Amyloid Beta Transport and Effects on Permeability in a Human Brain Endothelial Cell Line

Thesis

Amyloid Beta Transport and Effects on Permeability in a Human Brain Endothelial Cell Line

Leon M.Tai

A thesis submitted for the degree of Doctor of philosophy

Supervised by Dr Ignacio A. Romero and Dr A. Jane Loughlin

Department of Life Sciences

The Open University

Walton Hall

Milton Keynes

MK7 6AA

England

Submission date: 17 November 2008
Date of award: 26 January 2009

Acknowledgements

Firstly, I would like to thank my supervisors Dr Ignacio Romero and Dr Jane Loughlin for giving me this opportunity to study for a PhD. I would also like to thank you both for helping me to develop many skills that will help me through out my career and life in general! Thanks to the immunology and cell biology group, in particular Dr Hilary Macqueen and Professor David Male who have supported me during my time at The Open University. I would also like to acknowledge Dr Karen Logan, Hadassah Sade and Heather Davies who have provided me with laboratory support and all the other Open University staff who have helped my PhD run smoothly.

A big thank you to my family; Mum, Grandparents, Ian, Janet, James, Dad, Merlot and to Nicola who have always been there with support and love.

'Out, out, brief candle! Life's but a walking shadow, a poor player that struts and frets his hour upon the stage and then is heard no more: it is a tale told by an idiot, full of sound and fury, signifying nothing.' Macbeth Act 5, scene 5, 19-28.

Abstract

The clearance of neurotoxic amyloid beta (Aβ) from the brain represents a novel therapeutic target for Alzheimer's disease (AD). The ability of two blood-brain barrier (BBB) drug transporters, P-glycoprotein (P-gp) and the breast cancer resistance protein (BCRP), to transport Aβ was investigated using a human brain endothelial cell (BEC) line, hCMEC/D3. P-gp expression by hCMEC/D3 cells was stable over a high passage number, polarised on the apical membrane, consistent with the blood side *in vivo*, and comparable, albeit slightly reduced, to primary isolated human BECs. The P-gp inhibitors tariquidar and vinblastine prevented the efflux of rhodamine 123 from hCMEC/D3 cells, indicative of functional P-gp expression. hCMEC/D3 cells therefore constituted a suitable model to investigate P-gp substrate interactions *in vitro*. P-gp, and to a lesser extent BCRP, inhibition, increased the net influx and decreased the efflux of 0.1 nM ^{125}I Aβ 1-40 in hCMEC/D3 cells. Both P-gp and BCRP inhibition increased the apical-to-basolateral but not the basolateral-to-apical permeability of hCMEC/D3 cells to ^{125}I Aβ 1-40. This data is consistent with P-gp and BCRP, acting *in vivo* to prevent blood-borne Aβ peptides entering the brain but not to clear Aβ load from the brain.

Vascular dysfunction is emerging as a key pathological hallmark in AD, including increased BBB permeability. The effect of Aβ on the permeability of hCMEC/D3 cells was therefore investigated. Aβ 1-40 induced a marked increase in hCMEC/D3 cell permeability to the paracellular tracer 70 kDa FITC- dextran. Increased permeability was associated with a specific decrease in the tight junction protein occludin, but not claudin-5 or ZO-1, both at the protein and mRNA levels. JNK and p38MAPK inhibition prevented Aβ 1-40-mediated occludin down-regulation and increased paracellular permeability of hCMEC/D3 cells. Our findings suggest that the JNK and p38MAPK pathways might represent attractive therapeutic targets for preventing vascular dysfunction in AD.

Publication list

Poster

7th Cerebral Vascular Biology International Conference. June 24th -28th 2007. Ottawa Canada. P-glycoprotein mediates Amyloid beta efflux from human brain endothelial cells. L.M.Tai, A.J.Loughin, I.A.Romero.

Oral presentation

11th Symposium of the Blood-Brain barrier. September 18th-20th 2008, Amsterdam, The Netherlands. Amyloid β increases the permeability of immortalised human brain endothelial cells via down-regulation of occludin in a p38MAPK- and JNK-dependent manner. L.M.Tai, A.J.Loughlin, D.K.Male I.A.Romero

Research articles

Amyloid-β-induced occludin down-regulation and increased permeability in human brain endothelial cells is mediated by MAPK activation. L.M..Tai, K.A.Holloway, D.K.Male, A.J.Loughlin, I.A.Romero*. *In press.* Journal of Cellular and Molecular Medicine.

P-glycoprotein and Breast Cancer Resistance Protein restrict apical-to-basolateral permeability of human brain endothelium to amyloid-β. Leon M. Tai, A. Jane Loughlin, David K. Male, Ignacio A. Romero*. Submitted to Journal of Cerebral blood flow and metabolism.

Functional P-gp expression by an immortalised human brain endothelial cell line Leon M. Tai, Heather A. Davies, A. Jane Loughlin, David K. Male, Ignacio A. Romero*.Submitted to Journal of Neurochemistry.

Table of contents

List of figures

List of tables

Abbreviations

ACh	Acetylcholine
ATP	Adenosine triphosphate
AChEI	ACh esterase inhibitors
AJ	Adherens junctions
AD	Alzheimer's disease
Aβ	Amyloid beta
ADDL	Aβ derived diffusible ligands
Absent	Amyoid beta Synergistic endothelial and neuronal toxicity
APLP	Amyloid precursor like protein
APP	Amyloid precursor protein
Ang1	Angiopoietin-1
ABC	ATP-binding cassette transporter
BACE	β-site APP cleaving enzyme
BEC	Brain endothelial cell
BCRP	Breast cancer resistance protein
BBB	Blood brain barrier
BSA	Bovine serum albumin
CAA	Cerebral amyloid angiopathy
CNS	Central nervous system
CSF	Cerebrospinal fluid
CVOs	Circumventricular organs
Cl	Claudin family members
CATCH	Critically attained threshold of cerebral hypoperfusion
CT	Cycle threshold
DC	Detergent compatible
DMT1	Divalent metal transporter 1
DTT	D,L- dithiothreitol
EAE	Experimental autoimmune encephalomylitis
EC	Endothelial cell
EM	Electron microscopy
EGF	Epidermal growth factor
EDTA	Ethylene diamine tetraacetic acid

ERK	Extracellular signal regulated kinases
EB	Extraction buffer
X_G	Facilitative transporter of acidic amino acids
Y^+	Facilitative transporter of cationic amino acids
n	Facilitative transporter of glutamine
L1	Facilitative transporter of large essential amino acids
FBS	Foetal bovine serum
FITC	Fluoresceine-isothiocyanate
FGF	Fibroblast growth factor beta
FTC	Fumitremorgin C
GLUT-1	Glucose transporter -1
GSK-3β	Glycogen sythase kinase-3
GuK	Guanyl kinase like
HBSS	Hank's balanced salts solution
hTERT	human telomerase
hBEC	Human Brain Endothelial cell
HRP	Horse radish peroxidase
IDE	Insulin degrading enzyme
IGF-1	Insulin-like growth factor 1
IL-1 α/β	Interleukin-1
IL-6	Interleukin-6
ISF	Interstitial fluid
JAM	Junctional adhesion molecules
JNK	c-Jun N-terminal kinases
LTP	Long term potentiation
Lrp-1	Low-density lipoprotein receptor related protein
P-gp	P-glycoprotein
MAGUK	Membrane–associated guanylate kinase
MDCK	Madin Darby canine kidney epithelial cells
MTT	Methylthiazolyldiphenyl-tetrazolium bromide
MCI	Mild cognitive impairment
MS	Multiple sclerosis
NaCl	Sodium chloride
NFT	Neurofibrillary tangles
NF-KB	Nuclear factor NF-KB

NBD	Nucleotide-binding domain
NGS	Normal goat serum
PLP	Paraformaldehyde-lysine-periodate fixative
p	Passage
PMSF	Phenylmethylsulphonyl fluoride
PBS	Phosphate buffered saline
PDGF	Platelet derived growth factor
p38MAPK	p38 mitogen activated protein kinases
PET	Positron emission tomography
PKA	Protein kinase A
PKC	Protein kinase C
PDZ	PSD95-DLG-ZO
RAGE	Receptor for advanced glycation end products
rh123	Rhodamine 123
A	Sodium- dependent transporter alanine preferring
ASC	Sodium- dependent transporter alanine-, serine- and histidine- preferring
EAAT	Sodium- dependent transporter of the excitatory acidic amino acid family
LNAA	Sodium- dependent transporter of large neutral amino acids
N	Sodium- dependent transporter of nitrogen rich amino acids
SDS	Sodium dodecyl sulphate
TGF-β	Transforming growth factor-β
TJ	Tight junctions
TNF-α	Tumor necrosis factor α
TMD	Transmembrane domain
TBS	Tris buffered saline
VEGF	Vascular endothelial growth factor
ZO-	Zonula occludens

Chapter 1

General introduction

1.1 The blood-brain barrier (BBB)

The blood-brain barrier (BBB) is a term used to describe the restricted permeability of brain tissue capillaries, compared to capillaries of other organs, especially with regard to hydrophilic molecules. The BBB prevents the passage of molecules from the blood into the brain, maintaining a homeostatic neuronal extracellular fluid. It is important that the interstitial fluid (ISF) of the central nervous system (CNS) is regulated in terms of ion concentrations and signalling molecules, to allow efficient neuronal firing and brain function. Neuronal action potentials are dependent on the concentration of ions in both the ISF and within the neuron (e.g. Na^+, K^+ and Ca^{2+}). The ion concentrations must be maintained within a narrow range to allow efficient neuronal firing and neurotransmitter release, which in turn are vital for CNS activity. The relative impermeability of the BBB to ions means that any acute fluctuations in the circulating blood do not affect the brain ISF levels.

The BBB also protects the neuronal tissue from a range of substances that, although relatively non-toxic to peripheral organs, could interfere with neuronal functions and damage neurons if allowed to enter the brain. These agents could come from the diet (e.g. plant toxins) or drug therapies, and their exclusion is achieved not only by allowing limited movement from the blood to the brain, but also by specific transporters e.g. P-glycoprotein (P-gp) expressed by cerebral brain endothelial cells (BECs), which actively efflux a broad range of substances back into the blood. In addition to functioning as a barrier to certain molecules, the BBB also supplies nutrients and removes the waste products to and from the CNS, processes which are conducted by specific transporters [e.g. glucose transporter -1 (Glut-1)].

Increased BBB permeability can give rise to neuronal damage by allowing toxins or endogenous molecules to penetrate the BBB and also by the loss of cerebral homeostasis. Indeed, BBB malfunction is implicated in many disease states including Alzheimer's disease (AD). There are two aims to this thesis, both centred on the neurotoxic polypeptide amyloid beta (Aβ), believed to be at the root cause of AD pathogenesis. The first aim is to study the role of BEC efflux transporter proteins in the transport of Aβ across an *in vitro* human BBB model. The second aim is to investigate the effects of Aβ on the expression of proteins which regulate the permeability of BECs, and other transporter proteins associated with BEC phenotype. This introductory chapter will describe the unique properties of BECs and the potential role of the BBB in AD pathogenesis.

1.1.1 The history of the BBB

The concept of the BBB was first proposed as an explanation for the exclusion from the brain of hydrophilic dyes administered to the peripheral vasculature. Ehrlich in 1885 [1], whilst comparing the oxygen consumption of different organs using 'intravital dyes', observed for the first time, that some aniline derivatives stained many organs but did not penetrate the brain. The term BBB is reported to originate from the work of Lewandoski [2], who found that intrathecal application of potassium ferrocyanate was lethal in dogs and rabbits at 1 % (w/v) of the dose required by the subcutaneous route. Allegedly, Lewandoski first used the term *bluthirnschranke,* or BBB to describe this barrier function, although it is debated as to the exact date [3]. Goldman, Ehrlich's student, added further evidence for a barrier function protecting the brain, with the observation that trypan blue injected directly into the cerebral spinal fluid (CSF) stained all brain tissue cell types, whereas intravenous application did not [4]. These findings sparked a search for the cellular structure(s) of the BBB, and it was not until the advent of electron microscopy

(EM) that BECs emerged as a central component of the BBB. During the 1960's, horseradish peroxidase (HRP) had been employed as an enzymatic tracer for vascular transport studies due to its relatively high sensitivity and low molecular weight (MW 43,000). HRP had been demonstrated to pass from the circulation to extravascular spaces by diffusion through gaps between endothelial cells (ECs) and also via pinocytotic vesicles in cardiac and skeletal muscle [5]. In 1967, Reese and Karnovsky [5] demonstrated that HRP administered via the tail veins of mice was undetectable in the brain tissue, since HRP appeared not to cross the cerebral vascular endothelium. Critically, Reese and Karnovski established that neighbouring BECs overlap and are linked together by tight junctions (TJs), which prevented the intercellular/paracellular passage of HRP. The authors also found that BECs contained fewer micropinocytotic vesicles than peripheral ECs, which reduced (relatively) the intracellular transport of HRP. This type of experiment was possible due to high resolution EM, which could distinguish between the fine structures of cerebral capillaries. Subsequent experiments have yielded a detailed understanding of the BBB. However, these first investigations were vital to the identification of BECs as key components of the BBB.

1.1.2 The BBB as a neurovascular unit

The lumen of the cerebral vessels that penetrate brain tissue are enclosed by BECs, which are interconnected by TJ proteins. Whilst BECs are a key component of the BBB, other cell types are also associated with the development and maintenance of BEC characteristics. Pericytes are sparingly attached to the abluminal (brain side) surface of BECs in capillaries and both cell types are surrounded by a basal lamina. In addition, astrocytic end feet are contiguous with the basal lamina and surround BECs (Figure 1.1). The term neurovascular unit has recently been introduced to describe the interactions between BECs, astrocytes, pericytes and neurons to function as a unit and maintain BBB

properties (although fibres of the white matter and oligodendrocytes are sometimes also included) [6]. Whilst CNS resident cells including oligodendrocytes, glia and neurones can also alter the function of BECs, astrocytes and pericytes lie closest to BECs and form an intimate association. Through this close position, both cell types have been demonstrated to play a role in the maintenance and induction of the BBB.

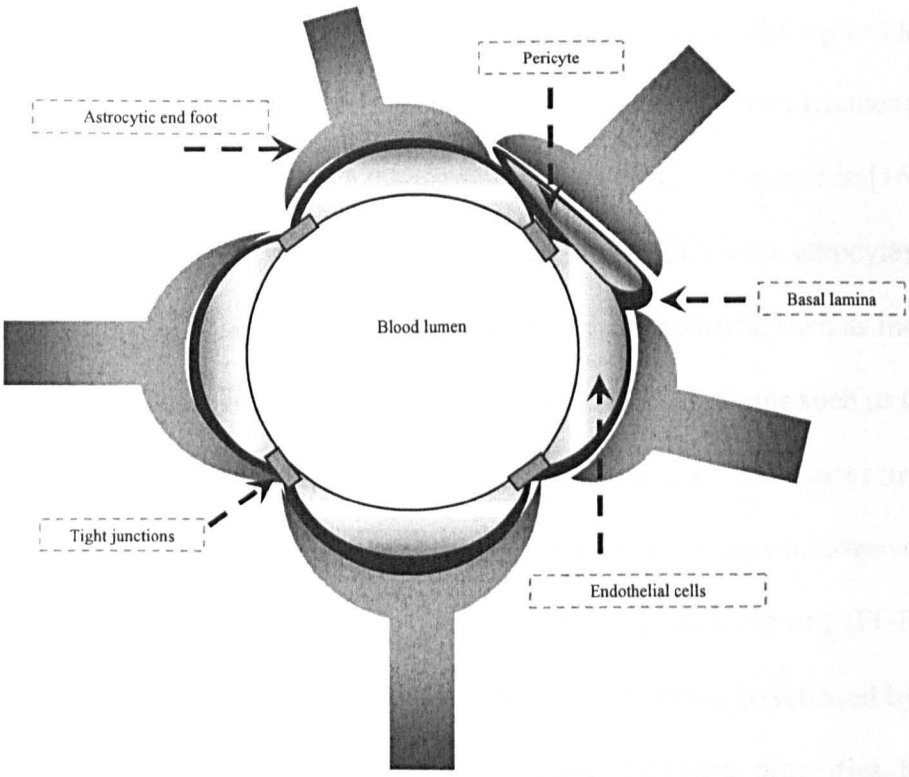

Figure 1.1 Schematic representation of the cellular components of the BBB. The lumen of cerebral capillaries is enclosed by BECs, which are interconnected by TJ proteins. Pericytes are attached to the abluminal surface of BECs and surrounded by a basal lamina. Astrocytic end feet are contiguous with the basal lamina and BECs.

1.1.2.1 Astrocytes

Astrocytes play a variety of active roles in maintaining neuronal physiology and homeostasis of the extracellular fluid surrounding neurones. Astrocytes are involved in the homeostasis of K^+ ions [7-9], glutamate and ammonia [10-12], to protect and ensure optimal neuronal function. K^+ ion concentrations must be tightly regulated in order to allow neuronal action potentials to occur. Astrocytes act as a spatial buffer and also take up

K^+ ions through carrier and pore-mediated transport [7, 9]. Astrocytes accumulate excess ammonia and convert glutamate to glutamine via glutamine synthase, thereby preventing excess neuronal excitation [11]. Recently, an additional astrocyte function has emerged in the metabolic coupling of neurons to astrocytes [12-15]. The astrocyte-neuron lactate shuttle hypothesis suggests that increased neuronal activity induces lactate production and secretion by astrocytes, and neurones then utilise this lactate as an energy source [12-15].

The close structural proximity of astrocyte foot processes to BECs provided the basis for the view that astrocytes contribute to the development and maintenance of the BBB. Indeed, astrocytes can influence the permeability of BECs (reviewed in [16-18]). *In vitro*, co-cultures of primary isolated BECs or immortalised BECs with astrocytes [19, 20] or astrocyte-conditioned media [20-23] improves BBB characteristics, such as increased tightness, decreased permeability and the up-regulation of BEC proteins such as Glut-1, P-gp, amino acid carriers, TJ proteins and γ-glutamyl transpeptidase. The exact astrocyte derived-factors responsible for the *in vitro* effects on BECs are unknown, however, transforming growth factor β (TGF-β) [24], basic fibroblast growth factor β (FGF) [25] and angiopoietin-1 [26], all appear to increase BECs tightness and may be released by astrocytes. It is worth noting that BECs can also influence astrocytic properties, for example increasing astrocytic anti-oxidant activity [27] and astrocyte differentiation [28].

1.1.2.2 Pericytes

The role of pericytes in the induction and maintenance of the BBB has not been as extensively investigated as astrocytes. However, it appears that pericytes may play a critical role in the development of BECs, in the control of capillary diameter and as a scavenger housekeeping cell (reviewed in [29-31]). Pericytes are more prevalent during the early stages of development and at maturation in rat neural capillaries than any other capillary type [32]. In fact, Balabanov and Dore-Duffy [29] have estimated the pericyte to

EC ratio to be 1:5 in rat brain capillaries, compared to 1:100 in skeletal muscle capillaries. This intimate association between BECs and pericytes appears to correlate with greater tightness and TJ protein expression. The recruitment of pericytes to BECs is considered to be a platelet derived growth factor (PDGF)-mediated response [33, 34], and PDGF-deficient mice develop numerous micro-aneurisms [34, 35], possibly due to capillary wall instability. A critical mechanism by which pericytes may influence the development of BECs is via angiopoietin-1 (Ang1) secretion, which acts via TIE2 receptors on BECs. Consistent with this theory is the finding that Ang1 and TIE2 knockouts do not develop mature brain blood vessels [34, 35]. In addition, Ramsauer *et al* [36] have demonstrated that co-cultured astrocytes, pericytes and BECs form capillary-like structures, which, unlike astrocyte-BEC co-cultures, were resistant to apoptosis induction. Furthermore, in co-cultures, pericytes can increase the expression of TJ components in rat BECs at the mRNA level [37] and reduce the paracellular permeability of immortalised mouse BECs to sodium fluorescein [38].

An early observation on pericyte ultrastructure by Herman and D'Amore [39], was that these cells contain contractile proteins. Oishi *et al* [40] have demonstrated that mouse pericytes cultured in a three-dimensional collagen gel, contract in response to acetylcholine (ACh) and noradrenaline, neurotransmitters that can be released in the vicinity of capillaries by neuronal fibres. In a novel experiment, Peppiatt *et al* [31] have shown that stimulation of rat retinal pericytes by superfused noradrenaline application caused capillary constriction in the cerebellum. Additionally, pericytes express receptors for catecholamines, endothelin-1, angiotensin II and vasopressin, which are all potential vasoactive mediators [29].

1.1.3 Characteristic phenotype of brain endothelial cells

BECs are characterised by reduced paracellular and transcellular permeability, and a high mitochondrial content compared to endothelial cells at other organs.

1.1.3.1 Low paracellular permeability

Although pericytes and astrocytes regulate the development of BECs, it is the properties of the BECs themselves that determine BBB function. Blood vessels throughout the human body are lined by ECs, which form the main site for nutrient exchange, leukocyte diapedesis, signalling molecule transport and all blood-tissue contact. In general, ECs fall into three types based on their structure; fenestrated, continuous and discontinuous.

Endocrine and exocrine glands, including the choroid plexus and intestinal villi, display discontinuous endothelia with fenestrae between them, and ECs in the liver, spleen and bone marrow are discontinuous in nature [41-43]. The increased leakiness offered by discontinuous and fenestrated capillaries allows secretory and sensory functions at these sites. Continuous ECs lack intracellular gaps and are found in skeletal muscle, lung and brain. BECs are of a specialised continuous type, as they are much more restrictive than other organs.

Due to this restrictive nature of the BBB, lipid solubility is the primary factor determining the permeability of a substance through the BBB [44]. A substance with a high oil/water partition coefficient can, in principle, diffuse freely through BECs and this is the primary route of entry and exit for small dissolved gasses to/from the CNS e.g. O_2. The permeability of BECs to hydrophilic macromolecules (e.g. albumin, HRP) and small ions is very low. This property is reflected by a high electrical resistance of pial vessels recorded in the frog and rat of 1000-2000 $\Omega.cm^2$ [45, 46], which is much higher than that in peripheral vessels (2-20 $\Omega.cm^2$) [45, 47].

The presence of continual complex TJ in BECs is considered to be the primary reason for the increased electrical resistance and decreased permeability at the BBB compared to discontinuous junctions in peripheral ECs. When BEC membranes containing TJs are freeze fractured and viewed via electron microscopy, fracture planes seprate the cytoplasmic leaflet of the inner membrane (P-face) from the extracellular leaflet (E-face).

TJs in BECs appear as strands on the P-face and grooves on the E-face, [48, 49] which allows continuous TJ formation [50-52]. The molecular composition and organisation of TJs is discussed in detail in section 1.1.4.

It should be noted that regions exist within the CNS in which the BECs are fenestrated and lack TJs. The choroid plexus (in cerebral ventricles) consists of a layer of fenestrated ECs surrounded by ependymal epithelium. The function of the choroid plexus is to produce cerebral spinal fluid (CSF), which circulates through ventricular cavities and the subarachnoid space. However, TJs are found at apical regions of the choroid plexus epithelium, which forms a blood-CSF barrier [53]. The other areas of the brain in which BECs are fenestrated are collectively called the circumventricular organs (CVOs) [54, 55]. CVOs are ventricularly located structures which carry out two main functions: 1) neuropeptide secretion (e.g. medial eminence, pineal gland, intermediate lobe of pituitary gland) and 2) to act as a sensor of circulating levels of hormones and neurotransmitters (e.g. subfornical organ, organum vasculosum).

1.1.3.2 High mitochondrial content

In addition to a high electrical resistance and the presence of TJs in most CNS regions, BECs also differ from periphery endothelia in terms of mitochondrial content. Oldendorf *et al* [56] calculated the mitochondrial content of rat BECs to be between 8 % and 10 % of total cytoplasmic volume, whereas in non-brain EC they represent between 2 % and 5 %. BECs contain numerous enzymes and transporters that are dependent on adenosine triphosphate (ATP). ATP-dependent transporters in BECs function to transport blood-borne harmful agents back into the blood (e.g. P-gp; see section 1.1.6.1), whereas a number of enzymes (e.g. monamine oxidase (A and B), cytochrome p450 monooxgenase, L-amino acid decarboxylase, epoxy hydolases, aminopeptidase A, superoxide dismutase [57-61]) are capable of degrading various peptides and reactive oxygen species that could

interfere with neuronal function or become neurotoxic. Thus, the high mitochondrial content in BECs may reflect the high energy requirements of these cells and their protective barrier function.

1.1.3.3 Low vesicular transport

In the original EM description of the BBB, Reese and Karnovsky [5] also noted a lower frequency of vesicles within ECs in cerebral vessels compared to other capillaries. Both the proportion and number of vesicles filled with HRP was much lower in BECs compared to cardiac ECs. A decreased vesicular content in BECs is a further indication of the barrier function of these cells in which blood-brain vesicular uptake is restricted.

Thus low transcellular transport, due to decreased vesicular transport, and low paracellular transport, as a result of TJs, together contribute to the barrier function of BECs.

1.1.4 Molecular organisation and regulation of brain endothelial cell tight junctions

BECs in the cerebral vasculature are linked together by both TJ and adherens junctions (AJs). AJs intermingle with TJs [62], and are expressed throughout the vasculature and play a role in EC adhesion, paracellular permeability, vascular growth and contact inhibition during vascular remodelling (reviewed in [63]). Vascular endothelial cell cadherin (VE-cadherin) is the transmembrane component of AJs [64], which is linked to the actin cytoskeleleton via β- and α- catenins, although the exact molecular components are under debate [64]. VE-cadherin is expressed by ECs in all tissues and its function is modulated by Ca^{2+} ions [65]. Abbruscato and Davis [66] have demonstrated using cultured bovine BECs, that hypoxic conditions cause a Ca^{2+}-mediated decrease in VE-cadherin expression. Although AJs are important for the development and function of BECs, it is the TJs that confer low permeability of BECs, when compared to other ECs. Multiple proteins

comprise TJs including; Junctional adhesion molecules (JAMs), occludin, claudin family members (Cl), zonula occludens 1, 2 and 3 (ZO-1 and 2, 3), cingulin, AF-6 and 7H6, associated directly or indirectly to a peri-cellular ring of actin filaments (reviewed in [6, 63, 67-69]). Generally, occludin, JAMs and the claudins form trans-membrane segments of the TJ complex whereas other TJ proteins serve as cytoplasmic anchors to the actin cytoskeleton (Figure 1.2).

(a)

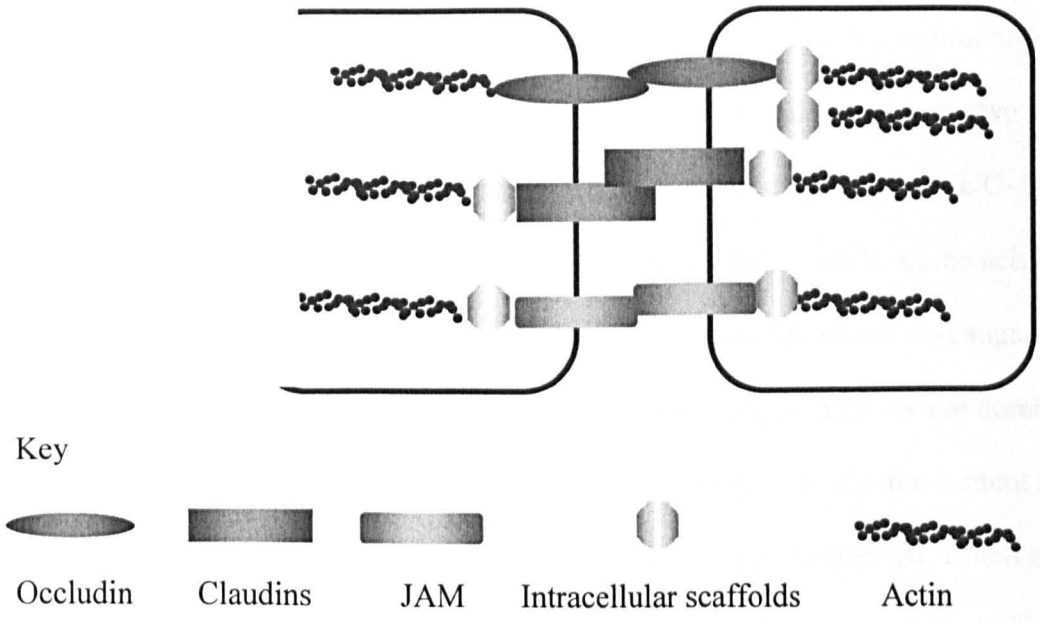

(b)

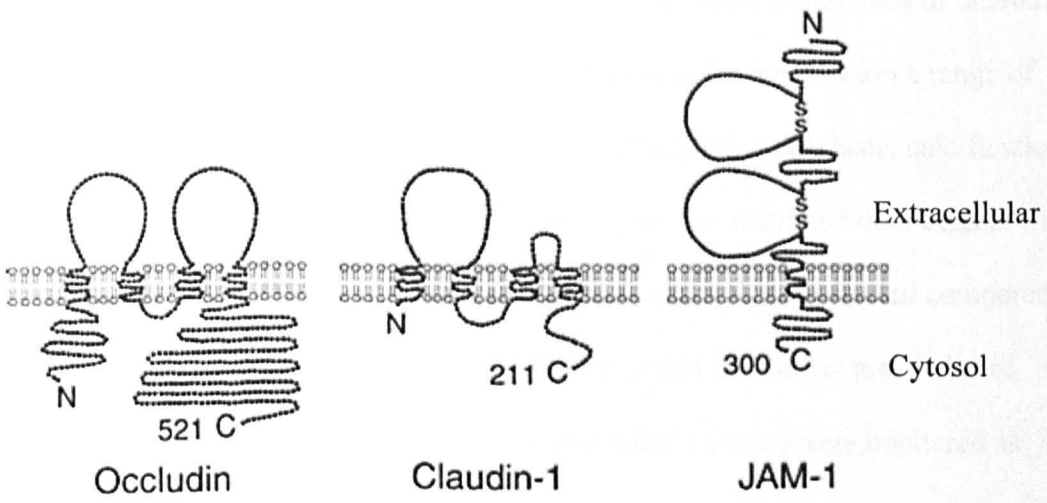

Figure 1.2 The tight junctional complex at the BBB. (a) BECs at the BBB are connected by TJ. Occludin, claudins and JAM form homodimers (claudins also form heterodimers) across the intercellular space and are held anchored to the actin cytoskeleton via scaffold proteins (ZO-1, -2, -3, AF6, 7H6 and cingulin). Actin can also be bound directly to occludin. **(b)** Representation of occludin, claudin and JAM structures [70].

1.1.4.1 Occludin

Occludin was the first TJ protein to be discovered in BECs. Furuse *et al* [71] developed rat antibodies directed against an isolated AJ fraction from chick liver, and found staining for a 65 kDa protein at epithelial and BEC TJs. Subsequently, continuous occludin expression was confirmed on rat [72], porcine [73] and human isolated brain capillaries [74, 75], whilst lower discontinuous expression is detected on non-cerebral ECs. Occludin expression is found at sites that display a high degree of tightness and is therefore considered to be actively involved in maintaining BBB permeability or function.

Structurally, occludin comprises four membrane spanning regions, two extracellular loops, a short cytoplasmic N-terminus and a long cytoplasmic C- terminus [71] (Figure 1.2). Human, murine and canine occludin share ~ 90 % amino acid similarity with each other but a divergence of ~ 50 % compared to chicken and rat-kangaroo occludin [74]. All species however share similarities in the two proposed functional domains: 1) the first extracellular loop of occludin which is rich in tyrosine and glycine content and is hypothesised to mediate cell to cell contact [74]; and 2) the C-terminus, which is responsible for the association with ZO-1 [76, 77].

There is conflicting experimental evidence as to the exact importance of occludin in TJ structure. Saitou *et al* [78] demonstrated that occludin-null mice develop a range of abnormalities such as chronic inflammation, gastric epithelium hyperplasia, calcification in the brain, testicular atrophy, and loss of cytoplasmic granules in striated duct cells of the salivary gland. However, the TJs of epithelial intestinal cells were unaffected compared to controls. In a follow up study, Schulzke *et al* [79] found that the barrier properties of epithelial cells in the stomach, bladder and throughout the intestine were unaltered as assessed by resistance measurements. The authors did find reduced acid secretion and morphological alterations in the gastric epithelium, which they attributed to a role for occludin in epithelial cell differentiation. It is of note that the permeability of the BBB was not investigated in either paper. In addition, mouse embryonic stem cells [80] deficient in

occludin, when differentiated into epithelial cells, form TJ structures that are impermeable to biotin.

However, there is considerable evidence that occludin confers increased tightness in TJ containing cells [81]. Many of these investigations have originated from epithelial cells, which also form TJ structures. McCarthy *et al* [82] have demonstrated that occludin over-expression in Madin Darby canine kidney epithelial cells (MDCK) increases the number of TJs and also the transepithelial resistance. The transfection of a C-terminal truncated mutant form of occludin into MDCK cells [83] or into Xenopus embryo cells [84] resulted in increased permeability to different paracellular tracers. Yu *et al* [85] used siRNA techniques to knock-down occludin expression in MDCK cells and found the permeability to small ionic cations such as Na^+, arginine and ethanolamine was increased.

Additional evidence for the role of occludin in the maintenance of TJs comes from observations that occludin down-regulation by different agents is associated with increased permeability. Antonetti *et al* [86, 87] have demonstrated using a streptozotocin-induced diabetes rat model, a concomitant increase in permeability to BSA and a decrease in occludin levels at the blood-retinal barrier. Other factors including histamine [88], CCL2 [89] and oxidised phospholipids [90] can phosphorylate occludin and induce leaky TJs. Occludin regulation therefore appears to play an important part in the TJ regulation of endothelial and epithelial permeability. Interestingly, occludin down-regulation and increased permeability of BECs has been reported in experimental animal models of neutrophil activation [91] inflammatory-induced pain [92], hypoxia [93] and Alzheimer's disease [94], further emphasising the importance of this protein in the regulation of BBB permeability.

1.1.4.2 Claudins

Furuse *et al* [95] upon re-examination of their isolated AJ fraction from chicken liver identified two further TJ proteins, claudin (Cl)-1 and 2. Subsequently, 24 members of the claudin family [96, 97] have been identified through database searches and genomic cloning.

Claudins are 20-27 kDa proteins with four transmembrane domains and one extracellular loop (~ 53 amino acids) much larger than the second (~ 24 amino acids) [95]. The C-terminus, as with occludin, has the ability to bind to ZO-1 and ZO-2 [98], whilst the extracellular loops of claudins can interact with each other via homophilic and heterophilic interactions [99]. The ability of claudins to form TJs has extensively been investigated in mouse L-fibroblast cultures. Cl-1 or Cl-2 expression in mouse L-fibroblasts results in the formation of TJ strands [100]. Furthermore, transfection of L-fibroblasts with paired combinations of Cl-1, 2 or 3 demonstrated that all transfected cells could form TJs, with the exception of those co-transfected with Cl-1 and -3 [99]. Interestingly, Furuse *et al* [100] also found that L-fibroblasts transfected with occludin do not form in TJs unless Cl-1 is also expressed.

The expression of claudins varies between cell types, and four particular Cls have been identified at the mammalian BBB: Cl-1 [101], 3 [102], 5 [103] and 12 [103]. The expression of Cl-1 by BECs has been brought into question, as the antibody used in many studies has been shown to cross-react with Cl-3 [102]. Nitta *et al* [103] have recently demonstrated the potential role of Cl-5 in the BBB using Cl-5-deficient mice. These mice die within 24 h of birth, indicating a developmental role for Cl-5. The development of the blood vessels was normal, and there were no signs of oedema, however paracellular tracer experiments revealed increased selective permeability for molecules <800 Da at the BBB. Whilst there was no detection of serum albumin leakage into the brain of Cl-5 deficient mice, the conclusion by these authors that Cl-5 exerts a size selective barrier at the BBB should be approached with caution. The tracer experiments by Nitta *et al* [103] were

carried out over a relatively short time period of 5 min, and the larger MW tracers used may have required longer to diffuse across the BBB than smaller ones and therefore to be detected in the brain parenchyma of Cl-5 deficient mice. The importance of Cl-3 at the BBB has recently been highlighted by the work of Wolburg *et al* [102], who demonstrated a selective loss of Cl-3 in autoimmune encephalomyelitis (EAE) mouse models and human glioblastoma multiforme tissue.

1.1.4.3 Junctional adhesion molecules

Members of an additional transmembrane protein family, termed junctional adhesion molecules (JAMs) are also present at TJs in BECs [104, 105]. JAMs are part of the immunoglobulin-like super-family of adhesion molecules and consist of three main members (JAM-1, -2,-3, also referred to as JAM-A, B and C). JAM -1 and -3, but not JAM -2, expression has been noted in rat brain blood vessels [106]. JAMs have been demonstrated to play a role in junction assembly [104, 107] and leukocyte migration [105] at the BBB (reviewed in [104]). Transfection of JAM-1 into Chinese hamster ovary cells (CHO) enhances endogenous ZO-1 expression and co-transfection of JAM-1 and occludin into the same cell type results in redistribution of JAM-1 to junctional areas [108]. JAM-1 can also bind to cytoplasmic accessory proteins such as ZO-1 and cingulin [108, 109]. However, the exact function of JAMs as BBB TJ proteins has not yet fully been explored.

1.1.4.4 Cytoplasmic accessory proteins.

There are several accessory cytoplasmic proteins that associate with the transmembrane components of TJs. However, the function of many of these proteins, e.g. cingulin [110, 111], AF-6 [109, 112, 113] and 7H6 [114, 115], has not been extensively investigated, especially with regards to the BBB. A notable exception is the ZO family of proteins, of which ZO-1 [116] was the first described TJ-associated protein. Stevenson *et al* [116] observed ZO-1 TJ staining in a variety of epithelia, and subsequently, two further

ZO family members, termed ZO-2 [117] and ZO-3 [118], were identified via co-immunoprecipitation of ZO-1 in MDCK cells.

The ZO proteins are members of the membrane–associated guanylate kinase (MAGUK) family, which generally enable multiple protein-protein interactions as intracellular scaffolds [119, 120]. ZO proteins share three core regions, a src homology 3 (SH3) domain, a guanylate kinase-like (GuK) domain and three PSD95-DLG-ZO (PDZ) domains which allow binding to different proteins. ZO proteins bind to each other [121], to occludin [76, 77, 108, 118, 122, 123] (via the SH3- GuK domains [123]), to claudins [98, 124] (via the PDZ domains), to JAM [109], to AJ proteins [112, 113, 125, 126] and to actin [76, 121] (via the C- terminus). Thus, the ZO proteins anchor transmembrane TJ proteins to the actin cytoskeleton, although it should be noted that occludin can also bind directly to the actin cytoskeleton [121].

Many studies have shown that ZO proteins are important for the stability of TJ architecture. Although epithelial cells lacking ZO-1 expression still form well developed TJs, loss of ZO-1 expression inhibits the Ca^{+}- induced re-formation of TJs previously disassembled by Ca^{2+} depletion [127, 128]. McNeil *et al.* [127] demonstrated that in ZO-1-depleted MDCK cells, formation of TJs is delayed after Ca^{2+} removal and this effect could be rescued by ectopic expression of the SH3 domain of ZO-1. In addition, Umeda *et al* [128] have demonstrated that suppression of ZO-1 and ZO-2 expression in a mammary epithelial cell line, Eph4, results in a lack of organisation of occludin, JAM-1 and Cl-3. One study has shown that ZO proteins may also play a role in development. ZO-1 knockout mice embryos are not viable and present with defective yolk sac angiogenesis and apoptosis of embryonic cells [129].

1.1.4.5 Regulation of paracellular permeability

There are multiple extracellular mediators that can induce a leaky BBB including cytokines, nitric oxide, free radicals, prostaglandins and histamine (reviewed in [46, 130]). These extracellular molecules can mediate increased permeability by TJ protein translocation at cell-cell contacts and/or a decreased expression of TJ proteins at the messenger level. Intracellular signalling pathways that have been shown to mediate TJ reorganisation include protein kinase C (PKC), protein kinase A (PKA), the small G-protein rho and the mitogen activated protein kinase family (MAPK) (reviewed in [131, 132]). As an example, when epithelial cells are cultured in low calcium medium, increased permeability and decreased transepithelial resistance is observed, which in some cases is accompanied by a membrane loss of ZO-1, ZO-2 and occludin at the membrane [133]. PKC activation and PKA inhibition have both been demonstrated to preserve the TJs after Ca^{2+} removal from epithelial cell cultures [134-136]. In contrast, the elevation of intracellular cAMP in BECs increases the TJ tightness and reduces paracellular permeability [46]. Therefore, PKA activation in BECs can enhance the barrier function, whilst in epithelial cultures may increase permeability.

Phosphorylation of TJ proteins is a further way in which permeability can be regulated. Ischemia, oxidative stress, Rho activation, and VEGF can cause phosphorylation of occludin and increased permeability to paracellular tracers in TJ containing cell lines [69, 131].

1.1.5 Nutrient transporters at the BBB

TJ expression and reduced vesicular transport in BECs combine to restrict the passage of hydrophilic molecules into the brain. However, the CNS shows a high metabolic demand, and essential brain substrates and nutrients require specific carriers and receptors to transport them into the brain across BECs. The transporters of glucose, iron, essential amino acids and ions are represented in Figure 1.3.

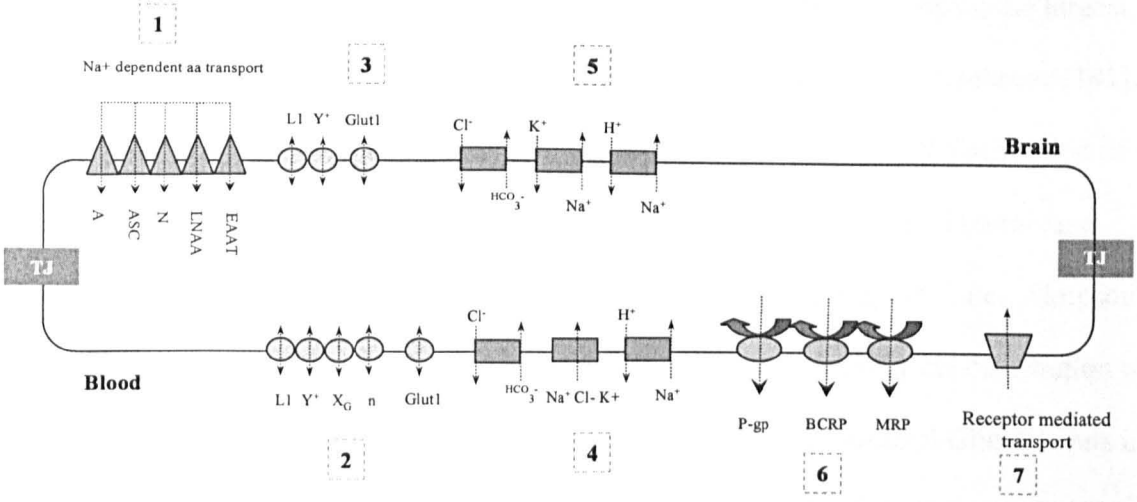

Figure 1.3. Transport mechanisms at the BBB. BECs contain a number of transport mechanisms to allow homeostatic control of nutrients, ions and signalling molecules. **(1)** Na^+ dependent transporters (A, ASC, LNAA, EAAT) eliminate non-essential, essential and excitatory amino acids from the brain, preventing excess accumulation. **(2)** Facilitative diffusion allows essential amino acids (L1, Y^+) and glucose (Glut-1) into the brain and elimination of excitatory amino acids (N, X_G) into the blood across the luminal and **(3)** abluminal membranes. **(4-5)** Ion transporters at the BBB regulate extracellular K^+ and Na^+ ions (Na^+ / K^+ ATPase) and intracellular pH. **(6)** ABC transporters (P-gp, BCRP, MRP) protect the brain from blood circulating toxins. **(7)** Receptor-mediated transport allows essential proteins and signalling molecules into the brain (e.g. Insulin receptor, transferrin receptor). Adapted from [137] [155].

1.1.5.1 Glucose

Glucose supply to the brain, either as glucose or as its breakdown product, lactate, is essential as an energy source for brain resident cells such as neurons. Glucose transport at the BBB is primarily mediated by facilitative diffusion via glucose transporters (Glut, reviewed in [138]). To date, 13 members of the Glut family have been identified, and amongst these Glut-1 is the major isoform present at the BBB. Pardridge *et al* [139] have found that over 90 % of glucose transport in bovine cortex blood vessels is attributable to Glut-1. Two different molecular weight forms of Glut-1 exist (44 and 55 kDa), which differ only in their extent of glycosylation [140]. At the BBB, the 55 kDa form is primarily present at both the luminal and abluminal membranes in addition to a large intracellular pool, although the exact sub-cellular distribution is not entirely clear [139, 141-147]. Farrell *et al* [144], using EM techniques on rat BECs, found a distribution of Glut-1 of 12

% luminal, 48 % abluminal and 40 % cytoplasmic and in a study in rabbits, the largest proportion of this transporter was similarly observed in the abluminal membrane [141]. More recently, Simpson *et al* [138] have suggested a more symmetrical distribution of Glut-1 expression. Lee *et al* [148] isolated bovine luminal and abluminal membrane vesicles and demonstrated a similar kinetic profile of glucose transport. Later, Simpson *et al* [147] corroborated this finding in bovine BECs, reporting symmetrical distribution of Glut-1. The intracellular pool of Glut-1, might serve to increase luminal Glut-1 levels in times of increased neuronal demand such as hypoglycaemia [149] and seizures [142]. Although Glut-1 is the most studied glucose transporter at the BBB, there is also evidence for a Na^+-dependent glucose transporter [148], which could play a role in glucose homeostasis if the glucose content in the neuronal environment is too high.

1.1.5.2 Iron

Iron is an essential trace element required for a plethora of functions including neurotransmission, myelination, as a component of the electron transport chain and cell division [150, 151]. In non-pathological conditions, virtually all iron circulates in the plasma bound to hydrophilic transferrin, which in principle would be excluded from the brain by the TJs at the BBB. However, BECs contain a receptor for iron-bound transferrin, the transferrin receptor [152, 153], which allows iron uptake by the brain. The exact mechanism of iron uptake by BECs is still unknown. Moos *et al* [151], have recently suggested a model of iron trafficking at the BBB. In this model, iron-transferrin binding to the transferrin receptor results in endosomal internalisation of the complex and abluminal vesicular release. In many cell types, the divalent metal transporter 1 (DMT1) causes the transport of iron into the cytoplasm, however DMT1 has not been detected in BECs [154]. Their theory is therefore, that under the acidic conditions of the endosome and an ATP-

citrate-rich abluminal membrane environment secreted by astrocytes, iron becomes available for cellular uptake.

1.1.5.3 Amino acids

The transport of amino acids at the BBB is complex and carried out by both facilitated diffusion and Na^+-dependent transport (reviewed in [155]). There are four facilitative amino acid carriers expressed by BECs; an essential neutral amino acids system (L1), a cationic amino acids system (Y^+), an acidic amino acids system X_G and a glutamine system (n). L1 expression was first identified when it was noted that the movement of neutral essential amino acids into the brain was greater than that of non-essential amino acids [156]. L1 is expressed on the luminal and abluminal membrane of BECs and functions to transport essential amino acids (e.g. Leucine, valine, isoleucine, phenylalanine, trypophan) into BECs and the brain [155, 157]. System Y^+, located on the abluminal and luminal membrane, is primarily a cationic amino acid transporter and acts to transport lysine, arginine and ornithine, whilst the presence of Na^+ allows association of neutral amino acids with this transporter [155, 158-160]. System n, on the luminal membrane, allows the facilitative diffusion of glutamine [161], whilst X_G (luminal) has affinity for glutamate and arginine [155, 162]. Collectively, L1 and y^+ allow access to the brain of all essential amino acids.

Analysis of the CSF composition, a rough indicator of brain extracellular fluid, reveals that, with the exception of glutamate, CSF amino acid levels are ~ 10 % of the plasma levels [155]. This led to the identification of five Na^+-dependent systems on the abluminal membrane of BECs, which allow the elimination of non-essential and/or toxic amino acids as well as maintaining homeostatic control over all amino acids. These five Na^+-dependent transporters (reviewed in [155]) are A (non-essential amino acid preferring e.g. alanine), ASC (alanine, serine, cysteine preferring), N (glutamine, asparagine and

histidine preferring), excitatory amino acid transporter family (EAAT, aspartate and glutamate preferring) and a Na^+-dependent L neutral amino acid transporter system (LNAA).

1.1.5.4 Ions

The free passage of ions through the BBB is limited by the presence of TJs. BECs contain a number of Na^+ and K^+ transporters to regulate their brain concentrations [163-165]. Na^+-K^+ ATPase is located on the abluminal EC membrane and serves the dual function of maintaining low extracellular K^+ levels to enable optimal neuronal action potentials, and maintaining a high extracellular Na^+ gradient to allow Na^+-dependent substrate transport to occur. There is also a Na^+/H^+ exchanger [165, 166] located on the luminal and abluminal membranes at the BBB. Further luminal ion transporters include a Na^+/Cl^- co transporter [163], a $Na^+/K^+/Cl^-$ co-transporter [167] and also a Na^+-Cl^-/HCO_3^- [168] dependent influx transporter.

1.1.6 ATP binding cassette (ABC) transporters

In addition to transporters involved in nutrient supply and homeostasis, BECs express a number of ATP-dependent binding cassette (ABC) transporters which act to prevent blood-to-brain transport of a broad range of substances, including xenobiotics and endogenously produced molecules. ABC transporters are a large family of membrane transporters expressed by a variety of cell types including many mammalian cells and bacteria. These transporters require ATP to transport molecules across plasma and intracellular membranes. To date, at least 48 ABC transporter genes have been identified and are classified into seven subfamilies ABCA to ABCG [169, 170]. At the BBB, ABCB1 (P-gp), ABCG2 (the breast cancer-related protein, BCRP) and ABCC [multidrug resistance proteins, (MRPs)] are the most significant (reviewed in [171]). Whilst the MRP family

members expressed at the BBB have a broad substrate range [172], a lack of specific inhibitors has hindered insight into their exact function at the BBB. P-gp and BCRP shall now be described in more detail, since they are the focus of the work described in this study on amyloid beta (Aβ) transport.

1.1.6.1 P-glycoprotein (P-gp)

Juliano and Ling [173] first discovered P-gp, a 170 kDa protein, which corresponded to the multidrug resistance activity of Chinese hamster ovary cells (CHO). Subsequent work revealed P-gp expression in other mammalian multidrug resistance cancer cell lines [174-176] and established a direct link between the MDR/ABCB1 gene and P-gp protein expression [175]. In humans, two types of P-gp exist, which are termed class I and class II [172]. Class I P-gp is encoded for by the MDR1/ABCB1 gene, located on the long arm of chromosome 7 [177, 178], whilst class II (MDR2/ABCB4), with a high sequence homology, is located adjacently [179]. Class I P-gp is expressed by the epithelia of many organs including the gastro-intestinal (GI) tract and kidney, and on ECs of the testes and brain (discussed below). Class II P-gp is expressed by canalicular hepatocytes and acts as a bile salt transporter [180, 181] and phosphatidyl flippase [182, 183]. In rodents, class 1 P-gp is subdivided into mdr1a (expressed at the BBB) and mdr1b (expressed in brain parenchyma) and are the equivalent of human MDR1. The rodent equivalent of human MDR2 is denoted mdr2.

Structurally, both P-gp types are around 1200 amino acids in length, and contain two nucleotide-binding domains and twelve transmembrane segments. P-gp is arranged in two halves, joined by a 75 amino acid linker region [184], with each half consisting of a transmembrane domain (TMD) made of six transmembrane segments, and an intracellular nucleotide-binding (NBD) domain (reviewed in [172, 185-187]). Both the N- and C-termini are located intracellularly (Figure 1.4). The two halves of P-gp are believed to form

a barrel-like configuration with the two NBD arranged to form a dimer. The exact mechanism of transport of substrates by P-gp is unknown. The most recent model involves first the binding of a ligand to the TMD, leading to a conformational change in the NBDs, increasing their affinity for ATP. ATP binding induces the formation of a closed NBD dimer, which in turn results in a conformational change in the TMD to induce ligand translocation [185]. ATP hydrolysis then causes the dissolution of the closed NBD dimer, releasing ADP and allowing P-gp to return to a state of high affinity for the ligand.

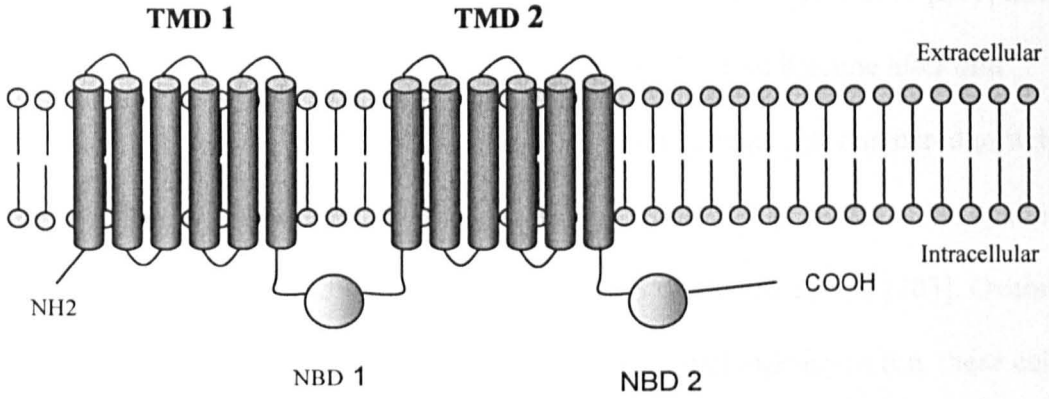

Figure 1.4. Structure of P-gp. P-gp is a transmembrane efflux transporter consisting of two TMD and two NBD. P-gp uses the energy derived from ATP to actively prevent the blood-to-brain transport of many substances

P-gp has a very large structurally diverse substrate list (Table 1.2), which includes many endogenous molecules (e.g. steroid hormones, cytokines, lipids), natural products and drugs in therapeutic use [172]. Multiple studies attempting to identify characteristics of P-gp substrates have been carried out [188-193]. However, a common feature is their amphipathic and, in some cases, hydrophobic nature. These properties allow for relatively easy diffusion across lipid membranes and have led to the notion that P-gp acts as a flippase transporter [186]. The flippase model states that lipophilic molecules associate with the inner leaflet of the lipid bilayer, and are flipped out by P-gp. In support of this notion, substrate binding sites have been located to the TMD of P-gp [176, 194], and phospholipid flipping is inhibited *in vitro* by the P-gp inhibitor vinblastine [195].

One of the most widely studied sites of P-gp expression is the GI tract. Canapro *et al* [196] have recently demonstrated P-gp expression in human tissue samples throughout the ileum, jejunum and stomach, at both the protein and mRNA levels. The majority of investigations into intestinal P-gp function have focused on whether P-gp limits the oral bioavailability of known P-gp substrates and anti-cancer drugs. *In vivo* and *in vitro* studies using mdr1a/1b (-/-) mice, caco-2 cell lines (a human carcinoma cell line) and human clinical trials have all been employed to that end. Several groups have suggested that the influence of P-gp on intestinal absorption is limited, since P-gp substrates have relatively higher absorption rates than expected [197-200]. In contrast, Ogihra *et al* [201] have demonstrated that in mdr1a/b-/- mice, the plasma levels of vinblastine after oral administration were increased, whereas that of verapamil was not, compared to wild type mice. Furthermore, in human volunteers, talinolol significantly increases the availability of digoxin [202], and similar findings have been noted with other agents [203]. Overall, P-gp in the intestine is located on epithelial cells on the luminal membrane (i.e. these cells are polarised with regards to P-gp), and, depending on the substrate, P-gp reduces oral availability.

The localisation and function of P-gp in the kidney, liver, placenta and lung appears to follow a similar theme of substrate efflux. In the kidney, P-gp expression is found on the luminal surface of epithelial cells of the proximal tubules and functions to excrete unwanted molecules into the urine [204]. In the liver, P-gp is found on the canalicular membrane of hepatocytes providing directional transport into the bile [205]. Placental expression of P-gp is localised to syncytiotrophoblasts, cytotrophoblasts and ECs in the trophoblast layer and, in general, P-gp is thought to play a role in protection of the foetus (reviewed in [206]). P-gp is found on ECs in both rat and human testes and Stewart *et al* [207] found P-gp staining in rat on both the luminal and abluminal membrane of testis EC. This suggests that the role in rat testis is to efflux substrates from the ECs themselves.

P-gp expression at the BBB has been noted in BECs and astrocytes [208, 209]. The expression of P-gp is frequently described as luminal, as P-gp expression has been found mainly on the luminal membrane of isolated capillaries from rat [210], mouse [211] and human [212]. There does exist however, some conflicting evidence with regards to the abluminal vs luminal expression of P-gp. Bendayan *et al* [213] observed P-gp staining along the nuclear envelope, in caveolae, cytoplasmic vesicles, Golgi complex, and rough endoplasmic reticulum (RER), using EM techniques and rat brain tissue. The presence of intracellular staining is unsurprising and could represent a basal P-gp production, or a pool of P-gp which could translocate to the membrane. However, the authors also demonstrated greater abluminal expression than luminal.

The most convincing indirect evidence for the polarisation of P-gp onto the luminal side of the BBB is found in P-gp knockout mouse models. In rodents, there are three P-gp genes, two encoding for P-gp type I (mdr1a and mdr1b) and one encoding for the equivalent of human MDR2 (mdr2). Schinkel *et al* [214, 215] were the first to describe mdr1a (-/-) mice. Mdr1a(-/-) mice were found to be viable and healthy, but treatment with the anti-parasitic drug ivermectin to treat a mite infection revealed a 100-fold increased neural tissue accumulation over wild-type mice, and resulted in virtually all the mdr1a(-/-) mice dying. Follow up studies on mdr1a(-/-) and mdr1a/b (-/-) mice revealed that after peripheral administration there were increased brain levels of many P-gp substrates, including cyclosporin A, digoxin, verapamil, vinblastine, steroid hormones, morphine, and HIV protease inhibitors, indicative of a brain protective role for P-gp (reviewed in [172, 216]). Further corroborative findings revealed that brain uptake of colchicine, vinblastine and paclitaxel was increased by co-administration of a P-gp inhibitor [217, 218] (see Tables 1.1 and 1.2 for lists of P-gp substrates and inhibitors, respectively).

Overall, P-gp is believed to play a protective role by secreting toxic xenobiotics and unwanted naturally produced molecules into the intestinal lumen, bile and urine as well as protecting specific organs i.e. brain, testes. However, undesirable effects of P-gp include

multidrug resistance of cancerous tissue and the prevention of therapeutic agents reaching their intended target organs e.g. BEC P-gp prevents anti-cancer agents and HIV treatments reaching brain tissue.

Substrate class	Examples
Anticancer agents	Actinomycin D, daunorubicin, docetaxel, doxorubicin, etoposide, imatinib, paclitaxel, methotrexate, mitoxantrone, vinblastine, vincristine, mitomycin C, teniposide, taxol,
Antihypertensive agents	Celiprolol, diltiazem, losartan, talinolol,
Anti-arrhythmics	Digoxin, digitoxin, quinidine, verapamil
β-adrenoreceptor antagonists	Bunitrolol, talinol
Antidepressants	Amitriptyline, nortryptiline, doxepin, paroxetine, venlafaxine
Antimicrobial agents	Doxycycline, erythromycin, rifampin, tetracyclines, fluoroquinolines
HIV protease inhibitors	Amprenavir, indinavir, nelfinavir, ritonavir, saquinavir
Anti-emetics	Ondansetron, domperidon
H2 receptor antagonists	Cimetidine, Ranitidine
Immunosuppressants	Cyclosporin A, valspodar, tacrolimus
Anti-epileptics	Phenytoin, carbamazepine, phenobarbital, topiramate
Steroid hormones	Aldosterone, cortisol, coticosterone, dexamethasone, hydrocortisone.
Opiods	Morphine, loperamide
Lipid lowering agents	Lovastatin, cerivastatin
Fluorescent dyes	Rhodamine 123, calcein-AM, hoechst 3342
Cytokines	IL-2, IL-4 IFN- γ

Table 1.1 P-gp substrate list. P-gp acts to prevent the blood-to-brain transport of a broad range of xenobiotics and naturally produced signalling molecules [171, 172, 176].

Generation	Examples
First generation	Verapamil, cyclosporin A, quinidine, verapamil, vinblastine
Second generation	Valspodar (PSC-833), biricodar (VX-710)
Third generation	ONT-093, zosuquidar (LY335979), tariquidar (XR9576), elacridar (GF120918).

Table 1.2. A selection of P-gp inhibitors. First generation P-gp inhibitors are compounds that are in clinical use for other indications e.g. cancer therapies although they also display P-gp inhibitory action. Second and third generation inhibitors are more specific for P-gp. The P-gp inhibitors names given by the drug companies are shown where appropriate, with other synonyms shown in brackets. In this study, the name given by the drug company was used unless otherwise stated. Adapted from [171, 172, 176]

1.1.6.2 The breast cancer resistance protein (BCRP)

Similarly to P-gp, BCRP was discovered in a drug-resistant cancer cell line. Chen *et al* [219] identified BCRP in a breast carcinoma cell line (MCF-7/AdrV) that was resistant to the cytotoxic effects of antracyclines, even in the presence of P-gp inhibition. Doyle *et al* [220, 221] subsequently identified and cloned BCRP cDNA from MCF-7 cells and found that transfection into MCF-7 cells resulted in the efflux of mitoxantrone, doxorubicin and daunorubicin. Two other independent groups also cloned an identical sequence from mitoxantrone-resistant human colon carcinoma cells [222] (MXR) and from human placenta [223] (PABCB). Currently, this transporter is referred to as BCRP/ABCG2 (reviewed in [224, 225]).

BCRP is a 70 kDa protein consisting of one NBD, one TMD containing six transembrane segments and N- and C- termini located intracellularly (Figure 1.5). Compared to P-gp, BCRP is often referred to as a half transporter, as it is considered to form a homodimer through disulphide bonded cysteine residues in order to function ([224, 225]). In support of this notion, Mitomo *et al* [226] have demonstrated that BCRP forms homodimers in HEK-293 cells, which can be broken by mercaptoethanol treatment, although the exact position of the cysteine(s) residue(s) within the BCRP sequence that mediate homodimer formation is still under debate.

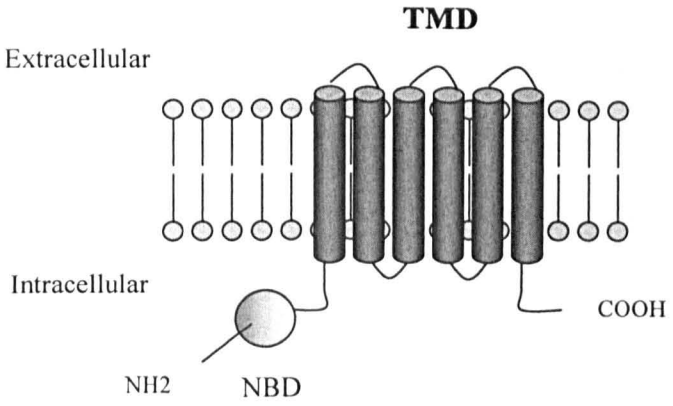

Figure 1.5. Structure of BCRP. BCRP contains contain one TMD and one NBD, and forms cysteine-dependent homodimers in order to function.

BCRP is found expressed in a large variety of tissues including placenta, liver, small intestine, brain, colon and lung, where, similarly to P-gp, it plays a role in organ protection. At the BBB, BCRP expression has been observed in BECs of porcine [227], mouse [228] and human origin [229]. Using confocal microscopy, Cooray *et al* [229] observed luminal BCRP expression in BECs of human tissue sections, indicative of barrier function. Sequencing of BCRP from normal tissue in comparison to that originally described from MCF-1 tumour cells, revealed a discrepancy in one amino acid at position 482 [230]. Wild type BCRP has an arginine (R482) where in many antracycline-resistant tumour cell lines there is a glycine or threonine (R482G/T). This difference in the amino acid sequence of BCRP has led to some confusion as to the substrate range. It appears as though both wild type and mutated BCRP can transport common drugs such as methotrexate and mitoxantrone, whilst only the mutated form shows preference for rh123 and enhanced activity towards daunorubicin and doxorubicin.

The transport function of BCRP for endogenous substances has not been extensively investigated, especially with regards to the BBB. mdr1a (-/-) mice have an enhanced BCRP expression of around three-fold in brain microvessels compared to wild type mice [228]. Furthermore, Cisternino *et al* [228] have shown that BCRP inhibition in mdr1a (-/-) mice results in enhanced prazosin and mitoxantrone accumulation in the brain.

Youdim *et al* [231] also demonstrated that the brain penetration of the flavanoid quercetin was increased by BCRP inhibition in rat models. The substrate range of BCRP shares an overlap with P-gp (e.g. Hoechst 3342 [232, 233], mitoxantrone [234], reserpine [235, 236]), and both P-gp and BCRP are inhibited by elacridar (GF120918) [237, 238]. Future investigations will yield a more detailed understanding of the role of BCRP at the BBB (see Table 1.3 for substrate list).

Substrate class	Examples
Anti-cancer drugs	Antracyclines, mitoxantrone, methotrexate, prazosin, topotecan,
Anti-HIV agents	Lamivudine
Natural compounds	Flavonoids, porphyrins, sulphated oestrogens
Fluorescent dyes	Mitoxantrone, Hoechst 3342
Inhibitors	Fumitremorgin C and analolgues e.g. KO143. Elacridar (GF120918), biricodar (VX-710), reserpine, prazosin.

Table 1.3. BCRP substrates and inhibitors. Substrates of BCRP are less well characterised than those of P-gp, however there is a large degree of overlap. The BCRP inhibitor names given by the drug companies are shown where appropriate, with other synonyms shown in brackets. In this study, the name given by the drug company was used unless otherwise stated. Adapted from [221, 225]

1.1.6.3 Regulation of efflux transporter expression

The regulation of P-gp is an area of extensive research, whilst the regulation of BCRP has not been extensively investigated as yet. Many extracellular molecules can alter P-gp function and/or expression by BECs. For example, ligands for PXR (ligand-activated transcription factors) can increase P-gp expression. Dexamethasone has been demonstrated to increase P-gp expression and cyclosporin A transport in isolated rat capillaries via PXR signalling [239]. Interestingly, the anti-nociceptive action of intravenous methadone, a P-gp substrate, was found to be reduced by 70 % in transgenic mice expressing human PXR

[240]. PXR ligand xenobiotics could therefore act to induce P-gp expression, self-limiting their passage across the BBB.

Inflammatory mediators can also affect the expression of P-gp. Intracranial ventricle injections of LPS reduce P-gp expression [241]. However, peripheral inflammatory pain can increase P-gp expression [242]. Recently, it has been demonstrated that TNF-α and endothelin-1 rapidly decrease P-gp transport activity after 1 h incubation, with no changes in P-gp expression at the protein level in rat brain capillaries [243]. However, this effect was transient and by 6 h P-gp expression and function had increased to double that of control levels. Overall, many agents can induce a decrease and increase in P-gp expression and/or activity (Table 1.4).

1.1.7 The role of the BBB in CNS pathologies

There is increasing evidence of a role for the BBB in the pathogenesis of many diseases affecting the CNS. Indeed, BBB dysfunction is a hallmark of many pathological states including Alzheimer's disease (AD), multiple sclerosis (MS) and cerebral ischemia, amongst others. In addition, the presence of an intact BBB may affect the success of potentially beneficial therapies for many CNS disorders. For example, P-gp and BCRP expressed by BECs hinder access to the brain of many drugs used to treat epilepsy (where increased P-gp expression is also found), brain tumours and depression (reviewed in [172]). Similarly, many drugs that are effective in peripheral infectious diseases are not effective in CNS infections, as is the case of cerebral malaria and HIV-1 encephalopathy. In this section, the role of the BBB in multiple sclerosis and cerebral ischemia will be briefly discussed before we consider in greater detail what is known about BBB dysfunction in AD.

Model	Agent	Effect on P-gp expression and/or function	Reference
Rat brain capillaries	Dexamethasone, pregnenolone.	Increased protein expression and transport activity.	[239]
Rat BEC cell line, GPNT	Dexamethasone, PKC activation.	No change in protein expression, increased activity.	[244]
Rat brain capillaries	TNF-α, ET-1	Biphasic response. After 1 h incubation decreased activity, after 6 h incubation increased protein expression and activity.	[243]
Human BEC cell line BB19	TNF-α	No change in protein expression, decreased activity.	[245]
Rat BECs cell line GPNT	TNF-α	Increased mRNA levels, decreased activity.	[246]
Primary rat BECs	Phenobarbital, phenytoin, carbamazepine,	Increased protein expression and activity.	[247]
Rat *in vivo*	Kainate induced seizures.	Increased protein expression.	[248]
Primary rat BECs	Glutamate	Increased mRNA levels, protein expression and activity.	[249]
Primary rat BECs	Hydrogen peroxide, hypoxia/reperfusion	Increased mRNA levels and activity.	[250]
Primary rat BECs	Repetitive hypoxia.	Increased protein expression and activity.	[251]
Mice *in vivo*, and mice BECs	HIV-Tat	Increased mRNA levels, protein expression and activity.	[252]
Mouse BECs cell line, MBE4	TGF-β	Increased activity.	[253]
Primary rat BECs	Glutathione depletion.	Increased protein expression and activity.	[254]
Mice BECs *in vivo*	Oral rifampin-treated mice overexpressing human PXR.	Increased activity.	[240]
Rat BECs *in vivo*	Intracranial LPS injections	Decreased mRNA levels and function.	[241]
Rat BECs *in vivo*	Lambda-carrageenan hind paw injection.	Increased protein expression and activity.	[242]

Table 1.4. A selection of modulators of P-pg expression and/or function by BECs

1.1.7.1 Multiple sclerosis

MS is the most common neurological condition affecting young adults, with around 85,000 people in the UK diagnosed with MS [255]. In many cases, MS follows a course of remission and relapse and is characterised by axonal demyelination and microvascular inflammation [256, 257]. Active CNS lesions, (manifested by areas of active demyelination) are characterised by the activation of microglia and macrophages, possibly via a T cell-mediated autoimmune response [256, 257]. Axons and astrocytes may also be affected in MS. Increased BBB permeability is a characteristic of MS [258, 259] and TJ disruption, including alterations in ZO-1 and occludin expression are frequently found in active MS lesions [260-262]. In animal models of MS (allergic encephalomyelitis, EAE), and MS patients, the cytokines interleukin-1, TNF-α and interferon- γ (IFN-γ) are increased (reviewed in [263, 264]). *In vitro*, all three of these cytokines can alter TJ expression, suggesting a potential mechanism by which BBB leakiness is induced in MS patients [265-270].

1.1.7.2 Cerebral ischemia

Cerebral ischemia is an event whereby parts of the brain do not receive sufficient blood supply to maintain neuronal function. Ischemic events e.g. stroke can lead to increased mirovascular permeability and oedema both clinically *in vivo* and *in vitro* (reviewed in [271]). TJ disorganisation might play a key role in the increased BBB permeability observed in ischemia. Witt *et al* [272] have demonstrated a concomitant reduction in occludin expression and increased permeability to sucrose using a low O_2 model of ischemic insult in rats. Fisher *et al* [273] have demonstrated *in vitro* using porcine BECs, that hypoxia induces increased permeability and ZO-1 down-regulation via VEGF production. The application of VEGF to *in vitro* cultures can reduce the expression of occludin and ZO-1 in bovine BECs [274]. Van Bruggen *et al* [275] have also found that

treatment of mice with a VEGF antagonist can reduce oedema and infarct size in a middle cerebral artery occlusion model of stroke. Nitric oxide (NO) is also considered a possible modulator of BBB permeability. Mark *et al* [276] have demonstrated *in vitro* that increased BECs permeability as a result of oxygen deprivation can be attenuated by inhibition of nitric oxide synthase. Thus, the increased BBB permeability that occurs as a consequence of ischemia, potentially exacerbates the symptoms found in stroke.

1.2 Alzheimer's disease (AD)

Dementia, as defined by the Diagnostic and Statistical Manual of Mental Disorders IV [277], is 'the development of multiple cognitive deficits (including memory impairment) that are due to the direct physiological effects of a general medical condition, to the persisting effects of a substance, or to multiple aetiologies'. In practise, dementia leads to the loss of skills needed to carry out daily functions. Globally, the direct and indirect costs of dementia were estimated by Winblad and Wimo [278] to be in the region of US $ 248 billion in 2003, which with an ageing population could rise considerably in the coming years. The incidence of dementia doubles every 5 yrs after 65 yrs of age, with around 1 in 5 individuals over 80 years of age affected by dementia [279-281]. As global demographics shift to an aging population, with more countries developed or developing (e.g. China, India), it is more than likely that dementia cases will rise. Indeed, Ferri *et al* [279] have calculated that dementia cases will double every 20 yrs to 81.1 million by 2040. AD accounts for 40 – 60 % [280, 282] of all dementia cases, and in 2007, in the UK, there were ~ 700,000 people who suffered from dementia, at a cost of over £17 billion [283]. Approximately 90-95 % of AD cases are idiopathic (no established cause) and occur over 65 yr of age, termed late onset/non-familial/sporadic AD (SAD) [284, 285]. The remainder of cases exhibit inherited patterns and occur frequently in patients under 65 yrs of age, termed early onset/familial AD (FAD).

1.2.1 The pathology of AD

Aloys Alzheimer, a German neurologist, was the first to describe a patient with what is currently known as AD. At a conference of psychiatrists in 1906, Alzheimer described [286-289] a deceased patient (D.Augustine), who had a five year history of progressive memory impairment, hallucinations, delusions and severely impaired social functioning, which are hallmarks of AD today. Currently, AD is recognised as a progressive neurodegenerative illness (clinical stages are shown in Table 1.5), whereby initial minor memory lapses develop into severe motor dysfunction, with death occurring 10-15 yrs after diagnosis.

Stage 1: No cognitive decline

No memory problems evident to a health care professional.

Stage 2: Very mild decline

Memory lapses (e.g. forgetting location of keys) not noticeable to friends or during medical examination

Stage 3: Mild cognitive decline

Friends, family and co-workers notice memory alterations. Memory problems can be recognised during medical examination and in some cases diagnosed with early stage AD. Problems include;

- Word/name recall problems
- Decreased name retention
- Losing/misplacing an object
- Decreased ability to plan/organise

Stage 4: Moderate cognitive decline/mild or early stage AD

Clearly noticeable issues in:

- Decreased current event and personal knowledge
- Impaired mental arithmetic ability
- The individual will appear withdrawn and subdued

Stage 5: Severe cognitive decline/mid stage AD

Major cognitive dysfunction emerges and assistance with day-day activities may be required. Symptoms include:

- Unable to recall address, telephone number, education history and can become confused with the date and day
- Require help choosing appropriate clothing and with mental arithmetic
- Usually can recall own name and do not require help eating.

Stage 6: Severe cognitive decline/moderately severe mid stage AD

In addition to worsening memory, personality changes emerge and individuals may;

- Lose awareness of recent experiences and events
- Recollect imperfectly personal history, however can recall own name
- Need help dressing and using the toilet, incontinence
- Hallucinations, delusions, repetitive behaviour

Stage 7: Very severe cognitive decline/late stage AD

In the final stage, AD patients often lose the ability to speak and control movement:

- Individuals lose the ability to form recognisable speech
- Need constant help eating and using the toilet
- Lose the ability to walk, smile and muscle become rigid
- Death 5-15 years post diagnosis

Table 1.5. Symptomatic stages of AD. AD is a chronic neurodegenerative illness, with memory and normal cognitive function loss becoming progressively worse during disease progression. Source [290]

In the context of AD pathology, Alzheimer, using silver impregnation microscopy staining, observed neuronal atrophy, extracellular 'miliary' deposits (which are now known as senile plaques) and intraneuronal neurofibrillary tangles (NFT) over the cerebral cortex of Augustine [286-289]. Since this initial description, the core of the plaques was found to consist of the polypeptide Aβ [291-294], whilst the NFT were shown to consist of paired helical filaments of hyperphosphorylated microtubule associated tau protein [295, 296]. Nowadays, complete diagnosis of AD is only fully confirmed by the identification of these findings in post mortem tissue and falls into different staging categories. Braaq and Braaq have investigated the distribution of NFT in the AD brain and describe six stages in AD pathogenesis (BRAAQ stages) [297]. Initially, NFT appear in the trans-enterorhinal region of the basal mediotemporal cortex (stages I and II), then they can be detected in the hippocampus (stages III and IV) and the neocortex (stages V and VI). Thal *et al* [298-300],

have more recently suggested that the expansion of Aβ deposits correlates with NFT and the development of cognitive deficits. These authors have observed five stages of Aβ deposition in the medial temporal lobe; stage 1 occurs in the neocortex, stage 2 in the enterorhinal region, stage 3 in the thalamus, basal ganglia and hypothalamus, stage 4 in the midbrain and medulla oblongata and stage 5 in the brain stem and cerebellum. It should be noted that for both NFT and Aβ progression in AD, the hippocampus is affected throughout the different stages.

A further characteristic of AD is the loss of cholinergic neurones in the basal forebrain of AD patients [301]. ACh is a neurotransmitter involved in the cognitive functions including learning and memory. In addition to the loss of cholinergic neurones, decreased choline acetyl transferase (the enzyme involved in ACh synthesis), choline uptake and ACh release have all been reported in AD patients.

Overall, AD is characterised by neuronal degeneration, NFT and Aβ deposits. Aβ is considered at the centre of AD pathogenesis, the evidence of which shall now be discussed in more detail.

1.2.2 Amyloid β (Aβ) cascade hypothesis

There is no clear defining theory for the underlying cause(s) of AD. The most widely accepted view is described as the Aβ cascade hypothesis [302, 303] (Figure 1.6), although more recently vascular alterations (discussed in section 1.2.4) have come to be considered critical events in AD pathogenesis. Under the Aβ cascade hypothesis, in AD patients, an event(s) occurs that causes increased levels of Aβ in the brain, potentially through increased production by brain resident cells or decreased clearance (section 1.2.3). Aβ has a high tendency to self-aggregate and forms soluble oligomers, fibrils and plaques, either intra or extra-neuronally. These increased Aβ species induce an inflammatory response, neuronal dysfunction and lead to the symptoms of AD disease.

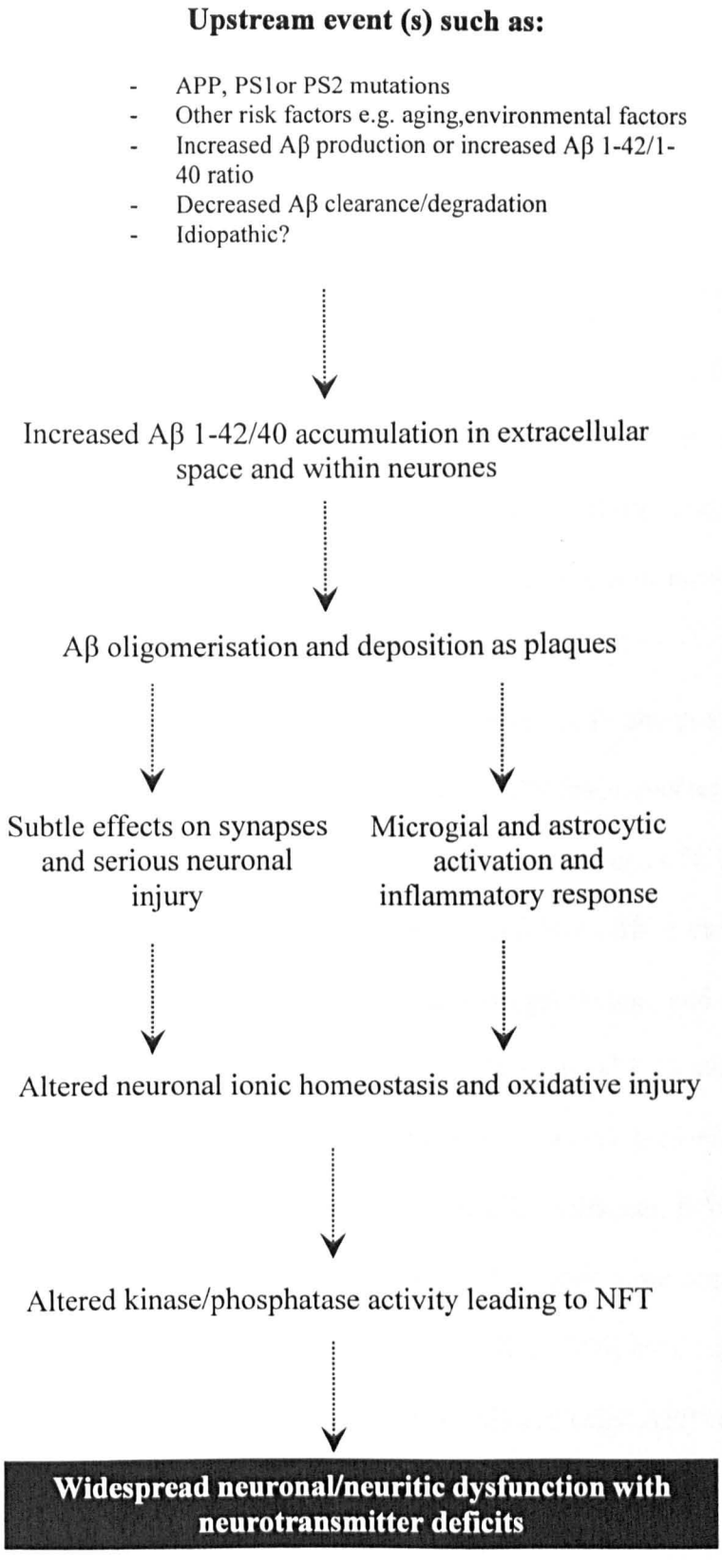

Figure 1.6 Aβ cascade hypothesis. Aβ is believed by many in the field to be the cause of AD. In the Aβ cascade hypothesis, increased Aβ levels in the brain of AD patients lead to widespread neuronal degeneration and inflammation which cause dementia. Adapted from [302-304].

1.2.2.1 Aβ processing

Shortly after the identification of Aβ as the main component of senile plaques, its precursor protein was identified and named as the amyloid precursor protein (APP) [292] (Figure 1.7). APP is part of a family of type 1 membrane glycoproteins, which in mammals includes APP-like protein 1 and 2 (APLP 1 and 2) (reviewed in [305-307]). The human *APP* gene is located on the long arm of chromosome 21 and codes for three main isoforms of 695, 751 and 770 amino acids in length. APP 751 and 770 contain a domain that is homologous to the kunitz-type serine protease inhibitors (KPI), and are expressed by virtually all cell types. APP695 lacks the KPI domain and is primarily expressed by neurones.

APP is processed by three proteinases termed α-, β- and γ- secretase. Cleavage of APP by α-or β-secretase generates larger soluble APP fragments termed APPsα and APPsβ and C-terminal fragments (CTFα and β). Subsequent cleavage of CTFα by γ- secretase produces a 3 kDa product whilst CTFβ cleavage produces Aβ of various amino acids in length, of which Aβ 1-40 and Aβ 1-42 are the most prominent, and the APP intracellular domain (AICD). The main neuronal β-secretase is β-site APP cleaving enzyme (BACE), whilst γ-secretase is a protein complex consisting of at least presenilin 1 and 2 (PS1 and 2), nicastrin, anterior pharynx defective-1 and presenilin enhancer. BACE, APP and the γ-secretase complex are most likely to degrade APP in endosome compartments and thus secrete Aβ via vesicular release. Thinakaran and Koo [306] have suggested that only 10 % of APP is present on the plasma membrane in cultured cells. APP can undergo axonal transport and Cirrito *et al* [308] have recently demonstrated Aβ vesicular release via synaptic exocytosis.

Aβ has a high tendency to self-aggregate, forming soluble dimers and oligomers and larger insoluble fibrils and plaques high in β-pleated sheet content. The solubility of an

Aβ species is generally defined as it ability to remain in the aqueous phase of a solution after high speed centrifugation (>100,000 xg, 1 h).

(a) Human APP 770

```
1     mlpglallll aawtaralev ptdgnaglla epqiamfcgr lnmhmnvqng
51    kwdsdpsgtk tcidtkegil qycqevypel qitnvveanq pvtiqnwckr
101   grkqckthph fvipyrclvg efvsdallvp dkckflhqer mdvcethlhw
151   htvaketcse kstnlhdygm llpcgidkfr gvefvccpla eesdnvdsad
201   aeeddsdvww ggadtdyadg sedkvvevae eeevaeveee eadddedded
251   gdeveeeeaee pyeeatertt siatttttt esveevvrev cseqaetgpc
301   ramisrwyfd vtegkcapff yggcggnrnn fdteeycmav cgsamsqsll
351   kttqeplard pvklpttaas tpdavdkyle tpgdenehah fqkakerlea
401   khrermsqvm reweeaerqa knlpkadkka viqhfqekve sleqeaaner
451   qqlvethmar veamlndrrr lalenyital qavpprprhv fnmlkkyvra
501   eqkdrqhtlk hfehvrmvdp kkaaqirsqv mthlrviyer mnqslsllyn
551   vpavaeeiqd evdellqkeq nysddvlanm iseprisygn dalmpsltet
601   kttvellpvn gefsldd lqp whsfgadsvp antenevepv darpaadrgl
651   ttrpgsgltn ikteeisevk mdaefrhdsg yevhhqklvf faedvgsnkg
701   aiiglmvggv viatvivitl vmlkkkqyts ihhgvvevda avtpeerhls
751   kmqqngyenp tykffeqmqn
```

(b)

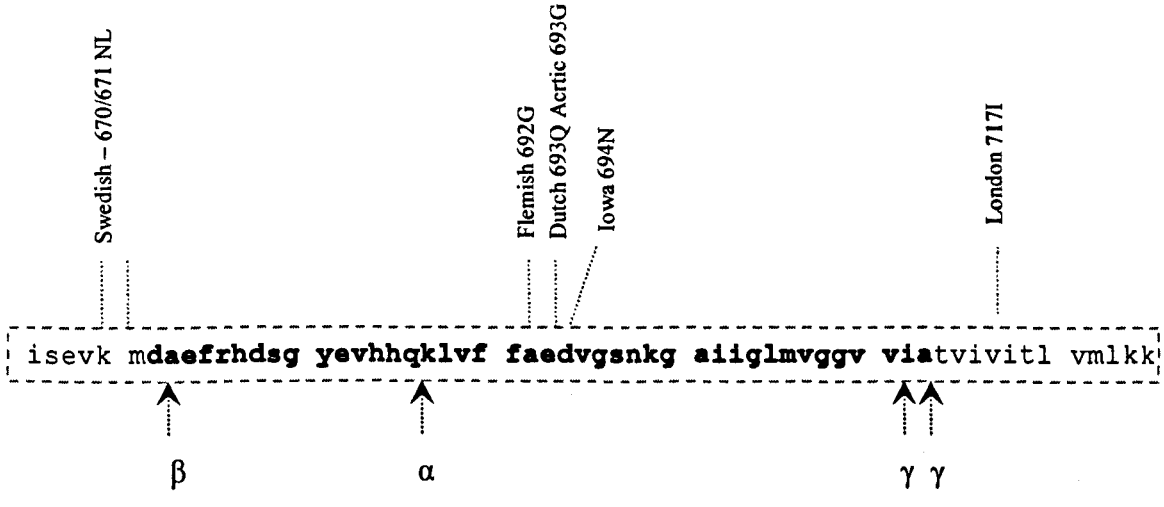

Figure 1.7. Production of Aβ from its precursor APP. (a) The amino acid sequence of APP with the Aβ 1-42 sequence in bold [309]. **(b)** APP is cleaved by the action of α-, β- and γ- secretases to produce Aβ 1-40 and Aβ 1-42. A selection of FAD mutations are also indicated, which increase the net production of Aβ, the ratio of Aβ1-42/1-40 or the aggregation properties of Aβ [309, 310].

1.2.2.2 Aβ levels in AD

The levels of Aβ in the plasma, cerebrospinal fluid (CSF) and total brain continue to be an area of intense research with the view to aid the diagnosis and understanding of disease progression (reviewed in [311-313]). Some researchers have argued that Aβ plaques do not to correlate with AD progression, since Aβ plaques are found in non-dementia patients, and in APP transgenic mice, memory impairment and alterations in neuronal function occur prior to amyloid deposition [314, 315]. In contrast however, increased insoluble, and, importantly, soluble Aβ oligomers are found in the brain tissue of AD patients (reviewed in [311]). For example, Gong *et al* [316], found an increase of up to 70-fold in levels of oligomeric species (main constituent 12-mer) in AD patient tissue, compared to controls. The increased retention of positron emission tomography (PET) agents, which can bind to the fibrillar form of Aβ, have also been demonstrated in AD patients and in a subset of patients with mild cognitive impairment that subsequently developed AD (reviewed in [317]). For example, the retention of the Pittsburgh compound-B (PIB) was higher in AD patients compared to controls and was inversely correlated with glucose metabolism [318].

Measurements of plasma Aβ levels have been inconclusive as to whether Aβ levels are increased or unaltered in AD (reviewed in [313]). The contradictory findings can originate from the inability of ELISA techniques to sufficiently measure aggregated Aβ levels, Aβ binding to plasma proteins and a high intra- and inter-individual variability. More recently, however, increased free [319] and total plasma Aβ levels [320] have been found in AD patients compared to healthy controls. Furthermore, Van Oijen *et al* [321] have found that high Aβ 1-40 levels in early life corresponded with an increased risk of developing dementia in later life, compared to those who did not develop dementia.

CSF levels of Aβ 1-42 are reduced in AD patients compared to controls, most likely as the result of sequestration and deposition in the brain [311, 312, 322]. Indeed,

CSF levels are inversely correlated with Aβ load after autopsy [323] and PIB labelling [324].

1.2.2.3 Genetic factors underlying AD pathogenesis

A key line of evidence for the role of Aβ in AD has originated from genetic studies. Down's syndrome is caused by a trisomy in chromosme 21, where the *APP* gene is located, and Down's syndrome patients display AD pathologies including increased levels of Aβ 1-40 and Aβ 1-42 in brain and plasma [325, 326], Aβ plaques [327, 328] and the development of dementia at an early age [329]. In a rare case of Down's syndrome, a point break mutation left a patient diploid for APP [330]. This patient lived until 78 years of age with no evidence of dementia and an autopsy revealed no Aβ deposition, highlighting a central role of Aβ in AD.

The genetic mutations found thus far in FAD all reside in the APP, PS1 or PS2 sequence (reviewed in [284, 285]). Mutations in the APP sequence are often named after the region of origin (e.g. Swedish, Dutch, Arctic, Iowa) and all have the net consequence of increasing the production of Aβ or increasing the ratio of Aβ 1-42 to Aβ 1-40 [284, 285]. In many cases the ability of these mutations to confer AD pathology has been confirmed in transgenic mouse models (reviewed in [310, 331, 332]). For example, the Tg 2756 mouse model expresses the 695 human isoform of the Swedish mutation of APP, and develops Aβ deposits at around 9 months of age. Mutations in PS1 and PS2 have the net result of increasing the production of Aβ 1-42, which is considered a more toxic species, as observed from the plasma and in the media of cultured skin fibroblasts from patients harbouring PS1 and/or PS2 mutations [333].

The majority of AD is sporadic, with the only high genetic risk factor being ApoE4 allele inheritance [334]. The *ApoE* gene is involved in nerve regeneration, immunoregulation and the activation of several lipolytic enzymes [335]. ApoE4 is

associated with a higher Aβ plaque burden [336, 337] in AD, although the mechanism through which this is caused is not clear [338]. Crossing APP transgenic mice with Apo E-deficient mice results in reduced cerebral Aβ deposition [339]. An interesting role of ApoE proteins is their ability to block Aβ transport from the blood into the brain. ApoE2 and 3 completely prevent the blood-to-brain transport of Aβ in a guinea pig perfusion model, whilst 85 % of Apo E4-Aβ crossed into the brain, which could increase the brain levels of Aβ and add to AD pathology [340].

1.2.2.4 Effects of soluble Aβ on neurons

There is a large body of work that has demonstrated that Aβ is toxic to neurones *in vitro* [341-353] and can cause neuronal dysfunction *in vivo* both in transgenic models and after intracerebral injection of Aβ [354]. More recently, soluble oligomeric Aβ species are emerging as the most neurotoxic Aβ forms (reviewed in [355-359]). As noted earlier, oligomers have been detected in AD patients at 70 fold higher levels than in control patients [316]. The first description of toxic non-plaque Aβ species was noted by Oda *et al* [360]. Astrocytic Apo J can prevent the formation of large aggregates, and was incubated with Aβ 1-42 and PC12 cells (cell line derived from a pheochromocytoma of the rat adrenal medulla) in an attempt to reverse toxicity. Oda *et al* [360] found enhanced neuronal toxicity, which was later attributed to smaller Aβ oligomers [361] named Aβ-derived diffusible ligands (ADDL) [356, 362]. ADDLs can be anything from dimer to 24 mer in size and impair synaptic plasticity and hippocampal long term potentiation (LTP) and induce neuronal cell death. ADDLs can induce hippocampal, but not cerebellar, neuronal death in *in vitro* mice cultures, mirroring AD pathology [356, 357, 362]. In addition, de Felice *et al* [363] have shown that oligomers isolated from human AD tissue can induce tau hyperphosphorylation in rat hippocampal neuronal cultures.

More recently, synaptic defects are thought to underlie the cognitive dysfunction found in AD. Aβ administration *in vivo* and *in vitro*, similarly to AD transgenic mouse models, leads to reduced dendritic spines and synapse number, and inhibition of LTP (reviewed in [364-368]). The inhibition of LTP, which is believed to be critical for memory formation, might, in part, be due to Aβ-induced loss of AMPA receptors and PSD-95 ([364-368]). Soluble oligomers can induce many of these changes *in vivo* [359] . For example, Klyubin *et al* [369] have recently found that Aβ-dimers, isolated from AD patients, impaired LTP, decreased hippocampal spine density and disrupted learned memory behaviour in rats, and these effects were inhibited by Aβ antibody treatment.

As described earlier, NFT are considered to be a consequence of Aβ in AD. NFT are not specific for AD and are found in other CNS disorders with (e.g. fronto-temporal dementia with Parkinsonism) and without dementia (e.g. progressive supranuclear palsy). NFT are insufficient to induce plaques. By contrast, Aβ has been shown to induce tau pathology. Gotz *et al* [370] have demonstrated that intracerebral injection of Aβ 1-42 into mutant tau over-expressing mice can increase the levels of NFT by 5-fold. Lewis *et al* [371] observed that transgenic mice expressing mutant tau and APP have increased levels of NFT in the olfactory cortex and limbic system compared to mice that expressed the tau mutation alone. Thus, whilst NFT are considered a key component of neuronal toxicity in AD, they are more likely to play a secondary role to Aβ [372].

1.2.2.5 Inflammatory response in AD

Another component of AD pathology is the presence of brain inflammation. The observed inflammatory response includes astrocytic end feet swelling [373], microglia activation [374] and either pericytic atrophy [375] or an increase in pericyte capillary coverage [376], which may constitute a second line of defence. The activation of astrocytes and microglia is often associated with an inflammatory response, and in AD patients the

cytokines IL-1 α/β, IL-6 and TNF-α are elevated [377]. Increased levels of Aβ might in part be responsible for the inflammatory response in AD. Aβ *in vitro* has been demonstrated to activate astrocytes and microglia to produce the cytokines mentioned above ([374, 377]), adding further evidence for the role of Aβ in AD. Whilst the relative contribution of inflammation to neuronal malfunction and death remains undetermined, it is interesting to note that inhibition of p38MAPK, activation of which is associated with increased production of cytokines by microglia, has beneficial demonstrable effects *in vivo*. Munoz *et al* [378] have recently demonstrated that p38MAPK inhibition suppressed hippocampal levels of TNF-α and IL-1 induced by intracerebroventricular Aβ 1-42 injections in mice, which was associated with an improvement in cognitive function.

1.2.3 Mechanisms of Aβ deposition

The increased levels of Aβ found in AD may be a direct consequence of increased production by brain resident cells, or of decreased clearance via the ISF or across the BBB.

1.2.3.1 Increased production of Aβ by brain resident cells

The increased levels of Aβ found in the CNS of AD patients are an indication of increased production by brain resident cells. Indeed, cultured neurones and astrocytes have been shown to produce Aβ [379], and neurones *in vivo* also produce Aβ [308]. Neuronal APP processing can occur during axonal transport and via the endosomal pathway. Cirrito *et al* [308] have demonstrated that synaptic activity is associated with vesicular Aβ release in Tg2756 mice. Mutations in PS1 and/or 2 and APP increase the production of Aβ by neurones *in vitro* [380, 381]. It is therefore considered that increased Aβ production by neurones might be a key pathogenic event in AD. However, there is currently no direct evidence of this in non-familial AD, and the mechanisms by which neurones might increase Aβ production in AD remains unclear.

1.2.3.2 Perivascular drainage of Aβ

Reduced perivascular drainage of Aβ might represent a mechanism by which CNS Aβ levels are increased (reviewed in [382]). The interstitial fluid (ISF) that surrounds the brain tissue, is roughly 280 ml in volume, and has a drainage rate of 0.11-0.29 µl/minute/g of brain [382]. ISF drains along the capillary and artery basement membrane to cervical lymph nodes. In AD, this pathway for Aβ elimination might be disrupted. Increased Aβ production by neurones, and stiffening of arteries during aging could reduce the clearance of Aβ via ISF drainage. Aβ is also found deposited on the blood vessels (arteries and capillaries) in many AD patients as a result of a process known as cerebral amyloid angiopathy (CAA), and is associated with a loss of smooth muscle cells in arteries [382]. A loss in smooth muscle cells might contribute further to reducing the perivasular drainage of Aβ.

1.2.3.3 Blood-brain barrier clearance of Aβ

Recently, Zlokovic *et al* [137, 383] have postulated that faulty clearance of Aβ at the BBB is key to the pathogenesis of AD. BECs express proteins capable of Aβ transport into the brain, most notably the receptor for advanced glycation end products (RAGE) and megalin, and from the brain, namely low-density lipoprotein receptor related protein (LRP-1) and P-gp (Figure 1.8).

RAGE is a multiligand receptor of the immunoglobulin superfamily, and is found expressed on microglia, neurones and BECs. The distribution of RAGE appears to be altered in AD. Donahue *et al* [384] observed an increased microvascular and decreased neuronal RAGE expression in the hippocampi of AD patients compared to controls. Miller *et al* [385] have recently confirmed this finding in hippocampal slices and found that RAGE levels were increased in cerebral BECs at the onset of AD and also in the progression to advanced BRAAQ stages. The interaction of Aβ with RAGE on neurones

can result in direct and indirect (via microglia activation) toxicity [386] and neuronal stress [387, 388], whilst in BECs a major consequence of Aβ-RAGE interaction is Aβ transcytosis across the BBB from the blood to the brain.

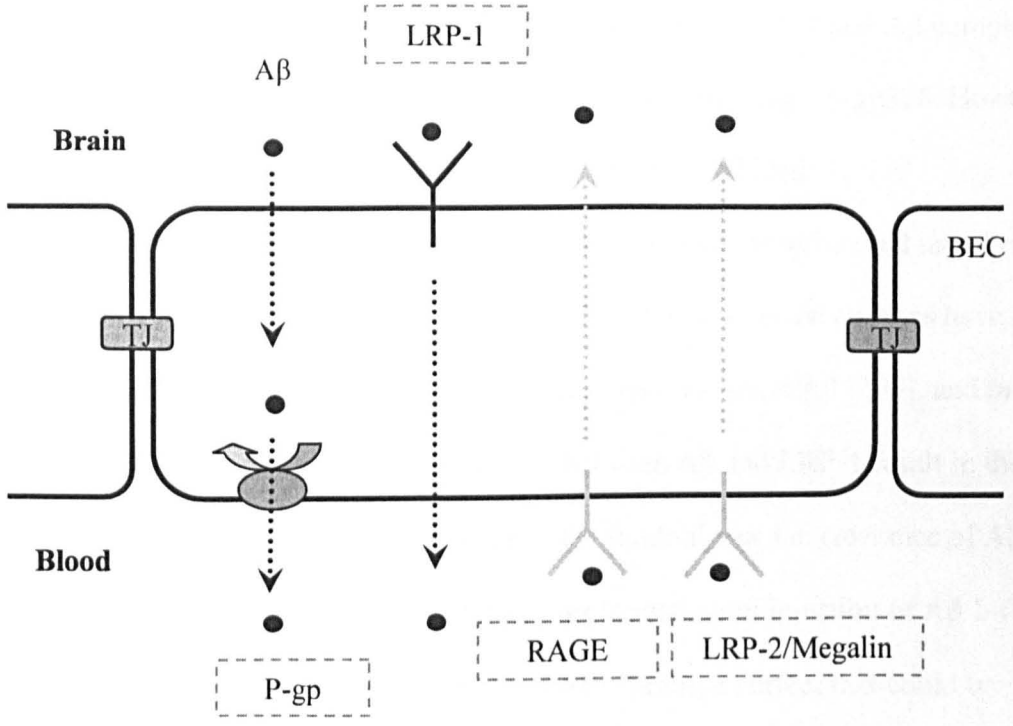

Figure 1.8. Proposed BBB transport routes for Aβ. Abluminal LRP-1 in addition to the ABC transporter P-gp, is considered to transport Aβ from the brain into the blood. RAGE mediates blood-to-brain Aβ transport. LRP-2/Megalin is also a proposed to mediate blood-to-brain transport of ApoJ-bound Aβ.

Using isolated primary hBECs, Mackic *et al* [389] demonstrated that RAGE transcytosed Aβ 1-40 from the luminal (blood) side to the abluminal side and was blocked by an anti-RAGE antibody *in vitro*. Deane *et al* [390] used an *in vivo* model, whereby Aβ 1-40 was intravenously infused into mice, and found RAGE-mediated Aβ transcytosis across the BBB. RAGE-Aβ interactions in the mouse model also led to the expression of inflammatory cytokines including TNF-α and IL-6, and induced vasoconstriction via endothelin-1 production. These authors also showed that in RAGE-null mice, the transport of Aβ into the CNS, was undetectable. Soluble RAGE (sRAGE), is a secreted form of RAGE, which can act as a signalling decoy receptor, and Emanuele *et al* [391] have recently reported decreased levels of sRAGE in the plasma of AD patients. In AD,

increased RAGE expression by BECs, together with decreased plasma sRAGE would therefore result in increased susceptibility to Aβ deposition in the brain.

A second blood-to-brain Aβ transporter at the BBB for Apo J-bound Aβ has also been described. Zlokovic *et al* [392] have shown that the infusion of ApoJ-Aβ complexes in guinea pigs, results in a high affinity brain uptake via LRP-2/megalin/gp330. However the significance of this interaction for AD has not been explored further.

LRP-1 is a multi-ligand scavager receptor expressed on the abluminal membrane of BECs and also on neurones. Data from *in vitro* fibroblast and neuronal cultures have demonstrated that LRP-1 binds to carrier (α2 macroglobulin)-bound Aβ [393], and *in vivo* LRP-1 binds to free Aβ. At the BBB, interactions between Aβ and LRP-1 result in the clearance of Aβ from the abluminal membrane to the luminal side i.e. clearance of Aβ from the CNS. Shibata *et al* [394] reported that after intracerebral injection of Aβ 1-40 in young mice, the peptide was rapidly removed from the brain, an effect that could be significantly reduced by LRP-1 antibodies. Deane *et al.*[395] further demonstrated *in vivo* the ability of LRP-1 to clear Aβ from the mouse brain and also identified two binding regions in LRP-1 which Aβ binds to: cluster II and IV. Subsequently, Sagare *et al* [319] found that treatment with recombinant LRP cluster IV (sLRP-IV) in APPsw +/- mice resulted in clearance of Aβ 1-40 and Aβ 1-42 from the hippocampus, cortex and whole brain. The increased clearance of Aβ appeared to be mediated by sequestration of Aβ in the plasma by sLRP-IV, and resulted in improvements in cognitive function as assessed by operant learning.

Alterations in LRP-1 expression are also found in AD. Kang *et al* [396] have described decreased LRP-1 expression at the BBB associated with increased plaque deposition in AD patients. Donahue *et al* [384] have also demonstrated reduced LRP-1 expression in cerebral microvessels of AD patients. Intriguingly, Sagare *et al* [319] have also found 30 % reduction in soluble LRP (sLRP) plasma levels in AD patients and an increase in free Aβ levels. There remains a degree of controversy as to the validity of *LRP-*

1 genetic mutations as a risk factor for AD. There are conflicting reports of a polymorphism of the *LRP-1* gene as an increased risk factor for developing AD. A positive correlation between with the C766T and C766C genotype but not the T766T genotype of LRP-1 has been observed in AD patients [397-401], although no correlation was observed in other studies [402-405]. In one study, carriers of the T766T genotype were observed to have decreased plaque numbers and increased LRP-1 expression by BECs, although all presented with AD [396]. Therefore in AD, a decreased LRP-1 expression at the BBB and sLRP-1 the plasma, could result in increased Aβ deposition in the brain. Currently, the application of sLRP to the treatment of AD is under investigation.

Lam *et al* [406] were the first to describe the ability of Aβ to bind to P-gp. The group found that transfection of MDR into a human embryonic kidney cell line (HEK293) previously stably transfected with human APP harbouring the Swedish mutation, or co-transfection with the Swedish mutation APP gene into wild type HEK293 cells, resulted in increased Aβ levels in the media. However, MDR1 transfection resulted in an increased APP expression in the cell line, which may account for increased Aβ production. Aβ was confirmed as a P-gp substrate, since Aβ 1-40 and Aβ 1-42 were shown to decrease the transport of colchicine into P-gp-enriched hamster vesicles and also to quench the fluorescence of labelled P-gp. Further *in vitro* [407] evidence for P-gp- mediated Aβ transport has been derived from a porcine derived kidney epithelial cell line (LLC). LLC cells transfected with human P-gp, showed increased Aβ 1-40 and Aβ 1-42 transport from the basolateral-to-apical chamber when grown on filter inserts compared to untransfected LLC cells. This increased Aβ transport was inhibited by cyclosporin A. In membrane vesicles derived from LLC-mdr1 cell lines, the transport of rh123 was increased compared to untransfected LLC cells and was also inhibited by Aβ 1-40 and Aβ 1-42 to a similar extent as that induced by verapamil.

Cirrito *et al* [408] have recently investigated P-gp-mediated Aβ transport *in vivo*. Initially, it was demonstrated that P-gp null mice cleared intracerebrally injected Aβ 1-40

and Aβ 1-42 at a much slower rate than wild type mice. However, the P-gp null mice also showed a marked decrease in expression of LRP-1, which may account for this effect. This group therefore went on to investigate the effect of a pharmacological P-gp inhibitor, tariquidar (XR9576), in Tg2576 mice. Tariquidar-treated animals showed increased ISF levels of Aβ compared to control animals. In addition, P-gp null mice when crossed with Tg2576 mice displayed increased hippocampal Aβ load, compared to Tg2576 mice. However LRP-1 down-regulation might have been responsible in part for this effect. Whilst an inverse correlation between P-gp expression and Aβ plaque deposition has been noted in non-dementia autopsies [409], the exact role of P-gp in AD is not fully understood and the contribution of P-gp to Aβ transport at the BBB warrants further investigation.

1.2.4 Role of vascular dysfunction in AD pathogenesis

The BBB may play an important role in the transport of Aβ into and out of the brain. In addition, multiple investigators have recently suggested that cerebrovascular dysfunction plays an important part in AD pathology (reviewed in [410-420]). This includes hypoperfusion and alterations in brain capillary function.

1.2.4.1 Brain hypoperfusion in AD

Using epidemological studies, multiple risk factors have been identified for AD (Table 1.6), and most, if not all of which are vascular in nature e.g. stroke, cardiac disease and atherosclerosis. De La Torre [421] has recently suggested that the risk factors occur prior to cognitive decline and result in a 'critically attained threshold of cerebral hypoperfusion' (CATCH hypothesis Figure 1.9) which, in combination with vascular abnormalities, may cause dementia in the elderly. A variable global decrease in cerebral blood flow (CBF) between 70 % and 90 % has been observed in AD patients, when compared to controls [413]. Ruitenberg *et al* [422] have observed that reductions in CBF

velocity and brain hypoperfusion precede the onset of dementia and hippocampal atrophy as observed via MRI. Hippocampal hypoperfusion as assessed by SPECT analysis, has been demonstrated to predict the progression from mild cognitive impairment to AD [423, 424].

Ischemic events, which are risk factors for AD, could lead to decreased CBF. Snowdon *et al* [425], examining AD patient autopsies, observed that multiple infarcts in the ganglia, thalamus, or deep white matter were a positive indicator for dementia severity. Results form Vermeer *et al* [426] corroborate these data with the finding that MRI-detectable infarcts more than double the risk of dementia development. Medial artery occlusion models in rodents can result in hippocampal neuronal damage, capillary irregularities, glial reactivity and glucose uptake deficiency, and bilateral occlusion of the carotid artery, can increase the production of Aβ [427, 428], adding to the evidence that brain hypoperfusion plays a significant role in AD pathogenesis.

Heart-related risk factors	**Peripheral risk factors**	**Brain-related risk factors**
Congestive heart failure	Smoking	Ageing
Cardiac arrhythmia	Alcoholism	Ischaemic stroke
Hypertension	High cholesterol	Silent stroke
Hypotension	High intake saturated fat	Head injury
Thrombotic episodes	Diabetes mellitus	Menopause
Atrial fibrillation	Haemorheological abnormalities	Migraine
Atherosclerosis		Depression

Table 1.6. Risk factors for AD. There are multiple identified risk factors for AD, many of which can be linked to vascular dysfunction. Adapted from [421]

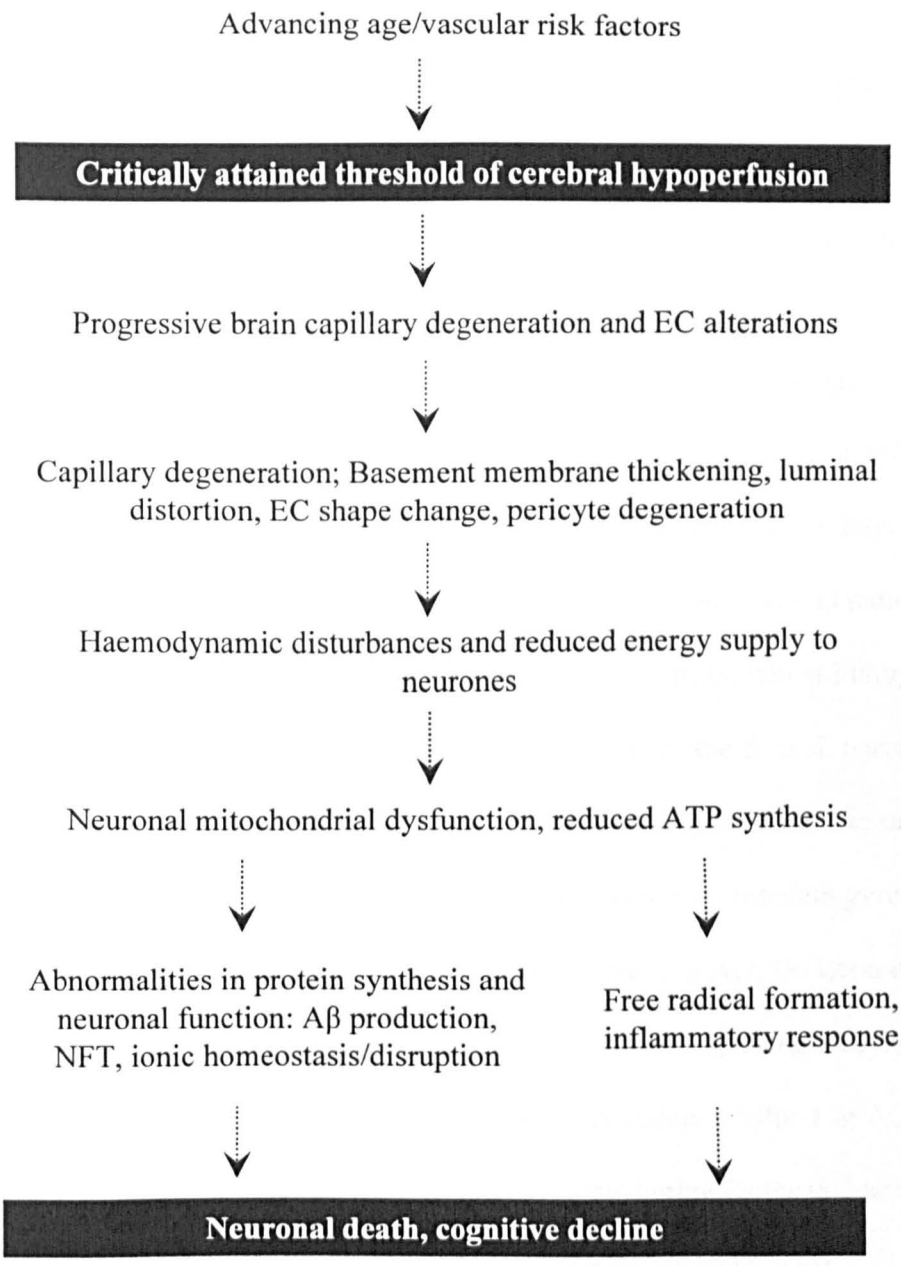

Figure 1.9. Critically attained threshold of cerebral hypoperfusion vascular hypothesis in AD. Torre has proposed that a convergence of aging and vascular risk factors leads to a critically attained threshold of cerebral hypoperfusion (CATCH). CATCH leads to capillary dysfunction, alterations in the neuronal homeostatic environment and a reduction in neuronal energy supply. Reduced neuronal metabolism triggers a cascade of events leading to the development of dementia [421].

1.2.4.2 Pathological changes of cerebral capillaries in AD

Multiple alterations throughout the vasculature have been described in AD patients. Cerebral capillaries appear fragmented and display atrophy, luminal buckling, decreased luminal diameter, basement membrane thickening, deposition of Aβ on the capillary wall and increased leakiness [413]. Morphological changes in small arteries in AD (e.g. pial and

intracerebral arteries) include CAA and decreased vascular smooth muscle content and can lead to the rupture of vessels. Capillary degeneration in AD may play a significant role in AD pathology which in turn may reflect a disturbance in angiogenesis. Wu *et al* [429] identified a gene that was under-expressed in AD BECs called mesenchyme homeobox 2 (MEOX-2), which is a transcription factor involved in vascular differentiation. Restoration of MEOX-2 in isolated BECs from AD patients resulted in angiogenesis, suppressed apoptosis and increased LRP-1 expression. In Meox-2 null mice, a reduction in brain capillary density, cerebral blood flow and angiogenic response to hypoxia was observed.

Decreased cerebral glucose utilisation is also found in AD patients. Hoyer *et al* [430] noted a 45 % decline in cerebral glucose utilisation, whilst Fukuyama *et al* [431] found a significant decrease in glucose metabolism in the frontal, parietal and temporal region as measured by PET in AD patients. Reduced glucose uptake or metabolism in the hippocampus [432, 433], enthorinal [434] and posterior cingulate gyrus [435] can also predict the conversion of mild cognitive impairment to AD. De Leon *et al* [436] have also demonstrated that the development of mild cognitive impairment in the elderly is predicted by reduced glucose metabolism. Decreased expression of Glut-1 in AD patient capillaries has been observed, which could be a major contributing factor to decreased glucose utilisation, and might contribute to neurodegeneration [437, 438].

The detection of plasma proteins such as albumin, thrombin and IgG in the brain parenchyma of AD patients is indicative of a leaky BBB [439]. An increase in BBB permeability is also observed in AD mouse models. Tg2765 mice display increased BBB permeability prior to the onset of pathology, which can be reversed by Aβ immunisation [440]. In an APP/PS1 transgenic mouse model, increased BBB permeability was associated with occludin down-regulation in mice fed on a high fat diet [94]. Intravenous infusion of Aβ can also lead to a disruption in BBB integrity in rats [441], and Aβ increases ECs permeability *in vitro* [442-444]. The pathological significance of increased

BBB permeability has not been fully explored, but in principle it could disrupt the neuronal homeostatic environment, further contributing to AD pathogenesis.

1.2.6 Combined neuronal and vascular dysfunction model for AD

The most commonly accepted view of AD pathology is the Aβ cascade hypothesis, whereby increased Aβ levels induce direct, or indirect via microglia activation, neuronal dysfunction and toxicity. The BBB may play a key role in the transport of Aβ out of or into the brain, and in part determine the brain amyloid load. However, what is absent in the amyloid beta cascade hypothesis is an understanding of how vascular dysfunction including increased BBB permeability, brain hypoperfusion and decreased Glut-1 expression may be linked to AD pathology. These vascular events could be the result of increased Aβ levels (Aβ cascade hypothesis), and might represent a further mechanism by which Aβ induces AD pathology. A second possibility is that one or more of these vascular events precede Aβ deposition and act as a causative factor in AD, such as the CATCH hypothesis. A third, unifying possibility, is that vascular events and Aβ production are interlinked in a more complex way. Indeed, as proposed by Roy and Rauk [419], an event(s) may occur in AD, that causes increased Aβ levels, which induce a synergistic toxicity of Aβ on BECs and neurones (Figure 1.10, Absent). Under their theory, in addition to inducing direct neurotoxicity, Aβ may also induce BEC damage, which in turn may lead to decreased glucose uptake into the brain, stroke and other vascular alterations, with the net consequence of inducing neuronal cell death. Whilst the initiating event(s) that causes AD is/are currently elusive, it remains a possibility that vascular dysfunction, decreased Aβ clearance across the BBB, and/or in combination with other predisposition(s) may all act to induce Aβ production.

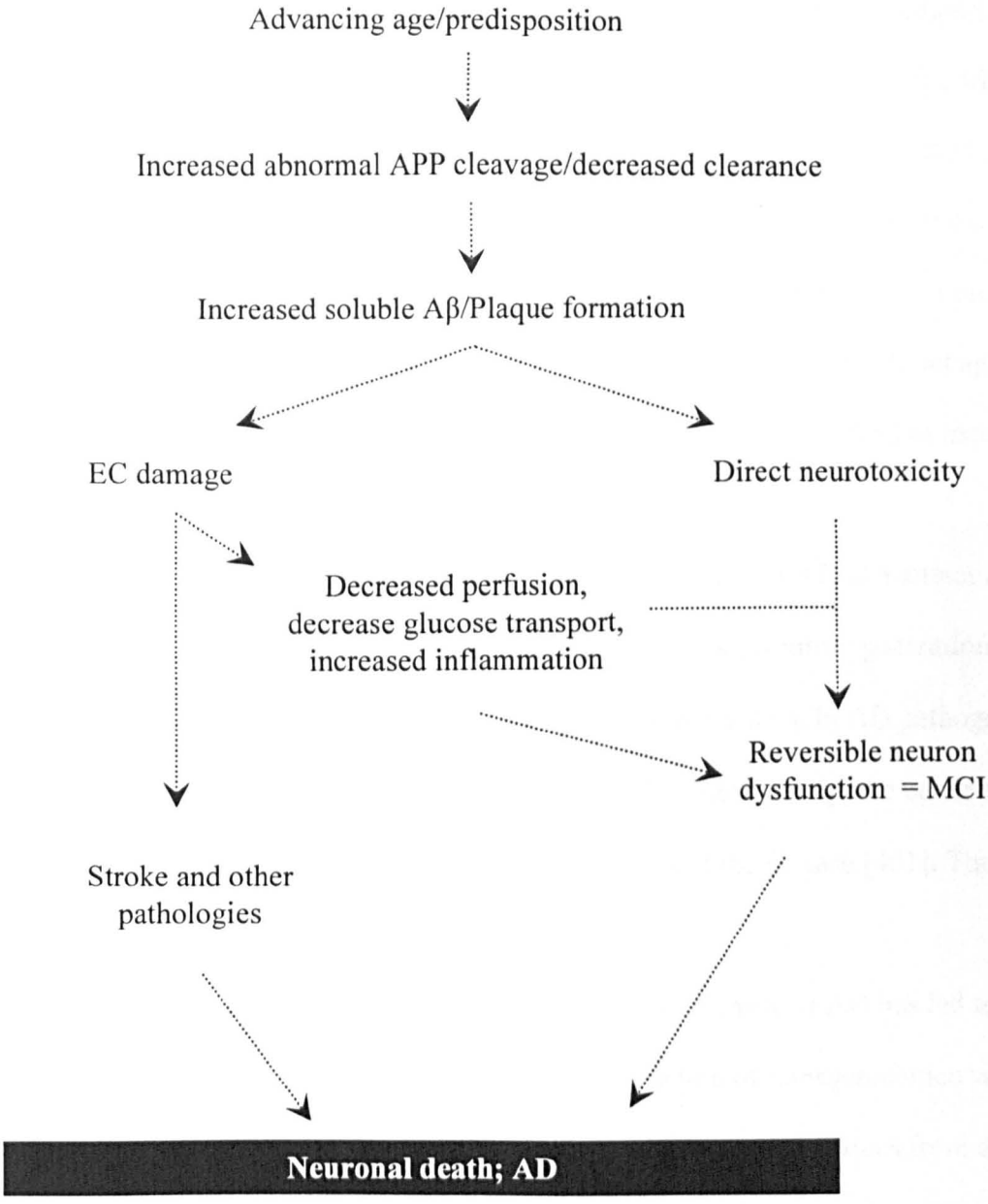

Figure 1.10 Aβ synergistic endothelial and neuronal toxicity hypothesis. Aβ production can lead to BEC damage, which in combination with neuronal cell death leads to AD [419].

1.2.7 Current therapies for AD

The only two current routine treatments for AD are based on strategies to prolong ACh signalling and prevent excitotoxicity. Cholinesterase inhibitors (targeting enzymes that degrade ACh, AChEI) were the first FDA-approved treatments for AD. These include tacrine, donepezil, rivastigmine and galantamine. Birks [445] has recently evaluated the results of 10 randomised double-blind placebo-controlled AD trials with donepezil,

rivastigmine and galantamine, and concluded that whilst they improved cognitive function, none of the effects were large. This is in agreement with other clinical trials, which demonstrate a slight improvement of symptoms [446, 447] or delayed onset in AD [448]. Treatment of mild cognitive impairment, a condition where there is cognitive or memory impairment that does not interfere with daily function and might represent a pre-clinical AD stage, with AChEI does not alter the conversion to AD [449]. The direct application of nicotine to AD patients does not improve memory function, but can lead to increased attention span [301].

The only other FDA-approved drug for the treatment of AD is memantine, a low affinity N-Methy-D-aspartate (NMDA) receptor antagonist. Neurodegeneration as a result of excess glutamate activity, is considered a possible mechanism in AD pathogenesis, and so mementine was approved for AD treatment [450]. Unfortunately, the benefits only appear marginal in AD and only to those in late stages of the disease [451]. Therefore there is a need to develop new AD treatments.

More recently, the assumption that Aβ is the root cause of AD has led to the design of vaccine strategies for the treatment of AD. Vaccination of transgenic mice with Aβ 1-42 or peptide fragments has shown great promise in the removal of plaques from the brain [452-460]. Schenk *et al* [456] immunised AD transgenic mice with Aβ 1-42 both before and after the onset on Aβ plaque formation and found the near-complete reduction in plaque deposits and astrocyte activation. Sigurdsson *et al* [458] have demonstrated that immunisation of transgenic mice which express the Swedish APP mutation (Tg2576), with an Aβ homologous peptide which does not form fibrils can reduce cortical and hippocampal Aβ levels by 89 % and 81 % respectively. In a follow up study, this group have observed improved cognition in Tg2576 mice possibly through IgM-mediated peripheral clearance [457]. Therefore immunisation not only clears Aβ plaques but also improves cognition in transgenic models. Morgan *et al* [455] used Aβ 1-42 with Freunds' complete adjuvant (inactive nitrobacteria) for immunisation in an APP/PS1 transgenic

mouse model. Using a water maze test, these authors demonstrated superior working memory compared to controls. Nasal immunisation using Aβ peptides can also result in the reduction of Aβ burden [454, 459]. Passive immunisation can also clear Aβ plaques. Bard *et al* [452] peripherally administered mice antibodies against Aβ or commercially available Aβ antibodies to an APP transgenic mouse model and reported reduction in amyloid burden in the cortex. The clearance they observed was via a Fc receptor mediated microglial phagocytosis, an effect that has been described by other research groups [460].

The advantageous effects of vaccination in transgenic models led to the clinical trial of a vaccine containing pre-aggregated Aβ 1-42 called AN1792 (reviewed in [461]). A phase 2 trial was conducted on 372 patients and unfortunately had to be stopped due to development of acute meningoencephalitis in 6 % of the patients, possibly due to over-activation of the Th1 mediated response. From autopsies of some of the trial participants, there was extensive clearance of amyloid plaques and this was associated with microglial phagocytotic activity; however amyloid deposition in the cerebral vessel walls and NFT remained. There was also very little evidence for any improvement in cognition. The relative failure of this trial might be related to the possibility that vaccination needs to start before the development of clinical pathology, and future vaccination studies are underway which should provide a clearer picture for AD treatment. There may also be a need however, to identify areas of treatment which can prevent the signalling of Aβ to immediately protect the vasculature and neurones in AD patients.

1.3 *In vitro* models to study Aβ effects on cellular function

Much information has been gained on the effect of Aβ using cell cultures to investigate AD pathogenesis. These include primary rodent [343] and human [342] neuronal cultures, stable neuroblastoma cell lines [353], microglial cells [462], primary human BECs [389] and BECs from other species [463]. Typically, dissolved Aβ peptides

have been added to the cell cultures to observe the effects on cell viability, signalling molecules and transport. The most commonly used Aβ fragments are Aβ 1-40 and Aβ 1-42 although in some cases an Aβ 1-40 or Aβ 1-42 isoform containing FAD mutation(s) is also used [464]. Smaller fragments of the Aβ peptide are also used in *vitro*. The most common is a fragment containing the amino acids 25-35 of full length Aβ. It has been proposed that Aβ 25-35 represents a biologically active region of the Aβ molecule [465]. Unlike full length Aβ, Aβ 25-35 forms β-sheet fibrils and aggregates immediately on dissolution and retains Aβ toxicity to neuronal cell cultures [466, 467]. However, fragments of Aβ may not behave as full length Aβ, in terms of their physical structure and ability to bind to receptors. Pre-aggregated Aβ is also frequently added to cell culture systems, and more recently, on the basis of observations in AD patients, soluble oligomers have been used [356, 357, 362]. A drawback of using these species is that it is not currently known what particular Aβ oligomers(s) is/are predominant in AD, or whether the synthetic oligomer(s) obtained *in vitro* correspond to the *in vivo* species.

1.3.1 An immortalised human brain endothelial cell for BBB study

In terms of studying Aβ effects on BEC function, non-BECs, and primary human BECs cultures have been used. A major driving force behind this study was to use BECs of human origin. Primary hBECs are phenotypically unstable and after a limited passage number undergo cellular senescence. The supply of human tissue is also limited and the use of primary human BECs in detailed experimentation is not feasible. A limited number of immortalised hBECs [468-472] are described in the literature. However, none are fully described with respect to the specific BEC phenotype. A major exception to this is the immortalised hBEC line referred to as hCMEC/D3 [473]. The hCMEC/D3 cell line was produced by lentiviral transduction of isolated human BECs from a female epileptic patient with the catalytic subunit of human telomerase (hTERT) and the SV40 large T antigen.

hTERT acts to prevent telomere shortening whilst SV40 large T antigen is an oncogene capable of transforming cell lines. hCMEC/D3 cells are utilised by an increasing number of laboratories worldwide [263, 474-481] as they retain most of the unique properties of the BBB. hCMEC/D3 cells grow to confluent monolayers and express TJ proteins, adhesion molecules, chemokine receptors and ABC transporter proteins.

P-gp and BCRP functional expression by hCMEC/D3 cells has been demonstrated using substrate uptake experiments. Intracellular rhodamine 123 levels, a fluorescence substrate of P-gp, are increased by co-incubation with a P-gp inhibitor (PSC833). Functional BCRP expression has also been demonstrated by assessing intracellular levels of ^{3}H daunorubicin (substrate for P-gp, MRP-1 and BCRP) in the presence and absence of KO-143 (BCRP inhibitor). hCMEC/D3 cells display restricted permeability to a variety of drugs (e.g. vinblastine and colchicine), in good agreement with *in vivo* perfusion studies in rats or mice. hCMEC/D3 cells are also highly restrictive with regards to FITC-dextran (a paracellular marker) of different sizes (4, 40, 70 kDa), inulin and sucrose permeability when compared to primary bovine BECs and rat BECs. For example, the permeability of the hCMEC/D3 cells to ^{14}C-sucrose is 1.65×10^{-3} cm/min, which although higher, is similar in value to a co-culture model of bovine BECs and astrocytes (0.75×10^{-3} cm/min) [473]. The only major discrepancy of hCMEC/D3 cells with regards to the *in vivo* situation is ionic permeability. The trans endothelial electrical resistance (TEER) of hCMEC/D3 cells, when grown on filters is in the range of 30-40 $\Omega.cm^2$, much lower than rat and porcine cell lines and BECs *in vivo*. Therefore, hCMEC/D3 cells do not form a restrictive barrier to ions.

hCMEC/D3 cells are currently the best characterised and most widely studied hBECs cell line. They retain many unique properties of the BBB and are therefore the most suitable *in vitro* tool for human BBB study.

1.4 Aims

The BBB may represent an important aspect of AD pathology. ABC transporters at the BBB may act to transport Aβ out of the brain, or to protect the brain from blood-borne Aβ peptides. To date, there are no experiments which have investigated the significance of P-gp and BCRP mediated Aβ transport by hBECs. In AD, a leaky BBB and decreased brain glucose uptake could be the result of a dysfunctional BBB. Increased levels of Aβ could in principle underlie many of these alterations. The aims of this study were:

1) To characterise the functional expression of P-gp and BCRP by hCMEC/D3 cells at the protein level and using a functional assay.

2) To investigate the role of P-gp and BCRP in Aβ transport by hCMEC/D3 cells using inhibitors for each transporter.

3) To study the effects of Aβ on the expression of TJ and other transporter proteins by hCMEC/D3 cells.

4) To determine the signalling or molecular pathways responsible for the changes found in aim 3.

Chapter 2

Characterisation of functional P-gp and BCRP expression by hCMEC/D3 cells

Abstract

The aim of the work described in this study was to investigate the expression of P-gp and BCRP by hCMEC/D3 cells. P-gp and BCRP expression by hCMEC/D3 cells was confirmed by western blotting, flow cytometry and immunocytochemistry. The expression of P-gp was stable between passages 23 and 38 and whilst primary isolated hBEC P-gp expression was ~ 30 % higher than that of hCMEC/D3 cells, the differences in P-gp levels were not statistically significant. Using differential detergent fractionation, P-gp was found to be associated with a membrane/organelle fraction. Immunogold staining indicated that P-gp is expressed at a higher level on the apical as opposed to basolateral membrane. Functional P-gp expression was confirmed using a rh123 efflux assay. rh123 efflux from preloaded hCMEC/D3 cells was time-dependent and inhibited by the P-gp inhibitors vinblastine and tariquidar but not by the BCRP inhibitor FTC. The results demonstrate that hCMEC/D3 cells express functional P-gp, located mainly on the apical membrane and therefore represent a suitable model to investigate Aβ transport across hBECs *in vitro*.

2.1 Introduction

ABC transporters at the BBB prevent the entry of unwanted endogenous signalling molecules and toxic xenobiotics into the brain (reviewed in [171, 172]). P-gp is the most extensively studied ABC transporter at the BBB, both *in vitro* and *in vivo*, and appears to prevent a broad range of lipophilic substances from entering brain tissue including many therapeutic drugs in use today (reviewed in [171, 172, 176, 186]). The function of BCRP at the BBB is not as extensively investigated as P-gp. However, some BCRP and P-gp substrates overlap and both play an important role in the protection of the brain from unwanted blood-borne molecules, with the undesirable effect of excluding therapeutic drugs (see Figure 1.4 for a comprehensive list).

P-gp expression has been described on the luminal membrane of rat brain capillaries [210, 482], isolated mouse BECs [211] and human brain microvessels [212, 483], although recently the polarised distribution of this transporter has been called into question [213]. Using EM techniques, Bendayan *et al* [213] have observed enhanced abluminal expression of P-gp in rat BECs. Further conflicting evidence on P-gp expression was described by Pardridge *et al* [209], who, using the antibody MRK16, reported no BEC P-gp staining but astrocytic expression in human brain sections. In subsequent studies, this group found P-gp co-localised with GFAP in human [208] and rhesus monkey brain tissue sections [484].

In vivo data supports the notion of a barrier function for P-gp at the BBB. Mice lacking either mdr1a or combined mdr1a/b genes display enhanced brain accumulation of many P-gp substrates, including verapamil, indinavir, vinblastine and morphine, compared to wild type control mice (reviewed in [171, 172, 216]). In addition, Drion *et al* [217] have demonstrated that treatment of rats with PSC-833 (a P-gp inhibitor) increases the brain concentrations of colchicine and vinblastine by 8.4 and 9.1, respectively.

BCRP expression has been observed on the luminal membrane of isolated human brain microvessels [229] and, like P-gp, acts to prevent certain substrates from entering the

brain. This is evident as BCRP inhibition causes enhanced brain uptake of prazosin and mitoxantrone in mdr1a(-/-) mice [228]. Youdim *et al* [231] have also demonstrated increased quercetin accumulation in the brain of rats by BCRP inhibition.

The focus of this study was to investigate the function of P-gp and BCRP in hBECs and so to further aid the understanding of substrate transport at the BBB. Whilst *in vivo* studies represent an important data source for evaluation of ABC transporter function at the BBB, they are highly costly and may be problematic due to species differences between the animal models and humans. For example, the comparison of P-gp expression by Bendayan *et al* [213] at the abluminal BEC membrane in rats, is in contrast to the data from mouse and human studies. It is useful therefore, to investigate the ability of ABC transporters to efflux a known/unknown substrate *in vitro* using BECs of human origin and to compare across species. Multiple cell lines are available for the study of P-gp from different tissues and species (Table 2.1). In terms of hBECs, primary and immortalised BEC cultures have been investigated. Human primary cell cultures are neither stable over passage 5 nor readily available and are therefore not suited for routine high throughput studies. There are only two extensively described immortalised hBEC cell lines; hCMEC/D3 [473] and BB19 [470] cells. The BB19 cell line has been shown to express P-gp, BCRP and MRP family members using mRNA analysis, immunostaining and western blotting, whilst the functionality of P-gp in this cell line has been demonstrated by increased uptake of daunomycin in cells treated with verapamil [470]. However, the BB19 cell line has not been used in any subsequent studies and is not fully characterised with respect to characteristic BEC protein expression. In contrast, the hCMEC/D3 cell line has been extensively characterised with respect to BEC-specific protein expression and permeability to paracellular tracers and has been used in multiple follow up studies [188, 474-476, 480, 481, 485, 486]. hCMEC/D3 cells express TJ proteins and are restrictive to molecules over 4 kDa in molecular weight. hCMEC/D3 cell P-gp expression has been demonstrated using western blotting and mRNA analysis, whilst P-gp function was also

shown using a fluorescent P-gp substrate, rhodamine 123 (rh123), and the P-gp inhibitor PSC-833 [473]. PSC-833 was demonstrated to increase the net influx of rh123, indicating active P-gp expression. Functional BCRP expression by hCMEC/D3 cells has also been demonstrated as the BCRP inhibitor KO143 increased the accumulation of ^{3}H daunorubicin in these cells. Given the limited availability of primary cells and their poor stability over passage number, hCMEC/D3 cells are the most suitable available option to study P-gp function in cells from human origin which retain characteristics of primary BECs.

The aim of this study was to confirm and investigate functional P-gp and BCRP expression by hCMEC/D3 cells, so that the role of these transporters in Aβ transport could be addressed in further studies. Comparisons were made with primary hBECs and the results demonstrate hCMEC/D3 cell suitability for investigating P-gp substrate interactions using the 3rd generation P-gp inhibitor tariquidar [487, 488], and the P-gp competitive substrate vinblastine.

Source	Type	Cell line example	Reference
Kidney epithelium	Madin-Darby canine kidney cells wild type and transfected with MDR1 gene.	MDCK II, MDCK II -MDR1	[489, 490]
	Porcine cells wild type and transfected with MDR1 gene.	LLC-PK1, LLC-PK1-MDR1	[183] [491]
Intestinal epithelium	Human colon carcinoma cell lines.	Caco-2, LS180	[492] [493]
Lung epithelium	Primary human bronchiolar and alveolar cells.	-	[494, 495]
	Primary porcine and rat pulmonary cells.	-	[495, 496]
	Human lung adenocarcinoma cells.	A549 NCI-H460	[497-499]
Hepatocytes	Primary rat and human cells.	-	[500, 501]
	Liver carcinoma cell lines.	HEP G2	[502]
Embryo	Immortalised syncytiotrophoblast cells.	TR-TBTs	[503]
Brain endothelium	Primary rat, human, mouse, porcine cells.	-	Reviewed [46, 172, 504]
	Immortalised rat, bovine, mouse, porcine, human cells.	Rat; RBE4, GPNT, GP8, rBCEC4.	Reviewed [505]
		Mouse; TMBB4 MBEC, bEnd.3, bEnd. 5.	[211, 506-508]
		Porcine; PBMEC.	[509, 510]
		Bovine; SV-BEC, t-BBEC-117.	[20, 511]
		Human; BB19, hCMEC/D3.	[470, 473]

Table 2.1. Summary of cell lines used for investigation of P-gp function. Multiple cell lines have been developed for the study of P-gp function, including kidney, intestinal and lung epithelial cells and ECs from the brain.

2.2 Methods

2.2.1 Culture medium

hCMEC/D3 cells were cultured in endothelial growth medium (EGM-2, Lonza, Wokingham, UK) supplemented with 2.5 % foetal bovine serum (FBS), ascorbic acid, gentamycin sulphate, hydrocortisone and ¼ volume of the supplied growth factor supplements [vascular endothelium growth factor (VEGF), epidermal growth factor (EGF), insulin-like growth factor 1 (IGF-1) and human basic fibroblastic growth factor (bFGF)]. Cambrex have optimised the composition of EGM-2 to induce endothelial cell proliferation and do not disclose the concentrations of the supplements. Primary hBECs were grown in EGM-2 media to which a full volume of the supplied growth factor supplements were added.

2.2.2 Growth surface preparation

Both primary hBECs and hCMEC/D3 cells were grown on tissue culture plastic flasks (Greiner, Gluocestershire, UK) coated with collagen type 1 from calf skin (Sigma-Aldrich, Dorset, UK). The collagen stock solution of 0.1 % w/v was diluted 1 in 20 in Hank's balanced salts solution (HBSS) (Sigma-Aldrich, Dorset, UK) and left for 1 h at room temperature (RT) on the plastic surface. The flasks were then washed once with HBSS and filled with EGM-2 medium in preparation for cell culture. For experiments that used transwell polyester membrane inserts (0.4 μm pore, 12mm diameter, Corning Costar, Buckingham, UK), the filters were coated with collagen and fibronectin which are required for optimal for hCMEC/D3 cell growth. For this, the filters were incubated for 1 h in collagen, washed in HBSS and incubated for 1 h with a 5 μg/ml solution of fibronectin from human plasma (Sigma-Aldrich, Dorset, UK).

2.2.3 hCMEC/D3 and primary human brain endothelial cell (hBEC) culture maintenance

hCMEC/D3 cells were grown until confluent (~ 1 x 10^5 cells/cm^2) on collagen-coated flasks at 37°C (5 % CO_2), with the culture medium changed every 2-3 days. Primary hBEC were typically grown to 90 % confluence, due the difficulty in trypsinising these cells at full confluence. To split cell cultures, both hCMEC/D3 cells and primary hBECs were washed in HBSS without Ca^{2+} and Mg^{2+} [HBSS w/o Ca^{2+} Mg^{2+} (Sigma-Aldrich, Dorset, UK)] at 37°C for 1-5 min and then incubated with 0.25% w/v porcine trypsin and 0.02 % w/v ethylene diamine tetraacetic acid (EDTA) (Sigma-Aldrich, Dorset, UK) at 37°C until detached. EGM-2 was then added to neutralise trypsin activity and cells were split at a ratio of 1:5 onto collagen-coated tissue culture flasks. For all experiments, hCMEC/D3 cells between passage (p) 23 and 33 were used, unless stated otherwise, whilst primary hBEC were used up to p4.

2.2.4 Isolation of primary hBECs

Solution A: HBSS w/o Ca^{2+} Mg^{2+} containing 10 mM HEPES (Sigma-Aldrich, Dorset, UK), 50 U/ml penicillin, 50 ug/ml streptomycin (Invitrogen, Paisley, UK), 2.5 μg/ml amphotericin B (Invitrogen, Paisley, UK) and 0.4 % w/v BSA (Sigma-Aldrich, Dorset, UK). Adjusted to pH 7.4 by eye and sterile filtered through 0.22 μm filter.

25 % w/v BSA: BSA dissolved in solution A, sterile filtered through 0.8 μm and 0.22 μm filters.

Collagenase/dispase: 1 mg/ml collagenase/dispase solution (Roche, West Sussex, UK) supplemented with 10 μg/ml DNase (Sigma-Aldrich, Dorset, UK) and 0.147 μg/ml N-p-tosyl-L-lysine chloromethyl ketone hydrochloride (Sigma-Aldrich, Dorset, UK).

Percoll gradient: Prepared immediately prior to use in an ethanol-sterilised (20 min, 70% ethanol) and blocked (solution A, 10 min) dupont tube. A 50% percoll solution (Sigma-

Aldrich, Dorset, UK) in HBSS was added to the dupont tube and centrifuged for 1 h at 25,000 xg, 4°C.

In procedures approved by ethical committiees at both Kings College London and The Open University, human brain tissue was obtained with written consent from patients undergoing cerebral cortical lobectomies, conducted at Kings College Hospital to relieve medically intractable seizures. The isolation of hBECs was carried out within 24 h post operation based on the protocol by Hughes and Lantos [512], and unless stated otherwise, all steps were carried out on ice or at 4°C.

The brain tissue was placed in a sterile petri dish and the meniges removed using autoclaved forceps. The tissue was then placed in 1 ml of solution A and cut into small pieces using a scalpel blade. Tissue fragments were then centrifuged at 300 xg for 10 min in 10 ml of solution A, the pellet resuspended in 15 ml of collagenase/dispase solution and incubated for 1 h at 37°C. The digest was then centrifuged (300 xg, 5 min, 4°C) and the resulting pellet re-suspended in 5 ml of solution A, using initially a glass pasteur pipette and subsequently a heated end glass pasteur pipette. The digest was then centrifuged (300 xg, 5 min, 4°C).

The capillaries were then isolated using density dependent centrifugation in 25% BSA. Brain tissue fragments were re-suspended in 20 ml of 25 % BSA solution and centrifuged for 15 min at 1000 xg at 4°C. The myelin plug was removed by gently turning the tube and poured swiftly into a separate tube leaving the initial tube upturned to prevent any BSA re-suspending the capillaries, since prolonged BSA can become toxic. The myelin was then resuspended and centrifuged a further couple of times (15 min, 1000 xg, 4°C) to increase the yield of pelleted capillaries. Capillary pellets were then pooled in solution A and centrifuged (300 xg, 5 min, 4°C). The capillaries then underwent a further 1 h digestion in 5 ml of collagenase/dispase for 1 h at 37°C.

A Percoll gradient was used to separate the capillary fragments from the red blood cells and surrounding cell contaminants. Pelleted capillary fragments (300 xg, 5 min, 4°C) were resuspended in 1.5ml of solution A and pipetted carefully on top of 7 ml of a prepared Percoll gradient and centrifuged at 1000 xg for 10 min. Three layers formed (the middle containing BECs), and each layer was carefully pipetted out into separate tubes containing 10 ml of solution A and centrifuged (300 xg, 5 min, 4°C). The resulting pellets were re-suspended in 10 ml of 1:1 solution A and EBM-2 medium, centrifuged (300 xg, 5 min, 4°C) and resuspended in 5 ml medium containing amphotericin B (2.5 μg/ml) and placed in collagen-coated 25 cm^2 tissue culture flasks. Each layer of the Percoll gradient was collected to increase the EC yield, as EC can sometimes reside in the top and bottom fractions. After 48 h the culture medium was replaced with fresh culture medium containing 0.5 μg/ml puromycin (Sigma-Aldrich, Dorset, UK), which was left in the culture medium for 5 days in order to selectively inhibit the growth of contaminating cells that lack P-gp expression and are therefore vulnerable to intracellular puromycin accumulation. The medium was changed every 48 h.

2.2.5 SDS-PAGE and western blotting

Lysis buffer: RIPA buffer (Sigma-Aldrich, Dorset, UK) containing 1mM phenylmethanesulfonyl fluoride [PMSF (Sigma-Aldrich, Dorset, UK)], 10 ng/μl of leupeptin (Sigma-Aldrich, Dorset, UK), pepstatin A (Sigma-Aldrich, Dorset, UK) and aprotinin (Sigma-Aldrich, Dorset, UK).

Laemmli's buffer reducing 4 X: 0.01 % w/v bromophenol blue (Sigma-Aldrich, Dorset, UK), 15 mg/ml D,L- dithiothreitol [DTT (Sigma-Aldrich, Dorset, UK)], 40 % v/v glycerol (Sigma-Aldrich, Dorset, UK), 8 % w/v sodium dodecyl sulphate [SDS (Sigma-Aldrich, Dorset, UK)] in 250 mM tris/HCl pH 6.8.

Running gel: 10 % v/v Protogel [30 % acrylamide, 0.8 % methylene bis-acrylamide, (National diagnostics, North Yorkshire, UK)], 0.1 % w/v SDS, 0.37 M tris/HCl pH 8.8, 0.05 % v/v tetramethyl-ethlenediamine [TEMED (Sigma-Aldrich, Dorset, UK)] and 0.1 % w/v ammonium persulphate [APS (Sigma-Aldrich, Dorset, UK)].

Stacking gel: 5 % v/v Protogel, 0.1 % w/v SDS, 0.12 M tris/HCl pH 6.8, 0.05 % v/v TEMED, and 0.1 % w/v APS.

Running Buffer: 25 mM Tris, 192 mM glycine, 0.01% SDS in deionised water [prepared from 10 x stock (National diagnostics, North Yorkshire, UK)].

Transfer buffer: 25 mM Tris and 192 mM glycine, [prepared from 10 x stock (National diagnostics, North Yorkshire, UK)] with 20 % v/v ethanol in deionised water.

Blocking buffer: 0.2 % v/v tween 20 (Sigma-Aldrich, Dorset, UK), 5 % w/v fat-free dried milk dissolved in PBS.

Washing solution: 0.2 % v/v tween 20 dissolved in PBS.

Full range molecular weight marker: Rainbow marker (Amersham, Buckinghamshire, UK).

Stripping solution: 2 % w/v SDS, 0.0625 M Tris pH 6.8, 0.008 % v/v β-mecaptoethanol.

hCMEC/D3 cells (p23) were grown to confluence (total ~ 1 x 10^7 cells) in a 75 cm^2 collagen-coated flask and left for 2 days. hCMEC/D3 cells were then detached and passed 1 in 5 into another 75 cm^2 flask. The remaining cells were washed twice in PBS and resuspended in 500 µl of lysis buffer. The suspension was left on ice for 5 min and then sonicated on ice 3 times for 5 seconds (Soniprep 150, MSE, London, UK). The cell lysate was then centrifuged at 8000 xg for 5 min at 4°C and the supernatant collected. This procedure was repeated for the cells every 3rd passage up to p44.

The protein concentration of the samples was calculated using the detergent compatible *(DC)* protein assay (Biorad, Hertfordshire UK), using BSA as a standard. For each lane of the western blotting gel, 20 µg of total protein in 1 x Laemmli' s buffer was

loaded on 10 % polyacrylamide resolving gels with a 5 % stacking gel. Prior to loading, the samples were denatured by heating at 95 °C for 5 min. The proteins were resolved on the gel by applying a 100-150 V potential until the dye front reached the end of the gel. Following electrophoresis, proteins were transferred onto nitrocellulose membranes (Amersham, Buckinghamshire, UK) using a wet blotting system run at a constant current of 0.15 A overnight at 4°C, with transfer buffer. Post-transfer, the nitrocellulose membranes were incubated with blocking buffer for 1 h at RT and incubated over-night at 4°C with 500 ng/ml of C219, an anti-P-gp antibody [mouse monoclonal IgG_{2a}, (Abcam, Cambridgeshire, UK)]. Membranes were then subjected to six 10 min washes in washing solution and a horse-radish peroxidise (HRP)-conjugated anti-mouse IgG secondary antibody [diluted 1/20000 (Pierce Biotechnology, Cheshire, UK)] was added for 1 h at RT. The membranes were then washed five times for 10 min with washing solution, followed by a 10 min wash in PBS. The membrane were then developed using an enhanced chemiluminescence (ECL) western blotting detection reagents system (Amersham, Buckinghamshire, UK), exposed to films (Amersham, Buckinghamshire, UK) and films were developed with an X-Omat 1000 automatic processor (Kodak, New York, USA). Film exposure times were adjusted to ensure adequate signal development.

In order to check for equal loading, the nitrocellulose membrane was subjected to a harsh stripping procedure. Membranes were placed in stripping buffer for 40 min at 50°C and washed for 30 min with frequent changes of washing solution. The membrane was then blocked as described above and re-probed using an anti-actin antibody [1 μg/ml, mouse monoclonal IgG_1, (Sigma-Aldrich, Dorset, UK)]. The signal intensities of the bands on the films were analysed using image J software and P-gp expression was normalised to actin expression.

2.2.6 Flow cytometry analysis

Permeabilisation/blocking buffer: 3 % v/v normal goat serum [NGS, (Sigma-Aldrich, Dorset, UK)], 0.1 % v/v triton X-100 (Sigma-Aldrich, Dorset, UK) in PBS.

hCMEC/D3 cells or primary hBECs were grown to confluence in 6 well tissue culture plates (total ~ 1 x 10^6 cells per well), detached, centrifuged (300 xg, 5 min, 4°C) and fixed in 4 % w/v *p*-formaldehyde (PAF, BDH, Dorset, UK) in PBS for 10 min at RT. After one wash in PBS, cells were incubated for 30 min in permeabilisation buffer, which contained 3 % NGS to prevent non-specific binding of antibodies. The cells were subsequently counted and 0.5 x 10^6 cells per treatment were incubated overnight at 4°C with 50-100 µl of permeabilisation buffer containing a primary antibody or isotype-specific control at a concentration of 5 µg/ml. The antibodies used were anti-BCRP BXP-21 [mouse monoclonal IgG_{2a}, (Merck, Nottinghamshire, UK)] or anti-P-gp JSB-1 [mouse monoclonal IgG_1, (Abcam, Cambridgeshire, UK)]. The isotype-specific controls were mouse IgG_{2a} (Sigma-Aldrich, Dorset, UK) or mouse IgG_1 (Sigma-Aldrich, Dorset, UK) as appropriate. JSB-1 rather than C219 was used for flow cytometry staining of P-gp as it proved more suitable for this staining technique.

After incubation with the primary antibody, the cells were washed three times in PBS and resuspended in permeabilisation buffer containing 10 µg/ml of a fluoresceinisothiocyanate (FITC) - conjugated goat anti-mouse IgG antibody (Chemicon, Hampshire, UK). After two final washes with PBS, the cells were suspended in 500 µl PBS and analysed using a FACSCalibur flow cytometer with Cellquest software [488 nm $\lambda_{excitation}$, 530 nm $\lambda_{emission}$, (Becton Dickinson, Oxfordshire, UK)]. For each sample the median fluorescence of 10,000 cells was determined.

2.2.7 Differential detergent fractionation

In order to investigate the localisation of P-gp, hCMEC/D3 whole cell lysates were separated into cytosolic, membrane/organelle, nuclear and cytoskeletal fractions using differential detergent fractionation as described by Ramsby *et al.* [513].

Extraction buffer 1 (EB1): 10 mM piperazine- 1, 4'-bis (2-ethanesulphonic acid) [PIPES, (Sigma-Aldrich, Dorset, UK)] pH 6.8, containing 300 nM sucrose (Sigma-Aldrich, Dorset, UK), 100 mM sodium chloride [NaCl (Sigma-Aldrich, Dorset, UK)], 3 mM magnesium dichloride [$MgCl_2$ (Sigma-Aldrich, Dorset, UK)], 5 mM [EDTA (Sigma-Aldrich, Dorset, UK)], 1.2 mM phenylmethylsulphonyl fluoride [PMSF (Sigma-Aldrich, Dorset, UK)] and 0.01 % w/v digitonin (Sigma-Aldrich, Dorset, UK).
Extraction buffer 2 (EB2): 10 mM PIPES pH 7.4, containing 300 mM sucrose, 100 mM NaCl, 3 mM $MgCl_2$, 3 mM EDTA, 1.2 mM PMSF and 0.5 % v/v triton X-100.
Extraction buffer 3 (EB3): 10 mM PIPES pH 7.4, containing 10 mM NaCl, 1 mM $MgCl_2$, 1.2 mM PMSF, 0.5 % v/v triton X-100, 1 % v/v tween-40, 0.5 % w/v sodium deoxycholate (Sigma-Aldrich, Dorset, UK).

hCMEC/D3 cells were grown until confluence in a 75 cm^2 flask (1 x 10^7 cells), detached by trypsinisation, washed once in HBSS and lysed in 250 µl of EB1 buffer. The whole cell lysate was incubated on ice for 10 min with occasional inversion to ensure solubilisation. After centrifugation (500 xg, 10 min, 4°C), the supernatant was collected (cytosolic protein fraction) and the pellet resuspended in 250 µl of EB2 buffer. The whole cell lysate was then incubated on ice for 20 min (with occasional inversion), centrifuged (5000 xg, 10 min, 4°C), and the supernatant collected (membrane/organelle fraction). The remaining pellet was resuspended in 125 µl of EB3, incubated on ice for 10 min and centrifuged (7000 xg, 10 min, 4°C). The supernatant contains the nuclear proteins, whilst

the pellet contains cytoskeletal proteins. The pellet was dissolved in 250 µl of 1 x Laemmli's buffer.

Laemmli's buffer was added to each fraction collected and the samples denatured at 95 °C for 5 min. Samples were then resolved using SDS-PAGE and western blotting as described in section 2.2.5. 20 µl of the cytosolic, membrane-organnelle and cytoskeletal fractions and 10 µl of the nuclear fraction were loaded per lane. Antibodies against the transcription factor Sp3 [200 ng/ml, mouse monoclonal IgG_{2a}, (Santa Cruz, California USA)], P-gp (500 ng/ml, C219), BCRP (200 ng/ml, BXP-21,) and actin (1 µg/ml), were used for western blotting detection as described in section 2.2.5. The intensity of the signals were analysed using image J software. For each protein, the intensity of the signal corresponding to each fraction (cytosolic, membrane/organelle, nuclear or cytoskeleton) was expressed as a percentage sum of the signals for all the fractions.

2.2.8 Immunocytochemistry

Permeabilisation/blocking buffer: 3 % v/v NGS, 0.1 % v/v triton X-100 (Sigma-Aldrich, Dorset, UK) in PBS.

hCMEC/D3 cells were grown to confluence on collagen-coated Labtek chamber slides (Nunc Scientific laboratory supplies, Nottinghamshire, UK), washed in PBS and fixed in 4 % PAF for 10 min. After three washes (PBS, 5 min each) permeabilisation/blocking buffer was added to each chamber for 30 min. Anti P-gp (JSB-1), BCRP (BXP-21) or isotype controls (IgG_1 or IgG_{2a} respectively) were added to the fixed cells at 5 µg/ml overnight at 4°C. After three 10 min washes in PBS, a FITC-conjugated goat anti-mouse IgG secondary antibody (as described in section 2.2.6) was added for 1 h at RT. After three further washes in PBS, a drop of 4',6-diamidino-2-phenylindole (DAPI) mounting media (Dako, Cambridgeshire, UK) was added for 5 min

and then, after a final wash in water, the slides were mounted with a glass coverslip and viewed with a fluorescent microscope (Olympus BX61,Olympus, Hertfordshire, UK).

For imaging via confocal microscopy, hCMEC/D3 cells were grown to confluence on collagen- and fibronectin- coated transwell polyester membrane inserts (0.4 μm pore, 12mm diameter, Corning Costar, Buckingham, UK) and stained as above with the exception that instead of DAPI, 5 μM DRAQ5 (Biostatus, Cambridegshire, UK) was added with the secondary antibody to stain nuclear DNA. hCMEC/D3 cells were then viewed with a confocal microsope, (Leica DMIRBE, Leica, Buckingham UK), taking XY and Z cross sections over a selected field to reconstruct a three dimensional image using Volocity software (Improvision, Coventry, UK).

2.2.9 Transmission electron microscopy combined with immunogold labelling

Phosphate buffer (PB): 0.018 M $NaH_2PO_4.H_2O$ (VWR, Leicestershire, UK), 0.082 M Na_2HPO_4 (VWR, Leicestershire, UK).

Paraformaldehyde-lysine-periodate fixative (PLP): 2 % w/v PAF, 0.01 M sodium metaperiodate (Sigma-Aldrich, Dorset, UK), 0.075 M lysine monohydrochloride (Sigma-Aldrich, Dorset, UK).

For the detection of P-gp at the ultrastructural level, the method of Bendayan *et al* [213] was followed with technical and experimental help from the EM suite at The Open University. hCMEC/D3 cells were grown to full confluence on collagen- fibronectin-coated transwell polyester membrane inserts (0.4 μm diameter pore, 12 mm diameter width) and left for 2 days. hCMEC/D3 cells were then fixed for 21 h (6 h RT, 15 h 4°C) with PLP. Post fixation, hCMEC/D3 cells were washed twice with PB (1–5 min) cut into 2 mm strips and processed using 'progressive lowering of temperature' with a Leica AFS2 automatic freeze substitution system (Leica, Buckingham UK). This method was used to dehydrate and prevent translocation of the antigen and involves the progressive lowering of

temperature from 0° to -30°C whilst increasing the methanol content of the solution (Table 2.2). hCMEC/D3 cells were infiltrated in the acrylic resin Lowicryl K4M (Agar Scientific, Essex, UK) and polymerised at -30°C under ultra violet (UV) light.

Ultrathin sections of the membrane insert were then cut (80 nm) using a Diatome diamond knife on a Leica ultra-microtome (Leica UCT, Leica, Buckinghamshire UK). The sections were mounted on formvar (Agar Scientific, Essex, UK) coated nickel slot grids, and all reactions were performed using 20 µl droplets on a parafilm lined box lid which was covered during incubation. Non-specific binding was blocked using 1 % w/v ovalbumin (Sigma-Aldrich, Dorset, UK) in 0.01 M PBS for 30 min at RT. Grids were incubated with droplets of anti-P-gp (5 µg/ml, C219, dissolved in PBS) or an isotype matched control (5 µg/ml, $IgG_{2a,}$) antibody overnight at RT in a humidified box. The grids were then washed by transferring from drop to drop (3 x 5 min in PBS), blocked (1 % ovalbumin, 10 min, RT) and incubated with a goat anti-mouse IgG conjugated to 10 nm gold secondary antibody for 2 h at RT (British Biocell International, Cardiff, Wales). The samples were then washed (3 x 5 min, PBS), fixed in 2.5 % w/v glutaraldehyde in PBS (Agar Scientific, Essex, UK), washed (2 x 5 min in PBS, 1 min with deionised water), allowed to air dry and counterstained with 4 % w/v aqueous uranyl acetate (Agar Scientific, Essex, UK) for 15 min. After a final three washes in distilled water the sections of immunolabelled hCMEC/D3 cells were examined using a JEOL JEM 1400 transmission electron microscope (JEOL, Hertfordshire, UK) operating at 80 kv. The images were acquired using an AMT XR60 11 mega pixel digital camera calibrated for magnification such that each image displayed a scale marker. Images of 7.5 µm lengths of membrane were taken every 2-3 frames for a total of 500 µm membrane. For both the apical and basolateral membranes, the number of gold particles within 100 nm was counted in each 7.5 µm length of membrane and expressed as gold particles per 1 µm of membrane.

Reagent	Temperature Start (°C)	Temperature End	Time (h)
30 % MeOH	0	0	0.5
50 % MeOH	0	-10	0.5
75 % MeOH	-10	-20	0.5
100 % MeOH	-20	-30	0.5
100 % MeOH	-30	-30	0.5
25 %K4M:75 % MeOH	-30	-30	1
50 % K4M: MeOH	-30	-30	1
80 % K4M: MeOH	-30	-30	1
K4M	-30	-30	1
K4M	-30	-30	15
K4M	-30	-30	1
K4M	-30	-30	48

Table 2.2. Protocol for progressive lowing of temperature for electron microscopy and immunogold staining. Fixed hCMEC/D3 cells were subjected to this protocol in order to prevent antigen translocation during dehydration and embedding for TEM immunolabelling (K4M: lowicryl K4M).

2.2.10 Methylthiazolyldiphenyl-tetrazolium (MTT) bromide cytotoxicity assay

The cytotoxicity of the P-gp inhibitors tariquidar (a kind gift from Xenova, Berkshire, UK), vinblastine (Sigma-Aldrich, Dorset, UK) and the BCRP inhibitor fumitremorgin C [FTC, (Axxora, Nottingham, UK)] were investigated using a Methylthiazolyldiphenyl-tetrazolium bromide [MTT, (Sigma-Aldrich, Dorset, UK)] toxicity assay.

hCMEC/D3 cells were seeded in 96 well tissue culture plates (3 x 10^4 per well), left for 2 days and the cell culture medium replaced with 100 µl of fresh culture media containing tariquidar (20-600 nM), FTC (0.3-22 µM), vinblastine (0.100 - 40 µM) in vehicle (DMSO or ethanol for vinblastine/FTC and tariquidar, respectively) or medium containing vehicle alone (< 1 % v/v), for either 24 h or 48 h at 37 °C. After the indicated time, 10 µl of MTT (stock 5 mg/ml) was added to each well to give a final concentration of 0.5 mg/ml and the plates left for 4 h at 37 °C. The media was then aspirated and the cells washed twice in PBS. Finally, 200 µl of isopropanol (Sigma-Aldrich, Dorset, UK) was added to lyse the cells and to solubilise precipitated formazan salts, produced by the action

of mitochondrial dehydrogenase in living cells on MTT. After complete solubilisation, the plates were read on a colourimeter (BMG, Offenberg, Germany) at a wavelength of 550 nm.

2.2.11 Rhodamine 123 (rh123) efflux assay

The principles underlying the rhodamine 123 (rh123) efflux assay are depicted in Figure 2.1. hCMEC/D3 cells were grown to confluence in collagen-coated 75 cm^2 flasks, detached, and the cells counted using a haemocytometer. For each test condition, 2.5 x 10^5 cells were used in duplicate. The test conditions for time-dependent efflux were: hCMEC/D3 cells preloaded with rh123 and kept at 4°C, rh123-preloaded hCMEC/D3 cells incubated at 15, 30, 60, 120, 180 and 360 min in the absence or presence of vinblastine, hCMEC/D3 cells that were not preloaded with rh123 in order to later subtract background fluorescence. For each experiment, two aliquots of 3.5 x 10^6 cells were centrifuged at 300 xg for 5 min at 4°C and re-suspended in efflux buffer [RPMI-1640, (Cambrex, Berkshire, UK) containing 1 % w/v BSA] at 4°C. From each aliquot of cell suspension, 2.5 x 10^5 cells were taken and placed on ice for the duration of the experiment (negative control). The remaining cells were then centrifuged (300 xg, 5 min, 4°C), re-suspended at 1 x 10^6/ml in efflux buffer containing 10 μg/ml (22 μM) rh123 (Sigma-Aldrich, Dorset, UK) and incubated on ice for 1 h. Rh123 preloaded cells were washed twice in efflux buffer and redistributed into different tubes according to each treatment. From each repetition, 2.5 x 10^5 cells rh123 preloaded cells were placed at 4°C in efflux buffer, whilst the remaining cells were incubated at 37°C with vinblastine (22 μM) in vehicle, or vehicle only, in efflux buffer. At 15, 30, 60, 120, 180 and 360 min intervals, 2.5 x 10^5 cells were removed and placed on ice/4°C for the duration of the experiment. After all samples had been collected, cells were washed twice in PBS and resuspended in 500 μl PBS. The samples were then read using a FACSCalibur with Cellquest software (488 nm $\lambda_{excitation}$, 530 nm $\lambda_{emission}$) and

the median fluorescence of 10,000 cells per sample recorded. The median fluorescence intensity of the negative control was subtracted from all the other treatments and the data expressed as a percentage of rh123 preloaded cells kept at 4°C. For each experiment the time taken for the fluorescence intensity to decline by 50 % was calculated, by plotting cellular rh123 levels against time, and using cells incubated at 4°C as time = 0 min.

For some experiments, the effects of inhibitors were tested on hCMEC/D3 cells both preloaded with rh123 alone or with an inhibitor and incubated at 37 °C for 1 h. The following inhibitors in vehicle or vehicle only were used; FTC (22 μM), vinblastine (22 μM) or tariquidar (300 nM).

2.2.12 rh123 permeability

The permeability of hCMEC/D3 cells grown on Transwell polyester membrane inserts (0.4 μm pore, 12mm diameter) to rh123 was investigated (Figure 2.2). hCMEC/D3 cells were cultured on collagen- and fibronectin-coated 12 well membrane inserts until confluent and left for 2 days. The cells were then washed with permeability buffer (DMEM, 2 % v/v FCS Sigma-Aldrich, Dorset, UK) and rh123 (22 μM), alone or in the presence of tariquidar (300 nM), vinblastine (22 μM) or FTC (22 μM), was added to the apical chamber (upper). The inserts were then transferred sequentially at 5 min intervals from well to well containing 1.5 ml of transport buffer (+/- appropriate inhibitors) for 30 min. The fluorescence diffusing to the basolateral (bottom) chamber was measured at an excitation wavelength of 485 nm and emission wavelength of 520 nm with a fluorescence plate reader (BMG, Offenberg, Germany). A vehicle control received DMSO (0.1 %) since ethanol had no appreciable difference in the efflux experiment.

Permeability coefficients of the hCMEC/D3 cell monolayers were calculated using the following calculations [473];

$$\text{Cleared volume} = (AUa - AUb)/Fi$$

The cleared volume (in µl/ml) represents the cumulative volume of rh123 solution passing through the cell monolayer at a particular time. AUa is the total fluorescence (arbitrary units) in the basal compartment, AUb is the background fluorescence, Fi is the fluorescence of the initial solution (AU/ml). The cleared volume is plotted against time and the permeability coefficients (P_e in cm/min) for the EC monolayer calculated as ;

$$1/PS = 1/PS_{ef} - 1/PS_f \text{ and } P_e = PS/S$$

PS_{ef} and PS_f correspond to the gradients of the curves for EC grown on filters or filters alone (ml/min). PS is the permeability surface area of the EC monolayer (ml/min) and S is the surface area of the filter. The higher the P_e value the more permeable the EC are to the fluorescent dye.

To investigate the basolateral-to-apical permeability, 1.5 ml rh123 (22 µM) was added to the basolateral chamber of a 12 well plate [+/- tariquidar (300 nM), vinblastine (22 µM) or FTC (22 µM)] and filters containing the appropriate inhibitors placed into the well. The filter was left in place for 30 min and the fluorescence of the apical and basolateral chambers measured. The P_e values were calculated using the assumption that the curve was linear:

$$PS_{ef} = [(AUa - AUb)/Fi] / 30$$

2.2.13 Statistical analysis

All data are represented as means +/- SEM and the number of experiments, n, indicated each time. For each data the statistical significance was calculated using ANOVA followed by Student's t test, comparing each treatment to the control (* $p < 0.05$). For the permeability experiments, a paired t-test was used, as there was an internal control specific for each experiment.

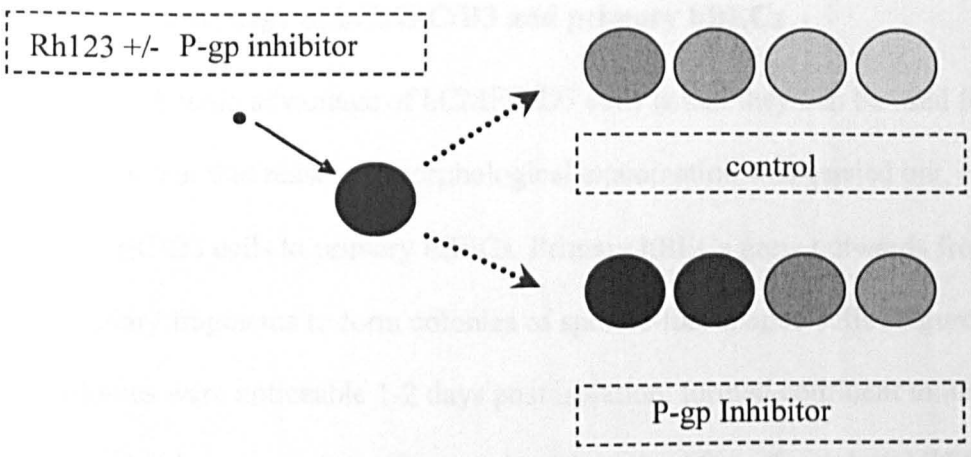

Figure 2.1. Principles underlying rh123 efflux experiment. rh123, a fluorescent P-gp substrate, is effluxed from preloaded hCMEC/D3 cells in a time-dependent manner. Inhibition of P-gp raises the intracellular levels, indicative of functional P-gp.

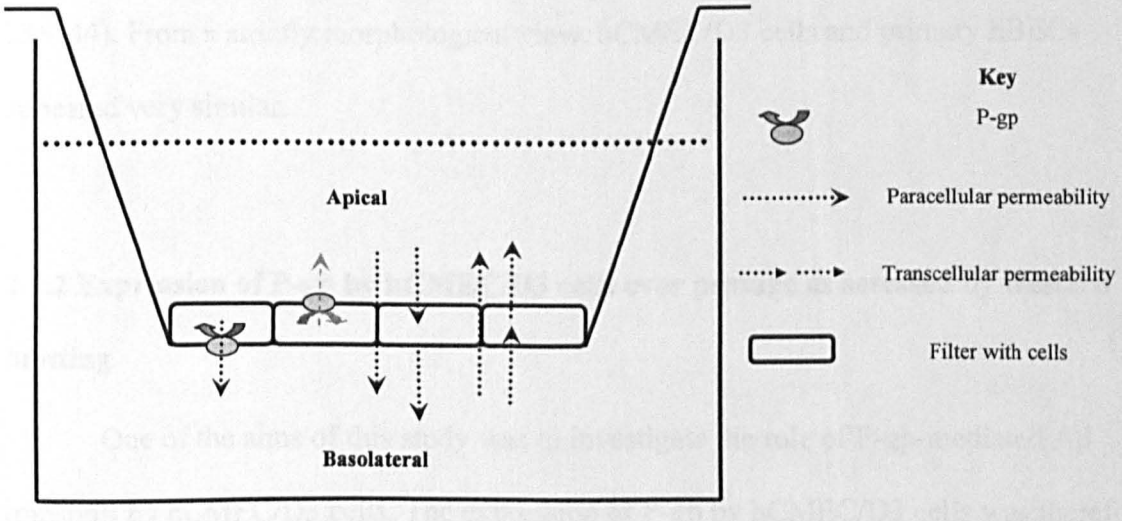

Figure 2.2. *In vitro* BBB model used to investigate hCMEC/D3 cell permeability to rh123. hCMEC/D3 cells were grown to confluence on transwell filters. A rh123 solution (22 μM) was added to either the basolateral or apical chamber with or without the inhibitors tariquidar, vinblastine and FTC. Ultrastructural localisation of P-gp (i.e. whether located on the apical or basolateral plasma membrane) is thought to influence the passage of rh123 from the compartment to which it was added to the other compartment.

2.3 Results

2.3.1 Morphology of hCMEC/D3 and primary hBECs

A main advantage of hCMEC/D3 cells is that they can be used for high throughput studies. For that reason, a morphological examination was carried out, comparing hCMEC/D3 cells to primary hBECs. Primary hBECs grew outwards from isolated capillary fragments to form colonies of spindle-like shaped cells (Figure 2.3a). These colonies were noticeable 1-2 days post isolation, formed confluent monolayers after 1-2 weeks and appeared free of contaminating cells. After p5, primary hBECs neither appeared completely spindle-shaped nor continued to grow at a sufficient rate to reach confluence. hCMEC/D3 cells, grew in a similar elongated spindle-shaped manner (Figure 2.3b) and reached confluence 2-3 days after a 1 in 5 passage. In contrast to primary hBECs, there were no alterations in shape or growth rates over the passage ranges used in this study (p 23 – 44). From a strictly morphological view, hCMEC/D3 cells and primary hBECs appeared very similar.

2.3.2 Expression of P-gp by hCMEC/D3 cells over passage as assessed by western blotting

One of the aims of this study was to investigate the role of P-gp-mediated Aβ transport by hCMEC/D3 cells. The expression of P-gp by hCMEC/D3 cells was therefore characterised, and compared to that of another ABC efflux transporter with an overlapping substrate range, BCRP. Firstly, the expression of P-gp over passage was investigated in order to determine the maximum passage in which this cell line could be used for further experimentation and also to ensure that results obtained between passages were comparable (Figure 2.4). Using western blotting techniques, P-gp expression was detected as a diffuse band of ~ 160 kDa, which probably reflects different glycosylation patterns of

the MDR1 product in hCMEC/D3 cells. P-gp expression was similar between p23 and 38 (n = 1), but at higher passages (> p41) appeared decreased (Figure 2.4a). In contrast, actin levels were maintained with the exception of the highest passage investigated (p44) expression declined. P-gp expression was quantified by measuring the signal intensity and normalised to actin as a control to account for loading differences (figure 2.4b). From this experiment, a maximum passage of 38 was selected for further experiments, as by comparison p 41 had a 30 % decrease in P-gp levels.

2.3.3 The expression of P-gp and BCRP by hCMEC/D3 and primary hBECs as measured by flow cytometry

To provide a more accurate quantitative method for protein expression, the expression of P-gp and BCRP by hCMEC/D3 cells was measured using flow cytometry (Figure 2.5). Flow cytometry showed a higher median fluorescence intensity when antibodies against P-gp (20.1 ± 1.5) and BCRP (30.96 ± 1.53) were used when compared to their controls [IgG_1 (4.6 ± 1.0,) and IgG_{2a} (3.9 ± 0.3), respectively] (n = 3, $P < 0.01$), indicating that both ABC efflux transporters are expressed by hCMEC/D3 cells.

The levels of P-gp expression were then compared between hCMEC/D3 cells and primary hBECs using flow cytometry to determine the suitability of the former cell line as a hBEC model. Both primary hBECs and hCMEC/D3 cells demonstrated a higher median fluorescence staining intensity compared to their controls (n = 3 experiments with duplicate samples, $P < 0.01$, Figure 2.6). Whilst primary hBECs expressed 37.6 % ± 8.0 more P-gp than hCMEC/D3 cells, these levels were not significant (for primary hBECs, n = 3 from 2 donors, $P > 0.05$). The results indicate that the expression of P-gp by hCMEC/D3 cells is close to that of primary hBECs cells and so they represent a suitable model for the study of P-gp expression.

2.3.4 The expression of P-gp by hCMEC/D3 cells as assessed by immunocytochemistry

The ability of P-gp to act as an efflux transporter is dependent on its localisation to the plasma membrane. Furthermore, the polarisation of P-gp to either the basolateral or apical membrane will determine the direction of efflux, which *in vivo* corresponds to the brain or blood side of the BBB respectively. Therefore, the sub-cellular localisation of P-gp was investigated by ICC. Using fluorescence microscopy, both P-gp and BCRP displayed a diffuse staining at the cytoplasm and membrane, but not in the nucleus (Figure 2.7, n = 3). As for fluorescence microscopy, the sub-cellular localisation of P-gp could not be discerned by confocal microscopy (Figure 2.8, n = 1). P-gp expression was not detected in the nucleus but appeared to be distributed throughout the cytoplasm and plasma membrane. The results indicate that either both techniques are not sufficiently sensitive to detect the sub-cellular localisation of P-gp, or that P-gp is distributed throughout hCMEC/D3 cells.

2.3.5 Sub-cellular localisation of P-gp as assessed by differential detergent fractionation

Since P-gp appeared distributed diffusely throughout hCMEC/D3 cells, a biochemical assay was employed to investigate the relative sub-cellular distribution of P-gp. hCMEC/D3 cells were separated into cytosolic, membrane/organelle, nuclear and cytoskeletal fractions using differential detergent fractionation. The expression of P-gp and BCRP in each fraction was determined by western blotting and compared to a nuclear marker, the transcription factor Sp3, and a cytoskeletal marker, actin (Figure 2.9).

Sp3 was found almost entirely in the nuclear fraction (89.3 % ± 5.4, n = 3), whereas actin was expressed highest in the cytoskeletal followed by nuclear and membrane fractions (75.2 % ± 9.5, 15.5 % ± 4.8 and 8.3 % ± 5.4, respectively, n = 3). P-gp and BCRP

were both predominantly expressed in the membrane/organelle fraction (78.5 % ± 2.6, 88.8 % ± 5.09, respectively, n = 3). Therefore, both efflux pumps under investigation were located on cellular membranes, which includes both plasma membrane and membranes of intracellular organelles.

2.3.6 Localisation of P-gp at the ultrastructural level

It is essential to determine whether P-gp expression is polarised on the plasma membrane as this would determine whether substrates would be effluxed on the apical or basolateral side of hCMEC/D3 cells, corresponding to the blood and brain sides respectively, *in vivo*. As ICC techniques were unable to demonstrate the polarised nature of P-gp, TEM and immunogold staining techniques were employed. Gold particles were observed in the apical, basolateral and intracellular compartments (Figures 2.10 a, b and c, respectively) in agreement with ICC staining. When quantified, the number of gold particles associated with the apical plasma membrane was 2.9 times greater than on the basolateral membrane (Figure 2.10 b, 66 images analysed over a 500 μm section of plasma membrane). Therefore, whilst P-gp molecules are distributed on both membranes, the majority are on the apical membrane, which corresponds to the blood side *in vivo*. Located on this membrane, P-gp would be situated to prevent the movement of unwanted substrates from the blood into the brain.

2.3.7 Cytotoxicity of P-gp and BCRP inhibitors

An aim of this chapter was to investigate the functional expression of P-gp by hCMEC/D3 cells using the P-gp inhibitors tariquidar, vinblastine and the BCRP inhibitor FTC. To determine non-cytotoxic doses of these inhibitors, an MTT assay was carried out encompassing a concentration range previously reported to inhibit drug efflux by the ABC transporters. Figure 2.11 shows that tariquidar (0 – 600 nM) and FTC (0 – 22 μM) did not

affect cell viability following a 48 h incubation period, indicating non-cyotoxicity to hCMEC/D3 cells over the range of concentrations tested. In contrast, vinblastine caused a concentration-dependent decrease in cell viability at 48 h with an IC 50 of 26.3 μM ± 6.1 (n = 3). The cytotoxicity was significant at concentrations of 0.5 μM and above when compared to the control (n = 3, $P < 0.05$). However, a 24 h incubation with the same doses of vinblastine (0 - 40 μM), did not decrease cell viability (n = 3, $P > 0.05$) over the entire concentration range investigated. In subsequent experiments, 22 μM vinblastine was used at incubation periods of 12 h or shorter, whilst 300 nM tariquidar and 22 μM FTC were used for periods shorter than 48 h.

2.3.8 P-gp-mediated efflux of rh123 by hCMEC/D3 cells

In the original characterisation of the hCMEC/D3 cell line, P-gp functional expression was demonstrated by an increase in the net influx of rh123 in the presence of PSC-833 [473]. The aim here was to expand on this evidence by investigating whether P-gp acts to efflux rh123 from preloaded hCMEC/D3 cells. Efflux is potentially a more sensitive assay than influx as a measure of activity, since it is dependent on the efflux activity of P-gp rather than a measure of the relative contribution of efflux versus influx mechanisms. Localisation of P-gp to the plasma membrane is also a prerequisite for the efflux function of P-gp, which has been demonstrated in Figure 2.10. hCMEC/D3 cells were preloaded with 22 μM rh123 (1 h, 4°C) and incubated at 37°C over 6 h (Figure 2.12). Compared to cells preloaded with rh123 and incubated at 4 °C, cellular rh123 levels decreased sharply in the first hour and then continued to decline. The $t_{1/2}$ was estimated to be 13.3 min ± 1.1 (n = 3). The addition of 22 μM vinblastine to the efflux buffer during incubation at 37°C resulted in a less steep decline and a $t_{1/2}$ of 112.2 min ± 3.7. At every time point measured (15, 30, 60, 120, 180 and 360 min), the median fluorescence intensity of cells treated with vinblastine was higher and statistically significant compared to those

treated with DMSO control (n = 3, $P < 0.05$). These results indicate that rh123 is effluxed from hCMEC/D3 cells via functional P-gp.

A mutation at arginine position 428 to glycine or threonine of BCRP can result in enhanced substrate specificity to rh123 [221], and so it remained a possibility that BCRP could act as a rh123 transporter in hCMEC/D3 cells. To further determine the relative contribution of P-gp or BCRP to rh123 efflux, the effects of tariquidar (300 nM), FTC (22 μM) and vinblastine (22 μM) were investigated. hCMEC/D3 cells were preloaded with 22 μM rh123 at 4°C for 60 min, followed by incubation at 37°C for 60 min with the different treatments (Figure 2.13). 300 nM tariquidar increased cellular rh123 levels compared to an ethanol control (n = 3, $P < 0.01$). 22 μM vinblastine, but not 22 μM FTC, also increased cellular rh123 levels compared the DMSO control (n = 3, $P < 0.01$). rh123-mediated efflux by hCMEC/D3 cells was therefore mainly mediated by P-gp and not BCRP.

Tariquidar has been demonstrated to have a long lasting, possibly irreversible inhibition on P-gp activity, whilst vinblastine acts as a competitive inhibitor. To investigate the mechanism of P-gp inhibition by tariquidar and vinblastine, hCMEC/D3 cells were pre-loaded at 4°C with 22 μM rh123 in combination with either tariquidar (300 nM) or vinblastine (22 μM), followed by incubation at 37°C for 60 min with either tariquidar, vinblastine or a control. After preloading hCMEC/D3 cells with rh123 and tariquidar, cellular rh123 levels were of similar high magnitude following incubation with tariquidar or a vehicle control (control 53.7 % ± 5.3, tariquidar 55.7 ± 4.3, n = 3). In contrast, after preloading hCMEC/D3 cells with rh123 and vinblastine, the presence of vinblastine during the incubation at 37°C was required to inhibit efflux of rh123 (control 5.8 % ± 1.4, vinblastine 50 % ± 12.2, n = 3). The results imply that tariquidar is a long lasting P-gp inhibitor that unlike vinblastine, can exert its effect after preincubation, even if absent during the efflux stage of an assay. The long lasting inhibition of P-gp by tariquidar might be caused by high affininty binding of tariquidar with P-gp, which persists even after washing steps.

2.3.9 The permeability of hCMEC/D3 cells to rh123

P-gp efflux activity may limit the permeability of its substrates across BEC monolayers since P-gp was located mainly on the apical membrane. Therefore the permeability of hCMEC/D3 cells grown on transwell filters to rh123 was investigated (Figure 2.14). Apical-to-basolateral permeability of hCMEC/D3 cells to 22 μM rh123 was unaffected by both 300 nM tariquidar and 22 μM vinblastine ($n = 3$, $P > 0.05$). The basolateral-to-apical permeability of hCMEC/D3 to rh123 was also unaffected by 300 nM tariquidar or 22 μM vinblastine compared to the control ($n = 3$, $P > 0.05$). The results show that hCMEC/D3 cells might not be suitable to measure the polarised transport of lipophilic molecules with a molecular weight of ~ 400 Da. Indeed, Weksler *et al* [473] have demonstrated that hCMEC/D3 cells are useful for investigating the permeability of paracellular tracers larger than or equal to 4 kDa in size.

(a) Primary brain endothelial cells

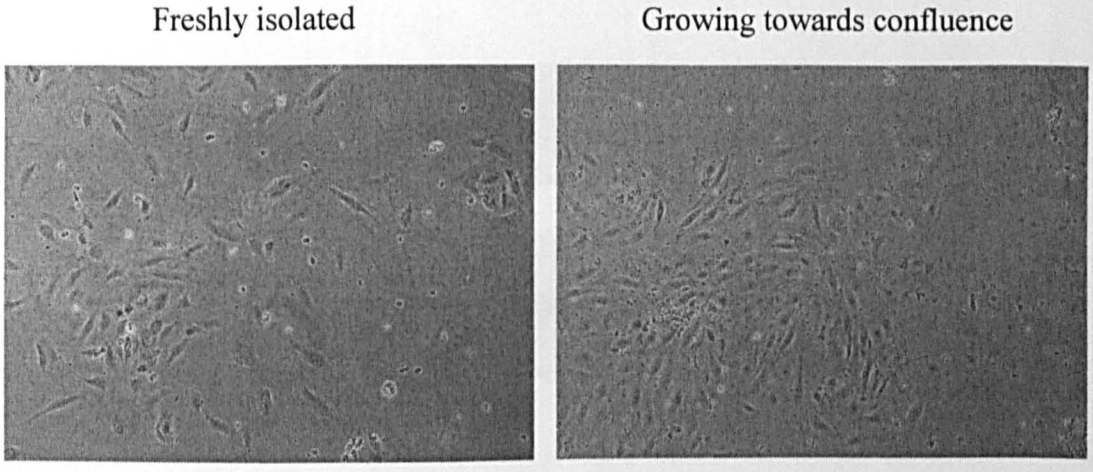

(b) hCMEC/D3 cells

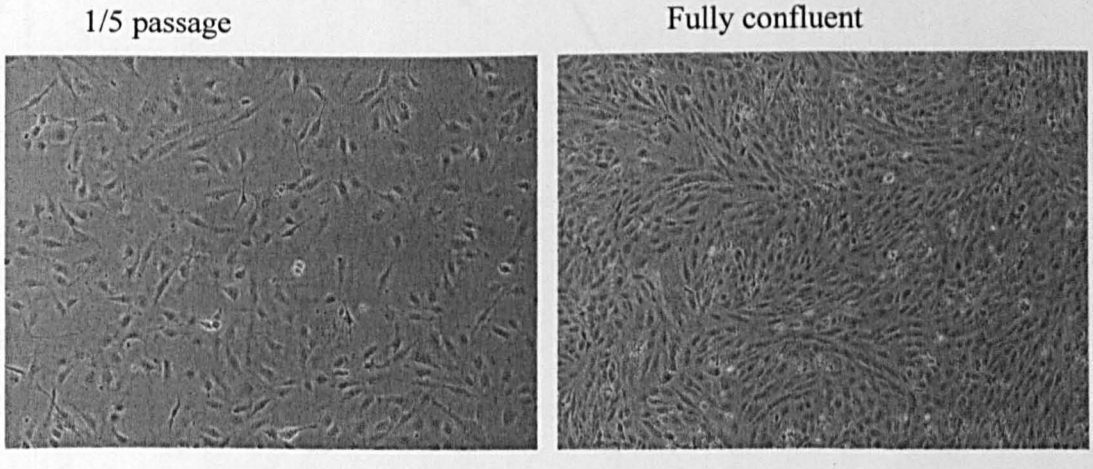

Figure 2.3. Morphology of hCMEC/D3 cells and primary hBECs viewed by phase contrast microscopy. (a) Freshly isolated primary hBECs grew outwards from isolated capillary fragments. One week after isolation, colonies of spindle shaped cells formed confluent monolayers. **(b)** hCMEC/D3 cells were split at a ratio of 1 in 5 onto collagen-coated tissue culture flasks. When confluent, ~ 2-3 days, hCMEC/D3 cells formed a monolayer of spindle shaped, tightly packed cells. Images taken on Nikon eclispse TS100.

(a)

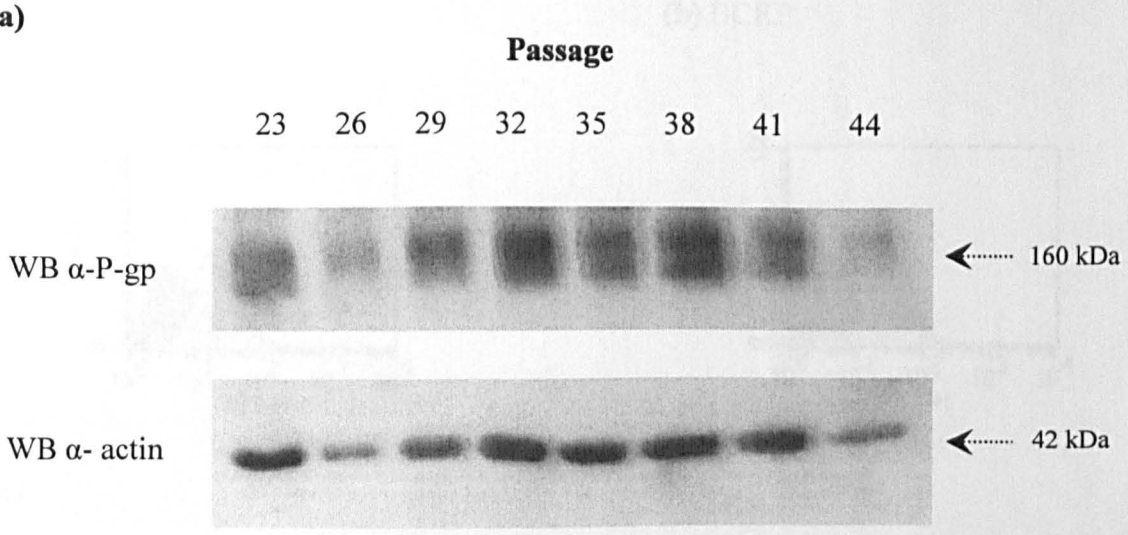

(b)

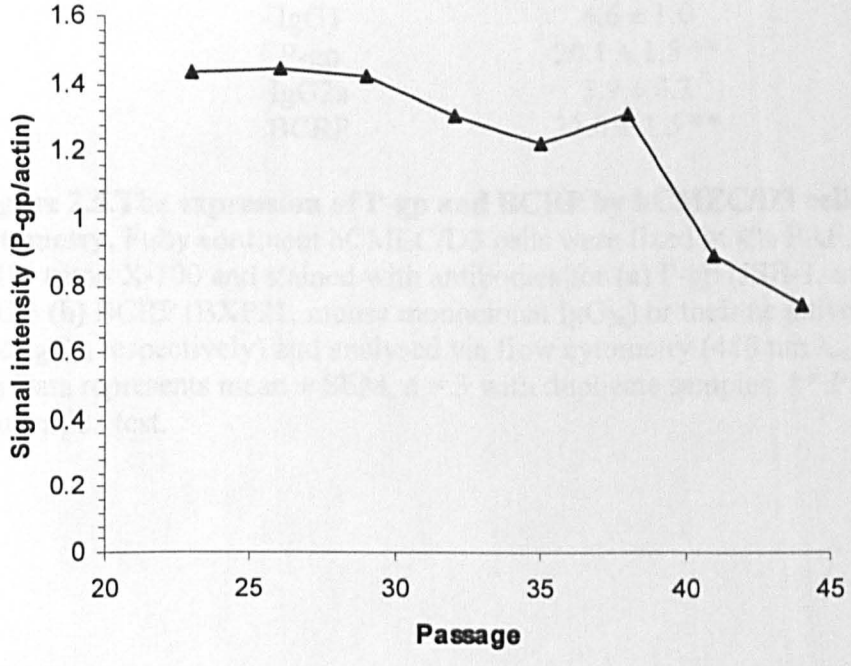

Figure 2.4.The expression of P-gp by hCMEC/D3 cells over passage. (a) Fully confluent hCMEC/D3 cells were lysed in RIPA buffer and the expression of P-gp (C219, mouse monoclonal IgG_{2a}) and actin (mouse monoclonal IgG_1) was determined over passage number from 23 to 44 using western blotting techniques.**(b)** The signal intensity of the bands corresponding to P-gp and actin were determined by image J and P-gp expression normalised. n = 1, with single samples.

(a) P-gp

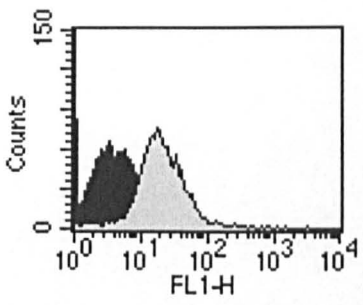

(b) BCRP

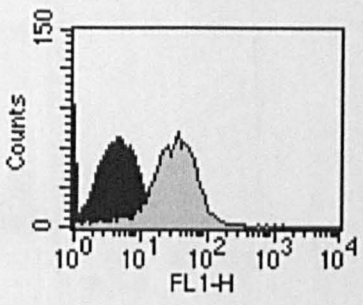

(c)

Antibody	Average median fluorescence
IgG1	4.6 ± 1.0
P-gp	20.1 ± 1.5 **
IgG2a	3.9 ± 0.3
BCRP	31.0 ± 1.5 **

Figure 2.5.The expression of P-gp and BCRP by hCMEC/D3 cells as assessed by flow cytometry. Fully confluent hCMEC/D3 cells were fixed in 4% PAF, permeabilised using 0.1% triton X-100 and stained with antibodies for **(a)** P-gp (JSB-1, mouse monoclonal IgG_1) **(b)** BCRP (BXP21, mouse monoclonal IgG_{2a}) or their negative controls (mouse IgG_1 and IgG_{2a} respectively) and analysed via flow cytometry (488 nm $\lambda_{excitation}$ 520 nm $\lambda_{emission}$) **(c)** Data represents mean ± SEM, n = 3 with duplicate samples. ** $P < 0.01$ using Student's t test.

(a) hCMEC/D3 cells

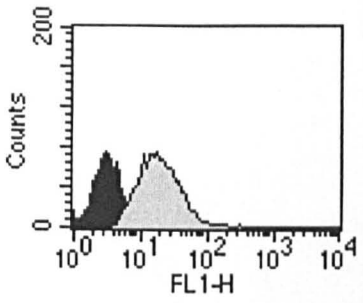

(b) Primary hBECs

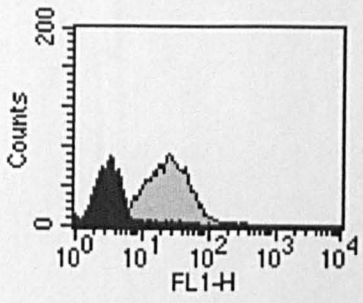

(c)

	Average median fluorescence
hCMEC/D3- IgG1	2.9 ± 0.1
hCMEC/D3 - P-gp	17.3 ± 1.6 **
Primary- IgG1	2.8 ± 0.1
Primary- P-gp	22.4 ± 1.6 **

Figure 2.6. The expression of P-gp by hCMEC/D3 cells and primary hBECs as assessed by flow cytometry. Fully confluent **(a)** hCMEC/D3 cells (p23-28) and **(b)** primary hBEC (p2-4) were fixed in 4% PAF, permeabilised using 0.1% triton X-100 and stained with antibodies for P-gp (JSB-1, mouse monoclonal IgG_1) or a negative control (mouse IgG1) and analysed via flow cytometry (488 nm $\lambda_{excitation}$ 520 nm $\lambda_{emission}$) **(c)** Data represents mean ± SEM, n = 3 with duplicate samples. ** $P < 0.01$ using Student's t test.

(a) P-gp Isotype control

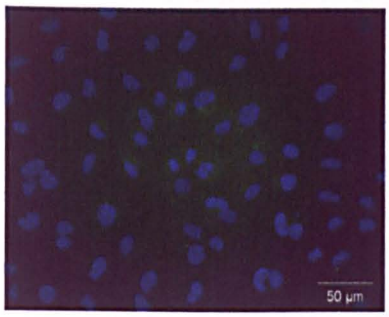

(b) α- P-gp

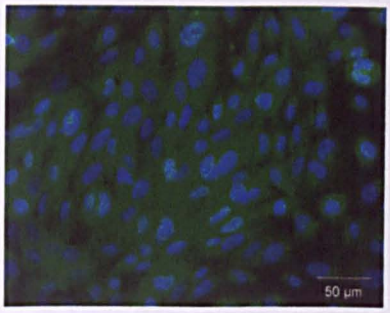

(c) BCRP Isotype control

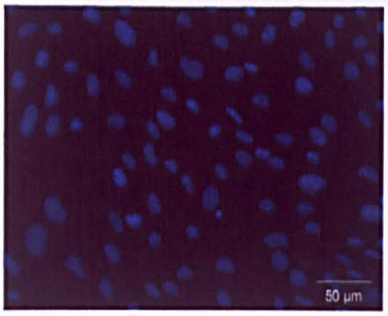

(d) α-BCRP

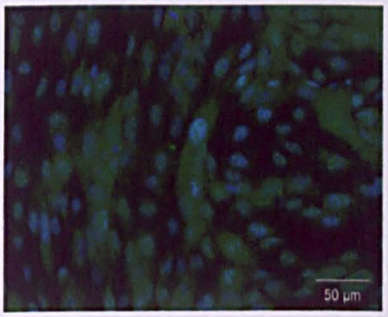

Figure 2.7. Expression of P-gp and BCRP by hCMEC/D3 cells as viewed by fluorescence microscopy. hCMEC/D3 cells were grown on collagen-coated Labtek slides until confluent, fixed (4 % PAF), permeabilised (0.1 % triton X-100) and stained for **(a,b)** P-gp [JSB-1 (mouse monoclonal IgG_1)] or isotype-matched control or **(c,d)** BCRP [BXP21,(mouse monoclonal IgG_{2a})], counterstained for the nucleus with DAPI and viewed via fluorescence microscopy. Images are a representation of hCMEC/D3 cells at p 26. (n = 3 with single samples)

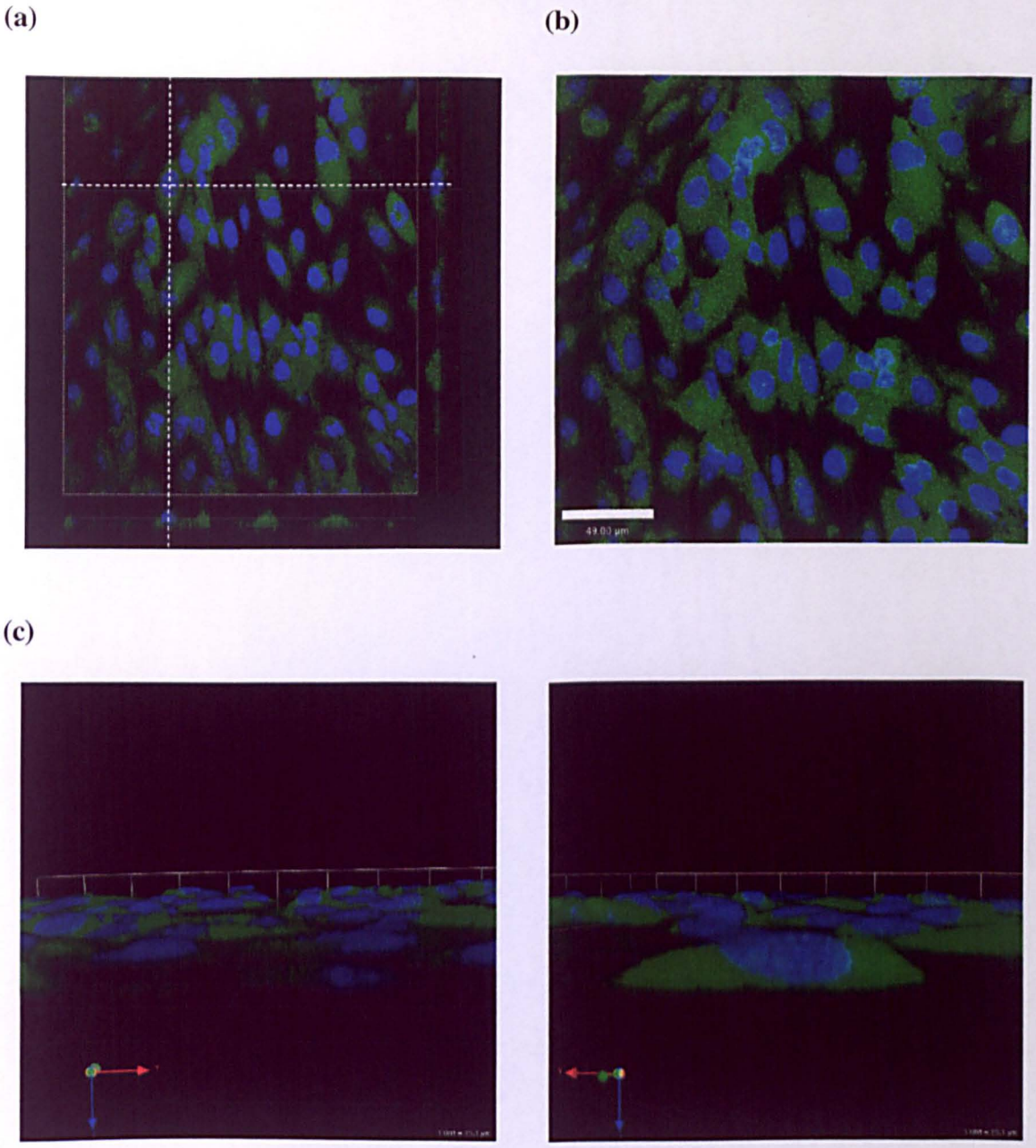

Figure 2.8. Expression of P-gp by hCMEC/D3 cells as viewed by confocal microscopy hCMEC/D3 cells (p 28) were grown to confluence on collagen- and fibronectin- coated transwell polyester membrane inserts (0.4 μm pore, 12mm diameter), fixed (4 % PAF), permeabilised (0.1 % triton X-100) and stained for P-gp (JSB-1, mouse monoclonal IgG_1) or an isotype control (mouse IgG1), counterstained with the nuclear stain DAPI and viewed on a confocal microscope. **(a)** An XY Z cross-section was taken over a selected field, enabling top down **(b)** and **(c)** three dimensional reconstruction with Volocity software. Images are from one experiment carried out in duplicate.

(a)

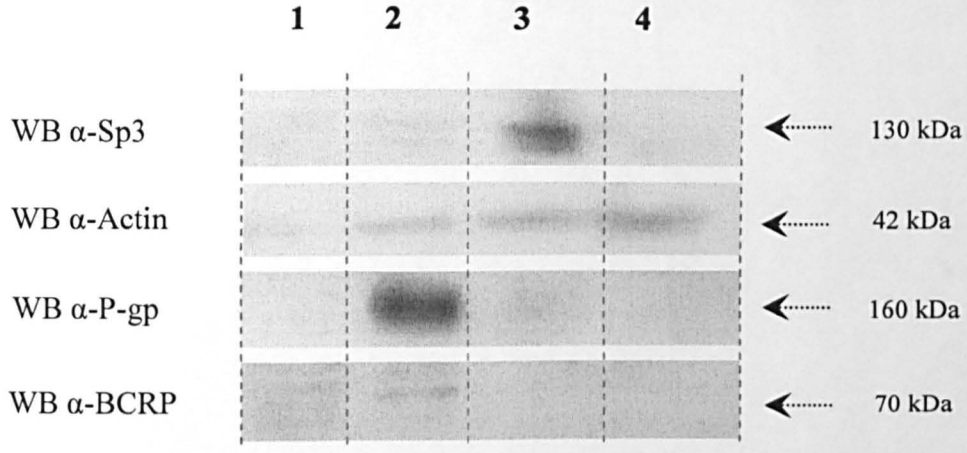

1 = Cytosolic. **2** = membrane/organelle. **3** = nuclear **4** = cytoskeletal

(b)

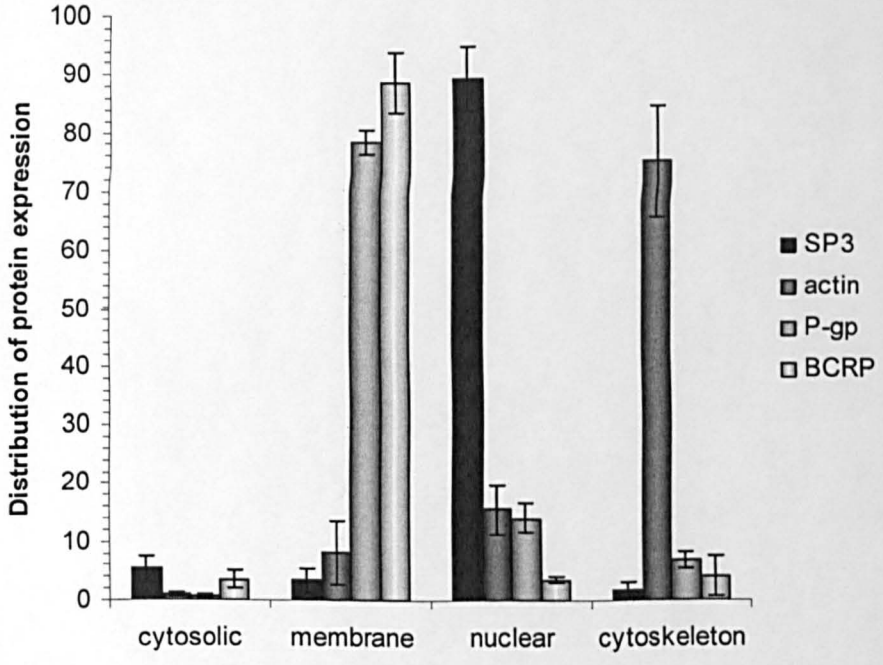

Figure 2.9. The sub-cellular localisation of P-gp, BCRP, Sp3 and actin in hCMEC/D3 cells as determined by western blotting after differential detergent fractionation. (a) Fully confluent hCMEC/D3 cells were separated into cytosol, membrane/organelle, nuclear and cytoskeletal components using differential detergent fractionation and the expression of Sp3 (rabbit polyclonal IgG), actin (mouse monoclonal IgG_1), BCRP [BXP21, (mouse monoclonal IgG_{2a} anti-human)] and P-gp [C219,(mouse monoclonal IgG_{2a}) was assessed by western blotting. **(b)** Relative expression of each protein in cytosol, membrane/organelle, nuclear and cytoskeletal fractions as a percentage of total expression. Data represents mean ± SEM, n = 3 with single samples.

(a) Abluminal expression

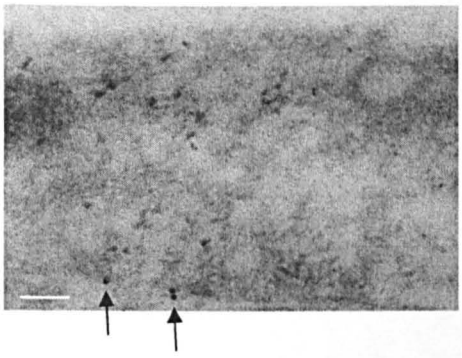

(b) Intracellular expression

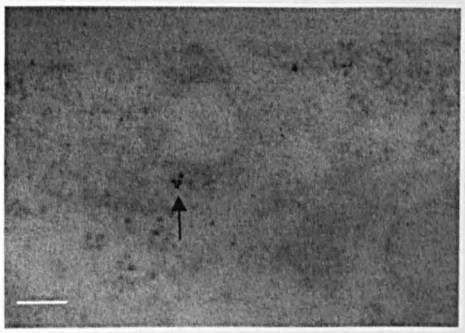

(c) Luminal expression

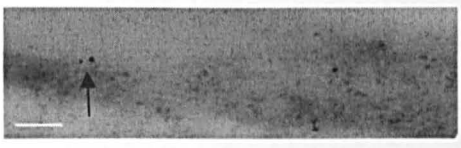

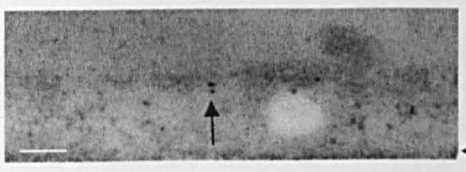

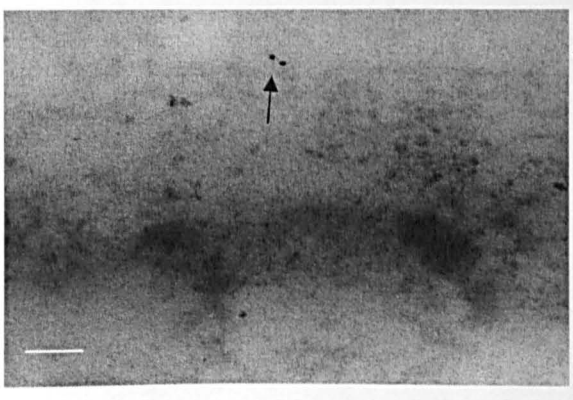

(d)

	P-gp		**Isotype control**	
	Apical	*Basolateral*	*Apical*	*Basolateral*
Average number of gold particles per µm	0.11 +/- 0.017	0.038 +/- 0.009	0.01 +/- 0.004	0.01 +/0.004

Figure 2.10. Expression of P-gp by hCMEC/D3 cells as assessed by TEM and immunogold staining. hCMEC/D3 cells (p 28) were grown to confluence on transwell polyester membrane inserts (0.4 µm pore, 12mm diameter), fixed (PLP), mounted on nickel slots, stained for P-gp [C219, (mouse monoclonal IgG_{2a}) or an isotype control (IgG_{2a}) and viewed in TEM. One frame length of 7.5 µm was taken every 2-3 frames **(a-c)** for a total of 500 µm, and the number of gold gold particles counted within 100 nm of the apical or basolateral membrane per image. **(d)** The average number of gold particles per µm was then calculated. ⟶ Indicates gold particles. Scale bar = 100 nm

(a) Tariquidar 48 h

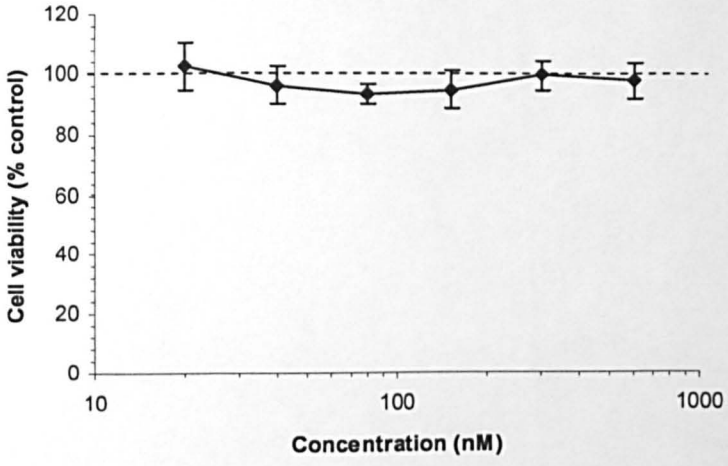

(b) FTC 48 h

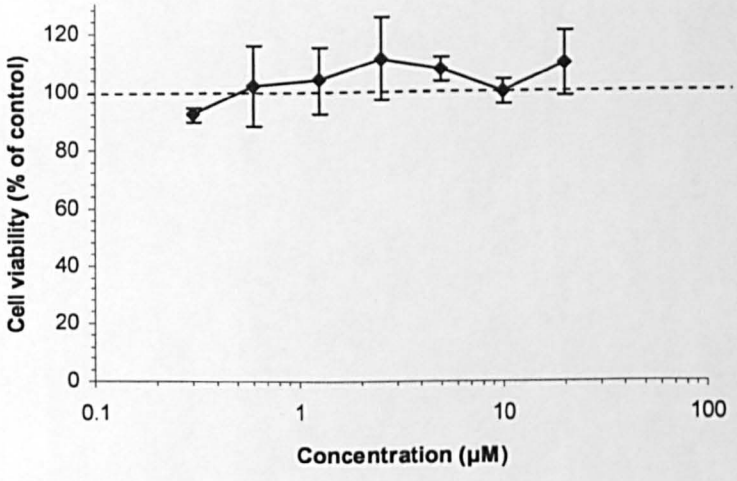

(c) Vinblastine at 24 h and 48 h

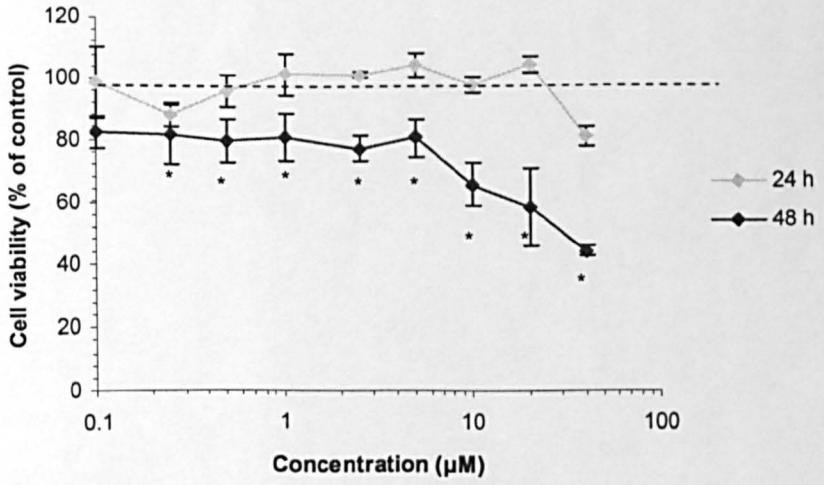

Figure 2.11. Cytotoxicity of vinblastine, tariquidar and FTC to hCMEC/D3 cells as assessed by an MTT assay. Cytotoxicity of **(a)** tariquidar, **(b)** FTC and **(c)** vinblastine in fully confluent hCMEC/D3 cells was assessed using an MTT assay. Data represents mean ± SEM, n = 3 with quintuplet samples. * $P < 0.05$ using Student's t test for raw data.

(a)

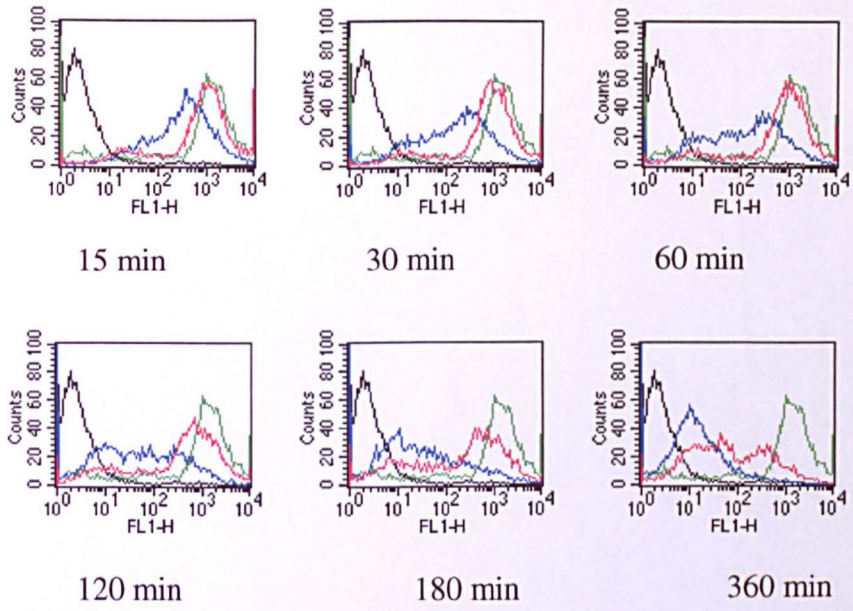

Key: Black = No Rh123. Green = 4°C. Pink =. vinblastine. Blue = 37°C.

(b)

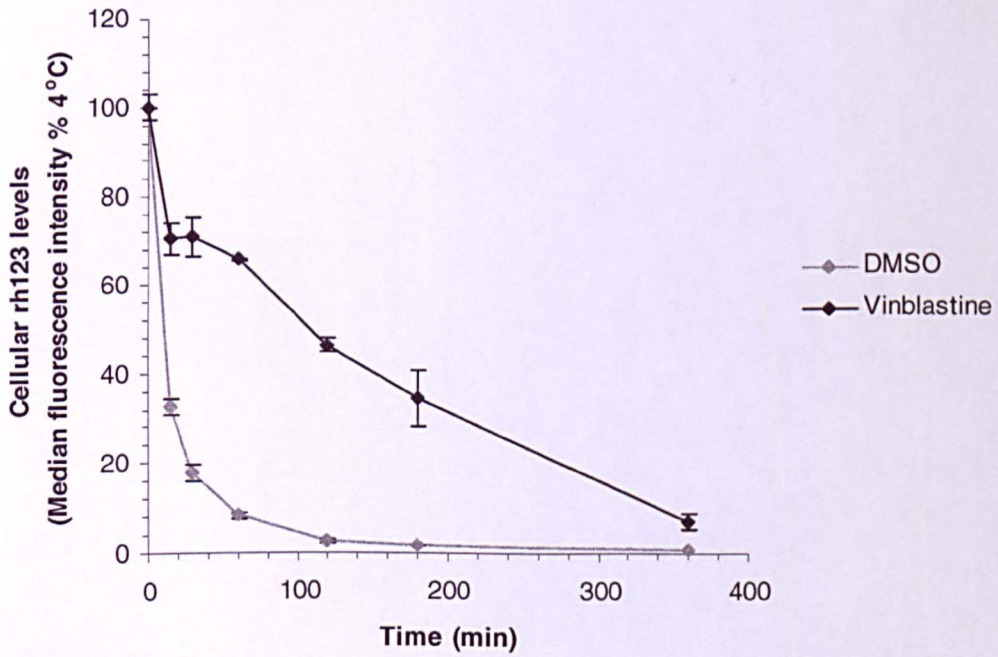

Figure 2.12. Time-dependent efflux of rh123 by hCMEC/D3 cells. (a) Fully confluent hCMEC/D3 cells were preloaded with rh123 (22 μM) for 1 h at 4°C and then incubated at 37°C in the presence of 22 μM vinblastine or DMSO for 15, 30, 60, 120, 180 or 360 min and analysed via flow cytometry (488 nm $\lambda_{excitation}$ 520 nm $\lambda_{emission}$). **(b)** The median fluorescence intensity was measured and expressed as a percentage of preloaded cells incubated at 4°C. Data represents mean ± SEM, n = 3 with duplicate samples. * $P < 0.05$, ** $P < 0.01$ using Student's t test comparing vinblastine to DMSO at each time point.

(a)

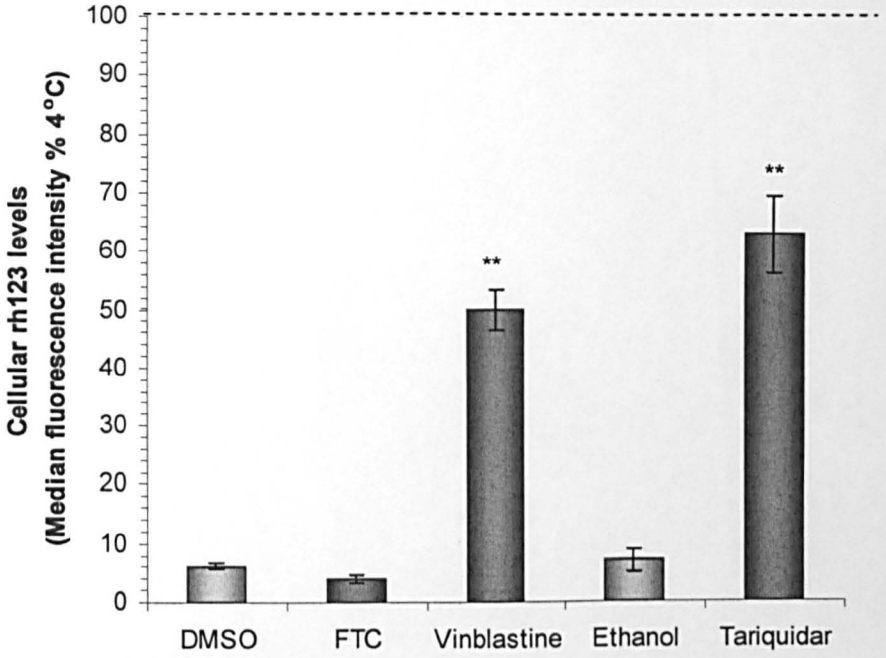

(b)

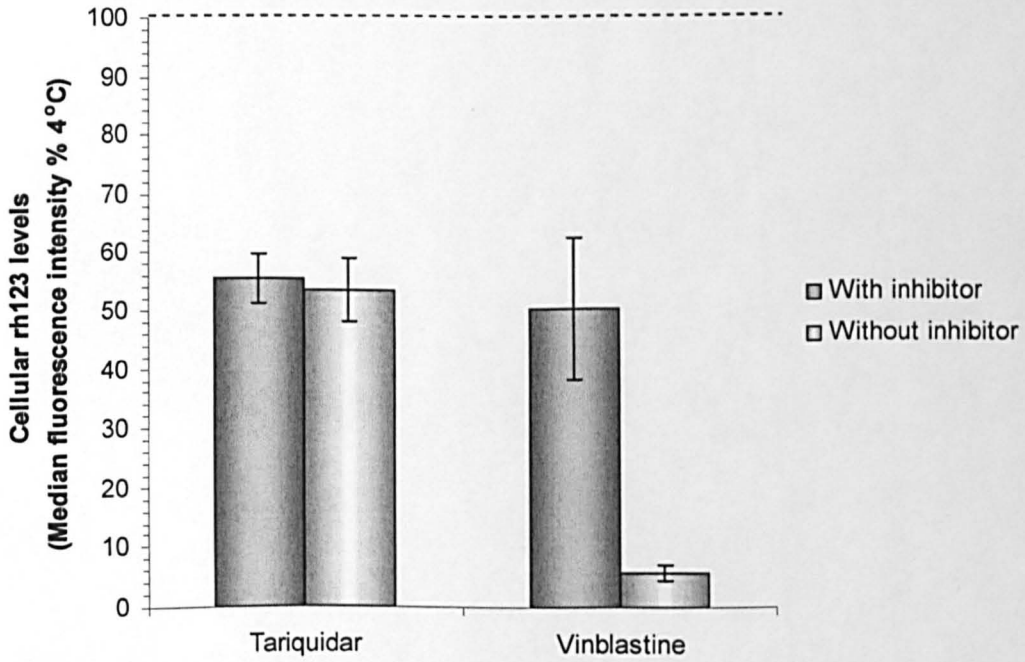

Figure 2.13. Rh123 efflux inhibition by tariquidar and vinblastine from hCMEC/D3 cells. (a) hCMEC/D3 cells were preloaded with rh123 (22 μM) at 4°C for 60 min followed by 60 min incubation at 37 °C in the presence of tariquidar (300 nM), vinblastine (22 μM), FTC (22 μM) or an appropriate control and the median fluorescence intensity measured by flow cytometry. Data represents mean ± SEM, n = 3 with duplicate samples. * $P < 0.05$, ** $P < 0.01$ using Student's t test comparing treatment to appropriate control. **(b)** hCMEC/D3 cells were preloaded with rh123 and either tariquidar (300 nM) or vinblastine (22 μM) for 60 min at 4°C followed by 60 min incubation at 37 °C in the presence or absence of the appropriate inhibitor. n = 3 with duplicate samples.

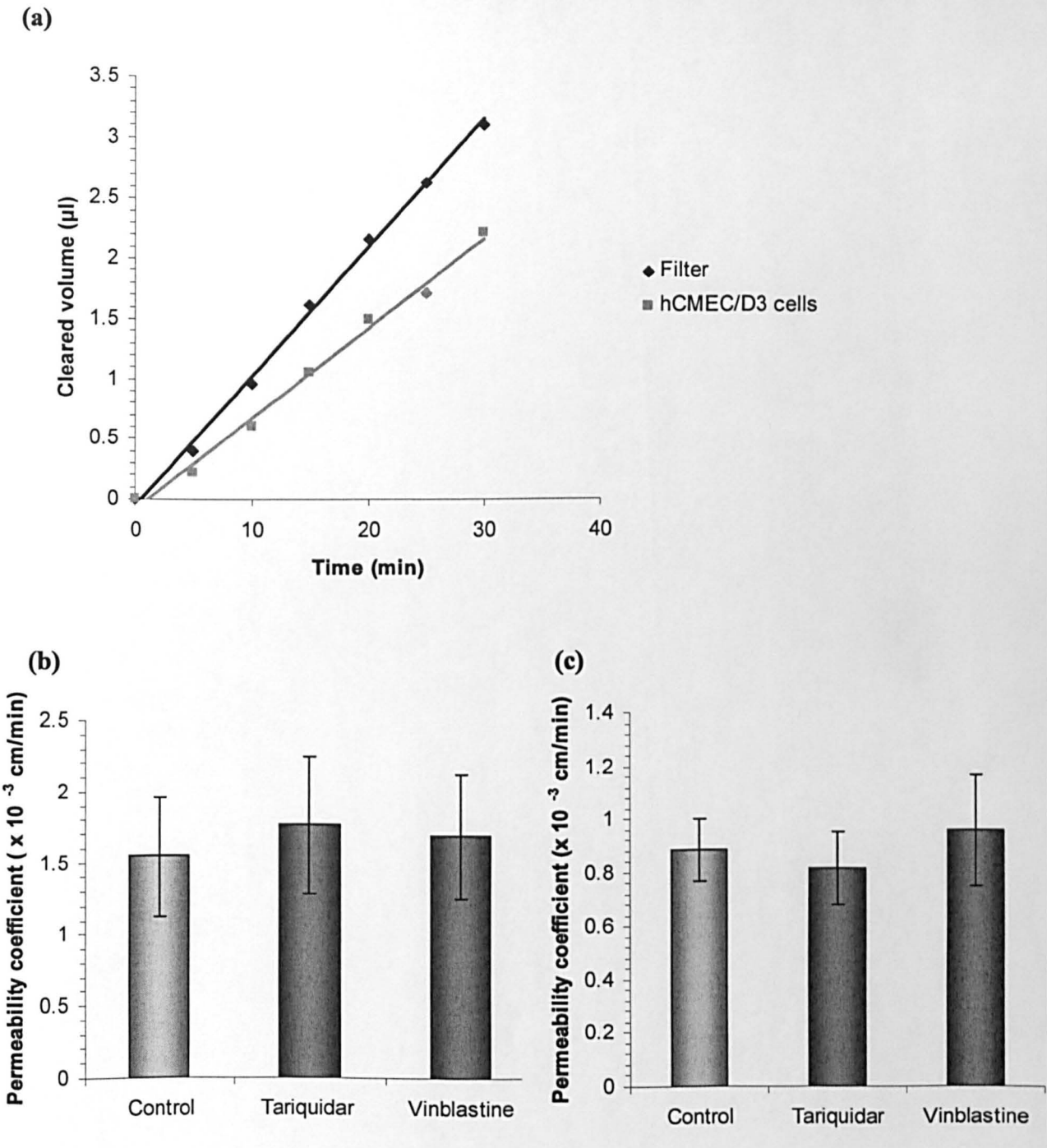

Figure 2.14. The permeability of hCMEC/D3 cells to rh123 in the presence or absence of tariquidar and vinblastine. hCMEC/D3 cell were grown to confluence on collagen- and fibronectin- coated filter inserts. rh123 (22 µM) was then added to the apical or basolateral side of the filter in the presence of tariquidar, vinblastine or DMSO and the amount of rh123 that crossed the filter was measured using a fluorescence plate reader. **(a)** Shows a typical curve of the volume of rh123 cleared versus time for apical to basolateral permeability. **(b)** The apical-to-basolateral permeability coefficient (P_e) of hCMEC/D3 cells was calculated using the slope of the curve. Data represents mean ± SEM, n = 3 with duplicate samples. $P > 0.05$. **(c)** Rh123 (22 µM) in the presence of tariquidar (300 nM), vinblastine (22 µM) or appropriate control was added to the basolateral chamber of fully-confluent hCMEC/D3 cells grown on filters. After 30 min the fluorescence was measured in the apical and basolateral chambers and the P_e calculated. Data represents mean ± SEM, n = 3 with duplicate samples. $P > 0.05$.

2.4 Discussion

2.4.1 P-gp expression by hCMEC/D3 cells

hBECs express P-gp which acts as a barrier for many therapeutic drugs and endogenous molecules, preventing their entry into the brain (reviewed in [172, 186]). The study of P-gp *in vitro* is a useful tool for identifying potential substrates and inhibitors. The overall aim of this chapter was to fully characterise P-gp expression by an immortalised hBEC cell line, hCMEC/D3 cells, previously suggested as a suitable *in vitro* human BBB model [473]. The data presented here shows that hCMEC/D3 cells express P-gp as assessed by flow cytometry, western blotting, ICC and TEM staining. This data is agreement with multiple studies that have demonstrated BEC P-gp expression at both the protein and mRNA level from *in vitro* cultures of both primary and immortalised cells of rat, mouse and human origin [172, 186, 210-212, 473, 482, 504, 506, 514, 515].

In terms of P-gp expression, the BEC phenotype appears to be preserved in hCMEC/D3 cells over a wide range of passages (up to p38) and P-gp expression was comparable, albeit slightly reduced, to primary BECs. It is likely that the primary BECs used here however would have a marked decrease in P-gp expression compared to isolated capillaries, which more closely mimic the *in vivo* situation as has been demonstrated in a number of animal and human studies. Regina *et al* [244, 516] demonstrated that compared to isolated rat brain capillaries, an immortalised rat BEC cell line, RBE4, and primary rat BECs express less P-gp when assessed by western blotting and by RT-PCR for mdr1a. The authors also found that P-gp expression was higher in primary rat BECs than in RBE4 cells, which is similar to the observations made in this study with hCMEC/D3 cells and primary hBECs. Barrand *et al* [517] have also demonstrated that isolated BECs express less P-gp than cerebral microvessels from rats. Seetharamam *et al* [212] have corroborated this finding in humans, reporting that isolated BECs express less P-gp, assessed by ICC when compared to brain capillaries. P-gp expression can be elevated in cell culture using a

variety of different agents including puromycin, dexamethasone, cAMP elevation and PKC activation [518] [244, 519]. hCMEC/D3 cells, however, have not been demonstrated to induce P-gp in response to a number of different agents (D.K.Male, The Open University personal communication) including TNF-α and puromycin.

2.4.2 P-gp cellular distribution in the CNS

There has been some controversy surrounding the expression of P-gp by BECs. In 1997, Pardridge *et al.* [209] found that MRK16, an antibody directed against an external epitope of P-gp, co-localised with GFAP but not with Glut-1 in isolated human brain microvessels and rhesus monkey tissue samples. GFAP is a typical astrocyte marker, whereas Glut-1 is an EC marker. In a follow up study, there was a similar finding in unfixed isolated human brain capillaries, whereby GFAP and MRK16 staining were co-localised in a discrete continuous pattern. This led the authors to conclude that P-gp was located on astrocytic foot processes on the abluminal side on ECs [208], although the activation state of the astrocytes in the post mortem tissue might have induced P-gp up-regulation. This finding has been challenged by several groups on the basis that only one P-gp antibody was used in the experiment and it has been suggested that in certain cell types, the glycosylation state of P-gp can mask the antibody binding site of MRK16 [172, 186, 515]. It is of interest to note that using a rabbit polyclonal anti-P-gp antibody, a group of researchers including Pardridge demonstrated P-gp expression on both astrocytes and ECs from normal primate brain [484]. Bendayan *et al* [213] have also noted astrocytic P-gp expression from human brain tissue sections using TEM. Whilst the numerous data describing BEC P-gp expression far outweighs the relatively few studies, described above, which do not show P-gp expression by BECs, this does not exclude the possibility that astrocytes do express P-gp. A recent study by Volk [248] indicated that in acetone-fixed rat brain tissue, P-gp is predominately expressed by capillary ECs and weakly by perivascular

astrocytes. After kainate induced seizures, P-gp was found unregulated in hippocampal neurones but not in astrocytes. Interestingly, however, in PAF- fixed sections, P-gp localisation was absent in BECs, whilst astrocytic P-gp expression was found up-regulated post-seizures [248]. This demonstrates that the fixation method can alter the pattern of P-gp expression, which could explain the results obtained by Pardridge. Astrocyte P-gp up-regulation has been observed in animal studies in response to seizure inducing agents [520] and increased astrocytic P-gp staining has been observed in epileptic brain tissue specimens [521]. Such observations may indicate a role for astrocytes as a second line of defence, to protect the brain after insult [522]

In this study P-gp expression was observed on both primary BECs and hCMEC/D3 cells, which is consistent with the P-gp staining found in isolated human brain capillaries [212] and tissue sections [483].

2.4.3 Sub-cellular P-gp localisation by hBEC

In this study, P-gp expression was localised to the membrane/organelle fraction, when isolated using differential detergent fractionation. Using TEM and immunogold staining, P-gp was found to be localised mainly in or at the apical membrane, although labelling in the cytoplasm and basolateral membrane was also observed. These results are in partial agreement with Bendayan *et al* [213] who found abluminal, luminal and cytoplasmic (cytoplasmic vesicles, Golgi complex, and rough endoplasmic reticulum) staining of P-gp in rat and human brain tissue. However, Bendayan demonstrated abluminal polarisation of P-gp in rat brain tissue and overall the number of gold particles per μm of membrane was much higher than that observed in our study (1.17 ± 0.04 abluminal, 0.85 ± 0.03 luminal compared to 0.038 ± 0.009 and 0.11 ± 0.017, respectively, in this study). These contrasting results might reflect species differences between rats and humans. Indeed, numerous lines of evidence point to the polarisation of P-gp on the

luminal membrane of BECs. Luminal P-gp expression has been observed in isolated human brain capillaries [212] and human tissue [483]. Virgintino *et al* [483] have demonstrated, using confocal microscopy, luminal microvessel P-gp expression in the human cerebral cortex. *In vivo*, Mdr1a or mdr1a/b knock out mice display enhanced accumulation of many intravenously injected P-gp substrates, including cyclosporin A, vinblastine, digoxin, morphine and digoxin, colchicine and morphine (reviewed [172, 186]). The polarised nature of BEC function has been demonstrated *in vitro* on isolated BECs grown on filter inserts, which show directional transport of cyclosporin A and vincristine in mouse BECs [211, 523].

In summary, the expression of P-gp by BECs is more likely to be luminal in nature as a protection mechanism from blood substrates. However, further research is required to clarify differences in the polarisation of P-gp expression by BECs across species.

2.4.2 Cytotoxicity of P-gp and BCRP substrates and inhibitors

FTC is a selective inhibitor of BCRP. The ability of FTC to block BCRP was first described by Rabindran *et al*, [524] who demonstrated that FTC was able to reverse the drug resistance of a human carcinoma cell line. Since that discovery, FTC has been used in a variety of cellular models at doses in the 5-10 μM range, to inhibit BCRP function [525-528] and its toxicity has been evaluated *in vivo* [529]. It has been suggested that FTC acts as a competitive inhibitor of BCRP [524]. The finding that FTC was non-toxic up to 22 μM for 48 h to hCMEC/D3 cells meant that subsequent experiments could be carried out in the μM range.

As mentioned in section 1.1.5.1, P-gp expression has been detected in many tumours, conferring tumour cell resistance to many anti-cancer drugs. To combat this multidrug resistance, many P-gp inhibitors have been developed (reviewed [530]). Tariquidar (XR9576) is a 3rd generation P-gp inhibitor that has been demonstrated to block

P-gp activity in cell cultures at concentrations in the nM range and is also effective *in vivo* [487, 531-537]. Tariquidar has been confirmed to have a superior potency than cyclosporin A and verapamil *in vitro*, and also to have a long duration of action, since it is not itself a P-gp substrate. In human and murine cell lines, Tariquidar was found to block the efflux of rh123 mediated by P-gp, and also to increase the cellular of ^{3}H daunorubicin levels, a P-gp/MRP-1 substrate [531]. In the current study, Tariquidar was found to be non-toxic to hCMEC/D3 cells at concentrations up to 600 nM for 48 h and so it was used at 300 nM in subsequently studies, a dose at which it effectively inhibited P-gp activity.

Vinblastine was found to be non-cytotoxic to hCMEC/D3 cells after 24 h incubation, but cytotoxic after 48 h incubation at concentrations over 0.5 μM. The maximum incubation time for that vinblastine was used at later studies was 12 h at 22 μM, i.e. non-cytotoxic concentrations. It is likely, however, that even at a non-cytotoxic dose, vinblastine was altering the protein expression and/or microtubule architecture of hCMEC/D3 cells. Vinblastine is a vinca alkaloid, which is used in cancer chemotherapy as it induces mitotic arrest. Vinca alkaloids bind to tubulin and prevent the assembly of microtubules, halting tumour cells in metaphase [538-540]. Vinblastine has demonstrable toxic effects on ECs [541-543]. In a co-culture model of porcine BECs and astrocytes, Van der Sandt *et al* [543] demonstrated that vinblastine caused a dose-dependent reduction in the TEER of porcine BECs between 0 and 1 μM, after 6 h incubation. This reduction in TEER was increased by the addition of cycloporin A, verapamil and PSC-833. Vinblastine has also been demonstrated to inhibit EC proliferation, motility and organisation at low concentrations [541, 542, 544] and also to up-regulate the expression of genes associated with cell cycle and apoptosis [545]. Pierre *et al* [546] have also demonstrated that treatment of primary isolated rat BECs with 5.51 μM vinblastine results in complete apoptosis of all cells. Tariquidar, FTC and vinblastine have no cytotoxic effects on hCMEC/D3 cells at the doses and incubations times selected for later experiments in this study.

2.4.3 P-gp activity in hCMEC/D3 cells

A rh123 efflux assay was used to determine functional P-gp expression in hCMEC/D3 cells. Rh123 is a low molecular weight (MW 380.82) fluorescent substrate of P-gp, which has been used to investigate P-gp activity in a range of different cell lines. Specifically for BECs, many groups have investigated the net influx of rh123 in the presence or absence of P-gp modulators (Table 2.3). Using this method and the P-gp inhibitor PSC-833, Weksler *et al* [473] have demonstrated that P-gp inhibition increases the intracellular accumulation of rh123 in hCMEC/D3 cells by 50 % after 1 h incubation. In this study, tariquidar and vinblastine inhibited the efflux of rh123 by ~ 55 % and 42 % compared to cells incubated at 4°C. Therefore, the sensitivity of P-gp-mediated inhibition appears similar for rh123 influx and efflux experiments. However, if the raw median fluorescence intensity data for tariquidar and vinblastine is divided by the control data, as carried out for influx data [473], the cellular levels are 779 % and 691 % higher than controls, respectively, revealing an increased sensitivity and improved P-gp functional assay than influx.

The efflux of preloaded rh123 (22 μM) was time-dependent with a $t_{1/2}$ of 13.3 min ± 1.1, whilst in the presence of vinblastine the $t_{1/2}$ was 112.2 ± 3.7 min. The $t_{1/2}$ obtained here is in agreement with Ji *et al.*[547], who obtained a $t_{1/2}$ of similar magnitude in rat primary BECs (~ 20 min). However, in contrast to the relatively modest increase in the $t_{1/2}$ caused by verapamil in that study, in the present study vinblastine caused a much more potent inhibition. These contrasting results could be explained by differences in methodology, since the rat BECs were loaded at 37°C and the data is expressed as a percentage of time zero, rather than cells left at 4°C. The levels of P-gp expression might also differ between the cell lines. Since vinblastine and tariquidar both inhibited rh123 efflux, there is strong evidence that rh123 efflux from hCMEC/D3 cells is mediated by P-gp. In agreement with other research groups, FTC in this study did not inhibit rh123 efflux [473, 548]. BCRP has been demonstrated to recognise rh123 as a substrate only when there

is a mutation at position 482 [221, 230, 549, 550]. Therefore it is likely that hCMEC/D3 express wild type, non-mutated BCRP, since BCRP activity has been demonstrated in hCMEC/D3 cells [473]

The inhibition of P-gp function by tariquidar was longer lasting than that of vinblastine. This observation is in agreement with *Misty et al,* [531] who reported an irreversible long- lasting inhibition of rh123 and ^{3}H daunorubicin efflux by tariquidar in a human ovarian carcinoma cell line, only if the inhibitor was present in the preloading stage. This evidence suggests that tariquidar might be a more suitable inhibitor than vinblastine for the study of the role of P-gp in the CNS penetration of drugs.

2.4.4 Permeability of hCMEC/D3 cells to rh123

The permeability of hCMEC/D3 cells grown on filters to rh123 was unaffected by P-gp inhibition in both the apical-to-basolateral and basolateral-to-apical directions. This result is consistent with Gaillard *et al* [551] who found no significant polarised transport of rh123 and doxorubicin in either direction across porcine BEC monolayers, unless co-cultured with astrocytes (Table 2.3). The lack of polarised P-gp transport may not reflect an unpolarised distribution of P-gp expression by hCMEC/D3 cells as strong luminal expression was observed in this study. Rather, it may reflect a reduced tightness of the EC layer. Rh123 is a small molecular weight molecule (MW 380.80) and the P_e values obtained for rh123 are similar to those obtained for sucrose (1.65×10^{-3} cm/min) in the original description of the hCMEC/D3 cells [473]. This permeability coefficient is high when compared to larger molecular weight molecules (4 kDa FITC- dextran 0.235×10^{-3} cm/min) and it has been suggested that the hCMEC/D3 cells are a good model for measuring the paracellular permeability of molecules over 4 kDa in MW, due to the relatively low TEER values. Thus the tightness of the hCMEC/D3 cells may not be sufficient to allow a barrier function for rh123, masking the contribution of P-gp to

polarised transport [473]. Rh123 is lipophilic whereas sucrose is hydrophilic, and so the main route of entry of sucrose is paracellular, whilst rh123 can cross hCMEC/D3 monolayers by paracellular and transcellular pathways. Therefore, if the hCMEC/D3 cell layers are not very tight, as indicated by the low TEER values obtained by Weksler *et al* [473], then the paracellular diffusion of rh123 will mask the influence of P-gp over its transcellular transport. Astrocytes in the co-culture system described by Gaillard [551] might have increased the TEER values of BECs to an extent that permeability might be solely transcellular in nature. Indeed, Kunhe *et al* [407] have demonstrated that in porcine kidney epithelial cells (LLC cells) transfected with the MDR1 gene, the basolateral-to-apical transport of rh123 was increased compared to untransfected cells. LLC cells form much tighter monolayers than BECs, which may allow rh123 to be used as a polarisation transport marker.

2.5 Conclusions

In this study, functional P-gp expression by hCMEC/D3 cells has been demonstrated. hCMEC/D3 cells were found to express P-gp polarised on the apical membrane as previously reported in isolated human brain capillaries and are therefore a good *in vitro* model for investigating the transport of P-gp substrates. P-gp expression was also found lower than primary BECs in agreement with the literature. The supply of human tissue is fairly limited for this study and so the hCMEC/D3 cell line represents the most suitable human *in vitro* BEC model for investigation P-gp function. Tariquidar and vinblastine were demonstrated to inhibit the efflux of rh123 and so can be used to inhibit P-gp function by hCMEC/D3 cells. Whilst P-gp was functional and polarised, rh123 cannot be used as a as a permeability tracer due to the hCMEC/D3 cells high permeability to low molecular weight molecules.

Type of rh123 experiment	Cell line	Result	Reference
Influx			
	Rat BECs	Net influx of rh123 (5 μM 90 min) increased after the addition of verapamil (10 μM) and amplodipine derivates (CJX1 and CJX2 1-10 μM). Verapamil increased influx by 297.3%	[547]
	Bovine BECs	Net influx of rh123 (4 μM, 20 min) increased after ultrasound induced hypothermia (74 % increase) and PSC-833 (1 μm, 60%).	[552]
	Rat BECs	Net influx of rh123 (2.6 μM, 60 min) increased by 2.5 fold by addition of cyclosporin A (50 μM) in hypoxic BECs.	[251]
	hCMEC/D3 cells	Net influx of rh123 (10 μM, 30 min) increased by 70% of control by PSC-833 (10 μM)	[473]
	Immortalised rat BECs	Net influx of rh123 (10 μM 1 h) increased by PSC-833 (10 μm, 30 min preloading) by ~ 70 %.	[504]
	Mice BECs	Net influx (10 μM, 60 min) decreased by TAT 1-72 partially overcome by verapamil.	[252]
	Bovine BECs	Cyclosporin A and verapamil increase the net intracellular accumulation of 3.2 μM rh123 afer 60 min.	[553]
	Rat BECs	Cyclosporin A (50 μM) and verapamil (200 μM) increase the cellular uptake of rh123 (200 μM).	[247]
	Rat BECs	Glutamate (100 μM, 30min) decreases rh123 accumulation (5 μM, 90 min) to 43 % of control.	[249]

Efflux			
	Rat BECs	BEC loaded with 5 μM rh123 for 90 min at 37°C, followed by incubation at 37°C +/- verapamil (10 μM). Control $t_{1/2}$ ~ 10 min and ~ 20 min with verapamil. Amlodipine derivates also increased cellular retention.	[547]
	Human BECs	BEC loaded with rh123 (10 μM rh123 15 min, followed by 1 h incubation +/- verapamil (30 μM). Cellular retention increased by 1.2-1.4 relative to control.	[554]
	Human Ovarian cancer cell line	2780AD cells loaded for 1 h with 2 μM rh123 +/ tariquidar (200,300nM) and then incubated minus inhibitors for 2 h. Cyclosporin A did no inhibit ($t_{1/2}$ ~ 20 min. Tariquidar caused complete inhibition	[529]
Permeability			
	Rat BECs	Apical-to-basolateral permeability of BECs to rh123 (4 μM) unaffected by PSC-833 (1 μM) after 30 min.	[555]
	LLC-MDR1	LLC-MDR1 cells have increased basolateral to apical transport of rh123 (10 μM), but not apical to basolateral, when compared to LLC.	[407]
	Bovine BECs	No polarised transport of rh123 by bovine endothelial cells alone, only when co-cultured with astrocytes	[551]

Table 2.3. rh123 assays used to investigate P-gp function in brain endothelial cells and epithelial cells.

Chapter 3

Role of P-gp and BCRP in Aβ transport across hCMEC/D3 cells

Abstract

The aim of this study was to investigate whether Aβ was a substrate for the brain efflux transporters P-gp and BCRP. The net influx of fluorescein-tagged Aβ 1-40 and Aβ 1-42 (fAβ 1-42 and fAβ 1-40 at 0.1 μM and 1 Mm, respectively) into hCMEC/D3 cells was unaltered by inhibitors for P-gp (tariquidar, vinblastine) or BCRP (FTC). In addition, the efflux of fAβ 1-40 and fAβ 1-42 from preloaded cells (1 μM, 24 h) was not affected by P-gp and BCRP inhibition. In contrast, at physiological concentrations of Aβ (^{125}I Aβ 1-40, 0.1 nM), influx was increased and efflux was decreased by the addition of P-gp inhibitors (vinblastine, tariquidar) in hCMEC/D3 cells. Importantly, the permeability of the hCMEC/D3 cells to ^{125}I Aβ 1-40 in the apical-to-basolateral direction, but not in the basolateral-to-apical direction, was increased by P-gp and BCRP inhibition. This finding was consistent with P-gp and BCRP acting to prevent blood-borne Aβ peptides entering the brain *in vivo*.

3.1 Introduction

Increased levels of neurotoxic Aβ in the brain are thought to be central in the pathogenesis of AD [302]. A potential therapy for AD is to increase the clearance of Aβ peptides from the brain, thus reducing the amyloid burden (reviewed in [137, 390, 556]). A number of transporters for Aβ have been demonstrated at the BBB which lead to Aβ transport into (RAGE, LRP-2/megalin) or out of (LRP-1, P-gp) the CNS.

LRP-1, a member of the low density lipoprotein receptor family, is the most extensively described brain-to-blood Aβ transporter at the BBB [319, 384, 394-396, 400, 401, 557-563], binding to both free Aβ [395] and Aβ bound to a carrier (ApoE, α2 macroglobulin) [396, 563, 564]. *In vitro*, both Aβ 1-40 and Aβ 1-42 bind with high affinity to two LRP-1 extracellular binding domains, called cluster II and IV [395], which results in internalisation [396] [563] and transcytosis [395] of the peptide in cultured BECs. *In vivo*, Aβ binds at the abluminal membrane of BECs via LRP-1 [395] and results in the transcytosis and clearance from the brain [319, 394, 395], whilst LRP-1 in the liver clears Aβ from the circulation [565] in rats. Recently, Sagare *et al*, [319] demonstrated that soluble recombinant LRP-1 cluster IV can reduce Aβ-related dysfunction in mice heterogeneous for the Swedish mutation of human APP, evidence that suggests treatment may be effective in AD.

RAGE acts to transport Aβ from the blood into the brain [389, 390], and increased microvascular RAGE expression has been observed in AD hippocampi sections compared to controls, whilst decreased BEC LRP-1 expression is found in AD patients [384]. Importantly, Deane *et al* [383] have calculated that if Aβ blood-to-brain transport was shut down, LRP-1 could remove all soluble Aβ from the ISF in the CNS in AD patients in ~ 40 min.

P-gp, similarly to LRP-1, appears to transport Aβ from the brain into the blood, although the interaction is much less well investigated. Lam *et al* [406] were the first to describe *in vitro* that both Aβ 1-40 and Aβ 1-42 bind to P-gp, using a human embryonic

kidney cell line (K269sw) enriched with the human MDR1 gene product and vesicles derived from the membrane of CHO cells. Further *in vitro* [407] evidence has shown that porcine kidney epithelial cells transfected with human MDR1 (LLC-MDR1), transcytose Aβ 1-40 and Aβ 1-42 from the basolateral-to-apical compartments when grown on filter inserts, and this transport is inhibited by cyclosporin A. *In vivo* data is consistent with *in vitro* observations. Cirrito *et al* [408] have found that Mdr1a/b(-/-) mice clear intracerebrally injected ^{125}I Aβ 1-40 and 1-42 from the CNS at half the rate of wild type mice. However, LRP- 1 was found to be down-regulated at the BBB of these mice. To clarify the contribution of P-gp to Aβ clearance, the same research group went on to show that Tg2576 transgenic mice (harbouring the human APP Swedish mutation gene), treated with a P-gp inhibitor (XR9576), have increased ISF levels of Aβ in the brain. Whilst there is no direct evidence of P-gp dysfunction in AD patients, it is of note that Vogelgesang *et al.* [409] found an inverse correlation between senile Aβ plaque deposition and P-gp expression in the median temporal lobe of non-demented subjects. There is also a reported P-gp down-regulation in Creutzfeldt-Jacob disease, a disease in which, at later stages, amyloid plaques and prion proteins are sometimes found aggregated [566].

There do, however, remain a few questions over the interactions between P-gp and Aβ at the BBB. The *in vitro* data collected thus far has originated from cell types that are not BEC in origin and so may express different levels of P-gp in addition to other Aβ transporters. Whilst the few *in vitro* studies too support the notion of P-gp functioning as a transporter for Aβ, a recent study using MDCK epithelial cells transfected with the human MDR1 gene (MDCK-MDR1 cells), found that the basolateral-to-apical transport of Aβ was the same for MDCK and MDCK-MDR1 cells [561]. Furthermore, using the P-gp inhibitors verapamil and quinidine, the brain-to-blood transport of human Aβ at the rat BBB *in vivo* has been demonstrated to be partially due to LRP-1, but not to P-gp [560].

In chapter 2, it was demonstrated that hCMEC/D3 cells express functional P-gp polarised to the apical membrane. The aim of this chapter was to investigate whether P-gp

and BCRP could act as transporters of Aβ at high concentrations (0.1-1 μM), using fluorescein tagged Aβ, and at physiological concentrations of Aβ, (0.1 nM) using ^{125}IAβ. To do this, the effects of P-gp and BCRP inhibition on the net influx of Aβ, and efflux of Aβ preloaded from hCMEC/D3 cells, were investigated. If Aβ is a substrate for P-gp or BCRP, then their inhibition would be expected to increase Aβ net influx and decrease efflux from hCMEC/D3 cells, as is noted with other P-gp substrates such as rh123. It should be noted however, that influx and efflux, as indicated by cellular levels, represents all process by which Aβ could associate and dissociate with the hCMEC/D3 cells. These include receptor mediated transport, diffusion, endocytosis, vesicular release and any 'sticking' to the cell membrane. In addition, the contribution of each transporter to the permeability of hCMEC/D3 cells to Aβ was investigated.

3.2 Methods

3.2.1 MTT cytotoxicity assay

Aβ 1-40, Aβ 1-42 (Bachem, Weil am Rhein, Germany), scrambled Aβ 1-40 and scrambled Aβ 1-42 (sAβ) (Covalence, California, USA) peptides were dissolved in DMSO (stock of 5 mM), and stored in Sigmacote (Sigma-Aldrich, Dorset, UK)-coated eppendorf tubes at -80°C. The toxicity of Aβ and sAβ peptides was investigated after 48 h incubation with a concentration range of 0.05 to 5 μM, in the presence of tariquidar (300 nM) or FTC (22 μM) in vehicle, or medium containing vehicle alone, using the MTT method described in section 2.2.10. The data is presented as a percentage of the vehicle control, however statistical analysis was performed on the raw data.

3.2.2 Influx of fluorescein-conjugated Aβ (fAβ) peptides

Fluorescein tagged Aβ (fAβ) peptides (Anaspec, California, USA) were dissolved and stored as for Aβ peptides (section 3.2.1). 1 x 10^5 hCMEC/D3 cells were seeded on collagen-coated 12 well plates, grown to confluence, and left for 1-2 days. 500 μl of fresh culture media was then added, containing 1 μM fAβ1-40 or fAβ1-42, and the hCMEC/D3 cells were incubated for 1, 6, 24 or 48 h at 37°C. At each time point, hCMEC/D3 cells were detached, washed twice in PBS and resuspended in 500 μl of PBS. The samples were then analysed using a FACSCalibur flow cytometer with Cellquest software (488 nm $\lambda_{excitation}$, 530 nm $\lambda_{emission}$) and the median fluorescence of 10,000 cells per sample was read. The median fluorescence intensity of a negative control, not incubated with fAβ, was used for statistical analysis.

To characterise the concentration-dependent influx of fAβ with BECs, hCMEC/D3 cells were grown to confluence and incubated with 0.001, 0.01, 0.1 and 1 μM fAβ 1-40 or fAβ 1-42 for 24 h and analysed via flow cytometry as described above.

In order to investigate the role of different transporters/receptors in the influx of fAβ with BECs, hCMEC/D3 cells were grown to confluence and either 1 μM fAβ 1-40 or 0.1 μM fAβ 1-42 was added for 24 h with 300 nM tariquidar, 22 μM vinblastine, 22 μM FTC, 200 nM receptor associated protein (RAP, an inhibitor of LRP, EMD Biosciences, California, USA), 2 μM Aβ 1-40, 2 μM sAβ 1-40, 2 μM Aβ 1-42, 2 μM sAβ 1-42 or a DMSO vehicle control. hCMEC/D3 cells were then detached and read via flow cytometry as previously described, with the exception that background fluorescence was subtracted from all treatments prior to statistical analysis.

3.2.3 Efflux of fAβ 1-40 and fAβ 1-42

hCMEC/D3 cells were grown to confluence as described in section 3.2.2 and preloaded with 1 μM fAβ 1-40 or fAβ 1-42 for 24 h. hCMEC/D3 cells were then detached, washed and incubated at 37°C in culture media for 1, 3, 6 and 12 h or incubated at 4°C for 12 h. The samples were kept at 4°C until all incubation time points had been collected and the samples were washed twice in PBS and resuspended in 500 μl of PBS. The fluorescence intensity of cells was then measured via flow cytometry as described in 3.2.2. The median fluorescence intensity of each sample after background subtraction was expressed as a percentage of that for fAβ preloaded cells that had been kept at 4°C.

In some experiments, hCMEC/D3 cells were preloaded with 1 μM fAβ 1-40 or fAβ 1-42 for 24 h, washed and incubated at 37°C in cell culture media for 6 h with 300 nM tariquidar, 22 μM vinblastine, 22 μM FTC or a DMSO vehicle control and the fluorescence measured by flow cytometry as described above.

3.2.4 Intracellular detection of fAβ by confocal microscopy

hCMEC/D3 cells were grown to confluence on collagen-coated 12 well tissue culture plates and incubated with 1 μM fAβ 1-40 or fAβ 1-42 for 24 h. hCMEC/D3 cells

were then detached, washed twice in PBS, fixed in 4 % PAF and incubated with 5 μM DRAQ5 in PBS for 1 h. After two washes, the cells were resuspended in PBS and ~ 5 x 10^4 cells were placed on a glass slide and mounted with a glass coverslip. hCMEC/D3 cells were then viewed with a confocal microscope (Leica DMIRBE, Leica, Buckingham UK), taking XY and Z cross sections over a selected field to reconstruct a three dimensional image using Volocity software (Improvision, Coventry, UK).

3.2.5 Influx of ^{125}I Aβ 1-40

hCMEC/D3 cells were seeded on collagen-coated 24 well plates (5 x 10^4 per well), grown to confluence and left for 2 days. Fresh culture media containing 0.1 nM ^{125}I Aβ 1-40 (1110 Ci/mmole, Weil am Rhein, Germany) was then added and the hCMEC/D3 cells were incubated for 0.5, 1, 3, 6 and 24 h. From all samples, the ^{125}I Aβ remaining in the media and in trypsinised hCMEC/D3 cells was measured using a γ-counter (Wallac Wizard, Perkin Elmer, Cambridgeshire, UK).

To further characterise ^{125}I Aβ 1-40 influx, hCMEC/D3 cells were grown to confluence as described above and incubated for 30 min with 0.1 nM ^{125}I Aβ 1-40 and vinblastine (2 μM), tariquidar (300 nM), FTC (2 μM), Aβ 1-40 (100 nM), sAβ 1-40 (100 nM), or a DMSO vehicle control. The ^{125}I Aβ 1-40 counts were then measured in the supernatant and trypsinised cells. For both experiments the amount of protein in each sample was determined using a DC protein assay. For data analysis, the hCMEC/D3 cellular levels of ^{125}I Aβ 1-40, in fentomoles, was related to the total protein in the cell suspension (fmoles/mg).

3.2.6 Efflux of ^{125}I Aβ 1-40

To measure ^{125}I Aβ 1-40 efflux from hCMEC/D3 cells, cells were grown as described in 3.2.5, preloaded with 0.1 nM ^{125}I Aβ 1-40 for 3 h, the culture media removed,

the amount of ^{125}I Aβ 1-40 counted, and fresh culture media added. hCMEC/D3 cells were then incubated for 7.5, 15, 30, 60 and 180 min at 37°C and the ^{125}I radioactivity measured in the trypsinised cells. A further treatment was also collected whereby preloaded cells were incubated at 4°C for 180 min. Cellular ^{125}I Aβ 1-40 levels were calculated as before. The $t_{1/2}$ was calculated with the assumption that the sample incubated at 4°C for 180 min represented the maximal cellular levels of ^{125}I Aβ 1-40 and also represented T = 0 min.

The effect of P-gp and BCRP inhibitors was then investigated on ^{125}I Aβ 1-40 efflux form hCMEC/D3 cells. Fully confluent hCMEC/D3 cells were loaded with 0.1 nM ^{125}I Aβ 1-40 for 3 h and then incubated for 10 min at 37°C in fresh culture media containing vinblastine (2 μM), tariquidar (300 nM), FTC (2 μM) or DMSO and the ^{125}I radioactivity measured in trypsinised cells as above.

3.2.7 The permeability of hCMEC/D3 cells to ^{125}I Aβ 1-40

hCMEC/D3 cells were grown on filter inserts (0.4 μm pore diameter, 12 mm diameter), until confluent and rested for 1-2 days. The permeability of hCMEC/D3 cells to ^{125}I Aβ1-40 and the paracellular tracer ^{14}C Inulin was then determined. Fresh media containing 0.1 nM ^{125}I Aβ and 0.1 mM ^{14}C Inulin (1-3 μCi/mg; MP biomedicals, Ohio, USA) in the presence of vinblastine (2 μM), tariquidar (300 nM), FTC (2 μM) or DMSO vehicle contol was added to the apical or basolateral chamber and left for 30 min. The amount of ^{125}I Aβ 1-40 in the apical medium, basolateral medium, trypsinised cells and filter was then counted. For ^{14}C inulin, the amount in the apical and basal compartments was measured (Wallac trilux, Perkin Elmer, Cambridgeshire, UK).

The data was analysed using an Aβ clearance quotient (Aβ CQ) as described by Nazer *et. al.* [561] with modifications:

$$A\beta\ CQ_{BL} = \frac{^{125}I_{AP} / {}^{125}I_{total}}{^{14}C_{AP}/^{14}C_{total}} \qquad A\beta\ CQ_{AP} = \frac{^{125}I_{BL} / {}^{125}I_{total}}{^{14}C_{BL}/^{14}C_{total}}$$

$^{125}I_{total}$ represents the total counts for the apical and basal compartments plus trypsinised cells plus the filter. $^{14}C_{total}$ is the total inulin counts for apical and the basolateral compartment. $^{125}I_{AP}$ are the apical counts whilst $^{125}I_{BL}$ represents basolateral counts. The amount of ^{125}I in the trypsinised cells only accounted for ~ 0.2% of total ^{125}I counts and so whilst not accounted for with the ^{14}C counts, the contribution was considered to be negligible.

3.2.8 Statistical analysis

All data are represented as means +/- SEM and the number of experiments, n, indicated each time. For all experiments, the statistical significance was calculated using ANOVA followed by Student's t test, comparing each treatment to the control (* $P < 0.05$, ** $P < 0.01$). For the permeability, influx and efflux experiments, a paired t-test was employed, since each experiment was carried out with paired control and treated samples.

3.3 Results

3.3.1 Cytotoxicity of Aβ 1-40 and Aβ 1-42 peptides to hCMEC/D3 cells

An aim of this chapter was to investigate the interactions of Aβ peptides with P-gp and BCRP at high and low concentrations. An MTT cytotoxicity assay was initially carried out to ensure that non-toxic concentrations of Aβ were used (Figures 3.1 and 3.2). Incubation of hCMEC/D3 cells with Aβ 1-40, sAβ 1-40, Aβ 1-42 or sAβ 1-42 for 48 h did not affect cell viability over the concentration range 0 - 5 μM as assessed by formazan production from MTT ($n = 3$, $P > 0.05$). Following co-incubation of Aβ and sAβ peptides with tariquidar (300 nM) or FTC (22 μM), there was no increase in Aβ-induced cytotoxicity to hCMEC/D3 cells ($n = 3$, $P > 0.05$). This suggests that if P-gp or BCRP inhibition increase Aβ levels in hCMEC/D3 cells, this was not sufficient to induce cell death at the concentrations used here. The highest concentration of Aβ used in subsequent experiments was 1 μM for 24 h incubation.

3.3.2 Sub-cellular localisation of fAβ peptides as assessed by confocal microscopy

In order to investigate the interaction of Aβ with hCMEC/D3 cells, fAβ was employed for ease of detection. fAβ differs from Aβ, by the addition of a fluorescein molecule on the N-terminus of the peptide and it should be noted that the fluorescence tag increases the molecular weight of Aβ 1-40 from 4329.86 to 4688.2 and Aβ 1-42 from 4514.1 to 4873.4. For Aβ to be effluxed from hCMEC/D3 cells by BCRP and/or P-gp, it should first access the intracellular compartment. Therefore, confocal imaging was carried out to investigate fAβ peptide sub-cellular localisation (Figure 3.3 and 3.4). Confocal imaging shows that both fAβ peptides appeared intracellularly but not in nuclear compartments. There is particularly strong staining in the area around the nucleus, where

the golgi apparatus, which is involved in the trafficking of vesicles, is located. These data indicate that a high proportion of fAβ peptides are located intracellularly.

3.3.3 Influx of fAβ peptides into hCMEC/D3 cells

Next, the effect of P-gp, BCRP and LRP-1 inhibition on fAβ influx was investigated. Initially, a time-course and dose-response curve of fAβ 1-40 and fAβ 1-42 influx into hCMEC/D3 cells was determined, in order to pick optimal conditions for subsequent influx experiments with inhibitors (Figure 3.5). 0.1 μM fAβ 1-42 influx into hCMEC/D3 cells increased with time, with a maximum at 24 h, and then a slight decrease after 48 h incubation to 70.4 % ± 1.8 of maximum levels ($n = 3$, $P > 0.05$). The pattern of fAβ 1-40 influx was similar, reaching a maximum at 24 h and then decreasing to 75.9 % ± 1.53 of maximum levels after 48 h incubation ($n = 3$, $P > 0.05$). However, from 6 h, the median fluorescence intensity values for fAβ 1-40 were much lower than those for fAβ 1-42 (e.g. 56 ± 16 and 20 ± 1.5 for fAβ 1-42 and 1-40, respectively, after 24 h incubation). For fAβ 1-40, the median fluorescence intensity was higher than background for all time points investigated ($n = 3$, $P < 0.01$) whilst for fAβ 1-42 the levels were only significant at 24 h and 48 h ($n = 3$, $P < 0.05$) due to the high variability at lower time points. The results indicate that the maximal influx of both fAβ species into hCMEC/D3 cells occurs at 24 h.

The concentration-dependent influx of fAβ peptides into hCMEC/D3 cell was next investigated. A concentration-dependent increase in fAβ 1-42 influx into hCMEC/D3 cells was observed after 24 h incubation, which was significant compared to background median fluorescence intensity at concentrations of 0.1 μM and 1 μM ($n = 3$, $P < 0.05$) but not at lower concentrations. For fAβ 1-40, influx into hCMEC/D3 cells was lower than that for fAβ 1-42, and was only significantly higher than background at the highest dose 1 μM ($n = 3$, $P < 0.05$). In subsequent influx experiments, 1 μM fAβ 1-40 and 0.1 μM Aβ 1-42 were used at 24 h incubation. These parameters were selected to ensure that fAβ 1-42 cellular levels were not maximal in hCMEC/D3 cells so that any increases due to P-gp or BCRP

inhibition could be detected. In the case of fAβ 1-40 only 1 μM could be used, due to the lack of detectable florescence at lower concentrations.

3.3.4 Role of P-gp, BCRP and LRP-1 in fAβ influx into hCMEC/D3 cells

An aim of this chapter was to investigate if Aβ is a substrate for P-gp or BCRP in hCMEC/D3 cells. The net influx of P-gp and BCRP substrates are enhanced by the addition of specific inhibitors as previously demonstrated for rh123 and daunorubicin in hCMEC/D3 cells [473].Whether this was the case for fAβ peptides was therefore investigated. The transcytosis of Aβ across EC monolayers has been described to be mediated by RAGE and LRP (reviewed in [137]) and as part of this process the Aβ peptide would be internalised. The effects of LRP inhibition and unlabelled Aβ peptides were investigated to determine the potential mechanisms of fAβ influx into hCMEC/D3 cells (Figure 3.6). Compared to control levels the influx of 0.1 μM fAβ 1-42 or 1 μM fAβ 1-40 into hCMEC/D3 cells was unaffected by co-incubation with 300 nM tariquidar, 22 μM vinblastine, 22 μM FTC, 200 nM RAP, 2 μM Aβ 1-42, 2 μM Aβ 1-40, 2 μM sAβ 1-42 or 2 μM sAβ 1-40 after 24 h incubation ($n = 3$, $P > 0.05$). These results imply that the influx of Aβ into hCMEC/D3 cells may not be a receptor-mediated event, and that P-gp and BCRP do not play a significant role in Aβ influx at concentration > 100 nM.

3.3.5 Role of P-gp and BCRP in fAβ efflux from hCMEC/D3 cells

The results described in chapter 2 implicated that the efflux of preloaded P-gp substrates from hCMEC/D3 cells is potentially a more sensitive measurement of P-gp activity than net influx as indicated by rh123. Therefore, efflux of preloaded fAβ from hCMEC/D3 cells was investigated using P-gp and BCRP inhibitors. Initially a characterisation of time-dependent efflux was carried out (Figure 3.7). After preloading hCMEC/D3 cells with fAβ peptides, (1 μM, 24 h), the efflux of each peptide was determined over time. Efflux (reduction in cell median fluorescence intensity expressed as

a % of 4°C treated cells) was time-dependent, with a $t_{1/2}$ of 203.2 min ± 14.3 and 216 min ± 3.1 min for fAβ 1-40 and 1-42, respectively (n = 3). For both peptides, the data was significantly different at time points over 6 h incubation when compared to preloaded hCMEC/D3 cells incubated at 4°C (n = 3, $P < 0.05$).

The efflux of hCMEC/D3 cells preloaded with fAβ 1-40 or fAβ 1-42 in the presence of tariquidar (300 nM), vinblastine (22 μM), FTC (22 μM) or a vehicle control was then investigated after 6 h incubation. There was no significant difference in median fluorescence intensity between any treatments compared to the control for both fAβ 1-40 or fAβ 1-42 (n = 8 for fAβ 1-42; n = 4 for fAβ 1-40; $P > 0.05$). The results indicate that, at high concentration of Aβ (1 μM), the contribution of P-gp and BCRP to Aβ efflux from hCMEC/D3 cells in negligible.

3.3.6 Effects of P-gp or BCRP inhibition on the influx of ^{125}I Aβ 1-40 into hCMEC/D3 cells

It is possible that high concentrations of fAβ saturated the transport capability of P-gp in hCMEC/D3 cells, or that the fluorescein tagged peptides are not P-gp substrates as they are more hydrophilic. Therefore, the influx of a lower concentration of 0.1 nM ^{125}I Aβ 1-40 was investigated, which is closer to physiological levels (reviewed in [313]). Firstly, a characterisation of the time-dependent influx of 0.1 nM ^{125}I Aβ 1-40 was carried out. 0.1 nM ^{125}I Aβ 1-40 influx into hCMEC/D3 cells was indeed time-dependent, reaching saturation between 3 and 6 h with a $t_{1/2}$ of 35 ± 5.0 min (Figure 3.10) (n = 3).

Next, the influx of 0.1 nM ^{125}I Aβ 1-40 after 30 min incubation with inhibitors for P-gp (300 nM tariquidar, 2 μM vinblastine), BCRP (FTC 2 μM), unlabelled Aβ or sAβ (100 nM) or a DMSO vehicle was investigated (Figure 3.10). Tariquidar significantly increased ^{125}I Aβ 1-40 influx by 20.9 % ± 0.6 .compared to the control (n = 3, $P < 0.05$). Whilst FTC and vinblastine both increased the influx of ^{125}I Aβ 1-40 into hCMEC/D3 cells

(19.6 % ± 1.1, 10.7 % ± 0.7 respectively) but levels did not reach statistical significance (P = 0.26 for FTC and 0.07 for vinblastine). Aβ 1-40 and sAβ1-40 did not alter ^{125}I Aβ 1-40 levels compared to the control (n = 3, $P < 0.05$). These results indicate, that P-gp, and possibly BCRP, might act to reduce cellular levels of ^{125}I Aβ 1-40 at 0.1 nM, and that Aβ influx is not a receptor-specific phenomenon in hCMEC/D3 cells.

3.3.7 The role of P-gp or BCRP on ^{125}I Aβ 1-40 efflux from hCMEC/D3 cells

To further explore the possibility that Aβ might be a P-gp or BCRP substrate in hCMEC/D3 cells, the efflux of ^{125}I Aβ 1-40 was investigated (Figure 3.11). After preloading hCMEC/D3 cells with 0.1 nM ^{125}I Aβ 1-40 for 3 h, efflux was time-dependent, with a $t_{1/2}$ of 11.6 min ± 0.88 (using preloaded hCMEC/D3 cells incubated at 4°C as a measure of maximal cellular levels).

hCMEC/D3 cells were preloaded with 0.1 nM ^{125}I Aβ 1-40 and incubated for 10 min with P-gp and BCRP inhibitors. Compared to the control, tariquidar (300 nM) and vinblastine (2 μM) both increased cellular levels of ^{125}I Aβ 1-40 by 62.2 % ± 17.6 and 53.8 % ± 7.2 , respectively (n = 3, $P < 0.05$). Whilst FTC (2 μM) increased cellular levels by 27 % ± 13.6, the levels did not reach statistical significance (n = 3, $P > 0.05$). The levels of cellular ^{125}I Aβ 1-40 in hCMEC/D3 cells incubated at 4°C for 10 min had increased by 157.8 % ± 21.1 of controls (n = 3, $P < 0.01$). These results indicate that P-gp, and to a lesser extent BCRP, contribute to ^{125}I Aβ 1-40 efflux from hCMEC/D3 cells, in addition to other mechanisms which may include receptor-mediated transport, vesicle-mediated secretion or diffusion from either inside the cells or from the membrane.

3.3.8 The permeability of hCMEC/D3 cells to ^{125}I Aβ 1-40

Since P-gp, and to a lesser extent BCRP, have roles in the influx and efflux of 0.1 nM ^{125}I Aβ 1-40, they may also be a factor in determining the permeability of hCMEC/D3 cells to ^{125}I Aβ 1-40. Although the results of chapter 2 have indicated that hCMEC/D3 cells

are not a suitable model for studying the permeability to small molecules (rh123), it has been proposed that they are adequate to study the paracellular permeability of tracers with a MW of 4 kDa or greater [473]. The permeability of hCMEC/D3 cells grown on filters to 0.1 nM ^{125}I Aβ 1-40 in the presence of tariquidar (300 nM), vinblastine (2 μM) and FTC (2 μM) or a vehicle control was thus investigated over 30 min (Figure 3.10 and 11). In order to take into account potential alterations in paracellular permeability, the permeability to ^{14}C inulin, which has a similar molecular weight, was used as a correction factor.

From the apical-to-basolateral chambers, the permeability of filter inserts to ^{125}I Aβ 1-40 was higher than that of hCMEC/D3 cells on filters, by around 250 % ($n = 6$, $P < 0.05$). This was also the case for the basolateral-to-apical transport, where in the absence of hCMEC/D3 cells, 185 % more ^{125}I Aβ 1-40 crossed into the apical chamber compared to hCMEC/D3 cells on filters ($n = 6$, $P < 0.05$). Higher total ^{14}C inulin also crossed from the apical-to-basolateral (152 %) and baolateral-to-apical side (420%) in the absence of cells, compared to cells of filters ($n = 3$, $P < 0.05$). The hCMEC/D3 cells therefore formed a barrier to the passage of both ^{125}I Aβ 1-40 and ^{14}C inulin (Figure 3.10).

The Aβ CQ_{AP} of hCMEC/D3 cells when compared to control levels was increased by 54.2 % ± 16.3 with tariquidar (300 nM), 40.8 % ± 19.9 with vinblastine (2 μM) and 18.9 % ± 4.0 by FTC (2 μM) ($n = 6$, $P < 0.05$). In contrast, the Aβ CQ_{BL} was unaltered by tariquidar, vinblastine or FTC ($n = 6$, $P > 0.05$). When ^{125}I Aβ 1-40 was applied on the apical side, cellular levels of ^{125}I Aβ 1-40 in hCMEC/D3 cells was increased by tariquidar (20 % ±16), vinblastine (46 % ± 23) and FTC (88 % ± 65), although these increases were not statistically significant. When ^{125}I Aβ 1-40 was applied to the basolateral side, no such increase in influx was observed with any of the inhibitors (Figure 3.11).

These results suggest that P-gp and BCRP act to prevent the movement of Aβ from the apical-to-basolateral side of the cells, which is consistent with the luminal P-gp expression observed in chapter 2.

(a)

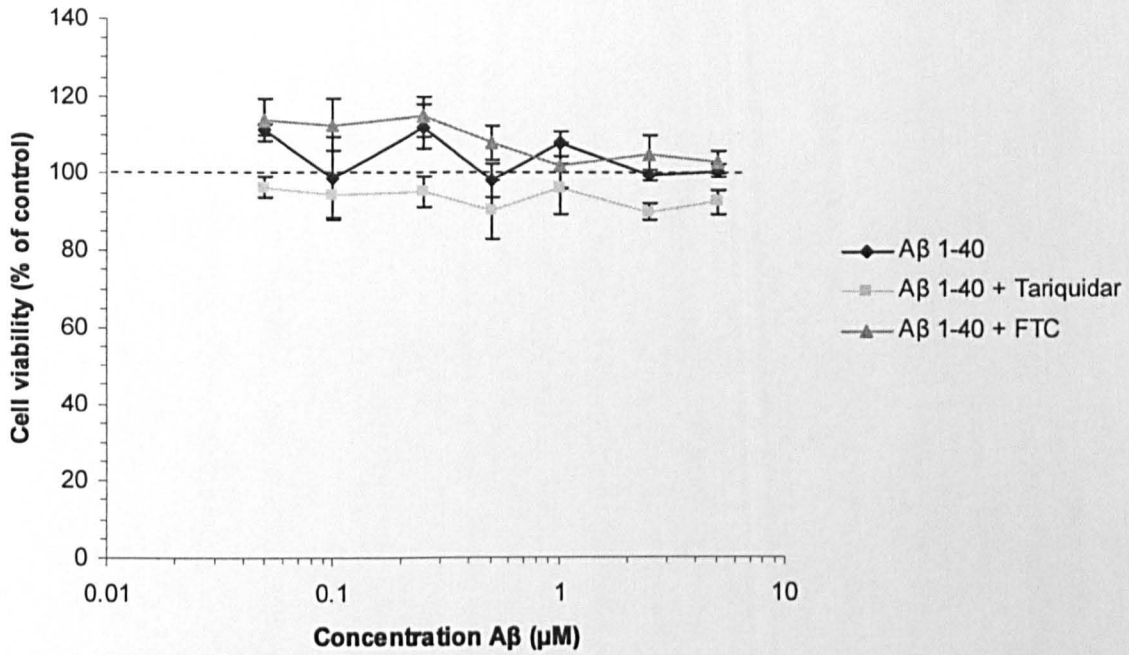

(b)

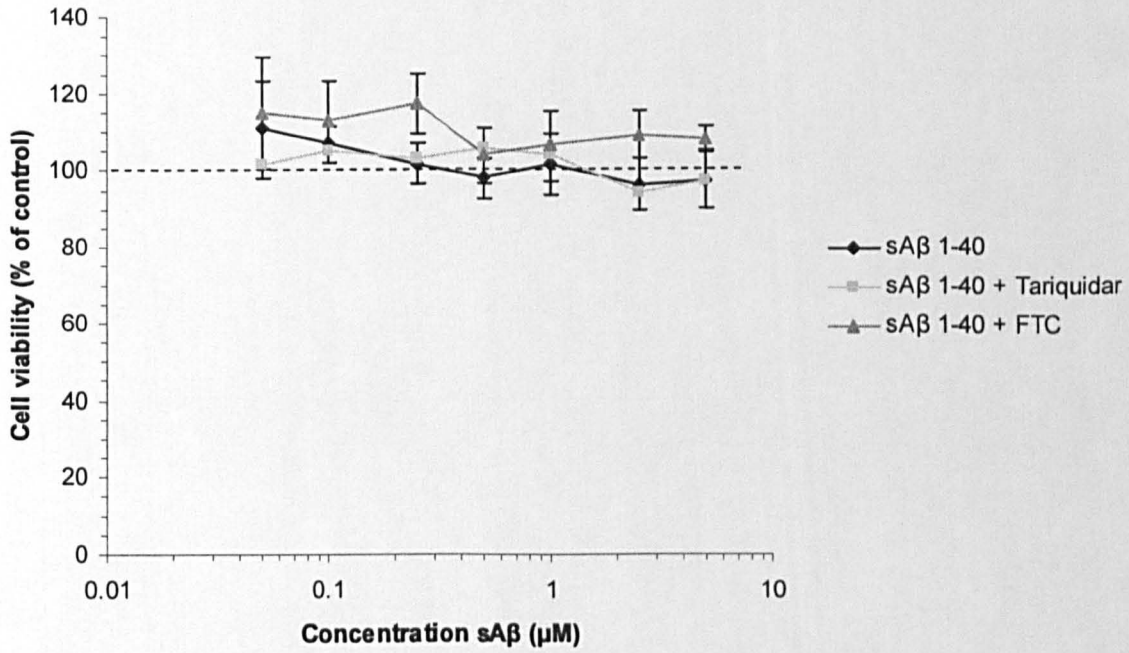

Figure 3.1. Cytotoxicity of Aβ 1-40 to hCMEC/D3 cells as assessed by an MTT assay. The cytotoxicity of **(a)** Aβ 1-40 or **(b)** sAβ 1-40 (0 - 5 μM) to fully confluent hCMEC/D3 cells was determined over 48 h in the presence of tariquidar (300 nM), FTC (22 μM) or a vehicle control using an MTT assay. Data represents mean ± SEM, n = 3 with quintuplet samples plotted on a semi-logarithmic scale. The SEM of controls values (100) were ± 12.1 and ± 16.7 for Aβ and sAβ, respectively. $P > 0.05$ using Student's t test for raw data compared to vehicle control.

(a)

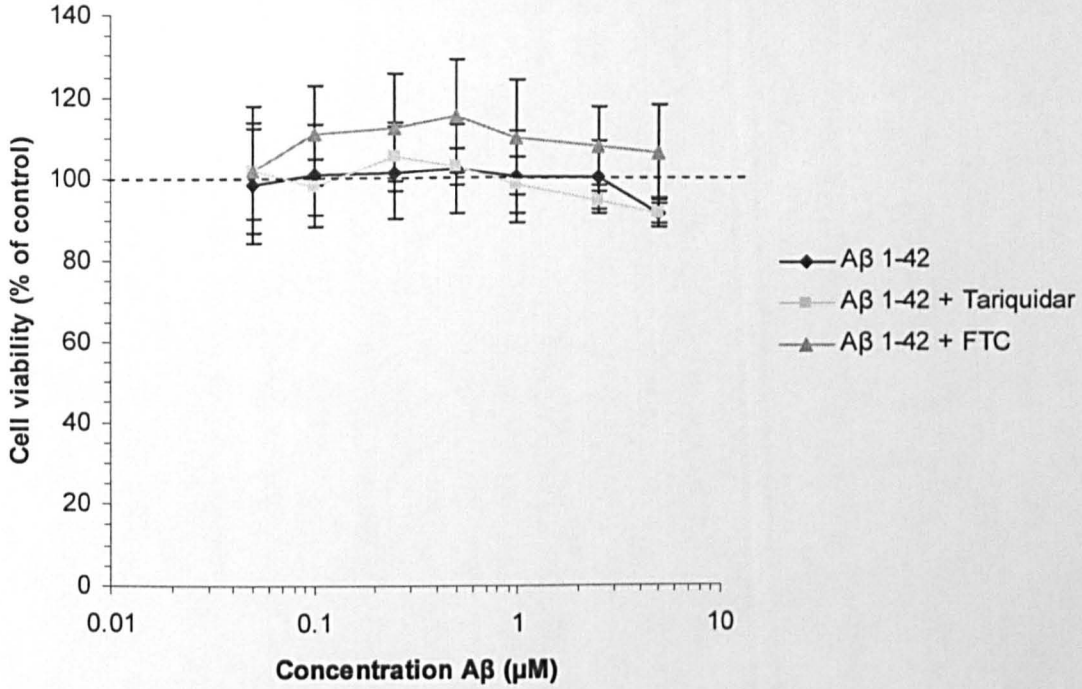

(b)

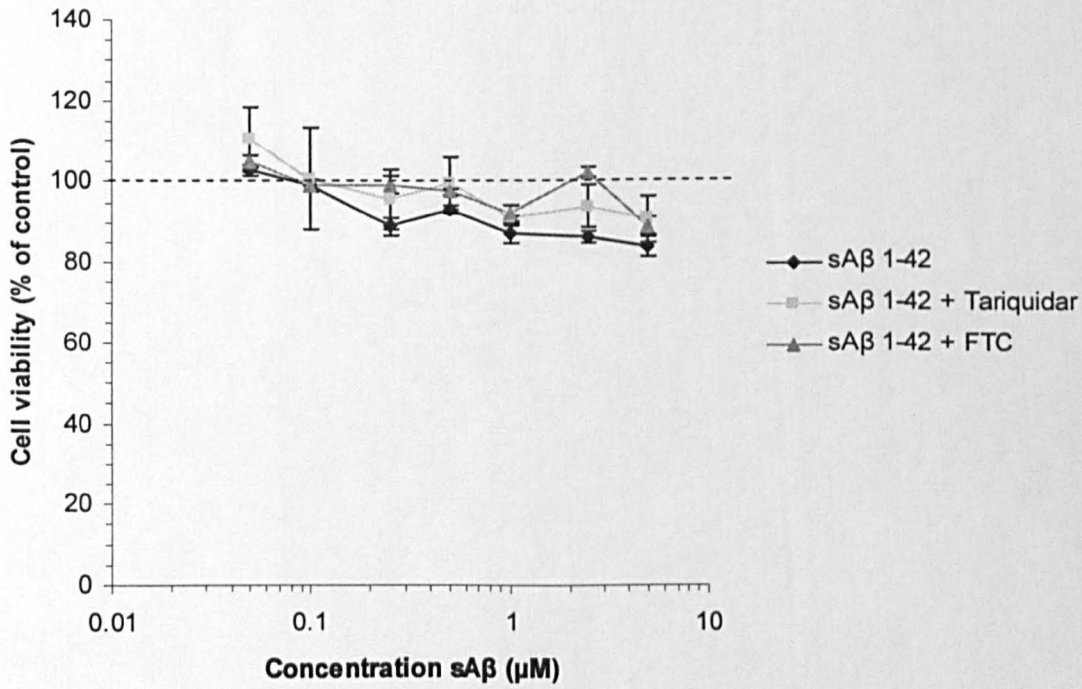

Figure 3.2. Cytotoxicity of Aβ 1-42 to hCMEC/D3 cells as assessed by an MTT assay. The cytotoxicity of **(a)** Aβ 1-42 or **(b)** sAβ 1-42 (0 - 5 μM) to fully confluent hCMEC/D3 cells was observed over 48 h in the presence of tariquidar (300 nM), FTC (22 μM) or a vehicle control using an MTT assay. Data represents mean ± SEM, n = 3 with quintuplet samples plotted on a semi-logarithmic scale. SEM of controls values (100) were s ± 12.1 and ± 16.7 for Aβ and sAβ respectively. $P > 0.05$ using Student's t test for raw data compared to vehicle control.

(a) (b)

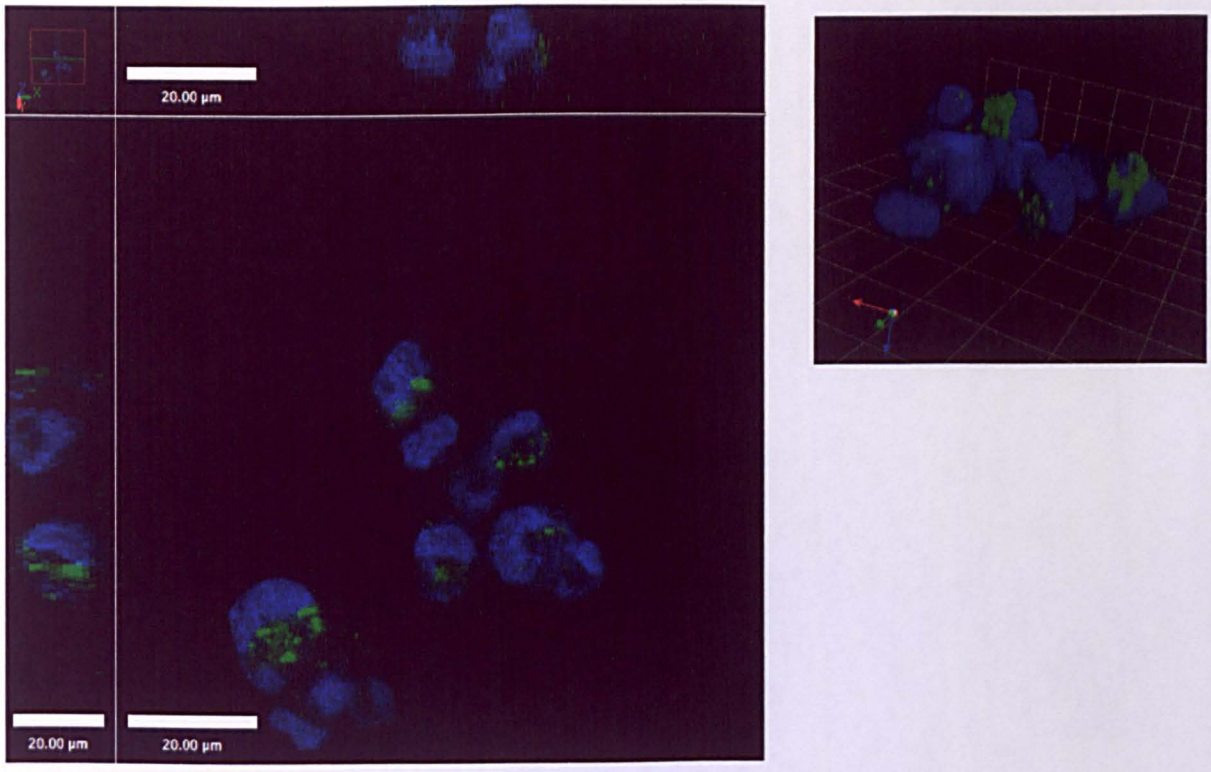

(c) (d)

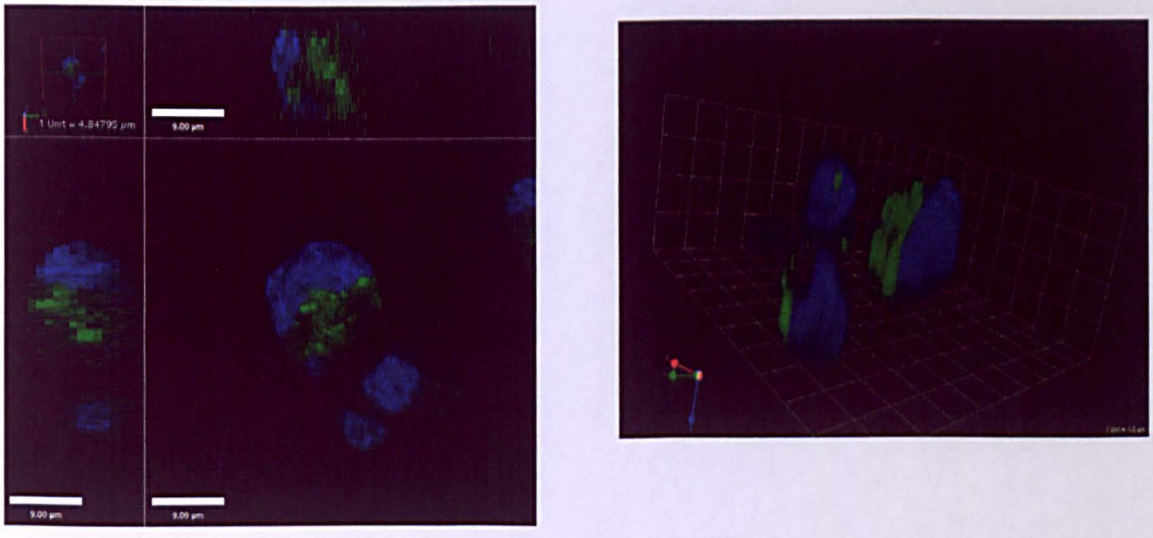

Figure 3.3. Sub-cellular localisation of fAβ 1-42 in hCMEC/D3 cells as viewed by confocal microscopy. hCMEC/D3 cells were grown to confluence in a 12 well collagen-coated plate, incubated with 1 µM fAβ 1-42 for 24 h, detached, fixed in 4 % PAF, stained with DRAQ-5, mounted and viewed on a confocal microscope. An XY Z cross-section was taken over a selected field **(a,c),** enabling a three dimensional reconstruction with Volocity software **(b,d)**. n = 1 with duplicate samples.

(a) **(b)**

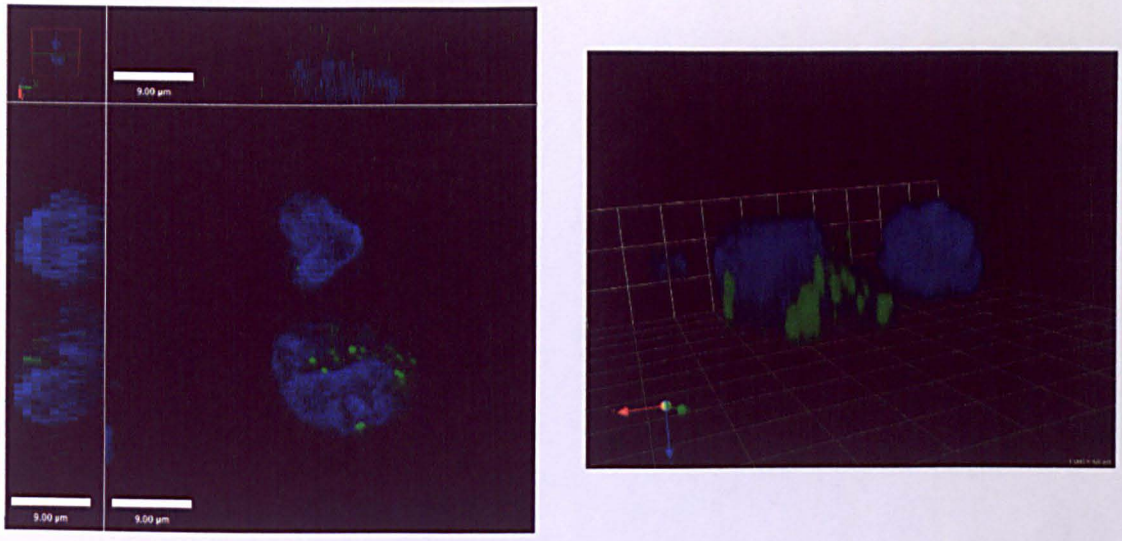

Figure 3.4. Sub-cellular localisation of fAβ 1-40 in hCMEC/D3 cells as viewed by confocal microscopy. hCMEC/D3 cells were grown to confluence in a 12 well collagen-coated plate, incubated with 1 µM fAβ 1-40 for 24 h, detached, fixed in 4 % PAF, stained with DRAQ-5 mounted an viewed on a confocal microscope. An XY Z cross-section was taken over a selected field **(a)**, enabling a three dimensional reconstruction with Volocity software **(b)**. n = 1 with duplicate samples.

(a)

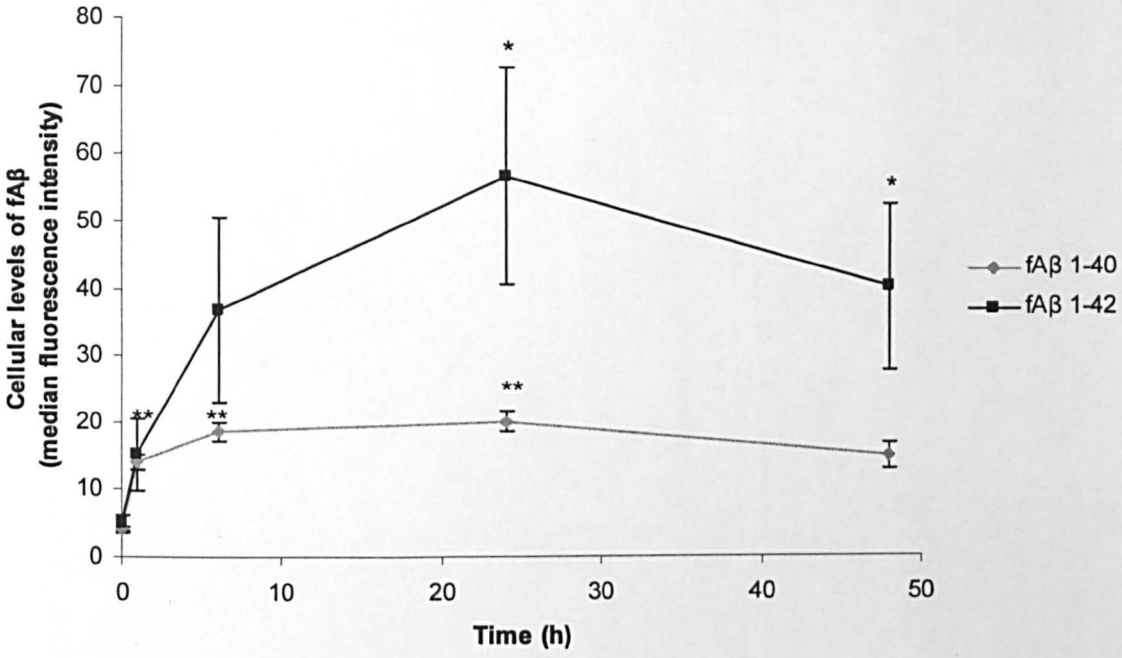

(b)

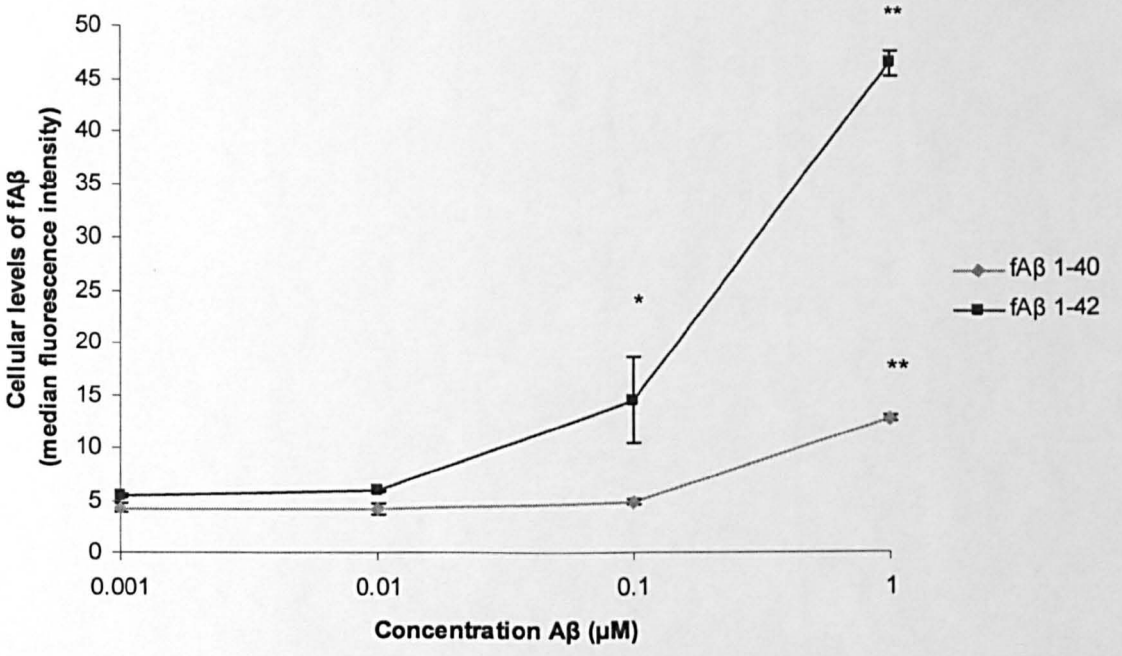

Figure 3.5. The effects of time and concentration on the influx of fAβ peptides into hCMEC/D3 cells. (a) hCMEC/D3 cells were grown to confluence on 12 well plates and incubated for 1, 6, 24 and 48 h with 1 μM fAβ 1-40 or 1-42. The cells were then detached and analysed via flow cytometry (488 nm $\lambda_{excitation}$, 520 nm $\lambda_{emission}$). **(b)** hCMEC/D3 cells were incubated for 24 h with either fAβ 1-40 or Aβ 1-42 at concentrations of 0.001, 0.01, 0.1 and 1 μM before analysis via flow cytometry (488 nm $\lambda_{excitation}$, 530 nm $\lambda_{emission}$). Data represents mean ± SEM, n = 3 with duplicate samples. * $P < 0.05$, ** $P < 0.01$ using paired t test comparing the fluorescence at each time point to background fluorescence, which in **(a)** is represented by time = 0 min on the graph.

(a) fAβ 1- 40 (1 μM, 24 h)

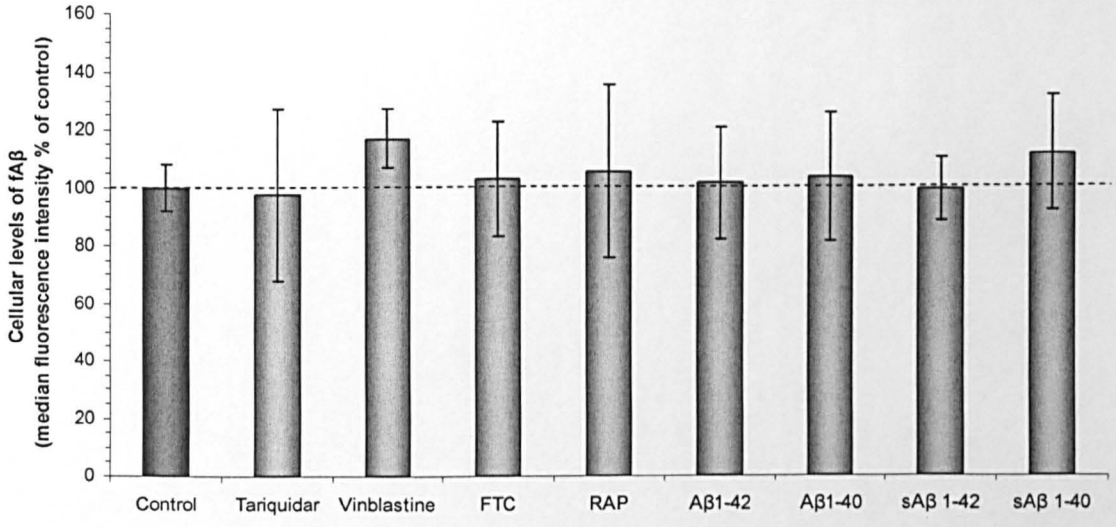

(b) fAβ 1-42 (0.1 μM, 24 h)

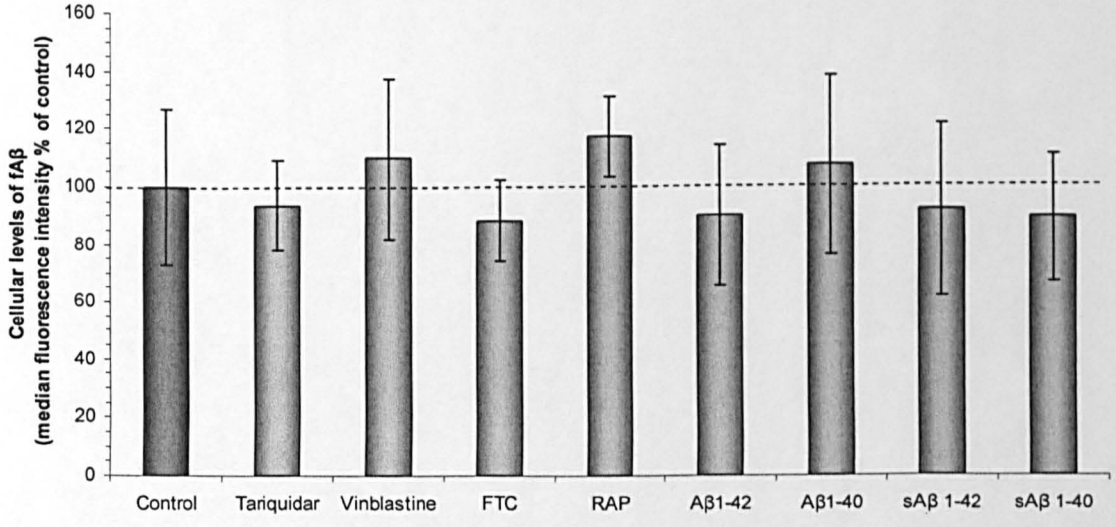

Figure 3.6. The effects of P-gp, BCRP or LRP-1 inhibition on the influx of fAβ peptides into hCMEC/D3 cells. hCMEC/D3 cells were grown until fully confluent, rested for 2 days, and the incubated for 24 h with ether **(a)** 1 μM fAβ 1-40 or **(b)** 0.1 μM fAβ 1-42 in the presence tariquidar (300nM), vinblastine (22 μM), FTC (22 μM), RAP (200 nM), unlabelled Aβ 1-40 or sAβ 1-40 or 1-42 (2 μM) or a DMSO vehicle control. The fluorescence was then measured via flow cytometry (488 nm $\lambda_{excitation}$, 530 nm $\lambda_{emission}$) and expressed as a % of the value for the vehicle control. Data represents mean ± SEM, n = 3 with duplicate samples.

(a)

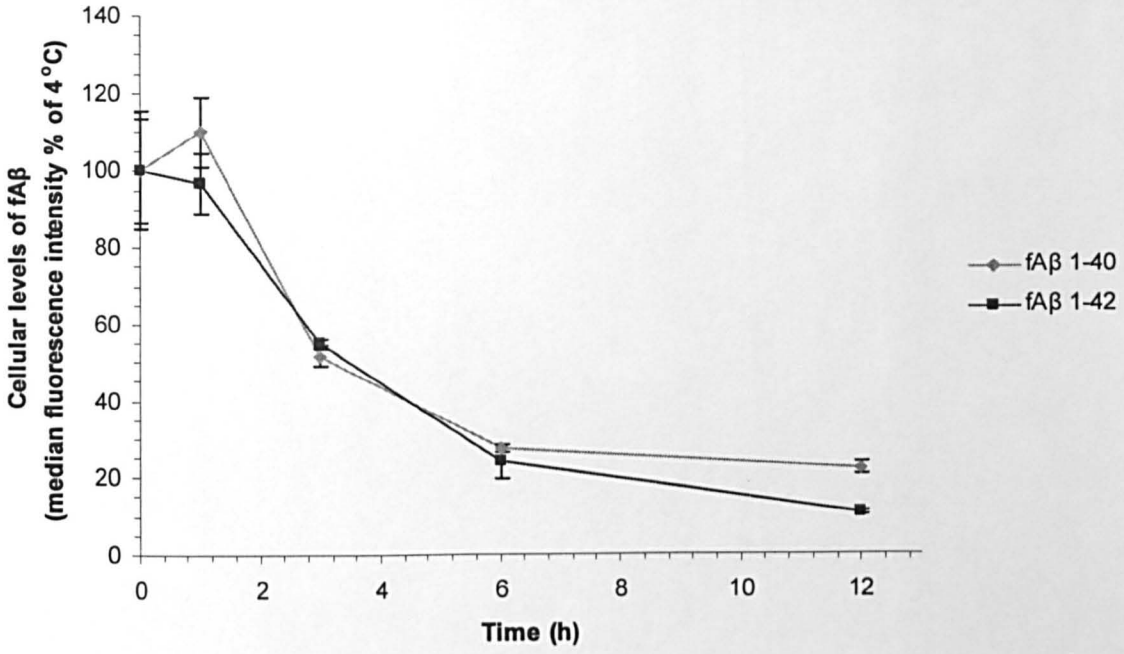

(b)

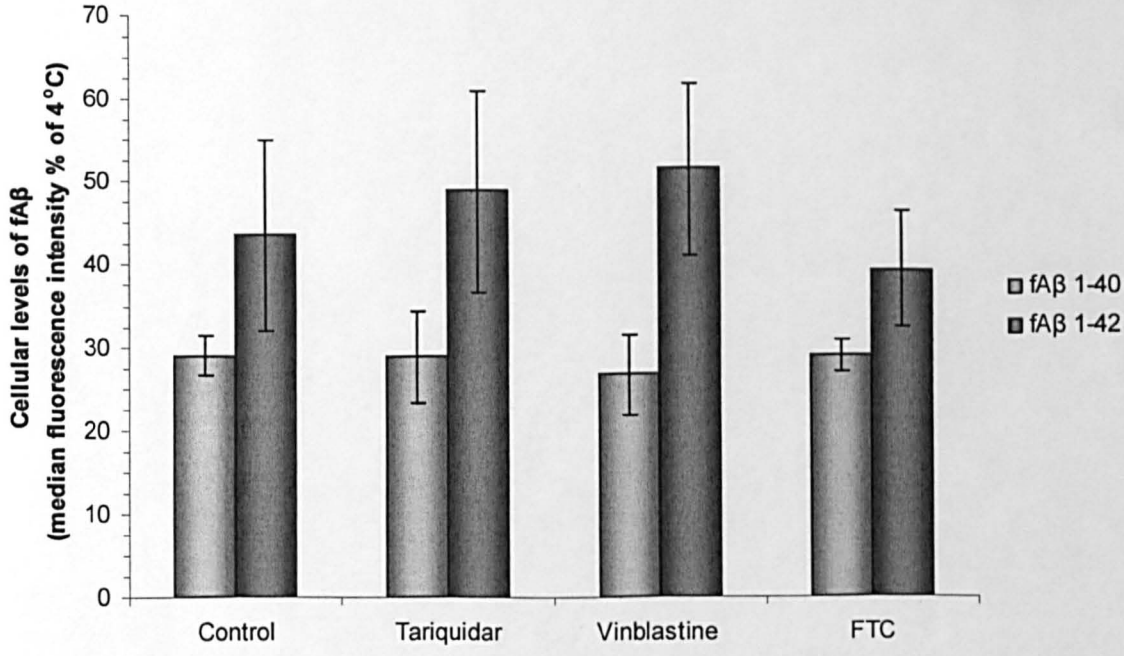

Figure 3.7. The effects of P-gp or BCRP inhibition on the efflux of fAβ peptides from hCMEC/D3 cells. (a) hCMEC/D3 cells were grown to confluence on 12 well plates and preloaded with 1 μM fAβ 1-40 or fAβ 1-42 for 24 h. Cells were then detached and incubated at 37°C for 1, 3, 6 and 12 h, or left at 4°C. The fluorescence was then measured by flow cytometry, and the data expressed as a percentage of fluorescence in cells left at 4°C. Data represents mean ± SEM, n = 3 with duplicate samples.**(b)** hCMEC/D3 cells were preloaded with 1 μM fAβ 1-40 or fAβ 1-42 for 24 h, and then incubated at 37°C for 6 h with tariquidar (300 nM), vinblastine (22 μM), FTC (22 μM) or DMSO vehicle control. The fluorescence was then measured by flow cytometry and the data expressed as a percentage of the 4°C treatment. Data represents mean ± SEM, n = 8 fAβ 1-42 and n = 4 for fAβ1-40 with duplicate samples. $P > 0.05$ using paired t test comparing the raw data to the control.

(a)

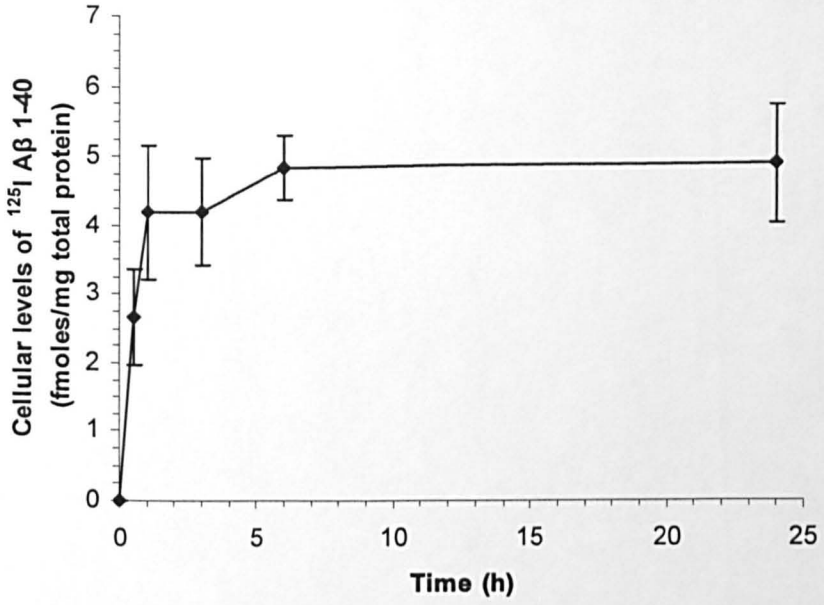

(b)

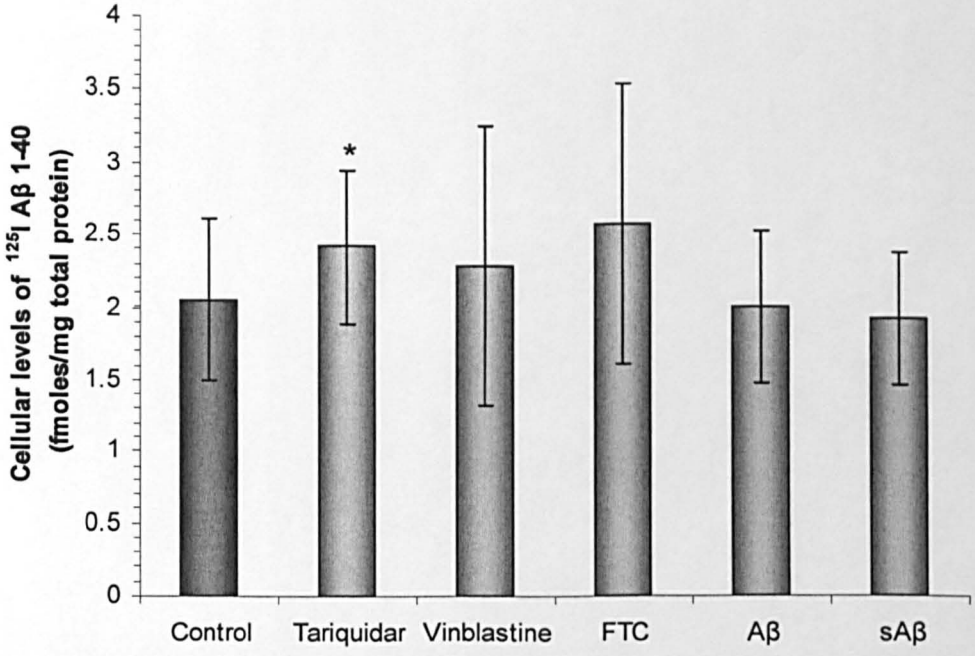

Figure 3.8. The effects of P-gp or BCRP inhibition on the influx of ^{125}I Aβ 1-40 into hCMEC/D3 cells. (a) Fully confluent hCMEC/D3 cells were incubated with 0.1 nM ^{125}I Aβ 1-40 for 0.5, 1, 3, 6 and 24 h, detached and the cellular levels of ^{125}I Aβ 1-40 (fmoles/mg of total protein) were measured using a γ-counter. Data represents mean ± SEM, n = 3 experiments with duplicate samples. **(b)** Fully confluent hCMEC/D3 cells were incubated with 0.1 nM ^{125}I Aβ 1-40 for 30 min in the presence of tariquidar (300 nM), vinblastine (2 μM), FTC (2 μM), Aβ 1-40 (100 nM), sAβ 1-40 (100 nM) or a DMSO vehicle control, and the cellular levels of ^{125}I Aβ 1-40 calculated. Data represents mean ± SEM, n = 4 experiments with duplicate samples. * $P < 0.05$, ** $P < 0.01$ for treatments compared to control using paired t test.

(a)

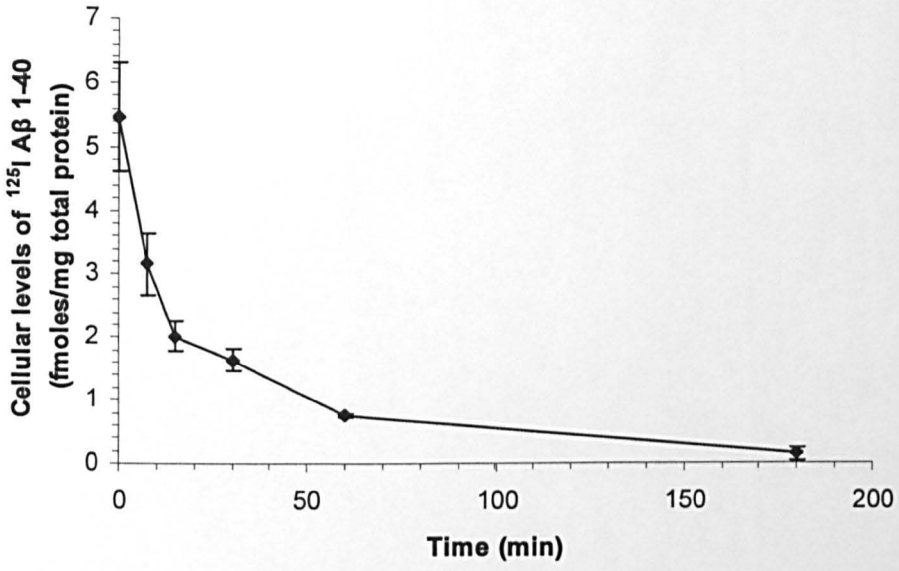

(b)

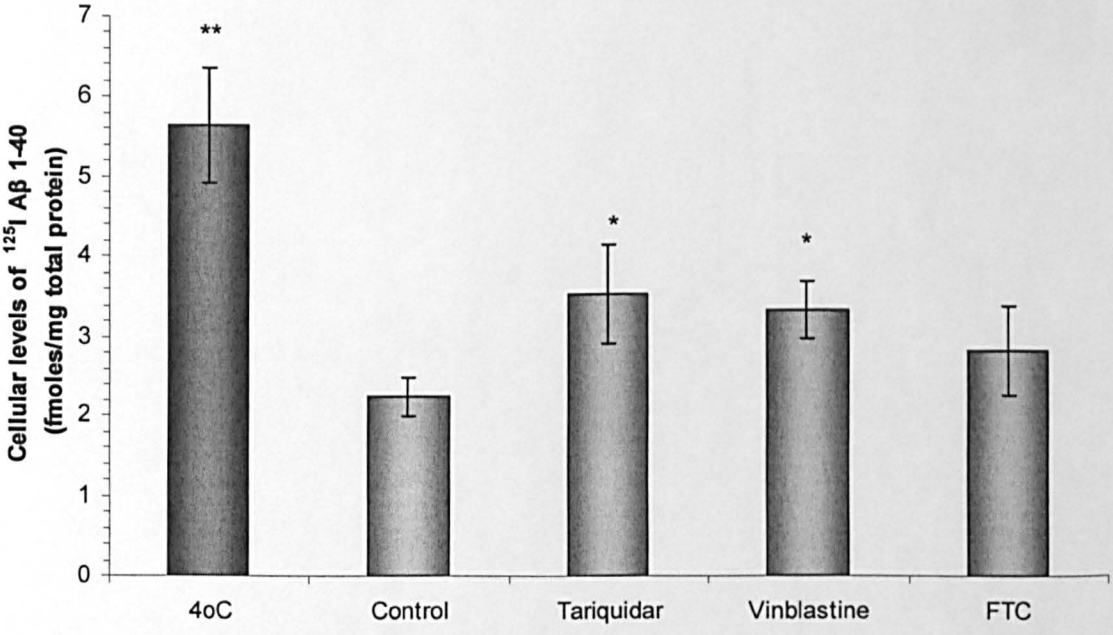

Figure 3.9. The effects of P-gp or BCRP inhibition on the efflux of ^{125}I Aβ 1-40 from hCMEC/D3 cells. (a) Fully confluent hCMEC/D3 cells were preloaded for 3 h with 0.1 nM ^{125}I Aβ 1-40, the cell culture media was changed and the cells were incubated for 7.5, 15, 30, 60 and 180 min at 37°C. At each time point the cellular levels of ^{125}I Aβ 1-40 (fmoles per mg of total protein) were measured using a γ-counter. Data represents mean ±SEM, n = 3 experiments with duplicate samples. **(b)** Preloaded hCMEC/D3 cells were incubated with tariquidar (300 nM), vinblastine (2 μM), FTC (2 μM) or a DMSO vehicle control for 10 min at 37°C, cellular levels of ^{125}I Aβ 1-40 (fmoles/mg of total protein) were measured using a γ-counter. Data represents mean ± SEM, n = 4 experiments with duplicate samples. * $P < 0.05$, ** $P < 0.01$ for treatments compared to the control using paired t test.

(a) Apical to basolateral permeability

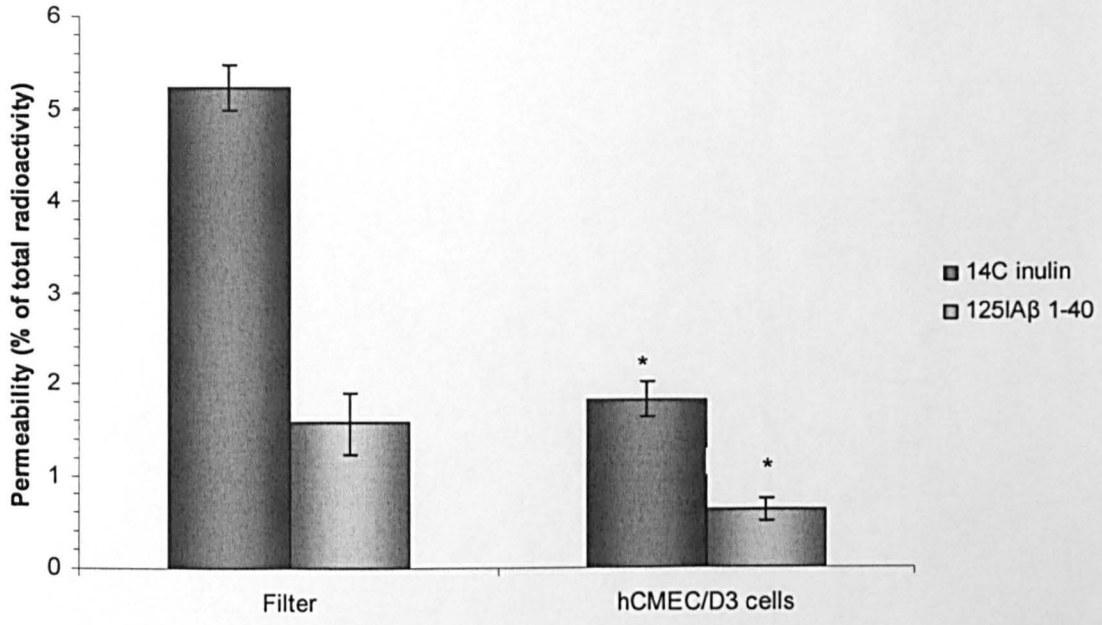

(b) Basolateral to apical permeability

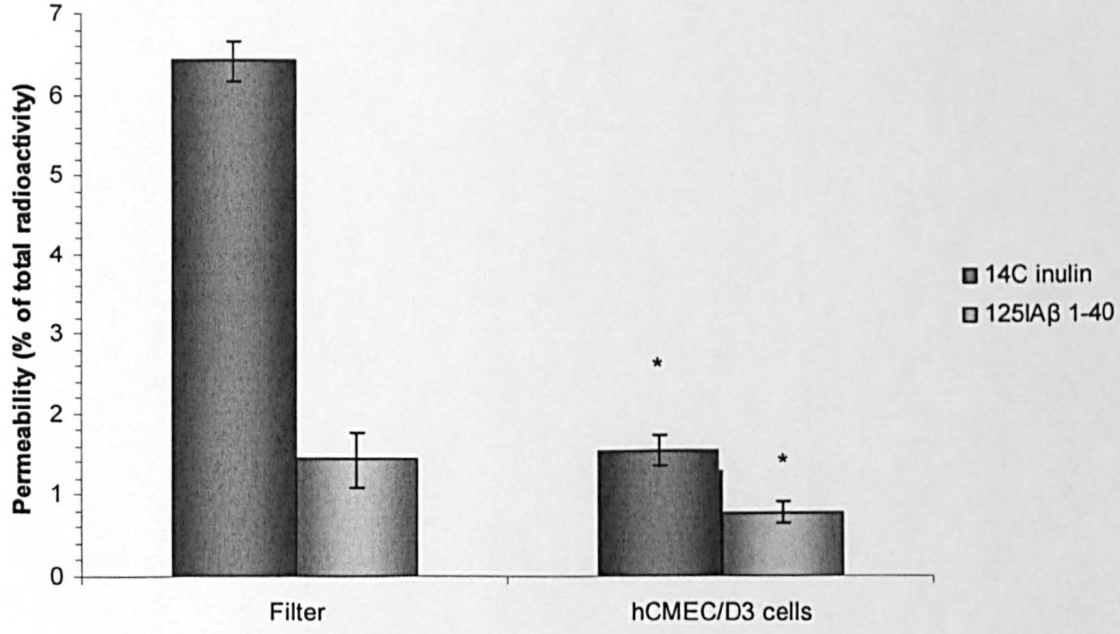

Figure 3.10. The permeability of hCMEC/D3 cells to ^{125}IAβ 1-40 and ^{14}C inulin. hCMEC/D3 cells were grown to confluence on filter inserts and 0.1 nM ^{125}IAβ 1-40 and 0.1 mM ^{14}C inulin was added to either the **(a)** apical or **(b)** basolateral compartments for 30 min. The total counts in each compartment were measured and the percentage crossing the filter calculated. Data represents mean ± SEM, n = 6 with single samples, * $P < 0.05$, compared to filters with no cells using paired t test.

(a)

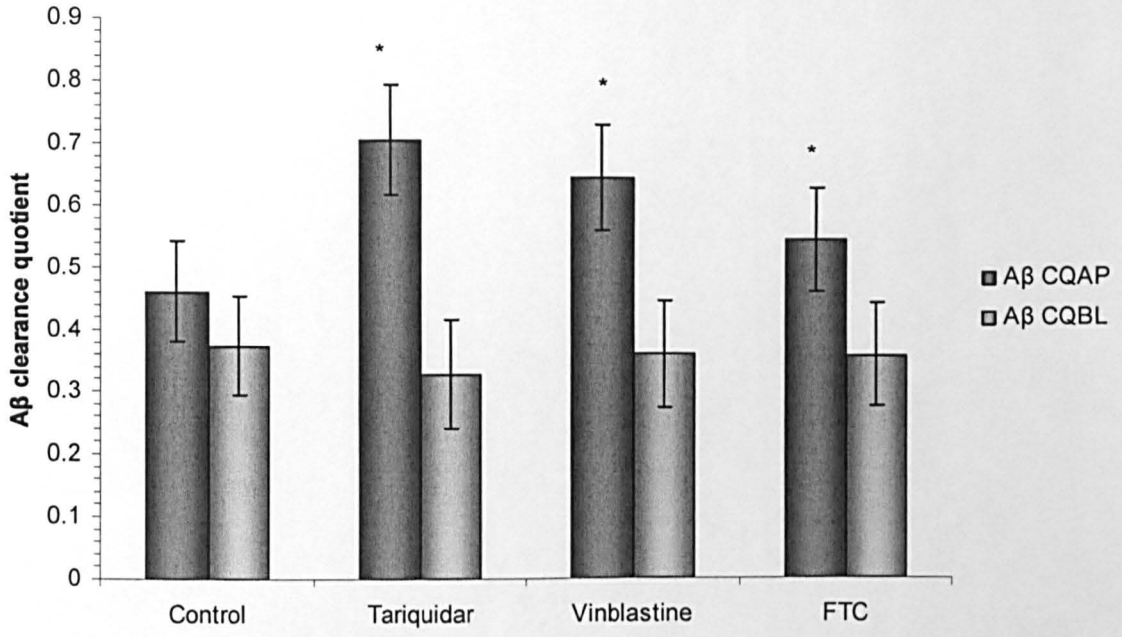

(b)

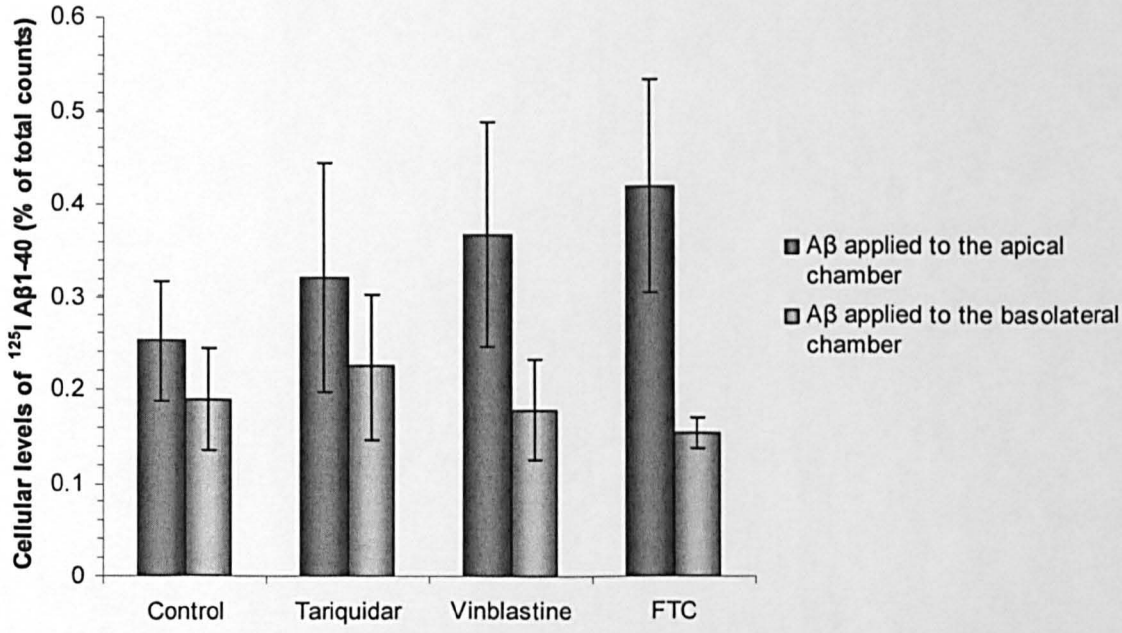

Figure 3.11. The effect of P-gp and BCRP inhibition on the clearance quotient of hCMEC/D3 cells to ^{125}I Aβ 1-40. (a) hCMEC/D3 cells were grown to confluence on filter inserts and rested for 48 h. Fresh culture media was then added to the apical or basolateral chamber containing 0.1 nM ^{125}I Aβ 1-40 and 0.1 mM ^{14}C inulin and tariquidar (300 nM), vinblastine (2 μM), FTC (2 μM) or a vehicle control for 30 min. The ^{125}I and ^{14}C counts were measured and the amyloid clearance quotient calculated. **(b)** Represents the total ^{125}I ^{125}I Aβ 1-40 recorded from the trypsinised cells as a percentage of the total ^{125}I Aβ 1-40 counts. For both experiments data represents mean ± SEM, n = 6 with single samples, * P< 0.05, comparing each treatment to the control using a paired t-test.

3.4 Discussion

3.4.1 Mechanism of Aβ influx and efflux in hCMEC/D3 cells

Aβ peptides have been previously reported to be a substrate for multiple receptors at the BBB, which mediate CNS Aβ transport in the brain-to-blood direction (P-gp, LRP-1) or in the blood-to-brain direction (RAGE, megalin). Increased P-gp activity and/or expression could therefore be therapeutically beneficial in AD, reducing the brain amyloid burden. In this study the roles of P-gp and BCRP, which shares a similar substrate overlap with P-gp, on Aβ transport by hCMEC/D3 cells were investigated. The results indicate that, at high concentrations of Aβ, the influx and efflux of Aβ is mediated by a non-receptor-mediated process, and both are unaltered by P-gp or BCRP inhibition. At lower more physiological concentrations of Aβ, influx also appeared dependent on a non-receptor mediated process. However, P-gp, and to a lesser extent BCRP inhibition, results in increased infux and decreased efflux of Aβ.

3.4.1.1 Role of LRP-1 and RAGE on Aβ influx in hBECs

The first interesting finding of this study was that LRP-1 inhibition and up to a 20 fold higher concentration of unlabelled Aβ did not affect the influx of fAβ into hCMEC/D3 cells. Confocal imaging demonstrated that a high proportion of fAβ appears intracellularly, rather than membrane-associated, and so the measurement of cellular fAβ levels most likely represented intracellular levels. This finding was confirmed using a low concentration of Aβ, as ^{125}I Aβ 1-40 influx into hCMEC/D3 cells was unaltered by the addition of 1000 times excess of unlabelled Aβ 1-40. Therefore, the influx mechanism of Aβ into hCMEC/D3 cells may not be receptor-mediated endocytosis and is possibly mediated by diffusion through the membrane, membrane binding or fluid-phase endocytosis.

There are two major receptors reported to be involved in the influx of Aβ into BECs and Aβ clearance at the BBB, LRP-1 and RAGE. Conflicting reports exist as to the role of LRP in the transport of Aβ at the BBB. Shibata *et al* [394] have demonstrated that after intracerebral injection of ^{125}IAβ 1-40 into mice, rapid clearance across the BBB occurs with a $t_{1/2}$ of < 25 min. The authors also found that ^{125}IAβ 1-40 transport was half saturated at 15.3 nM with full saturation at 70-100 nM, which was inhibited by antibodies against LRP-1 and α-2 macroglobulin (an Aβ binding partner and LRP-1 ligand). Ito *et al* [560] have confirmed this finding in rats, where the clearance of intracerebral microinjections of ^{125}IAβ 1-40 was inhibited by 20.3 % by RAP (LRP-1 inhibitor), although this result does imply that other routes of brain-to-blood transport are present. Deane *et al* [395] have demonstrated that Aβ binds with high affinity to LRP recombinant fragments (binding clusters I and IV) and that microinjections of ^{125}IAβ 1-40 are cleared across the mouse BBB, which was found to be inhibited by RAP and LRP-1 neutralising antibodies. In addition to transcytosis of Aβ, LRP can mediate internalisation. Deane *et al* [395] demonstrated that mouse capillaries internalise Aβ 1-40 and Aβ 1-42 via LRP-1. Kang *et al* [396] have found that in mouse fibroblasts transfected with human LRP-1, uptake of Aβ only occurs if α2 macroglobulin is present to form a complex. Ito *et al* [559] have found contrasting results as to the ability of LRP ligands to form binding partners with Aβ and mediate transcytosis. This research group has found that Aβ dimer formation and pre-incubation of Aβ with α2 macroglobulin and ApoE results in a reduced elimination of ^{125}IAβ 1-40 injected intracerebrally into the rat brain compared to freshly dissolved Aβ. However, the uptake of Aβ was found to be increased after ApoE 2,3 and 4 preincubation in a multiple myeloma cell line (MEF-1).

The very nature of LRP-1-mediated Aβ transcytosis has also been called into question. Nazer *et al* [561] have demonstrated that MDCK cells transfected with LRP binding domain IV (MDCK-mLRP4) internalise and degrade, but do not transcytose intact

Aβ peptides. The authors found that LRP-1-mediated Aβ transport across cells grown on filters only occurred for degraded Aβ fragments.

The above data indicates that LRP-1 can mediate the transcytosis of Aβ across the BBB. However, this might not be only route of brain-to-blood transport, and *in vitro* the internalisation of Aβ by BECs mediated by LRP might be dependent on monomeric Aβ species and binding to an LRP-1 ligand. The finding in this study that LRP-1 is not a major pathway involved in Aβ influx into hCMEC/D3 cells might reflect the absence of LRP-1 ligands binding to Aβ in the culture media, or the absence of functional LRP-1 expression by hCMEC/D3 cells. Concerning the latter, it is important to note that Nazer *et al.* [561] discovered that ^{125}I Aβ 1-40 uptake and degradation (0.1 nM, 24 h) was inhibited by 500 nM RAP in hCMEC/D3 cells, as determined by cell lysate counts. In addition, this research group went on to demonstrate that hCMEC/D3 cells exhibited a time-dependent uptake of HiLyte Fluor 55 Aβ 1-40 (100 nM, 6 and 24 h), which was inhibited by 500 nM RAP. The contrast between these results and the present study might, in some part, be due to the fact that in the study by Nazer *et al.*, hCMEC/D3 cells, when used for fluorescence uptake studies, were at around 10 % confluence if compared to the cells used in this current study (fully confluent). Fully confluent hCMEC/D3 cells might be a better refection of fully mature BECs, whilst at 10 % confluence the uptake of Aβ by proliferating ECs may be dependent on a different pattern of transporter receptor expression. Whilst LRP-1 expression was demonstrated via western blotting in that study, LRP-1 levels were much less than those expressed by HUVEC, MDCK-mLRP4 and possibly even wild type MDCK cells. Indeed, the proportion of fluorescent hCMEC/D3 cells after incubation with HiLyte Fluor 55-conjugated Aβ 1-40 was found to be ~10 %, which was comparable to MDCK cells (~ 10 %) but not to MDCK-mLRP4 cells (~ 40 %). Therefore, hCMEC/D3 cells might not express high enough levels of LRP-1 to allow significant internalisation of Aβ compared to diffusion.

RAGE has been demonstrated to mediate Aβ transport in primary isolated hBECs. Mackic *et al* [389] found that the binding of ^{125}I Aβ 1-40 (0.5 nM over 1 h) to primary hBECs was time-dependent, polarised to the apical membrane, and inhibited by 63 % by co-incubation with an anti-RAGE antibody and CHO cells transfected with human RAGE internalise Aβ. In the current study however, the contribution of RAGE to Aβ internalisation is unlikely, as excess unlabelled Aβ did not block the influx of either fAβ or ^{125}I Aβ 1-40 with hCMEC/D3 cells. It is possible that isolated hBECs express increased RAGE compared to hCMEC/D3 cells as is the case for P-gp (chapter 2). The results of this study demonstrate that Aβ influx into hCMEC/D3 cells is likely to be mediated by bulk flow and that further *in vivo* investigations should be carried to take into account this potential route of Aβ entry into BECs.

3.4.1.2 Role of P-gp and BCRP on Aβ influx and efflux in hBECs

The second interesting finding of the present study was that P-gp inhibition only increases influx and decreases efflux at low concentrations of Aβ. There are a number of possibilities that could explain the lack of a contribution of P-gp in the influx and efflux of fAβ. Firstly, the high concentrations of fAβ used for influx and efflux might have masked the comparatively small contribution of P-gp mediated transport, which was indistinguishable by flow cytometry. An additional variable of time might also have impacted on the results. hCMEC/D3 cells were incubated for 24 h with fAβ and 30 min with ^{125}I Aβ 1-40 for influx followed by 3 h or 10 min (3 h preloading for ^{125}I Aβ 1-40) for efflux respectively. In addition, the fluorescein tag might have altered the physiochemical properties of Aβ, since fluorescein is hydrophilic, and could have altered the ability of fAβ to be a substrate for P-gp or BCRP.

Another possibility factor is that after 24 h incubation with fAβ, the peptides are at sites inaccessible to P-gp, such as organelle- or vesicle- bound in hCMEC/D3 cells.

Confocal imaging does not rule out this possibility, as fAβ appears mainly located in the cytoplasm surrounding the nucleus where the golgi apparatus is located. To be a P-gp substrate, localisation to the membrane is considered a prerequisite. Exactly how the fAβ then efluxes from the hCMEC/D3 cells remains unknown. It is possible that another transporter or mechanism such as vesicular transport is partially responsible for efflux or that diffusion through the membrane is the limiting step for both influx and efflux at high concentrations of Aβ.

An additional possibility is that for both influx and efflux, fAβ undergoes significant degradation, and Aβ fragments may not readily be transported by P-gp. BECs express enzymes capable of Aβ degradation (reviewed in [567]) including neprilysin (NEP), [568, 569] insulin degrading enzyme (IDE) [570], endothelin converting enzyme (ECE-1 and 2) [571] and angiotensin converting enzyme [572]. A possibility therefore, is that, rather than efflux, degradation is the main route of Aβ elimination from hCMEC\D3 cells once it has been internalised. Multiple sites exist within the Aβ protein sequence for enzymatic cleavage by NEP, IDE and ECE, producing various fragments in length ([573, 574]). For example, Iwata *et al.*[569] found that ^{125}I Aβ injected into the hippocampus of rodents was degraded with a half life of 17.5 min with the major catabolic intermediate, Aβ 10-37, generated by NEP activity. Leissrung *et al* [575] have demonstrated using a kinase assay that IDE hydrolysis can cleave Aβ to form various fragments of 1-13, 1-14, 1-19, 1-29 and 20-40 in length, whilst NEP produced Aβ 20-30, 20-28, 20-29 and 14-25. Eckman *et al* [571] found that CHO cells transfected with ECE-1 were able to reduce the extracellular concentration of Aβ 1-40 by up to 90 % with the production of Aβ fragments 1-17, 1-19 and 20-40 over a 24 h period. The location of the fluorescein tag on the N terminus of fAβ raises the possibility that if fragments of 1-x in length were produced, they would be detected by flow cytometry. In addition, the most lipophilic region of the Aβ peptide is within the C-terminus. It is thus possible that non-fluorescently labelled Aβ fragments are transported out of cells by P-gp. The degradation of Aβ by hCMEC/D3 cells

has been noted by Nazer *et al* [561], who found that after incubation of 1 nM ^{125}I Aβ1-40 for 24 h that 44.2 % of the ^{125}I Aβ counts in the whole cell lysate originated from degraded Aβ in hCMEC/D3 cells. The group also demonstrated that after the addition of 1 nM ^{125}I Aβ1-40 to the basolateral compartment of MDCK-LRP cells grown on filters, only degraded fragments are released into the apical compartment. This data would indicate that a proportion of the degraded peptides still remain intracellular, and that degraded peptides can be either transcytosed or effluxed from cell cultures. Since in the present, study hCMEC/D3 cells were preloaded for efflux and incubated for influx for 24 h, the fAβ measured via flow cytometry and confocal microscopy most possibly reflected a combination of degraded and 'whole' Aβ, which may more accurately reflect the *in vivo* situation rather than short term exposure.

In contrast to high concentrations of fAβ, the influx and efflux of ^{125}IAβ 1-40 was increased by P-gp inhibition, and although not statistically significant, by BCRP inhibition. To date, there are no published experiments that have investigated the influx and efflux of Aβ with P-gp inhibitors in cultured hBECs and none which have reported a possible role for BCRP in Aβ efflux. The permeability of cell cultures to Aβ (see section 3.4.2) and *in vitro* studies however does imply Aβ is a P-gp substrate. Lam *et al.* [406] showed that the fluorescence of membrane vesicles from CHO cells transfected with the human MDR1 gene and labelled with a fluorescence marker, was quenched upon increasing additions of Aβ peptides with a binding affinity comparable to other P-gp substrates. This research group also demonstrated that Aβ 1-40 and Aβ 1-42 both compete for the uptake of ^{3}H-colchicine in MDR1 over expressing-CHO cells, with an IC50 of 27 μM and 22 μM for Aβ 1-40 and Aβ 1-42, respectively. Intriguingly, the authors do not state the concentration of ^{3}H-colchicine used, and instead refer to previous papers in the methods section where they use 1 μM. If that is the case, then these results imply that interaction between P-gp and Aβ is not very strong in nature, as very high concentrations of Aβ were needed to block the uptake of ^{3}H-colchicine. More specific vesicle binding of Aβ was observed by Kuhne *et al.*

[407], who established that rh123 (10 μM) was transported by an ATP-dependent mechanism into LLC-MDR membrane vesicles, and this was inhibited to 25 % of control levels by 10 μM Aβ 1-40 and Aβ 1-42. Furthermore, cyclosporin A (10 μM) and verapamil (100 μM) reduced the uptake of FITC-conjugated Aβ1-40 and Aβ 1-42 to 65 % of control levels in inside-out vesicles. Whilst the ability of amyloid peptides to block rh123 uptake is apparent, the rather modest inhibition of Aβ uptake by cyclosporin A implies other mechanisms mediating Aβ efflux are at work in addition to that mediated by P-gp. The results of the above studies were from P-gp over-expressing cell lines and using membrane vesicles. Whilst they do indicate that P-gp may function as an Aβ transporter, the results in the present study indicate that in hBECs this may only be so at physiological concentrations of Aβ.

3.4.2 The permeability of ^{125}I Aβ 1-40 to hCMEC/D3 cells

Fully confluent hCMEC/D3 monolayers formed a barrier to the passage of both ^{125}IAβ 1-40 (< 1 %) and ^{14}C inulin (< 2 %) in both the apical-to-basolateral and basolateral-to-apical directions. ^{14}C inulin predominantly crosses BECs via paracellular diffusion, and to a much lesser extent, fluid phase endocytosis, whereas the permeability of BECs to ^{125}IAβ 1-40 is dependent on several processes: paracellular diffusion, fluid phase endocytosis and receptor-mediated transcytosis. Several factors may contribute to the differences in permeability between ^{14}C and ^{125}IAβ 1-40 in untreated hCMEC/D3 cells. 1) Aβ may aggregating in the culture media increasing its molecular weight; 2) Aβ is highly hydrophobic and may stick to the filter and/or plastic; and 3) the molecular shape of ^{14}C inulin and ^{125}IAβ 1-40 may be different affecting their ability to diffuse within the culture media. For example, ^{14}C inulin may form a more globular structure than ^{125}IAβ 1-40, a property which would result in increased paracellular diffusion compared to Aβ. The results of this current study indicate that BCRP and P-gp both play a role in preventing the

apical-to-basolateral, but not the basolateral-to-apical, permeability of hCMEC/D3 cells to ^{125}I Aβ 1-40. Whilst the data was not significant, increased cellular levels of ^{125}I Aβ 1-40 were also observed following P-gp and BCRP inhibition, indicative of a barrier function of each transporter to Aβ.

It is unlikely that the transported ^{125}I Aβ 1-40 in the present study represented degraded peptide fragments. Mackic *et al* [389] have demonstrated > 94 % of cellular ^{125}I Aβ 1-40 remains intact after 60 min incubation with primary hBECs. Whilst Nazer *et al* [561] have found that MDCK-mLRP4 cells only transport degraded fragments, and 44 % of hCMEC/D3 cellular levels of ^{125}I Aβ 1-40 represented the degraded peptide, the incubations times used were 24 h, much longer than the 30 min used in this study.

The role of P-gp in the permeability of the BBB to Aβ is an area of controversy. Kunhne *et al*, [407] found that compared to LLC cells, LLC-MDR1 cells have enhanced basolateral- to-apical permeability but not apical-to-basolateral permeability to 5 μM FITC-Aβ 1-40 and Aβ 1-42. This enhanced permeability, in cells over-expressing P-gp, was inhibited by 10 μM cyclosporin A after 1 h incubation. In the same study, it was also noted that transport of rh123 (10 μM) was increased only in the basolateral-to-apical direction in LLC-MDR1 cells compared to LLC cells alone, and this effect was inhibited by Aβ peptides with an IC 50 of ~ 50 μM. Whilst the expression of P-gp LLC-MDR1 cells was demonstrated to be polarised on the apical membrane with little or no intracellular or basolateral staining, it was carried out using confocal microscopy of cells grown on glass coverslips not filter inserts, which may have altered the distribution of P-gp expression. In contrast, Nazer *et al* [561] found that the basolateral-to-apical transport of 1 nM ^{125}I Aβ 1-40 at 24 and 48 h in MDCK cells over-expressing human MDR1 (MDCK-MDR) is not increased compared to wild type MDCK cells. It would have been interesting if in that study the apical-to-basolateral permeability had been investigated. Mackic *et al* [389] have demonstrated that in isolated hBECs, ^{125}I Aβ 1-40 (0.5 nM 30 and 60 min) exclusively binds to the apical membrane and is transported towards the basolateral membrane, not

vice- versa, in agreement with the present study. However, these authors demonstrated that Aβ binding to hBECs was inhibited by non-tagged Aβ and was 63 % attributable to RAGE. Whilst the results of the current study do not exclude the binding of RAGE to Aβ in hCMEC/D3 cells, the influx data indicates that is unlikely to be significant. Differences in Aβ concentrations, incubations times and cell types makes comparisons between studies very difficult. The permeability results found in the present study are consistent with P-gp and BCRP protecting the brain from blood-borne Aβ species but not transporting Aβ from the brain. Interestingly, there are no reports on the role of BCRP and on Aβ transport in the literature.

In vivo data has also produced conflicting results with regards to the role of P-gp in Aβ transport at the BBB. Cirrito *et al* [408] have found intracerebrally injected Aβ 1-40 and Aβ 1-42 accumulates in the brain of mdr1a/b(-/-) mice at higher rates than wild type mice (although LRP-1 was also down regulated in the mdr1a/b(-/-)). In the same study, it was also found that tariquidar treated Tg 2576 mice have increased basal ISF Aβ levels in the CNS compared to control after 8 h treatment. Although it should be noted that astrocytes may also express P-gp in addition to epithelial cells throughout the body, which may have impacted on the results. For example, P-gp inhibition could increase cellular retention of Aβ by astrocytes, reducing brain ISF Aβ levels. In contrast to these findings, Ito *et al* [560] have demonstrated that the brain elimination of intracerebrally injected ^{125}I Aβ 1-40 is unaltered by quinidine and verapamil (both P-gp inhibitors). The differences between these two studies could be explained by the finding that in one finding from rat tissue, Bendayan *et al* [213] found that P-gp was primarily located on the abluminal membrane. However, there is also evidence for luminal expression in rats [210], and as described in section 1.1.1.6.1, the majority of mice and human studies have indicated that P-gp is expressed in higher amounts on the luminal membrane at the BBB. The results presented in the present study, might in part explain the discrepancy described above. The increased ISF fluid Aβ levels in Tg 2756 mice after P-gp inhibition described by Cirrito *et*

al [408] may be due to the increased blood-to-brain permeability of the BEC. In the results described by Ito *et al* [558], there was no brain-to-blood P-gp mediated Aβ transport, which is consistent with the *in vitro* data described here.

Increased Aβ levels in the brain are believed to be key in the pathogenesis of AD, and some research groups argue that decreased BBB clearance is a key component of AD. Increased plasma levels of Aβ are reported in AD patients compared to controls [576]. For example Sagare *et al* [319] have noted a 300-400 % increase in free Aβ levels compared to control patients. The results of this study imply that P-gp might protect the CNS from this Aβ pool and at higher concentrations of Aβ found in AD patients may become saturated. P-gp saturation, RAGE up-regulation and LRP down-regulation in BECs in AD [384], might significantly add to the brain Aβ load. In addition many drugs which are prescribed for elderly patients, such as lipid lowering agents and antidepressants, are substrates for P-gp and in principle might act as competitive substrates for Aβ at the BBB, potentially increasing the risk of developing AD.

3.5 Conclusions

The results presented here indicate that P-gp, and to a lesser extent BCRP, act to decrease influx and increase efflux of low Aβ concentrations in hBECs. However, at high concentration of Aβ over longer periods of time, neither transporter affects the influx of efflux of Aβ. At both concentrations of Aβ, the influx mechanism is a non-receptor mediated process. Importantly, P-gp and BCRP both prevented the apical-to-basolateral permeability of human brain endothelial cells to Aβ, which is consistent with blood-brain protection *in vivo*.

Chapter 4

Effect of Aβ on tight junction and transporter protein expression by hCMEC/D3 cells

Abstract

The aim of this study was to investigate the effects of Aβ on the expression of tight junction and transporter proteins by hCMEC/D3 cells. A 48 h treatment with a non-cytotoxic dose (5 μM) of Aβ 1-40 or Aβ 1-42 decreased the expression of Glut-1 but not P-gp or the transferrin receptor by hMCEC/D3 cells as assessed by western blotting. These treatments also decreased the expression of the tight junctional protein occludin but not of claudin-5 (Cl-5) or ZO-1, as determined by western blotting and flow cytometry. When viewed via immunocytochemistry, Aβ 1-40 reduced occludin expression intracellularly and at the level of the tight junctions. At the mRNA level, Aβ 1-40 decreased occludin levels after 24 h, with partial recovery by 48 h. Cl-5 mRNA levels were unaltered up to and including 48 h treatment with Aβ, whilst increased ZO-1 mRNA levels were detected after 48 h but not 24 h. Tight junctional proteins restrict endothelial cell paracellular transport of molecules. Thus the permeability of hCMEC/D3 cells to the paracellular tracer molecules 4 kDa and 70 kDa FITC – dextran was investigated. Whilst Aβ 1-40 or Aβ 1-42 incubation did not alter the permeability to 4 kDa FITC-dextran, both peptides increased the permeability to 70 kDa FITC-dextran. These results demonstrate that Aβ can directly induce a leaky BBB *in vitro*, potentially via the down-regulation of occludin expression.

4.1 Introduction

Vascular dysfunction is emerging as a key pathological hallmark in AD, with features that include brain hypoperfusion (reviewed in [410, 421]) reduced glucose uptake [430, 431, 436], detrimental BEC morphological alterations [413, 414] and increased permeability of the BBB [577-581]. Increased BBB permeability could have potentially disastrous consequences for the homeostatic neuronal environment, especially with regards to alterations in the levels of soluble ions, insulin, glucocorticoids, glutamate and pathogens.

Aβ *in vitro* evokes direct cytotoxic effects in BECs, with increased superoxide [582, 583] and decreased nitric oxide [412] production proposed as key detrimental factors. Aβ peptides have also been demonstrated to increase the paracellular permeability of porcine artery ECs [442] and BECs of human [443] and porcine origin [444] in culture. *In vivo*, increased BBB permeability has also been noted in AD transgenic animal models [94, 440, 584], and after the intravenous infusion of Aβ in rats [441]. Furthermore, blood-borne molecules have been detected in the CNS parenchyma of tissue samples from AD patients indicative of a leaky BBB [577-581]. TJ proteins are critical to restrict the paracellular leakage of molecules at the BBB. In principle, TJ protein alterations may in part be responsible for the increased leakiness found in AD. Indeed, Marco and Skaper [486] found that Aβ 1-42 decreased occludin levels in cultures of rat BECs after 24 h incubation, whilst Cl-5 and ZO-1 levels remained unaltered via western blotting. In addition, Aβ 1-40 soluble oligomers have recently been demonstrated to induce ZO-1 translocation from junctional areas in primary hBECs [443]. Furthermore, Takechi *et al* [94] recently demonstrated substantially reduced occludin expression in APP/PS1 mice compared to wild type mice and significant plasma protein (IgG) extravasation, indicative of a leaky BBB. This evidence implies that alterations in TJ protein expression might play a role in the increased BBB permeability observed in AD.

Other proteins expressed by BECs are also altered in AD. Decreased Glut-1 expression has been observed in AD patients in neurons [585] and BECs [146, 438, 586, 587]. Alterations in Glut-1 expression would have the net result of reducing the amount of glucose available to neurons and BECs, potentially leading to energy deprivation and neuronal and BEC death. Indeed, decreased cerebral glucose utilisation has been observed in AD patients [430, 431]. In addition, an inverse correlation of P-gp levels with Aβ plaques has also been demonstrated in non-demented subjects [409]. Reduced P-gp expression would compromise the barrier properties of brain endothelium to a range of drugs and signalling molecules.

The aim of this chapter was investigate the effects of Aβ on the expression of transporter and TJ proteins by hBECs and the resulting physiological consequences i.e. altered permeability. The results of this study are important since they could provide information on whether Aβ could directly induce alterations in the BBB function, as observed in AD patients.

4.2 Methods

4.2.1 Cell culture conditions

The cell culture conditions used in this study are different to those used in other chapters. It was observed by Dr K.Logan (The Open University, personal communication) that maximal expression of occludin (as assessed by western blotting) occurred when hCMEC/D3 cells were maintained without a change in culture medium for 2-3 days post confluence. Therefore, for all experiments described here, hCMEC/D3 cells were grown to confluence as indicated previously (2.2.3), with culture media changes every 2-3 days, then rested for 2-3 days after confluence and treated with Aβ in the same media.

4.2.2 MTT cytotoxicity assay

hCMEC/D3 cells grown in collagen-coated 96 well plates were treated with Aβ 1-40, Aβ 1-42, sAb1-40, or sAβ 1-42 at concentrations of 0, 0.5, 1, 5 and 10 μM for 48 h. An MTT toxicity assay was then carried out as described in section 2.2.11.

4.2.3 SDS PAGE and Western blotting

hCMEC/D3 cells were grown on collagen-coated 6 well plates and Aβ 1-40, Aβ 1-42, sAβ 1-40 or sAβ 1-42 was then added to the culture media to give a final concentration of 0.5 or 5 μM, and cells were incubated for 24 h or 48 h. At the appropriate time point, hCMEC/D3 cells were washed in HBSS and 250 μl of lysis buffer (RIPA buffer containing 1 mM PMSF, 10 ng/μl leupeptin, pepstatin and apotinin) was added to each well for 5 min at 4°C. Each well was then scraped using a cell scraper (Greiner, Gloucestershire, UK) and the resultant lysate was collected and subjected to the same procedure as in 2.2.5. The expression of P-gp (C219, 500 ng/ml, mouse monoclonal IgG_{2a}), Glut-1 (1 μg/ml rabbit polyclonal IgG, Abcam, Cambridge, UK) transferrin receptor (1 μg/ml mouse monoclonal

IgG_1, Santa Cruz, CA USA), occludin (1 μg/ml of rabbit polyclonal IgG, Zymed, California, USA), Cl-5 (1 μg/ml mouse monoclonal IgG_1 Zymed, California, USA) and ZO-1 (1 μg/ml rabbit polyclonal IgG, Zymed, California, USA) was then determined using appropriate HRP-conjugated secondary antibodies (Anti-mouse/rabbit IgG diluted 1 in 20,000, Pierce Biotechnology, Cheshire, UK) and visualised by ECL. Membranes were then stripped and re-probed for actin (1 μg/ml, mouse monoclonal IgG_1) as described in section 2.2.5. The signal intensities of the bands on the films were analysed using image J software and protein expression was normalised with actin.

4.2.4 Flow cytometry

hCMEC/D3 cells grown on collagen-coated 12-well plates were incubated with 5 μM Aβ 1-40, Aβ 1-42, sAβ 1-40 or sAβ 1-42 for 48 h. The expression of occludin (2.5 μg/ml rabbit polyclonal IgG) or Cl-5 (2.5 μg/ml mouse monoclonal IgG_1) was then measured using flow cytometry (488 nm $\lambda_{excitation}$, 530 nm $\lambda_{emission}$) as described in section 2.2.6, with the alteration that the primary and secondary [10 μg/ml Alexa Fluor-488-rabbit polyclonal IgG (Invitrogen, paisley UK) or FITC-conjugated goat monoclonal IgG] antibodies were incubated for 1 h at RT. Statistical analysis was performed on the raw data. However, for illustrative purposes, Cl-5 or occludin expression by hCMEC/D3 cells was expressed as a percentage of cells treated with Aβ compared to those treated with the sAβ peptide.

4.2.5 Immunocytochemistry

hCMEC/D3 cells were grown on collagen-coated glass cover slips and Aβ 1-40 or sAβ 1-40 (5 μM) was added to the culture medium for 48 h. hCMEC/D3 cells were then fixed for 10 min in ice-cold methanol (Sigma-Aldrich, Dorset, UK) and ICC staining was carried out described in section 2.2.9, using 2.5 μg/ml of an anti-occludin rabbit polyclonal

IgG as the primary antibody, and 10 μg/ml of Alexa Fluor-488-rabbit polyclonal IgG as the secondary antibody applied for 1 h at RT. Mounted cells were viewed with a fluorescent microscope (Olympus bx61).

4.2.5 Quantitative RT-PCR

hCMEC/D3 cells grown on collagen-coated 12 well plates were incubated with 5 μM Aβ 1-40, Aβ 1-42 , sAβ1-40 or sAβ 1-42 for 24 h or 48 h. Total RNA was then extracted using TRIzol reagent (Invitrogen, Paisley, UK). hCMEC/D3 cells were washed with HBSS, incubated with 1 ml per well of TRIzol for 5 min at RT, collected with a cell scraper and transferred to a microfuge tube. Chloroform [0.2 ml/ml (Sigma-Aldrich, Dorset, UK)] was then added, and tubes were mixed vigorously for 15 seconds and incubated for 3 min at RT. After centrifugation (9000 xg, 15 min, 4 °C), the upper aqueous phase containing RNA was collected. To precipitate the RNA, isopropyl alcohol (0.5 ml per tube) was added to each sample and incubated for 10 min at RT, followed by centrifugation (6000 xg, 5 min). The supernatant was then removed and the pellet washed with 75 % ethanol. After centrifugation (6000 xg, 5 min, 4°C), the supernatant was removed, the pellet air-dried for 5 min at RT and redissolved in 50 μl of DNase/RNAse - free water. The concentration and purity of RNA was then calculated using UV spectrophotometery at λ_{260} and λ_{280}. First strand DNA synthesis was then carried out using a Reaction Ready First strand cDNA synthesis kit (Superarray, Maryland, USA), as directed by the manufacturer's protocol. Briefly, 1 μg of RNA was added to 1 μl of buffer P and dissolved in RNase-free water to a final volume of 10 μl. The mixture was then placed in a thermal cycler (Bio-Rad, California, USA) at 70°C for 3 min, cooled to 37°C and held for 10 min. A cocktail containing reverse transcriptase and RNAse inhibitor was then added to the annealing mixture, incubated at 37°C for 60 min, heated to 95°C for 5 min and held at 4°C. Real time PCR was then carried out using SYBR green and primer

sets for Cl-5, occludin, ZO-1 and actin according to the manufacturer's protocol (Superarray, Maryland, USA). Briefly, a mixture was made containing 1 µl of cDNA template, 1 µl of primer mix, 12.5 µl of 2x RT^2 Real-Time™ SYBR green PCR master mix in a final volume of 25 µl water. The mixture was then placed in a thermal cycler (DNA engine Opticon 2, Bio-Rad, CA, USA), using a 40 cycle program (95°C, 30 sec; 55°C, 30 sec; and 72°C, 30 sec). Using this method, cycle threshold (CT) values are obtained, which corresponds to the cycle number at which the fluorescence curve crosses a predetermined threshold (3 x Standard deviation over cycle range). The threshold is designated for the data during the logarithmic phase of the graph.

The data was then calculated using a comparative method. First the difference in CT between the target (i.e. occludin, Cl-5 or ZO-1) and housekeeping gene (actin) was calculated:

$$CT_{target} - CT_{actin} = \Delta CT$$

Then the difference between each treatment and that of the control was then calculated

$$\Delta CTA\beta\text{-}\Delta CTsA\beta\text{-} = \Delta\Delta CT$$

The data was then transformed into absolute values;

$$\text{Comparative expression levels} = 2^{-\Delta\Delta CT}$$

This method is appropriate for primers with similar efficiencies. Dr Logan calculated the primer efficiencies of actin, Cl-5, occludin, and ZO-1 to be 1.81, 2.07, 1.70, 1.58. Due to the difference in primer efficiency between Cl-5 and actin the Pfaffl method [588] was employed, which takes these alterations into account:

$$\text{Ratio} = \frac{\text{E target}^{\Delta CT\ target}}{\text{E ref}^{\Delta CT\ ref}}$$

Where E represents the primer efficiencies.

However, it was found using this method that there was no difference between the Pfaffl and comparative method and so all data is shown as calculating using the comparative method.

Actin was considered an appropriate control, since the difference between the CT values of the different samples was low (~ 0.5 CT value). In addition, the primer efficiency of actin was similar compared to ZO-1, Cl-5 and occludin.

4.2.6 Permeability of hCMEC/D3 cells to 4 kDa and 70 kDa FITC-dextran

hCMEC/D3 cells were grown on collagen-and fibronectin-coated transwell polyester membrane inserts (0.4 μm diameter pore, 12mm diameter) and incubated with 5 μM Aβ 1-40, sAβ 1-40, sAβ 1-42 or 1-42 for 48 h. The permeability of hCMEC/D3 cells to 2 mg/ml of 4 kDa or 70 kDa FITC-dextran (Sigma-Aldrich, Dorset, UK) added to the apical chamber was investigated using the method described in section 2.2.14. Pre-and post-Aβ incubation, the trans endothelial electrical resistance (TEER) of hCMEC/D3 cells was measured using an Endohm 12 chamber and an Endohmeter (World precision instruments, Florida, USA).

4.2.7 Statistical analysis

All data are represented as means +/- SEM and the number of experiments, n, indicated each time. Statistical significance was calculated using ANOVA followed by Student's t test, comparing each treatment to the control (* $P < 0.05$, ** $P < 0.01$). For the western blotting, RT-PCR and permeability experiments, a paired t-test was employed. For RT-PCR, analysis was carried out using ΔCT values as the $2^{-\Delta\Delta CT}$ method standardised all data so that the sAβ value is always 1.

4.3 Results

4.3.1 Cytotoxicity of Aβ 1-40 and Aβ 1-42 to hCMEC/D3 cells

The aim of this study was to investigate the effects of non-toxic concentrations of Aβ on hCMEC/D3 cell protein expression. The cell culture conditions used here are different from those in previous chapters and so a separate MTT assay was carried out (Figure 4.1). Aβ 1-42 and Aβ 1-40 incubations did not alter cell viability of hCMEC/D3 cells as assessed by the MTT assay at 0.5, 1 or 5 μM. However, cell viability was reduced at 10 μM ($n = 3$, $P < 0.05$) after incubation with both Aβ peptides. Aβ 1-42 and Aβ 1-40 incubation at 10 μM decreased hCMEC/D3 cell viability by 26 % ± 7.0 and 30 % ± 7.08 respectively compared to a vehicle control. These results show that both Aβ species were toxic to hCMEC/D3 cells at 10 μM after 48 h incubation and therefore 5 μM was used to investigate regulation of protein expression by Aβ in hCMEC/D3 cells.

4.3.2 The effect of Aβ on the expression of transporter proteins by hCMEC/D3 cells

Reduced expression of Glut-1 [146, 437, 586, 587] and increased brain levels of iron [589] have been observed in brain sections of AD patients in addition to an inverse correlation between plaque deposition and P-gp expression in non-demented elderly patients [409]. The transferrin receptor is capable of transporting transferrin bound iron at the BBB [150, 151]. The effect of Aβ on the expression of P-gp, Glut-1 and the trasnferrin receptor was investigated using western blotting (Figures 4.2-4.4).

Incubation with a sub-cytotoxic concentrations of Aβ 1-40 or Aβ 1-42 did not alter the expression levels of P-gp (Figure 4.2) or transferrin receptor (Figure 4.4) after 24 or 48 h incubation, when compared to cells incubated with sAβ peptides ($n = 3$, $P > 0.05$). By contrast, Aβ 1-42 reduced Glut-1 expression levels to 69.5 % ± 1.2 of sAβ 1-42 levels after 24 h and to 51.7 % ± 12.2 after 48 h incubation (Figure 4.3, $n = 3$, $P < 0.05$). Aβ 1-40 also

reduced Glut-1 levels to 60.5 % ± 5.3 after 48 h incubation (n = 3 experiments, $P < 0.05$) but not after 24 h. These results provide evidence that sub-cytotoxic Aβ concentrations do not affect P-gp or transferrin receptor protein expression but specifically reduce Glut-1 expression in hCMEC/D3 cells.

4.3.3 The effect of Aβ on the expression of tight junction proteins by hCMEC/D3 cells

There is evidence for a leaky BBB in both AD patients [579] and in transgenic mouse [440, 584] models of AD. The aim of this part of the study was to investigate whether Aβ could decrease the expression of TJ proteins, which could lead to increased hCMEC/D3 cell permeability (Figure 2.5-2.8). Occludin, Cl-5 and ZO-1 are key components of the TJ complex and were the focus of this study.

ZO-1 and Cl-5 levels were unaltered after 24 h and 48 h incubation with both Aβ peptides compared to the sAβ peptides (Figure 4.5 and 4.6, n = 3, $P > 0.05$). Occludin levels, though unchanged after 24 h, were reduced after 48 h Aβ incubation compared to sAβ incubation [n = 3, $P > 0.05$, (Figures 4.7)]. Aβ 1-40 and Aβ 1-42 incubation decreased occludin expression to 49.0 % ± 8.3 and 58.4 % ± 7.1, respectively, compared to cells incubated with sAβ peptides (Figure 4.8). The decreased occludin expression after 48 h was concentration-dependent, since 0.5 μM of both Aβ species did not alter occludin levels by hCMEC/D3 cells (Figure 4.8, n = 3, $P > 0.05$). The results presented here show that incubation of hCMEC/D3 cells with either Aβ 1-40 or Aβ 1-42 results in specific occludin down-regulation, but not Cl-5 or ZO-1, after 48 h incubation.

4.3.4 The effect of Aβ on the expression of occludin and claudin-5 by hCMEC/D3 cells as assessed by flow cytometry

For a more quantitative measurement of Aβ-mediated occludin down-regulation, flow cytometry was employed (Figure 4.9). After 48 h incubation with 5 μM Aβ 1-40,

occludin levels were reduced to 73.8 % ± 1.14 compared to cells treated with sAβ 1-40 (n = 20 experiments, $P < 0.01$). Aβ 1-42 incubation induced a similar significant decrease in occludin levels to 73.5 % ± 3.3 (n = 3 experiments, $P < 0.05$). To confirm the specificity of Aβ mediated occludin down-regulation, the expression of Cl-5 after 48 h incubation with Aβ 1-40 or sAβ 1-40 was investigated. In agreement with the western blotting findings, there was no decrease in Cl-5 levels in cells incubated with Aβ 1-40 compared to cells incubated with sAβ 1-40. These results have confirmed the western blotting findings, in that Aβ 1-40 and Aβ 1-42 both specifically reduce occludin levels after 48 h incubation in hCMEC/D3 cells.

4.3.5 The effect of Aβ 1-40 on the expression of occludin by hCMEC/D3 cells as assessed by immunocytochemistry

Whilst flow cytometry and western blotting data demonstrate occludin down-regulation mediated by Aβ, they give no indication as to the sub-cellular location of occludin. Therefore, the expression of occludin was investigated after 48 h incubation with Aβ 1-40 or sAβ 1-40 using ICC (Figure 4.10). Occludin expression after sAβ 1-40 incubation was strongly detected at the cell-cell borders between hCMEC/D3 cells, indicative of TJ localisation, and intracellularly, albeit at lower levels. In comparison, Aβ 1-40 incubation of hCMEC/D3 cells caused a decreased staining both at the cell borders and intracellularly. For some hCMEC/D3 cells, a complete loss of occludin was observed at the cell junctions. Aβ induced the loss of occludin at the TJ, which suggests that the paracellular permeability of hCMEC/D3 cells may be increased.

4.3.6 The effect of Aβ on the expression of tight junction mRNA levels by hCMEC/D3 cells

A decrease in both intracellular and cell junctional occludin was observed suggesting that overall levels of occludin may be reduced by Aβ. To assess whether Aβ affected the mRNA levels of occludin in addition to the protein levels, quantitative RT-PCR techniques were used (Figure 4.11). After 24 h incubation, neither Aβ 1-40 nor Aβ 1-42 significantly altered the mRNA levels of Cl-5 or ZO-1 ($n = 4$, $P > 0.05$) by hCMEC/D3 cells. By contrast, occludin mRNA levels were decreased significantly in hCMEC/D3 cells ($n = 4$, samples $P < 0.05$) after incubation for 24 h with Aβ 1-40 by ~ 55 % compared to cells treated with sAβ 1-40, and whilst the levels were also decreased with Aβ 1-42, they did not reach significance ($n = 4$, $P > 0.05$). After 48 h incubation with Aβ 1-40, mRNA levels of Cl-5 remained unaltered ($n = 3$, $P > 0.05$). Occludin mRNA levels were reduced in cells incubated with Aβ 1-40 after 48 h by ~ 30 %, compared to those incubated with sAβ1-40, however this effect was not significant ($n = 3$, $P > 0.05$). Interestingly, ZO-1 mRNA levels were significantly increased by ~ 30 % after 48 h incubation with Aβ 1-40 ($n = 3$, $P < 0.05$). These results show that occludin is suppressed at the mRNA level after 24 h incubation with Aβ 1-40, whilst at the protein level changes are observed at 48 h (Figure 4.7).

4.3.7 The effect of Aβ on the permeability of hCMEC/D3 cells to 4 and 70 kDa FITC-dextran

The permeability of hCMEC/D3 cells to the paracellular tracers 4 and 70 kDa FITC- dextran after Aβ incubation was investigated to see whether occludin down-regulation was associated with BBB dysfunction (Figure 4.12).

After 48 h incubation, neither Aβ 1-40 nor Aβ 1-42 altered the permeability of hCMEC/D3 cells to 4 kDa FITC-dextran compared to cells incubated with the sAβ

peptides (n = 3, P > 0.05). In contrast, Aβ 1-40 incubation significantly increased hCMEC/D3 cell permeability to 70 kDa FITC-dextran by 53 % ± 10.1 compared to sAβ 1-40 treated cells (n = 6, $P < 0.01$). After 48 h incubation, Aβ 1-42 also increased the permeability of hCMEC/D3 cells to 70 kDa FITC-dextran (an increase of 28 % ± 17), however this increase did not reach statistical significance (n = 3, $P > 0.05$). It is interesting to note that the TEER values of hCMEC/D3 cells were unaltered by Aβ incubation (Figure 4.13, n = 6 and 3 for Aβ 1-40 and Aβ 1-42, respectively, $P > 0.05$). As indicated by the low TEER values pre-incubation, hCMEC/D3 cells do not form an extensive barrier to ions when grown on filters. It is therefore no surprise that Aβ treatment did not alter this already low value.

These results demonstrate that Aβ can increase the paracellular permeability of hCMEC/D3 cells to 70 but not to 4 kDa FITC-dextran. This implies that the occludin down-regulation observed at the protein and mRNA levels might have the net result of increasing leakiness of hCMEC/D3 cells to paracellular tracers.

(a)

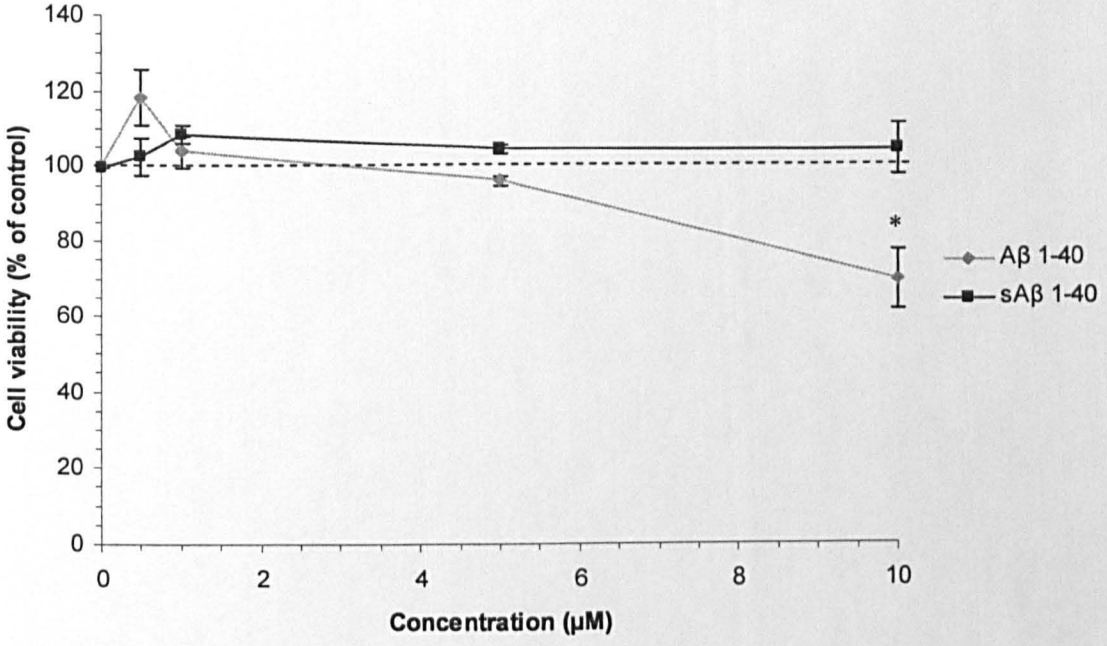

(b)

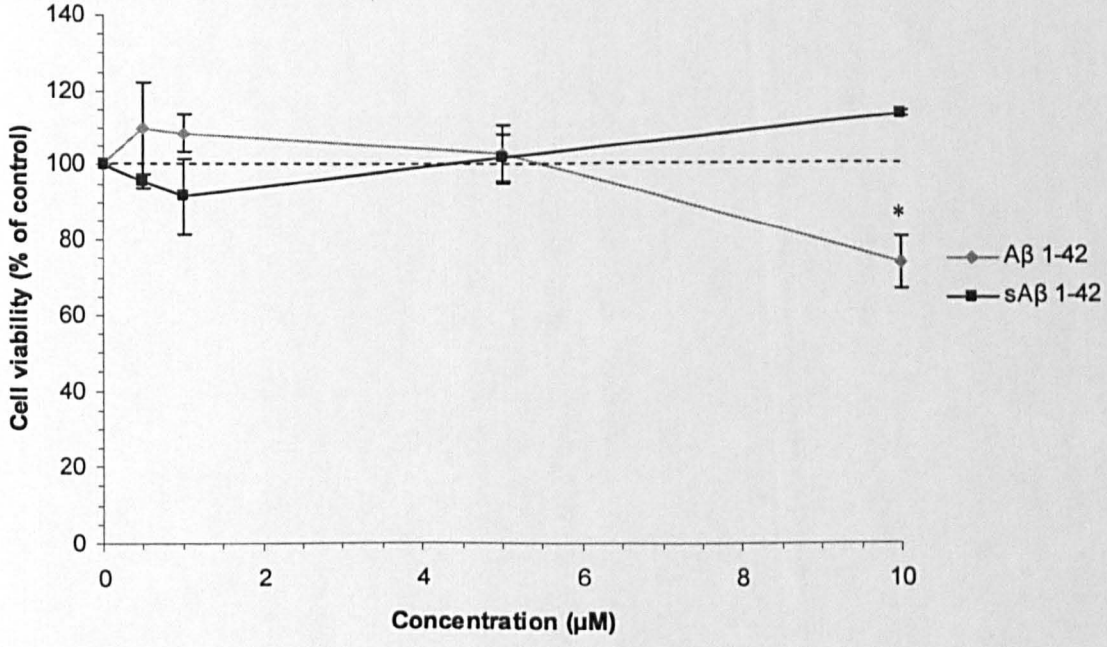

Figure 4.1. Cytotoxicity of Aβ 1-40 and Aβ 1-42 to hCMEC/D3 cells after 48 h incubation as assessed by an MTT assay. (a) The cytotoxicity of Aβ 1-40 or sAβ1-40 and **(b)** Aβ 1-42 or sAβ 1-42 was investigated in hCMEC/D3 cells cultured as described in section 4.2.1, using an MTT assay, over a 48 h incubation period. Data represents mean ± SEM, n = 3 experiments with quintuplet samples. * $P < 0.05$ comparing each data to vehicle control.

(a)

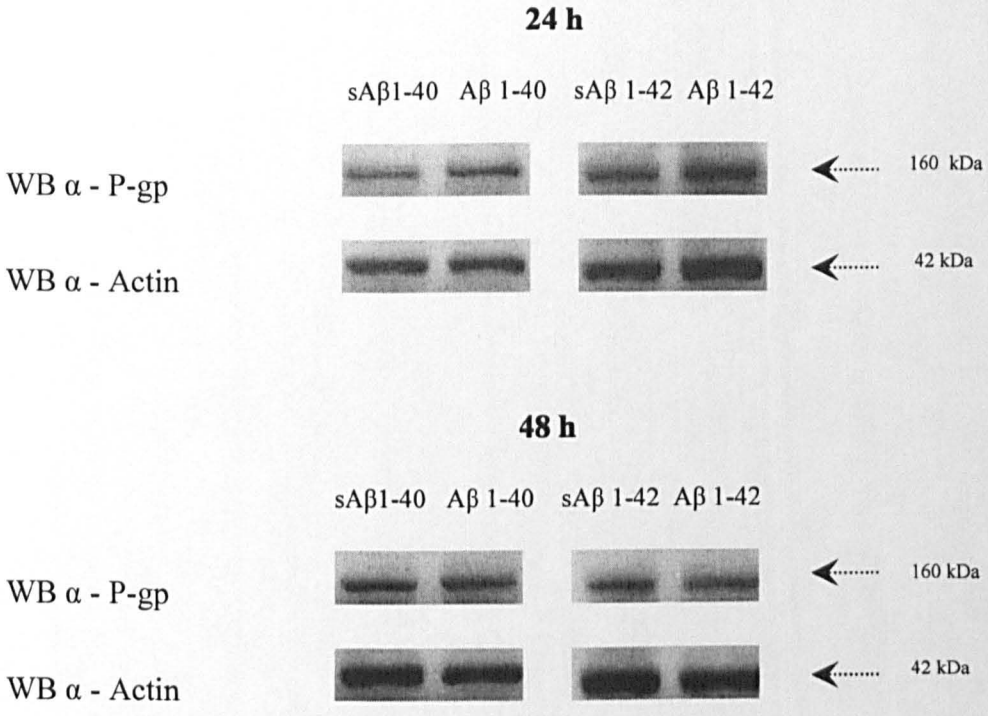

(b)

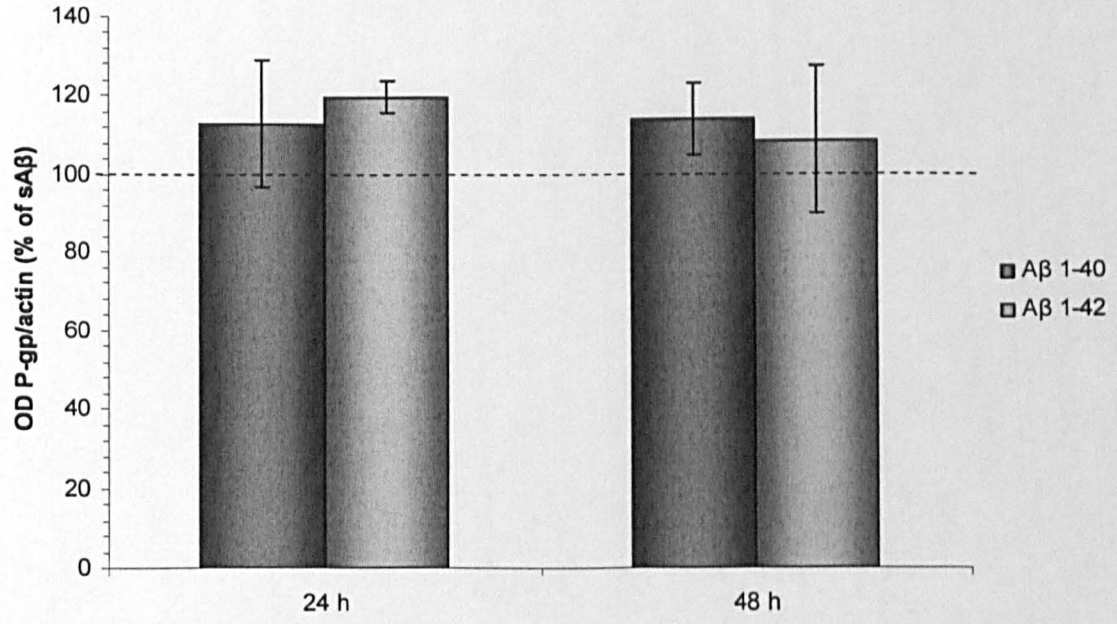

Figure 4.2. The effects of Aβ 1-40 and Aβ 1-42 on the expression of P-gp by hCMEC/D3 cells. (a) Fully confluent hCMEC/D3 cells were incubated with 5 μM Aβ 1-40, Aβ 1-42, sAβ1-40 or sAβ1-42 for 24 h or 48 h, and the expression of P-gp (mouse monoclonal IgG_{2a}) or actin (mouse monoclonal IgG_1) was then assessed by western blotting. **(b)** The optical density corresponding to P-gp (arbitrary units) was divided by the optical density corresponding to actin and data was normalised with their respective sAβ controls. Data represents mean ± SEM, n = 3 experiments with single samples. $P > 0.05$ comparing sAβ to Aβ raw data values using a paired t test.

(a)

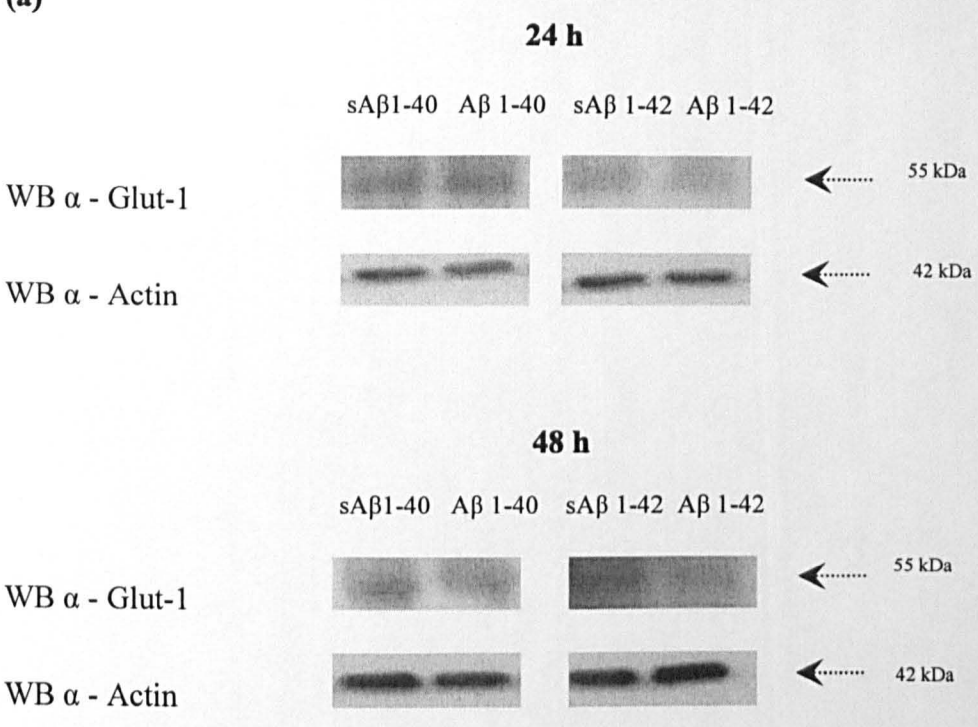

(b)

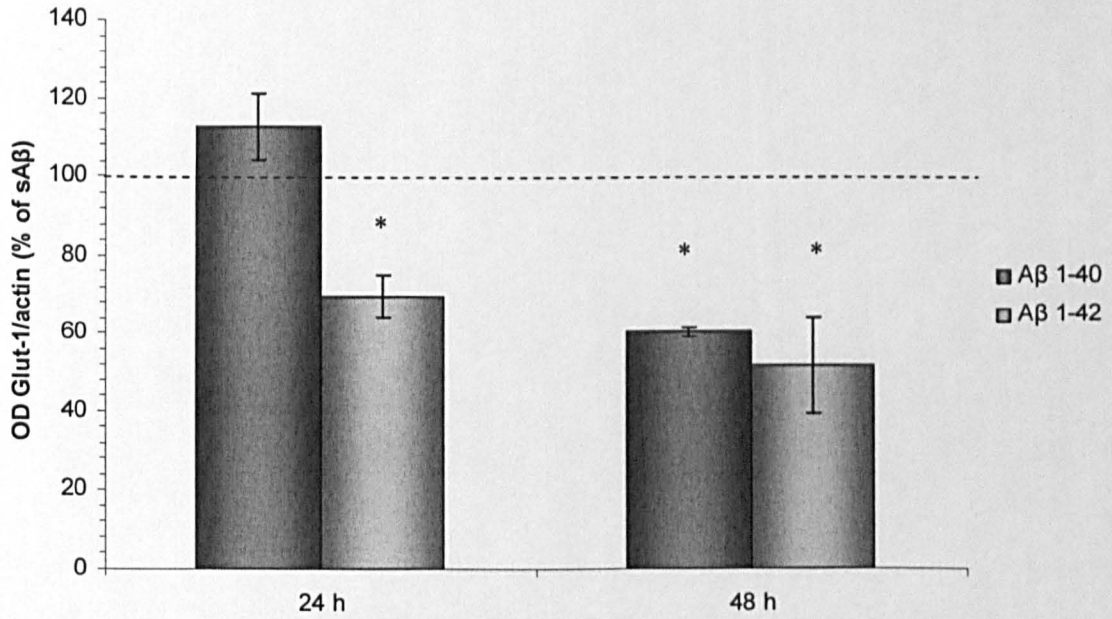

Figure 4.3. The effects of Aβ 1-40 and Aβ 1-42 on the expression of Glut-1 by hCMEC/D3 cells. (a) Fully confluent hCMEC/D3 cells were incubated with 5 μM Aβ 1-40, Aβ 1-42, sAβ1-40 or sAβ1-42 for 24 h or 48 h and the expression of Glut-1 (rabbit polyclonal IgG) or actin (mouse monoclonal IgG_1) was then assessed by western blotting. **(b)** The optical density corresponding to Glut-1 (arbitrary units) was divided by the optical density corresponding to actin and data was normalised with their respective sAβ controls. Data represents mean ± SEM, n = 3 experiments with single samples. * $P < 0.05$ comparing sAβ to Aβ raw data values using a paired t test.

.

(a)

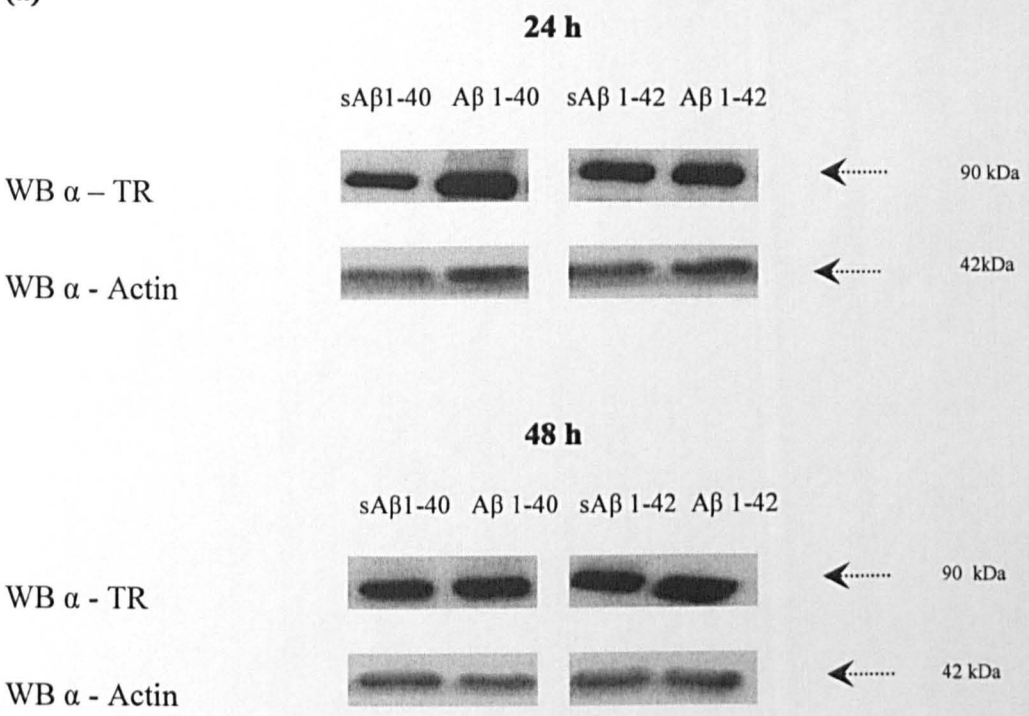

(b)

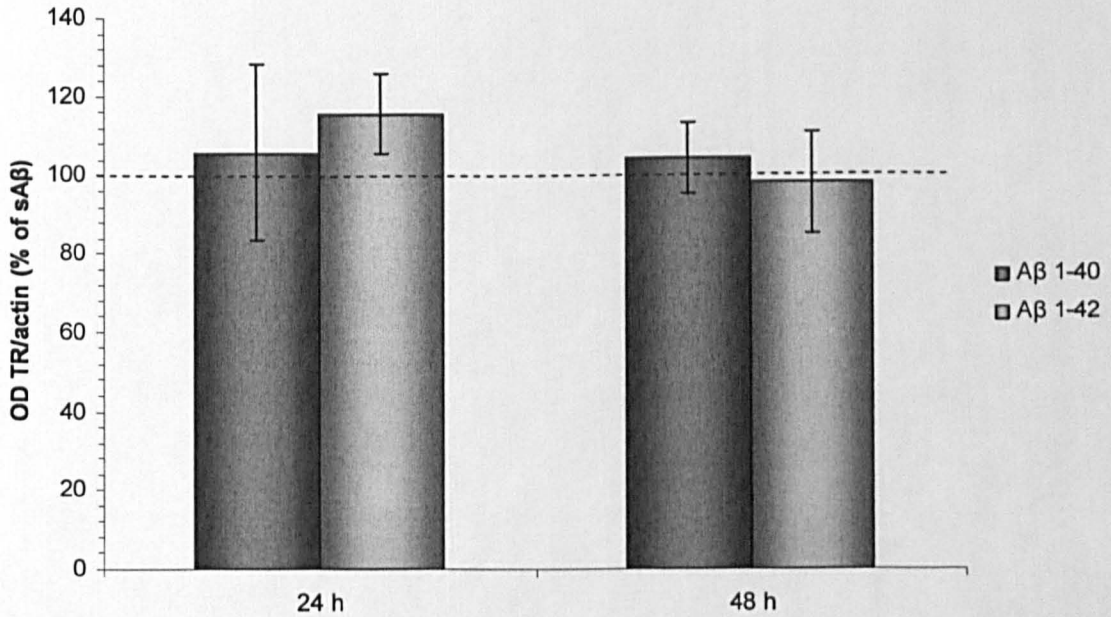

Figure 4.4. The effects of Aβ 1-40 and Aβ 1-42 on the expression of the transferrin receptor by hCMEC/D3 cells. (a) Fully confluent hCMEC/D3 cells were incubated with 5 μM Aβ 1-40, Aβ 1-42, sAβ1-40 or sAβ1-42 for 24 h or 48 h and the expression of the transferrin receptor (TR, mouse monoclonal IgG_1) or actin (mouse monoclonal IgG_1) was then assessed by western blotting. **(b)** The optical density corresponding to the TR (arbitrary units) was divided by the optical density corresponding to actin and data was normalised with their respective sAβ controls. Data represents mean ± SEM, n = 3 experiments with single samples. $P > 0.05$ comparing sAβ to Aβ raw data values using a paired t test.

(a)

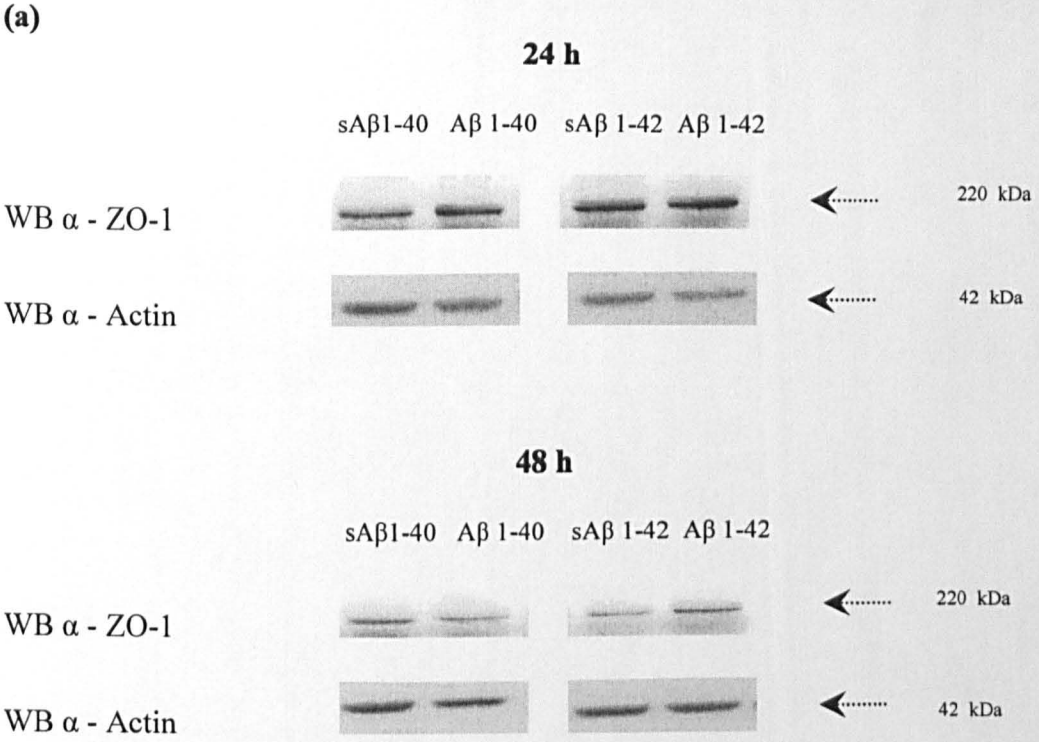

(b)

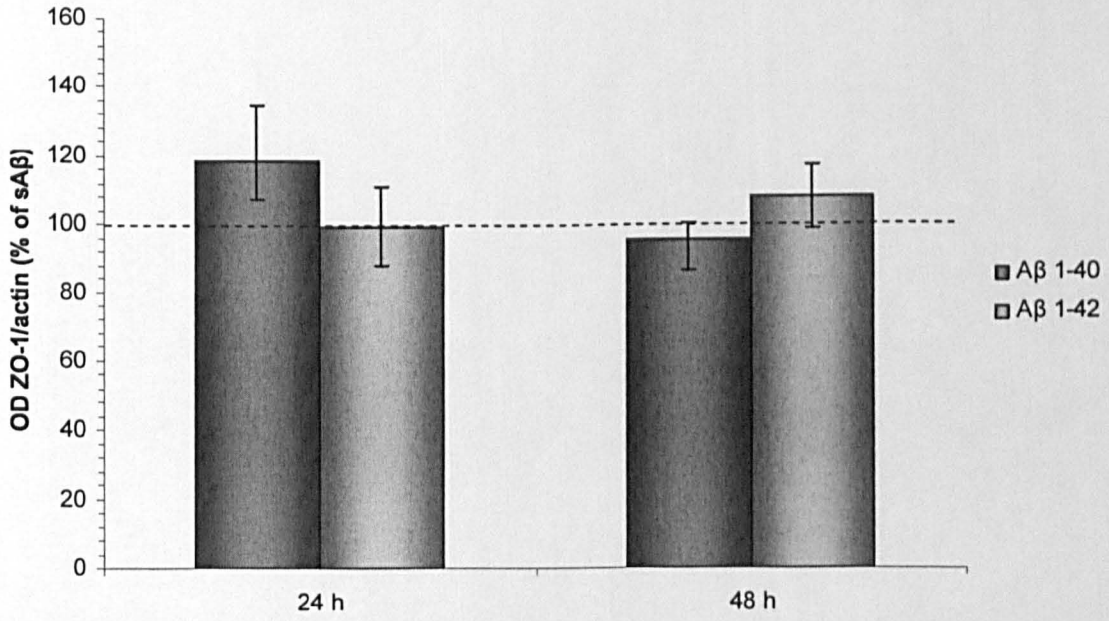

Figure 4.5. The effects of Aβ 1-40 and Aβ 1-42 on the expression of ZO-1 by hCMEC/D3 cells. (a) Fully confluent hCMEC/D3 cells were incubated with 5 μM Aβ 1-40, Aβ 1-42, sAβ1-40 or sAβ1-42 for 24 h or 48 h and the expression of ZO-1 (rabbit polyclonal IgG) or actin (mouse monoclonal IgG_1) was then assessed by western blotting. **(b)** The optical density corresponding to ZO-1 (arbitrary units) was divided by the optical density corresponding to actin and data was normalised with their respective sAβ controls. Data represents mean ± SEM, n = 3 experiments with single samples. $P > 0.05$ comparing sAβ to Aβ raw data values using a paired t test.

(a)

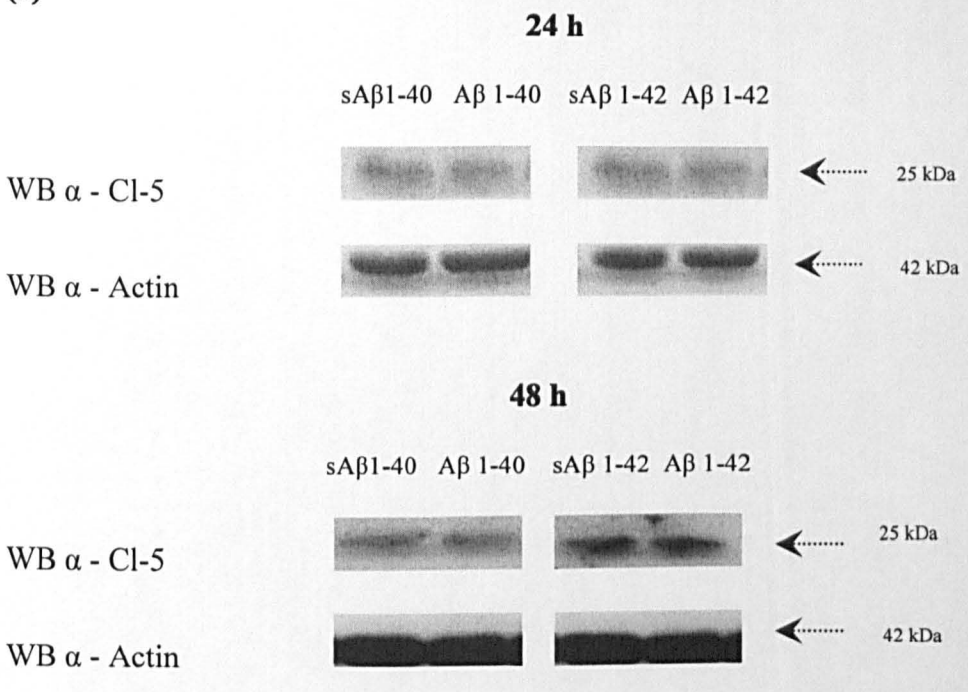

(b)

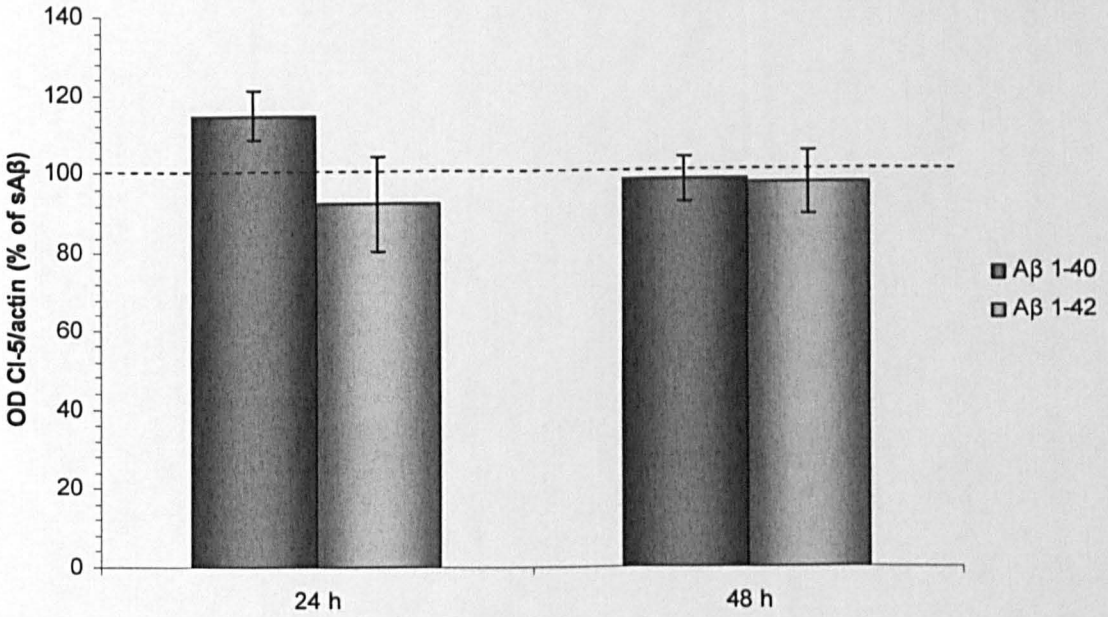

Figure 4.6. The effects of Aβ 1-40 and Aβ 1-42 on the expression of Cl-5 by hCMEC/D3 cells. (a) Fully confluent hCMEC/D3 cells were incubated with 5 μM Aβ 1-40, Aβ 1-42, sAβ1-40 or sAβ1-42 for 24 h or 48 h and the expression of Cl-5 (mouse monoclonal IgG_1) or actin (mouse monoclonal IgG_1) was then assessed by western blotting. **(b)** The optical density corresponding to Cl-5 (arbitrary units) was divided by the optical density corresponding to actin and data was normalised with their respective sAβ controls. Data represents mean ± SEM, n = 3 experiments with single samples. $P > 0.05$ comparing sAβ to Aβ raw data values using a paired t test.

(a)

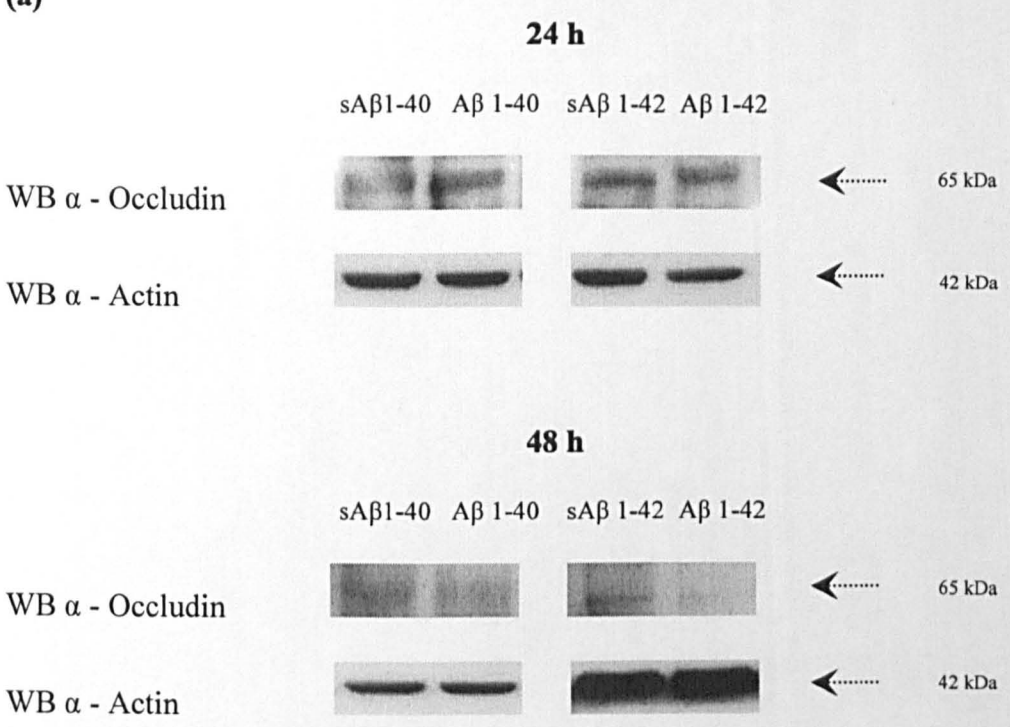

(b)

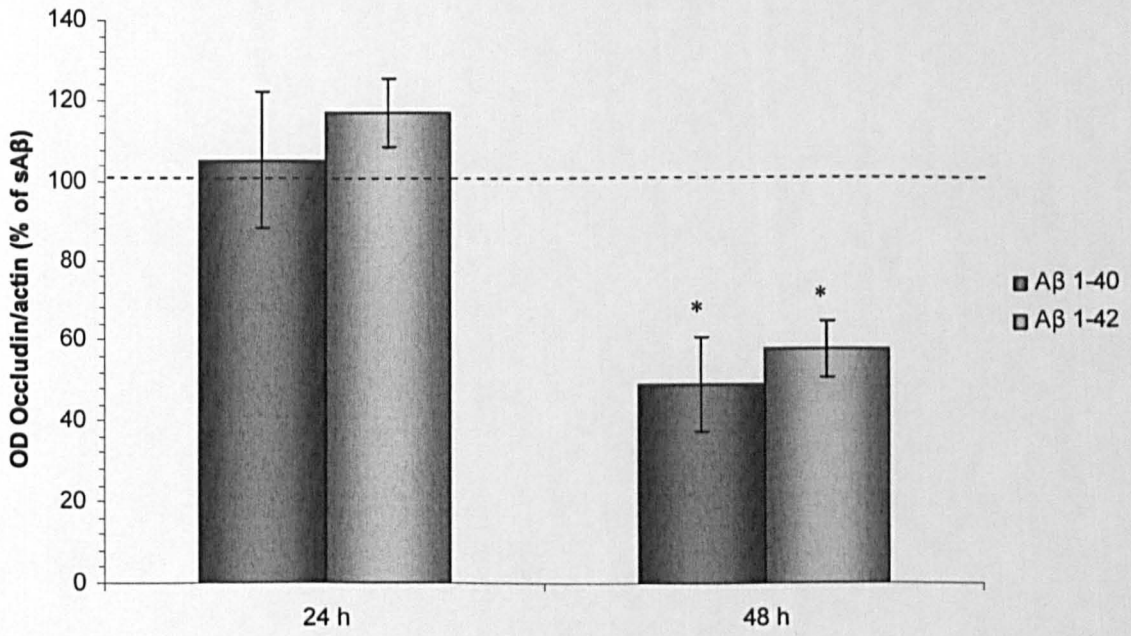

Figure 4.7. The effects of Aβ 1-40 and Aβ 1-42 on the expression of occludin by hCMEC/D3 cells. (a) Fully confluent hCMEC/D3 cells were incubated with 5 μM Aβ 1-40, Aβ 1-42, sAβ1-40 or sAβ1-42 for 24 h or 48 h and the expression of occludin (rabbit polyclonal IgG) or actin (mouse monoclonal IgG_1) was then assessed by western blotting. **(b)** The optical density corresponding to occludin (arbitrary units) was divided by the optical density corresponding to actin and data was normalised with their respective sAβ controls. Data represents mean ± SEM, n = 3 experiments with single samples. * $P < 0.05$ comparing sAβ to Aβ raw data values using a paired t test.

(a)

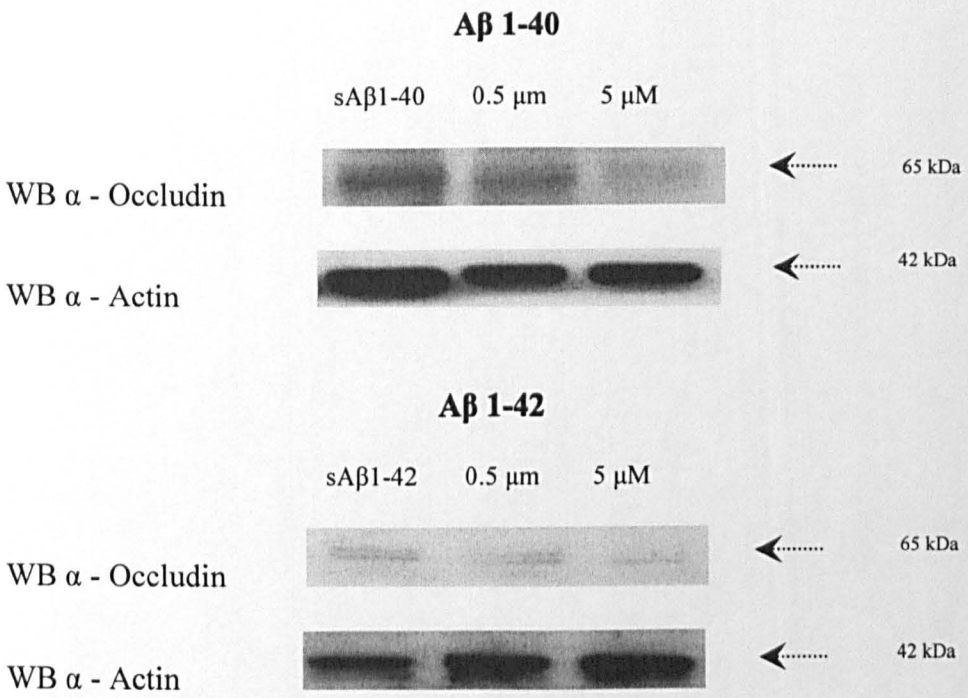

(b)

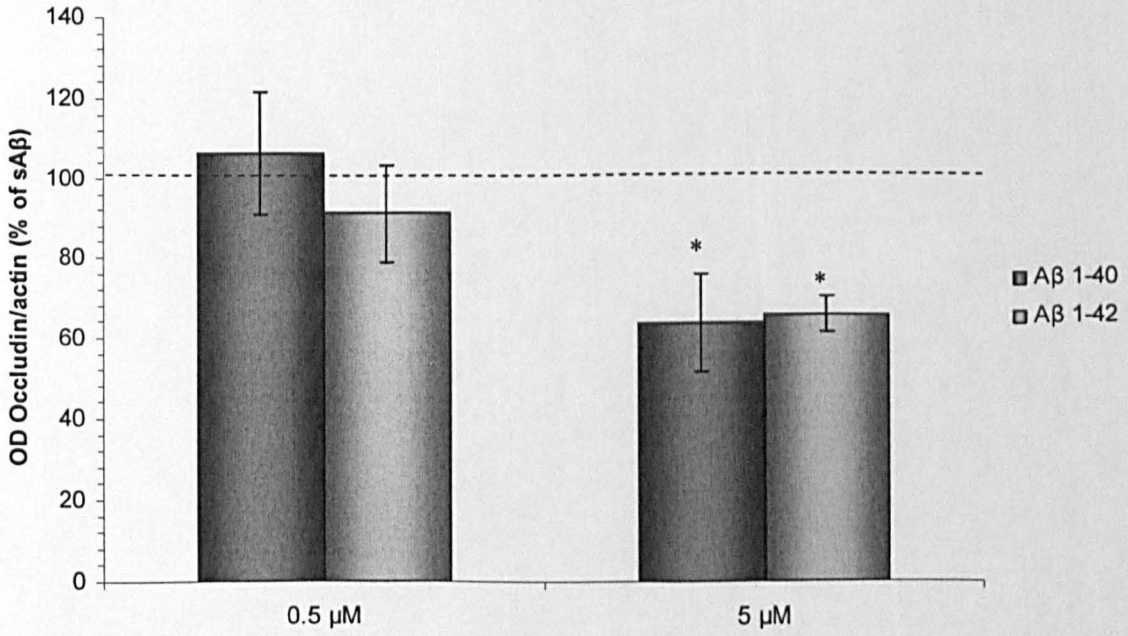

Figure 4.8. The concentration-dependent effects of Aβ 1-40 and Aβ 1-42 on occludin expression in hCMEC/D3 cells after a 48 h incubation period. (a) Fully confluent hCMEC/D3 cells were incubated with 0.5 or 5 μM Aβ 1-40, Aβ 1-42 or 5 μM sAβ 1-42 or sAβ1-40 for 48 h. The expression of occludin (rabbit polyclonal IgG) or actin (mouse monoclonal IgG_1) was then assessed by western blotting **(b)** The optical density corresponding to occludin (arbitrary units) was divided by the optical density corresponding to actin and data was normalised with their respective sAβ controls. Data represents mean ± SEM, n = 4 experiments with single samples. * $P < 0.05$ comparing sAβ to Aβ raw data values using a paired t test.

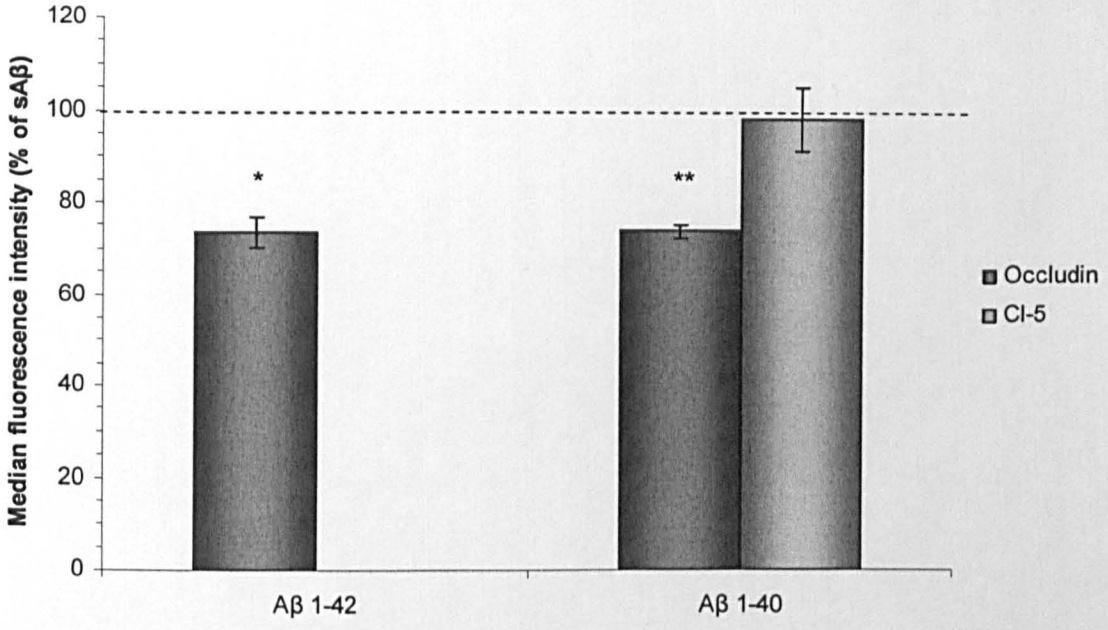

Figure 4.9. The effects of Aβ 1-40 and Aβ 1-42 on the expression of occludin and Cl-5 by hCMEC/D3 cells after a 48 h incubation period as assessed by flow cytometry. Fully confluent hCMEC/D3 cells were incubated with 5 μM of either Aβ 1-40, Aβ 1-42, sAβ 1-40 or sAβ 1-42 for 48 h. The cells were then fixed in 4 % PAF, permeabilised with 0.1 % triton x 100 and the expression of occludin or Cl-5 measured by FACS analysis. Data represents mean ± SEM. n = 3 experiments with duplicate samples for Aβ 1-42 and n = 20 for Aβ 1-40 occludin expression. n = 3 experiments with duplicate samples for Cl-5 expression. * $P < 0.05$, ** $P < 0.01$ comparing the raw data for sAβ to Aβ using a paired t test.

(a) sAβ 1-40 **(b)** Aβ 1-40

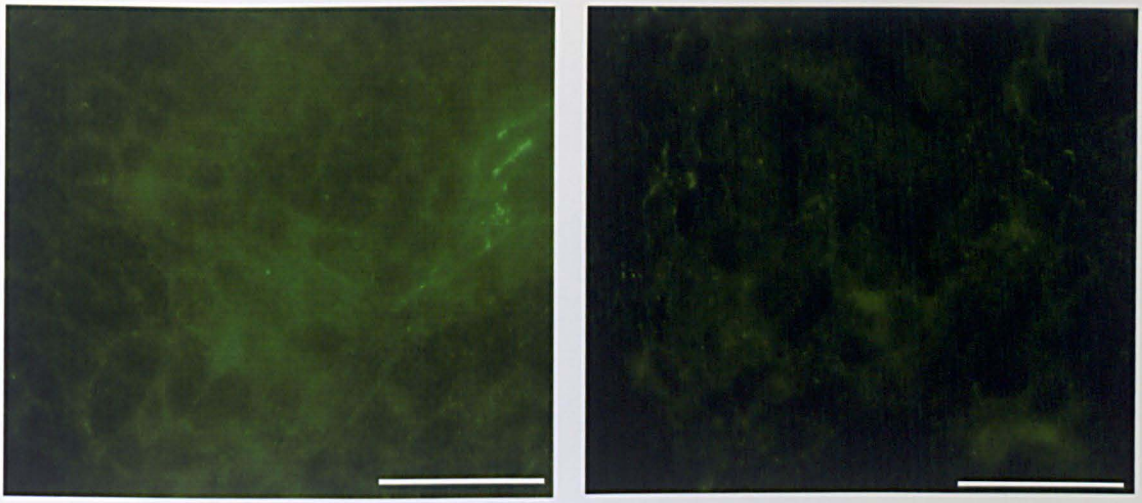

Figure 4.10.The expression of occludin by hCMEC/D3 cells after 48 h Aβ 1-40 incubation as assessed by immunocytochemistry. Fully confluent hCMEC/D3 cells were incubated with 5 μM **(a)** sAβ 1-40 or **(b)** Aβ 1-40 for 48 h. The cells were then fixed in methanol, permeabilised with 0.1 % triton x 100 and the expression of occludin (rabbit polyclonal IgG) measured by ICC. Results are from one experiment representative of 2. The scale bar represents 50 μM.

(a) 24 h

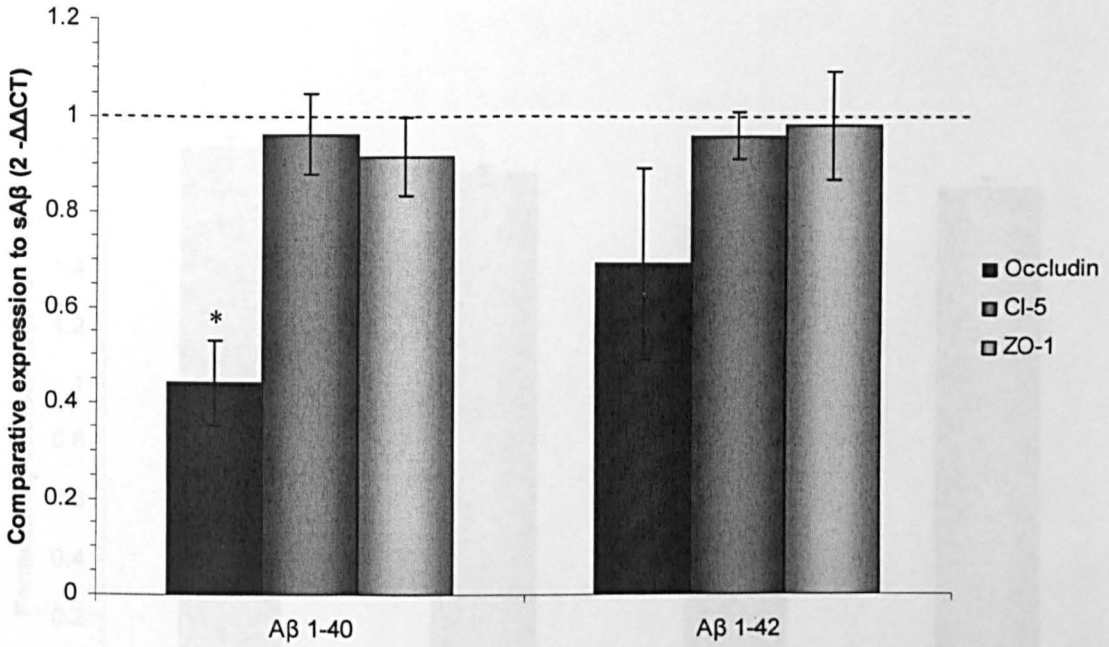

(b) Aβ 1-40 at 48 h

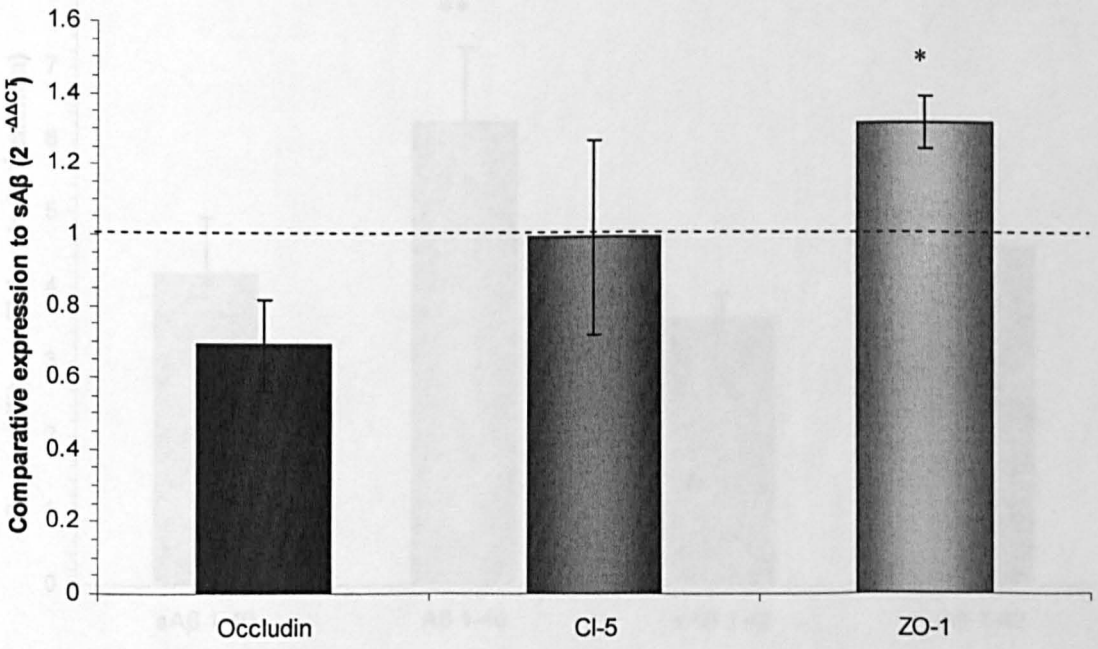

Figure 4.11. The effects of Aβ peptides on the mRNA levels of occludin, ZO-1 and Cl-5 after 24 and 48 h incubation in hCMEC/D3 cells. (a) Fully confluent hCMEC/D3 cells were incubated with 5 μM Aβ 1-42, Aβ 1-40, sAβ1-40 or sAβ 1-42 for 48 h and the mRNA levels of Cl-5, occludin and ZO-1 was calculated using RT-PCR Data represents mean ± SEM. n = 4 experiments with duplicate samples. * P <0.05 comparing ΔCT values using a paired t test. **(b)** mRNA levels of the TJ proteins were assessed after 48 h incubation with Aβ 1-40. Data represents mean ± SEM. n = 3 experiments with duplicate samples * $P < 0.05$ comparing ΔCT values.

(a)

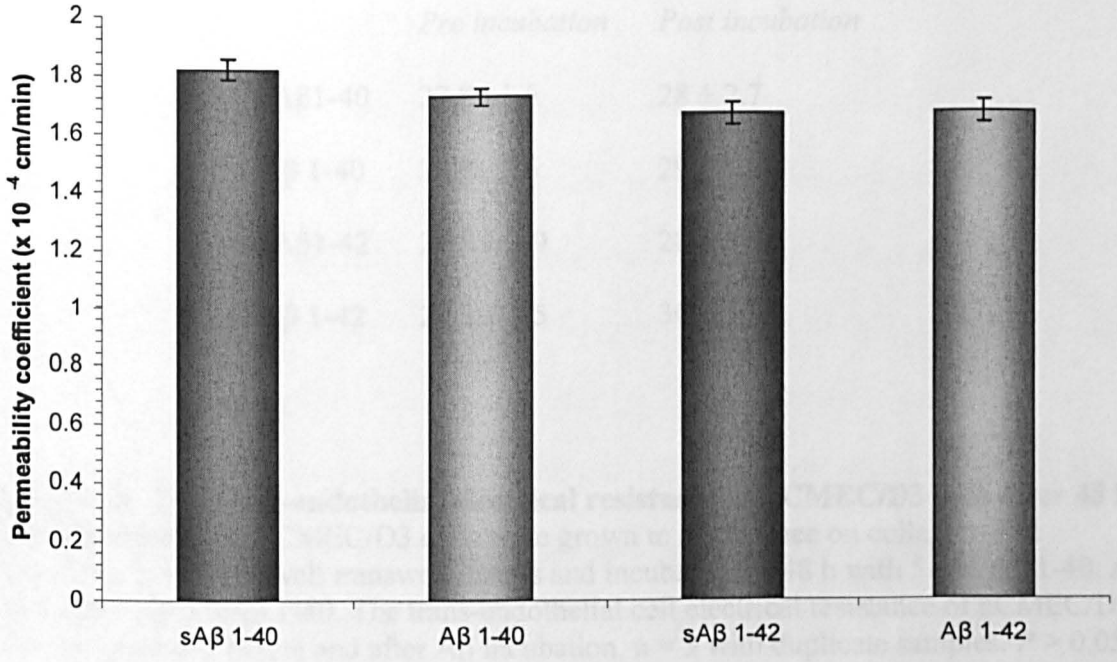

(b)

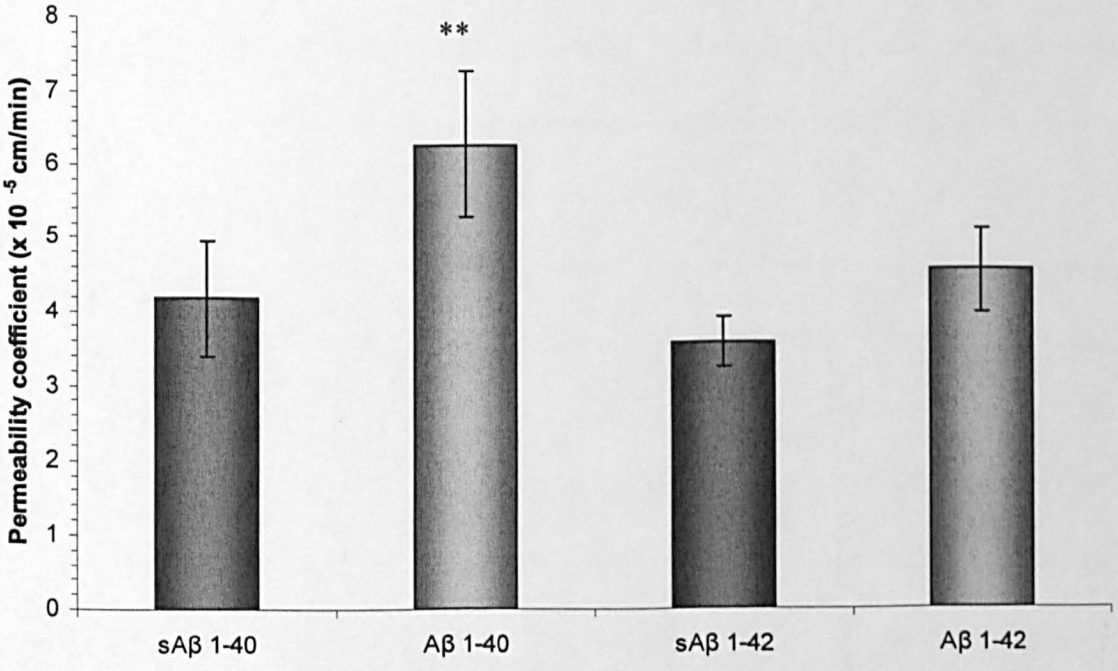

Figure 4.12. Permeability coefficient of hCMEC/D3 cells to 4 and 70 kDa FITC-dextran after 48 h Aβ1-40 or Aβ 1-42 incubation. hCMEC/D3 cells grown to confluence on transwell filter inserts were treated with 5 μM Aβ 1-40, Aβ 1-42, sAβ 1-42 or sAβ 1-40 for 48 h. The permeability of the cells to the paracellular tracers **(a)** 4 kDa or (b) 70 kDa FITC-Dextran was then investigated. Data represents mean ± SEM. n = 3 with duplicate samples for with the exception of Aβ 1-40 and sAβ 1-40 in **(b)** where n = 6 with duplicate samples. * $P < 0.05$, ** $P < 0.01$ using a paired t test.

	TEER ($\Omega.cm^2$)	
	Pre incubation	*Post incubation*
sAβ1-40	27.8± 1.6	28 ± 2.7
Aβ 1-40	28.5± 2.6	29.7 ± 3.8
sAβ1-42	27.8 ± 2.9	28.5 ± 3.7
Aβ 1-42	28.8 ± 3.5	30 ± 3.9

Figure 4.13. The trans-endothelial electrical resistance of hCMEC/D3 cells after 48 h incubation with Aβ. hCMEC/D3 cells were grown to confluence on collagen- and fibronectin- coated 12 well transwell inserts and incubated for 48 h with 5 μM Aβ 1-40, Aβ 1-42, sAβ 1-42 or sAβ 1-40. The trans-endothelial cell electrical resistance of hCMEC/D3 cells was recorded before and after Aβ incubation. n = 3 with duplicate samples. $P > 0.05$ using a paired t test.

4.4 Discussion

4.4.1 Cytotoxicity of Aβ to hCMEC/D3 cells

In the current study, both Aβ 1-40 and Aβ 1-42 peptides were only toxic at concentrations of 10 μM (when compared to their scrambled counterparts) to hCMEC/D3 cells after 48 h incubation. Results from other groups have found a large variation in concentrations needed to evoke toxic effects ranging from 100 nM to 20 μM using different EC types (Table 4.1). The toxicity of Aβ to ECs is believed to involve caspase activation [582], superoxide oxide production [582] and decreased nitric oxide production [412]. The confluent state of ECs might constitute a factor which can affect the cytotoxicity of Aβ. Using bovine aortic ECs, Balcells *et al* [590] found that Aβ 1-42 secreted from CHO cells co-transfected with APP and mutated PS genes was not toxic to confluent ECs, but displayed toxic properties to sub-confluent ECs. In this study, fully confluent hCMEC/D3 cells were used and both Aβ 1-40 and 1-42 only displayed modest toxicity after 48 h incubation. This result is in partial agreement with Eisenhower *et al* [464], who found that Aβ 1-40 was only toxic to primary hBECs at 20 μM, to but not at 2 μM. In contrast however, this group found that Aβ 1-42 displayed toxic effects at much lower concentrations, between 2 and 20 μM. It is worth mentioning that concentrations as high as 20 μM Aβ 1-42 have been added to primary rat BECs and shown no appreciable toxicity [486]. In addition to EC confluence, Aβ aggregation might in part explain the differences in concentrations needed to elicit toxic responses. Eisenhower *et al* [464] have demonstrated that aggregated Aβ 1-40 is more toxic to primary BECs than unaggregated Aβ 1-40. Recently, soluble oligomers have been hypothesised as the more toxic species of Aβ. Shankar *et al* [591] demonstrated that Aβ dimers isolated directly from AD patients are capable of impairment of synaptic plasticity and memory in rodents. Furthermore, Klein *et al* [357] have demonstrated that Aβ 1-42 oligomers are up to 40 times more toxic to neuronal cell cultures than unaggrgeated Aβ 1-42, with oligomer concentrations as low

as 10 nM eliciting a cytotoxic response. The overall consensus from this study, and other publications, is that Aβ can cause direct toxicity to BECs *in vitro*, albeit at high concentrations if unaggregated. Brain capillaries in AD display a number of morphological changes including basement membrane thickening, pericyte degeneration, endothelial shape changes, endothelial degeneration and luminal buckling [413]. This has led some researchers to argue that these events occur prior to the onset of AD symptoms as a result of cerebral blood flow reduction [421]. However, the observation that Aβ causes EC death *in vitro*, implies a further possible mechanism for BBB dysfunction in AD. Accumulation of Aβ as cerebrovascular deposits, could act to disturb the function of the BBB and provide a further neuropathogenic mechanism for AD.

4.4.2 Effects of Aβ on the expression of transporter proteins by hCMEC/D3 cells

The protein levels of P-gp were unaltered by Aβ. Currently, there are no reports on the effect of Aβ on the expression of P-gp by BECs *in vitro* and only one report from tissue samples [409]. Vogelgesgang *et al* [409] reported an inverse correlation between Aβ plaque deposition and P-gp expression in the medial temporal lobe of non-demented subjects. The results from the present study, however, do not demonstrate a direct link between Aβ and P-gp protein expression. Unpublished data from Margery Barrand (University of Cambridge, personal communication) has demonstrated P-gp down-regulation in capillaries from AD patient tissue samples. This apparent discrepancy might suggest that Aβ is not directly linked to P-gp down-regulation in AD, rather that other indirect mechanisms might contribute to this effect. For example, Aβ might act on other cell types such as astrocytes, pericytes, or microglia, which could secrete factors that mediate P-gp down-regulation. Astrocytic end feet swelling [373], microglia activation [374] and either pericytic atrophy [375] or an increase in pericyte capillary coverage [376], as a potential second line of defence, have been observed in tissue sections from AD

patients. In the CSF, plasma and brains of AD patient's, the cytokines IL-1 α/β, IL-6 and TNF-α are found elevated and Aβ *in vitro* can induce astrocytes and microglia to produce these cytokines [374, 377]. TNF-α has been demonstrated to decrease the activity of P-gp in an immortalised rat BEC cell line (GPNT)[246], whilst IL-6 can down-regulate P-gp expression in cultured rat hepatocytes [592] and *in vivo* in mice after intraperitoneal injection [593] (reviewed [594]). IL-1β is also found to decrease P-gp expression in rat hepatocytes *in vitro* [592]. P-gp down-regulation in AD might therefore be mediated by an indirect mechanism induced by Aβ or as a result of inflammation.

Iron accumulation has been observed in different brain regions in AD including the hippocampus and cerebral cortices [589]. The interaction of iron with Aβ causes ROS production and Aβ aggregation and it has been hypothesised that redox active iron is a key mediator in Aβ toxicity [595, 596]. The transferrin receptor is a key transporter molecule for iron at the BBB, acting to transport iron into ECs from the blood [150, 151]. In this chapter, Aβ did not alter the protein levels of the transferrin receptor. This result implies that increased levels of iron in the brain, would not be due to Aβ-induced transferrin receptor up- regulation and hence iron transport. This is in agreement with Kalaria *et al* [597], who noted that ^{125}I transferrin binding was decreased in hippocampal regions. However, in this current study there were no differences in cerebral microvessel binding in AD patients compared to controls. Morris *et al* [598] have also found decreased transferrin receptor levels in brain regions most prone to senile plaques, notably the hippocampus, though not at the microvessel level. The increased iron found in AD patients might originate from brain resident cells such as microglia, which can release iron from ferritin *in vitro* [599], or by binding of iron to Aβ deposits rather than from an absolute increase in iron levels in brain ISF. Increased iron concentrations in the brain might also be the result of BBB changes in AD patients. The up-regulation of an alternate iron receptor, such as melanotransferrin [600] could mediate blood-to-brain iron transport. Also, since there are

increased levels of iron in the plasma compared to CSF levels, a leaky BBB as found in AD patients, could allow diffusion of iron into the brain [150, 151, 601].

In the present study, Aβ 1-40 and Aβ 1-42 were both shown to decrease the expression of Glut-1 by hCMEC/D3 cells after 48 h incubation. This finding is in agreement with investigations in AD patients, where decreased glucose utilisation has been observed [431]. Reduced glucose metabolism in the hippocampus [432], neocortex [434] and posterior cingulate gyrus [435] has been noted in patients with AD. The decreased glucose metabolism might be due in part to a decreased uptake of glucose into the brain across the BBB. Glut-1 is highly expressed by BECs and is responsible for the transport of glucose across the BBB [138]. Using both immunolabelling and covalent binding of cytochalasin B, decreased Glut-1 levels have been observed in brain tissue from AD patients at the level of the BBB [146, 586, 587]. Mooradian *et al* [438] have further demonstrated in AD patients that Glut-1 is altered at the protein level, but not at the mRNA level. There is also evidence that Aβ can cause Glut-1 down-regulation *in vivo*. Using APP/PS1 mice, Hooijmans *et al* [437] found that Aβ load in the hippocampus precedes Glut-1 reduction, and that Glut-1 density per capillary was decreased. *In vitro*, Aβ 25-35 has also been demonstrated to decrease the uptake of glucose in porcine pulmonary ECs, however Glut-1 levels were not assessed [442]. Taken together, the results of the present study and the data described above indicate that Aβ can cause a down-regulation in the Glut-1 receptor, which could contribute to reduced neuronal activity contributing to the pathogenesis of AD.

4.4.3 Effect on Aβ tight junction protein expression by hCMEC/D3 cells

The results from this present study have demonstrated that Aβ incubation induces occludin down-regulation at the protein and mRNA level and increased hCMEC/D3 cell paracellular permeability. These results suggest that the two findings are interlinked, i.e. occludin is a key component of endothelial cell permeability. The importance of occludin

in conferring restrictive TJs has been demonstrtaed *in vitro* [84, 85, 134] and *in vivo* [91, 92, 276]. Transfection of truncated occludin or siRNA knockdown in MDCK cells or Xenopus embryo cells results in increased paracellular permeability [84, 85, 134]. Occludin down-regulation and increased permeability has been observed in animal models of oxidative stress [276], IL-1-induced neutrophil BBB breakdown [91] and inflammatory pain [92]. Occludin down-regulation, as observed in the current study, is in partial agreement with Marco and Skaper [486], who observed that Aβ 1-42 at 20 μM induced occludin down-regulation in rat BECs at 24 h, but not at 48 or 72 h incubation. In addition, these authors did not detect any alterations in overall Cl-5 or ZO-1 levels, in agreement with our study, although they reported that Cl-5 translocated to the cytoplasm and they did not investigate endothelial cell permeability. Soluble Aβ 1-40 oligomers, but not unaggregated Aβ 1-40 species, have also been demonstrated to increase the paracellular permeability of hBEC cultures after 24 h incubation, which was associated with ZO-1 translocation to the cytoplasm and nucleus from the cell membrane [443]. In that study, the expression of occludin was not investigated, and the total levels of ZO-1 were not quantified. Therefore, whilst in this current study total levels of ZO-1 were not decreased, as assessed by western blotting, it cannot be ruled out that ZO-1 could have translocated away from the membrane after Aβ 1-40 incubation.

Decreased occludin expression and increased BBB permeability has been noted by Takechi *et al* in APP/PS1 mice [94]. Stewart *et al* [376] have described that in AD patients there is a reduction in the number of TJs per vessel length. Therefore the evidence suggests that TJ disorganisation and occludin down-regulation might contribute significantly to the pathology in AD.

4.4.4 BBB permeability in AD

The results of this study have shown that incubation with Aβ 1-40 increases the permeability of hCMEC/D3 cells to the paracellular tracer FITC-dextran of 70 kDa but not

that of 4 kDa. The lack of an effect of Aβ 1-40 incubation on the permeability of hCMEC/D3 cells to 4 kDa FITC-dextran may be related to the relatively high permeability of the hCMEC/D3 cells to smaller molecules prior to Aβ treatment. Indeed, the P_e of hCMEC/D3 cells to 4 kDa FITC-dextran was ~ 5 fold higher than that to 70 kDa FITC-dextran.

Some studies have shown increased CSF/plasma protein ratios of albumin and IgG, suggesting that a leaky BBB is a common occurrence in AD patients [577-581]; however other studies have not confirmed this finding [602-604]. The most compelling evidence for an increased BBB permeability in AD was provided by Zipser *et al* [439], who found that prothrombin leakage from the blood into the CNS was significant in advanced stage AD. Matsumoto *et al.* [579] recently demonstrated, using CSF measurements and MRI, that increased BBB permeability to albumin was associated with medial temporal atrophy in AD patients. Other evidence, using AD animal models, also suggests that an increased BBB permeability can be induced by Aβ. Using Tg 2576 mice, Ujii *et al* [584] observed increased BBB permeability after 4 months of age, prior to plaque deposition and disease onset, which can be reversed via Aβ peptide immunisation [440]. Su *et al* [441] have also demonstrated that intravascular jugular vein injections of Aβ 1-40 can induce a leaky BBB and microglia activation in rats. Aβ 25-35 and Aβ 1-40 have also been demonstrated to increase the permeability of EC cultures *in vitro* including porcine BECs [442], human BECs [443] and porcine pulmonary ECs [444].

The increased BBB permeability induced by Aβ *in vitro*, as noted by others and in this study, is in agreement with data found in AD patients and *in vivo* models. This raises the question as to what extent a leaky BBB would induce alterations in CNS function. Increased BBB permeability has been proposed as a key pathogenic mechanism in other diseases such as stroke [605], multiple sclerosis [606] and the progression of epilepsy [607]. TJs at the BBB serve to limit the permeability of hydrophilic substances from the blood into the CNS, although transporters allow transfer of molecules. A breakdown of the

BBB in principle could lead to enhanced brain content of insulin, glucocorticoids [608], glutamate [155], plasma proteins and ions [609]. Insulin entry into the brain could compete with insulin degrading enzyme for the degradation of Aβ, increasing Aβ brain load. Extravasation of serum proteins in the brain has been linked to epilepsy and, interestingly, BBB breakdown is correlated with seizure frequency in mannitol-treated rats [607]. Similarly, the efflux of glucocorticoids by P-gp would be disrupted by a leaky BBB, which in turn could cause neuronal catabolism [610]. A leaky BBB would also decrease the efflux capability of all ABC transporters at the BBB, allowing unwanted potentially toxic xenobiotics entry to the CNS. Increased glutamate in the brain as a result of a leaky BBB could results in excitotoxic events. As mentioned previously, increased iron concentrations are found associated with AD plaques, in addition to other heavy metal ions. Transferrin-bound iron exists at much higher concentrations in the plasma than in brain tissue. A potential route of entry could therefore be via a leaky BBB.

The abnormal presence of serum-derived proteins in AD patients, via a leaky BBB, might act to cause inflammation and neuronal degeneration. Albumin levels are much higher in blood than the brain, and albumin has been demonstrated to activate microglia [611], and induce cholinergic cell death *in vitro* [612]. Albumin is also bound to Aβ in the plasma [613] and plasma proteins are frequently found as a component of Aβ plaques [614, 615]. A leaky BBB in AD patients could lead to the diffusion of serum proteins into the brain, which in turn could cause direct and indirect, via Aβ aggregation, neuronal degeneration. It would be expected that increased permeability of the BBB to serum proteins would lead to oedema as is the case in stroke. However, there are no reports suggesting the presence of oedema in AD patient's brains. This suggests that the BBB leakiness in AD patients may be subtler in nature.

Recently, Stone [616] has hypothesised that capillary haemorrhages might be an underlying cause of AD. Stone suggested that microhaemorrhages cause ischemia, which results in oxidative damage and increased neuophil Aβ production, and the release of

haemoglobin into the neuropil, which binds to Aβ to produce oligomers. Whilst the results of this study do not demonstrate a causative role for BBB leakiness in AD, they do provide a further mechanism of BBB dysfunction in this disease. Increased Aβ production could induce a leaky BBB, resulting in haemoglobin extravasation into the CNS. Haemoglobin could bind to Aβ and promote oligomer formation. In line with this view, haemoglobulin has been demonstrated to promote the formation of Aβ oligomers *in vitro* and is associated with senile plaques in AD patients [617].

A further consequence of BBB permeability could be the access of the brain of pathogens. Interestingly, increased levels of herpes simplex virus have been noted in the elderly and in AD patients [618], and pathogens have been proposed by some researchers to be a causative factor in AD [619, 620]. Increased BBB permeability caused by Aβ could increase the susceptibility of the brain to infection.

Whilst evidence that the BBB is compromised in AD patients is compelling, and numerous studies *in vitro* and in animal models have suggested possible mechanisms by which a leaky BBB might contribute to the pathogenesis of AD, unfortunately, to date, there is no evidence for direct BBB dysfunction underlying neuronal degeneration in AD patients.

4.5 Conclusions

The results of the present study demonstrate that Aβ can down-regulate Glut-1 expression in BECs, which may consequently reduce the amount of glucose available to neurones and promote neuronal degeneration. At the TJ level, non-toxic concentrations of Aβ induce a decrease in occludin expression by BECs, which was associated with an increased paracellular permeability. These results suggest that Aβ-induced BBB dysfunction, might contribute significantly to the pathogenesis of AD patients.

Cell type	Concentration of Aβ required for toxicity	Pathway involved	Assessed by	Reference
Bovine post capillary heart venular ECs	5 μM Aβ 1-40/1-42 evoke 71% and 62 % of control cell growth	Aβ induced ROS and caspase -3 activation	MTT	[582]
Primary human BECs	Aβ 1-40 toxic at 20 μM, whilst Aβ 1-42 toxic at 2 and 20 μM	-	MTT	[464]
Rat BECs	1 – 100 nM Aβ 1-40 and Aβ 1-42 enhance necrosis and apoptosis after 3 h but not 48 h	-	TUNEL, lactate dehydrogenase	[621]
Bovine aortic ECs	Aβ 25-35 and Aβ 1-40 ~ 1 μM induces apoptosis.	Decreased NO production and K+ ion channel disruption	MTT	[622]
Rat BECs	Aβ at concentrations of 100 nM and higher were toxic	Possibly NO	-	[623]
Rodent coronary ECs	5-100 nM proliferation of EC, 500 nM and above toxic of Aβ 1-40.	ERK/1/2 inhibition possibly mediated via decrease in FGF-2 production	Cell counts	[624]
Bovine aortic ECs	Aβ 1-40 50 μM caused endothelial cell death.	-	Hoesrst	[625]
Bovine aortic ECs	Aβ1-40 1 μM induce apoptosis.	Toxicity deceased after SOD addition. Also NO dysfunction.	Light microscopy	[583]
Murine BECs	Aβ1-40 caused 40 % toxicity after 48 h. 25-35 also evoked a strong endothelial cell death.	Reversed by caspase and an anti-oxidant both decreased cell death	MTT	[626]
Bovine aortic ECs	Aβ secreted from CHO over secreting Aβ cells. Not toxic unless ECs were sub confluent	-	Cell counts	[590]

Table 4.1. Selected references on the toxicity of Aβ to ECs

Chapter 5

Molecular mechanisms mediating Aβ 1-40- induced occludin down-regulation and increased hCMEC/D3 cell permeability

Abstract

The aim of this study was to investigate the pathway(s) involved in Aβ 1-40-mediated occludin down-regulation in hCMEC/D3 cells. Pharmacological inhibitors of signalling pathways which Aβ is known to activate (GSK-3β, NF-KB, JNK, p38MAPK, ERK) and others implicated in the regulation of occludin levels (Src, ROCK, PI3K, PKC) were used. Inhibitors of JNK (SP600125, TAT-TI-$JIP_{153-163}$) and p38MAPK (SB203580) selectively prevented Aβ 1-40- mediated occludin down-regulation as assessed by flow cytometry. All three MAPK family members (p38MAPK, JNK-46 kDa and ERK2) were activated at 24 h and 48 h by Aβ 1-40. After 48 h incubation with Aβ 1-40, SB203580 inhibited p38MAPK and JNK activation by Aβ 1-40; however, SP600125 and TAT-TI-$JIP_{153-163}$ only blocked JNK activation. JNK and p38MAPK inhibitors prevented the Aβ 1-40-mediated increase in hCMEC/D3 cell permeability to 70 kDa FITC-dextran. The aggregation of Aβ 1-40 as a possible mechanism mediating this effect was also investigated. When assessed by western blotting, using an anti-Aβ antibody, it was observed that levels of the 4 kDa Aβ 1-40 monomer decreased over 48 h in the supernatant and cell lysates, whilst a large 150 kDa protein was detected from 24 h. This 150 kDa band did not correspond to endogenous APP and might represent the activating Aβ species, since it appeared at the same time as MAPK activation. These results demonstrate that the JNK pathway is critical in the signalling of Aβ 1-40 mediating occludin down-regulation and increased paracellular permeability in hCMEC/D3 cells. JNK inhibition could represent a therapeutic target for AD to prevent BBB dysfunction found in AD patients.

5.1 Introduction

Aβ has been shown to induce several signalling pathways in many cell types, with investigations focused mainly on neuronal and EC death, or glial cell activation (reviewed in [627]). The toxicity of Aβ to neurones involves complex molecular mechanisms, potentially involving multiple pathways, both extra and intracellular, such as ROS and cytokine release [627]. Three main intracellular signalling pathways are commonly described as being activated by Aβ in neurones or in different cell types, namely GSK-3β, JNK and NF-kB.

GSK-3β forms part of the PI3K-Akt mediated cell survival pathway and is proposed to play multiple roles in AD [628, 629], including tau hyperphosphorylation, Aβ production and neuronal apoptosis. Recently, it has been demonstrated that GSK-3β inhibition [345] and PI3K activation [347], which in turn leads to GSK-3β inactivation, prevents Aβ- induced neuronal cell death in rat hippocampal neurones. Akt and GSK-3β are also implicated in Aβ toxicity to ECs. HUVEC cells transfected with APP, have been demonstrated to produce Aβ 1-42, which is associated with reduced AKT and increased GSK-3β activation, inducing apoptosis [630].

The JNK pathway also represents a potential therapeutic target in AD (reviewed in [631]). In brain tissue from AD patients, JNK activation has been found associated with both intracellular Aβ in neurones from the cerebral cortex [632], and Aβ plaques and NFT in the hippocampus [633]. *In vitro*, JNK activation can be induced following incubation of cultured neurones with Aβ [353, 634-636]. Wei *et al.* [353] have demonstrated, using the neuroblastoma cell line SH-SY5Y, that Aβ 25-35 and Aβ 1-42 rapidly induce JNK activation and cell death, which is prevented by JNK inactivation, albeit indirectly via insulin-like growth factor. Bozyczko-coyne *et al* [634] and Troy *et al* [636] have also demonstrated that direct JNK inhibition can prevent Aβ- induced cell death in rat cortical neurones and PC12 cells, respectively.

There is conflicting evidence regarding the role of NF-kB in AD. NF-kB has been reported to be activated in neurones and astrocytes surrounding early amyloid plaques in the cortex and hippocampus of AD patients brains [637]. NF-kB activation has also been described in the neurones of the hippocampus and enterohinal cortex [638, 639] and also, in large cholinergic neurones in AD patients [640]. Aβ can also induce the activation of NF-kB in primary rat cerebellar granule cells [637] and human neuroblastoma cells [641]. *In vitro*, NF-kB inhibitors have been demonstrated to prevent Aβ toxicity in rat primary neurones [351]. In contrast, Kaldschmidt *et al* [344] showed that NF-kB inhibition can potentiate the toxicity of Aβ 1-40 in rat primary neurones, and demonstrated a reduction in NF-kB staining in neurones surrounding plaques in AD brain tissue, compared to age-matched controls. The authors have explained this discrepancy by suggesting that a certain threshold levels of NF-kB is protective, whilst too high or low levels are neurotoxic [642].

The overall aim of this chapter was to investigate the signalling pathway(s) involved in occludin down-regulation and increased permeability mediated by Aβ. Aβ 1-40 was used in preference to Aβ 1-42 in this study, since this particular species is most abundant in AD patients plasma and whole brain homogenates [313]. In addition, Oijen *et al* [321] also found that high plasma concentrations of Aβ 1-40 are associated with an increased risk of developing dementia, and Aβ 1-40 is the species found at the highest levels in cerebrovascular deposits [643]. Therefore, in this study, inhibitors for JNK, GSK-3β and NF-kB, the main signalling pathways mediating Aβ actions, were initially used in an attempt to reverse the Aβ 1-40- mediated occludin down-regulation in hCMEC/D3 cells. Other pharmacological inhibitors were also employed for PI3K, ROCK, Src and PKC pathways which have been previously shown to regulate occludin expression and/or induce post-translational changes at the protein level.

5.2 Methods

5.2.1 Signalling pathway inhibitors

For this study, various inhibitors of signalling pathways, or soluble receptor antagonists for cytokines were employed (Table 5.1). For each inhibitor, concentrations were used that have been previously shown to inhibit the pathway under investigation *in vitro*, either reported in the literature, or as previously demonstrated in the laboratories at The Open University (Dr Ignacio Romero, personal communication). Two exceptions were the soluble cytokine receptors, and the JNK 2/3 inhibitor N-(3-Cyano-4,5,6,7-tetrahydro-1-benzothien-2-yl)-1-naphthamide. For the cytokine receptors, at least a 10 x higher concentration than the IC50 described by the data sheet was used. For N-(3-Cyano-4,5,6,7-tetrahydro-1-benzothien-2-yl)-1-naphthamide, as yet, there are no reported *in vitro* studies that have used this inhibitor. Initial experiments conducted as part of this study found N-(3-Cyano-4,5,6,7-tetrahydro-1-benzothien-2-yl)-1-naphthamide to be toxic to hCMEC/D3 cells. Therefore, an MTT assay (0.25, 0.5, 1, 5, 10, 20 μM) was carried out to determine non-toxic concentrations for use in subsequent experiments (Figure 5.1).

5.2.2 Flow cytometry

Fully confluent hCMEC/D3 cells (grown as in 4.2.4) were pre-incubated for 30 min in the presence or absence of the pharmacological inhibitors/antagonists listed in Table 5.1. 5 μM Aβ 1-40 or sAβ 1-40 was then added to the supernatant for 48 h, and the expression of occludin measured by flow cytometry as described in section 4.2.4.

Modulator	Pathway inhibited	Concentration	Source	Reference
SP600125	JNK 1, 2 and 3	10, 50 μM	Calbiochem NJ, USA.	[644]
TAT-TI-$JIP_{153-163}$	JNK 1, 2 and 3	1, 5, 10 μM	Calbiochem NJ, USA.	[645]
N-(3-Cyano-4,5,6,7-tetrahydro-1-benzothien-2-yl)-1-naphthamide.	JNK 2 and 3	0.5 μM	Calbiochem NJ, USA.	[646]
SB203580	p38MAPK	20 μM	Calbiochem NJ, USA	[647]
PD98059	MEK	50 μM	Calbiochem NJ, USA	[648]
pp2	Src family	10 μM	Calbiochem NJ, USA	[649]
Y-27632	ROCK inhibitor	700 nM	Calbiochem NJ, USA	[650]
Bisindolylmaleimide -1 (Bis-1)	PKC	10 μM	Calbiochem NJ, USA	[651]
LY294002	PI3-kinase	300 μM	Calbiochem NJ, USA	[652]
Lithium chloride (LiCl)	GSK-3β	5 mM	Sigma-Aldrich, Dorset, UK	[345]
sn50	NF-kβ	200 μM	Calbiochem NJ, USA	[653]
sn50-m	Control sn-50	200 μM	Calbiochem NJ, USA	-
sIL-1ra	IL-1	10 ng/ml	Prospec, Rehovot, Israel	IC 50- 0.5 ng/ml
sTNF-R1	TNF - α	10 ng/ml	Prospec, Rehovot, Israel	IC 50- 0.4-1 ng/ml
sIL-6 R	IL-6	10 ng/ml	Prospec, Rehovot, Israel	-

Table 5.1. Signalling pathway modulators and soluble cytokine receptors used to investigate Aβ 1-40 - mediated occludin down-regulation in hCMEC/D3 cells.

5.2.3 Permeability of hCMEC/D3 cells to 70 kDa FITC-dextran

hCMEC/D3 cells were grown to confluence in collagen- and fibronectin- coated transwell polyester membrane inserts (0.4 μm pore diameter, 12mm diameter). SP600125 (50 μM), TAT-TI-JIP$_{153-163}$ (10 μM), SB203580 (10 μM) or a vehicle control was then added to the apical chamber for 30 min. sAβ 1-40 or Aβ 1-40 was then added to the culture medium in the apical chamber for 48 h. The permeability of hCMEC/D3 cells to 70 kDa FITC-dextran was determined as described in section 4.2.6 in addition to the trans endothelial electrical resistance (TEER).

5.2.4 SDS-PAGE and Western blotting

hCMEC/D3 cells were grown to full confluence in collagen-coated 6-well plates and incubated with sAβ 1-40 or Aβ 1-40 for 0, 1, 5, 15, 30 and 60 min or 1, 3, 6, 24 and 48 h. A further experiment was carried out whereby hCMEC/D3 cells were pre-incubated with SP600125 (50 μM), TAT-TI-JIP$_{153-163}$ (10 μM), SB203580 (10 μM), N-(3-Cyano-4,5,6,7-tetrahydro-1-benzothien-2-yl)-1-naphthamide (0.5 μM), or a vehicle control and then incubated with Aβ 1-40 or sAβ 1-40 for 48 h. Cell lysates were then obtained as described in section 4.2.3. The expression of active JNK, p38MAPK and ERK was then assessed by western blotting using specific antibodies for the phosphorylated form of each signalling molecule (Table 5.2). To normalise the results, the western blots were stripped as described in section 2.2.5 and re-probed with antibodies specific for total JNK, p38MAPK or ERK2 (Table 5.2). As a positive control, hCMEC/D3 cells were placed under UV for 30 min, lysed and processed as above

Anti-	Species	Concentration	Source
Phospho- Thr183/Tyr185 JNK	rabbit polyclonal	1 in 1000 dilution	Cell signalling, Massachusetts, USA
Phospho- Thr180/Tyr182 p38MAPK	rabbit polyclonal	1 in 1000 dilution	Cell signalling, Massachusetts, USA
Phospho- Thr185/Tyr187 ERK1/2	mouse IgG_1 monoclonal	1 in 1000 dilution	Biosource, California, USA
JNK	rabbit polyclonal	1 in 1000 dilution	Cell signalling, Massachusetts, USA
p38MAPK	rabbit polyclonal	1 in 1000 dilution	Cell signalling, Massachusetts, USA
ERK2	mouse IgG_{2a} monoclonal	1 in 1000 dilution	Upstate California USA

Table 5.2. List of antibodies used for western blotting.

5.2.5 Aβ peptide in whole cell lysates and culture supernatants as assessed by SDS-PAGE and western blotting

hCMEC/D3 cells were grown to full confluence in collagen-coated 6-well plates, and incubated with Aβ 1-40 for 1, 3, 6, 24 and 48 h. To determine Aβ aggregation in the absence of cultured cells, Aβ 1-40 was added to collagen- coated tissue culture plates, with no hCMEC/D3 cells, for the same time points. 20 µl of each culture medium sample was added to 5 µl of 4 X Laemmli's buffer, whereas cells or collagen-coated wells were scraped and treated as described in section 4.2.3. Aβ levels were then assessed in both the cell lysates and medium samples using SDS-PAGE on 15 % and 8 % gels and western blotting techniques (Antibody 6E10 directed against Aβ 1-16, 1 in 100 dilution, mouse monoclonal IgG_1, Abcam, Cambridge, UK). The membranes were stripped and reprobed, as described in section 2.2.5, for APP (22C11 directed against APP 66-81, diluted 1 in 100, mouse monoclonal IgG_1, Chemicon, Mannheim, Germany).

5.2.5 Statistical analysis.

All data are represented as means +/- SEM and the number of experiments, n, indicated each time. Statistical significance was calculated using ANOVA followed by Student's t test, comparing each treatment to the control (* $P < 0.05$, ** $P < 0.01$). For the permeability experiments, a paired t-test was employed.

5.3 Results

5.3.1 Signalling pathways involved in Aβ 1-40- mediated occludin down-regulation by hCMEC/D3 cells

The aim of this experiment was to investigate the contribution of various signalling pathways in Aβ- mediated occludin down-regulation. Initially pathways known to be activated by Aβ (NF-κB, GSK-3β, JNK) [627], and others that have been previously shown to regulate TJ expression (Rock, Src, PKC) were investigated [131] (Figure 5.2).

Aβ 1-40 caused a decrease in occludin expression by 29 % ± 6.3 (compared to sAβ 1-40) in hCMEC/D3 cells. Pre-incubation with inhibitors of Src (pp2), ROCK (Y-27632), PKC (Bis-1), NF-κB (sn50), GSK-3β (LiCl) or PI3K (LY294002) did not prevent Aβ 1-40-induced occludin down-regulation (Figure 5.2a). However, this effect was completely blocked by pre-incubation with 50 μM SP600125, a JNK inhibitor.

JNK is a member of the mitogen activated protein kinase (MAPK) family of which there are three members, p38MAPK, JNK and ERK. Therefore, to investigate the specificity of the JNK pathway involvement in Aβ-induced occludin down-regulation, hCMEC/D3 cells were pre-incubated with two further inhibitors of JNK (TAT-TI-$JIP_{153-163}$ and N-(3-Cyano-4,5,6,7-tetrahydro-1-benzothien-2-yl)-1-naphthamide), a p38MAPK inhibitor (SB203580) or an indirect inhibitor of ERK (PD98059) at different concentrations (Figure 5.2b). JNK exists as three isoforms (JNK1, 2 and 3). JNK1 and 3 are described as important for Aβ-mediated toxicity to neurones [654]. N-(3-Cyano-4,5,6,7-tetrahydro-1-benzothien-2-yl)-1-naphthamide [646] is reported to be specific for JNK2/3 and so was used in an attempt to elucidate the isoform responsible for Aβ signalling in hCMEC/D3 cells. SP600125 at a lower concentration of 10 μM inhibited the Aβ 1-40- mediated occludin down-regulation ($n = 3$, $P < 0.05$) as found with the 50 μM dose (Figure 5.2a and b). 10 μM TAT-TI-$JIP_{153-163}$ rescued occludin down-regulation in hCMEC/D3 cells ($n = 3$, $P < 0.05$), although 5 μM and 1 μM doses were not effective. N-

(3-Cyano-4,5,6,7-tetrahydro-1-benzothien-2-yl)-1-naphthamide was toxic to hCMEC/D3 cells at concentrations of 1 μM and upwards (Figure 5.1). When used at 0.5 μM, however, there was no inhibition of occludin down-regulation, and similarly the MEK inhibitor PD98059 also had no effect ($n = 3$, $P > 0.05$). Interestingly, 20 μM SB2035580 completely blocked the down-regulation of occludin ($n = 3$, $P < 0.05$). These results demonstrate that p38MAPK and JNK inhibition both attenuate Aβ-mediated occludin down-regulation in hCMEC/D3 cells.

5.3.2 Time-dependent activation of JNK, ERK and p38MAPK as assessed by western blotting

The next issue to be addressed was whether JNK and p38MAPK were activated in hCMEC/D3 cells by Aβ 1-40 treatment (Figures 5.3- Figure 5.5). The activation of ERK was also investigated to determine the specificity of MAPK activation. Neither JNK nor p38MAPK were activated at early time points of 1, 5, 15, 30 and 60 min (Figure 5.3). By contrast, activation of all three kinases was observed after 24 h and 48 h incubation with Aβ 1-40 (Figures 5.4 and 5.5).

JNK activation was detected as early as 6 h post incubation with Aβ 1-40 and increased with time up to 48 h, but no JNK activation was observed following sAβ 1-40 incubation. JNK resolves as two bands of 52 kDa and 46 kDa. Aβ 1-40 activated 46 kDa JNK but not 52 kDa, whilst the positive control (UV light, 30 min) stimulated both. ERK was also activated by Aβ 1-40 at 24 h and 48 h. Two forms of ERK exist, ERK1 (44 kDa) and ERK 2 (42 kDa) and Aβ 1-40 appeared to exclusively activate ERK 2. p38MAPK activation was determined following 24 h and 48 h incubation with Aβ 1-40, however the band resolved was very weak and difficult to fully identify.

The activation of JNK, p38MAPK and ERK after 48 h incubation with Aβ 1-40 was then investigated, in the presence or absence of their specific inhibitors (Figure 5.6 and

5.7): 10 μM TAT-TI-$JIP_{153-163}$, 20 μM SB203580, 50 μM SP600125 and 10 μM PD98059. Both JNK inhibitors (TAT-TI-$JIP_{153-163}$ and SP600125) reduced the activation of JNK caused by Aβ 1-40, but did not inhibit the activation of p38MAPK or ERK2. Similarly, PD98059 decreased the activation of ERK but not that of JNK or p38MAPK. By contrast, SB203580 inhibited both JNK and p38MAPK activation but not ERK2. These results show that SB203580 also prevented JNK activation and so might not be specific for the p38MAPK pathway, or that p38MAPK signalling mediates the activation of JNK through an as yet undefined mechanism.

N-(3-Cyano-4,5,6,7-tetrahydro-1-benzothien-2-yl)-1-naphthamide) increased the activity of ERK, p38MAPK and JNK, indicating that hCMEC/D3 cells were under stress (Figure 5.8). It is therefore unsurprising that this compound did not prevent Aβ-mediated occludin down-regulation, since it activated rather than inhibited JNK.

5.3.3 The effect of soluble cytokine receptors on Aβ 1-40-mediated occludin down-regulation by hCMEC/D3 cells

The activation of p38MAPK is associated with the production of inflammatory mediators, which in principle could act to decrease the expression of occludin by hCMEC/D3 cells in a JNK-dependent manner. IL-1β, TNF-α and IL-6 are all elevated in AD patients [377] and IL-1β [265-270] or TNF-α [655, 656] can alter the expression of TJ proteins. In this study, sTNF-R1, sIL-1ra, combined sTNF-R1/sIL-1ra or a sIL-6 R all failed to prevent occludin down-regulation (Figure 5.8). These results suggest that either another unknown secreted factor is released by Aβ-stimulated BECs, or a direct activation of JNK or p38MAPK is crucial in the observed down-regulation of occludin levels by hCMEC/D3 cells. However, the lack of activation of p38MAPK as assessed by western blotting at early time points appears to rule out the possibility of the secretion of an unknown mediator by hCMEC/D3 cells, unless it is released via a p38MAPK-independent

mechanism. Indeed, p38MAPK, JNK and ERK activation were all observed at the same time of 24 h upwards, indicative of co-activation. The fact that TAT-TI-$JIP_{153-163}$, SP600125 inhibit JNK and not p38MAPK, and SB203580 inhibits both, implies that JNK is the critical pathway in occludin down- regulation mediated by Aβ.

5.3.4 The effect of JNK and p38MAPK inhibition on Aβ 1-40-mediated increased hCMEC/D3 cell paracellular permeability

Since TAT-TI-$JIP_{153-163}$, SB203580 and SP600125 all attenuated occludin down-regulation mediated by Aβ 1-40, their effect on the Aβ-mediated increase in hCMEC/D3 cell permeability was investigated (Figure 5.10 and 11). The TEER of hCMEC/D3 cells was unaltered by Aβ 1-40 incubation and also by the incubation of 10 μM TAT-TI-$JIP_{153-163}$, 20 μM SB203580 or 50 μM SP600125 (Figure 5.10, n = 3, $P > 0.05$). These results imply that none of the treatments sufficiently alter the permeability of hCMEC/D3 cells to small ions, probably due to the relatively poor basal TEER of the hCMEC/D3 cells.

Aβ 1-40 increased the permeability coefficient of hCMEC/D3 cells to 70 kDa FITC-dextran compared to the sAβ peptide by 69.7 ± 8.5% (Figure 5.11, n = 3, $P < 0.05$). This effect was inhibited by pre-incubation with TAT-TI-$JIP_{153-163}$, or SP600125 prior to Aβ 1-40 incubation (n = 3, $P > 0.05$). There was also no increased paracellular permeability after pre-incubation with SB203580 and subsequent Aβ 1-40 incubation (n = 3, $P > 0.05$). Although, it should be noted, that pre-incubation of hCMEC/D3 cells with SB203580 slightly increased the permeability coefficient when incubated with both s1-40 and Aβ 1-40 by 33.8 ± 22.5 % and 26.7 ± 12.6 %, respectively, when expressed as a percentage of vehicle pre-incubated sAβ 1-40 control, however the data was not significant (n = 3, $P > 0.05$). These results show that JNK and p38MAPK inhibition can prevent the Aβ 1-40 mediated increase in hCMEC/D3 cell permeability to 70 kDa – FITC dextran, most likely via occludin down-regulation.

5.3.5 Aβ peptide in whole cell lysates and culture supernatants as assessed by SDS-PAGE and western blotting

Aβ has a high tendency to self aggregate and there is some debate as to the most toxic form of Aβ (reviewed [359]). To investigate which Aβ species might be responsible for occludin down-regulation in hCMEC/D3 cells, Aβ levels in cell lysates and culture medium were assessed via western blotting. Using a 15 % acrylamide gel, a time-dependent reduction of a 4 kDa protein in both the supernatant and cell lysate was observed when Aβ 1-40 was incubated with fully confluent hCMEC/D3 cells, but not in the absence of cells (Figure 5.12). Interestingly, at 6, 24 and 48 h, increasing amounts of a large protein of ~150 kDa was detected in both cell lysates and the culture medium. To further investigate the identity of this protein, samples were electrophoresed on an 8 % acrylamide gel (Figures 5.12 and 5.13), which was blotted for Aβ, then stripped and re-probed for APP. As observed on the 15 % acrylamide gel, a 150 kDa protein was observed in hCMEC/D3 cell lysates and culture medium (Figure 5.12 and 5.13). In addition, in the supernatant of hCMEC/D3 cells incubated with Aβ 1-40, a decreased expression of a 50 kDa protein was observed using an APP antibody. The results suggest that either Aβ of 4 kDa is degraded by hCMEC/D3 cells or that Aβ aggregates with other Aβ molecules or with another protein(s), without the production of intermediate species.

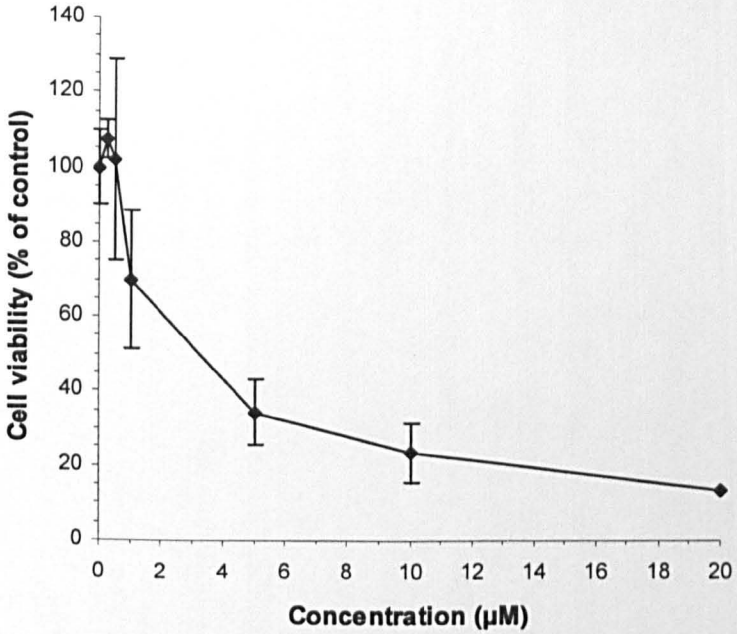

Figure 5.1. The toxicity of N-(3-Cyano-4,5,6,7-tetrahydro-1-benzothien-2-yl)-1-naphthamide to hCMEC/D3 cells. Fully confluent hCMEC/D3 cells were incubated with different concentrations of N-(3-Cyano-4,5,6,7-tetrahydro-1-benzothien-2-yl)-1-naphthamide for 48 h and the cell viability measured using an MTT assay. Data represents mean ± S.D. n = 1 experiment with quintuplet samples.

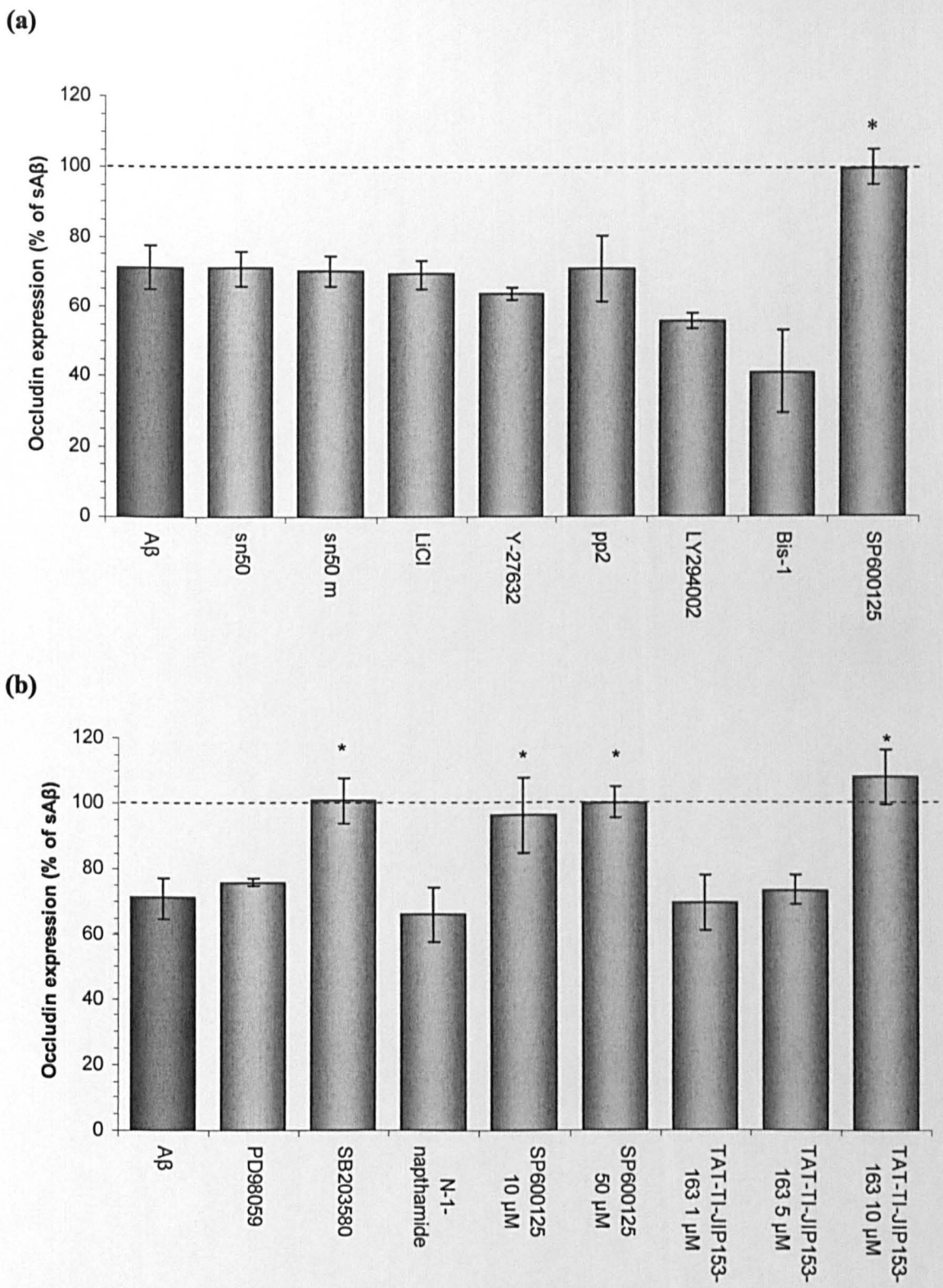

Figure 5.2. The role of signalling pathway inhibition on occludin expression by hCMEC/D3 cells following Aβ 1-40 incubation for 48 h. (a) Fully confluent hCMEC/D3 cells were pre-incubated for 30 min with inhibitors for the PI-3K, NF-κB, GSK-3β, Src, ROCK, PKC and JNK pathways and subsequently incubated for 48 h with either Aβ 1-40 or sAβ 1-40, and the expression of occludin assessed via flow cytometry. **(b)** Fully confluent hCMEC/D3 cells were pre-incubated with inhibitors for the MAPK family before sAβ 1-40 or Aβ 1-40 incubation. Data represents mean ± SEM. n = 3 experiments with duplicate samples. * $p < 0.05$ using a Student's t test comparing each treatment to the control.

(a) JNK

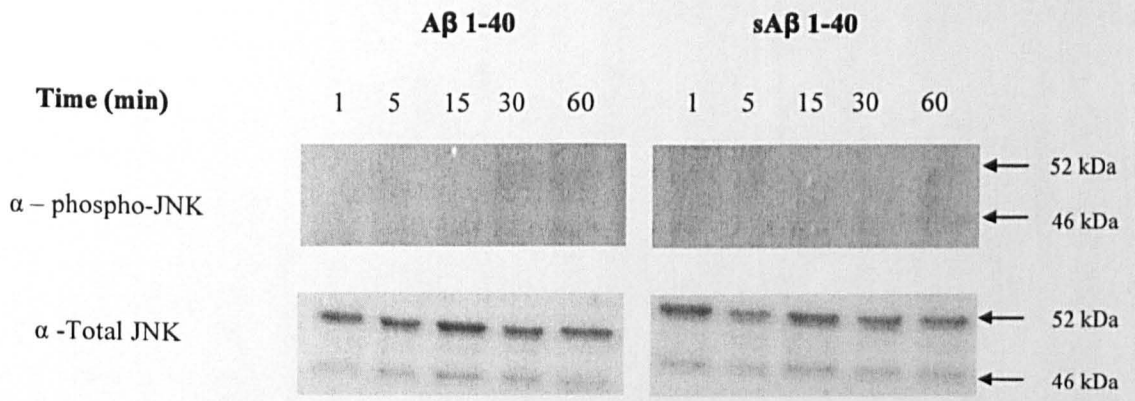

(b) p38MAPK

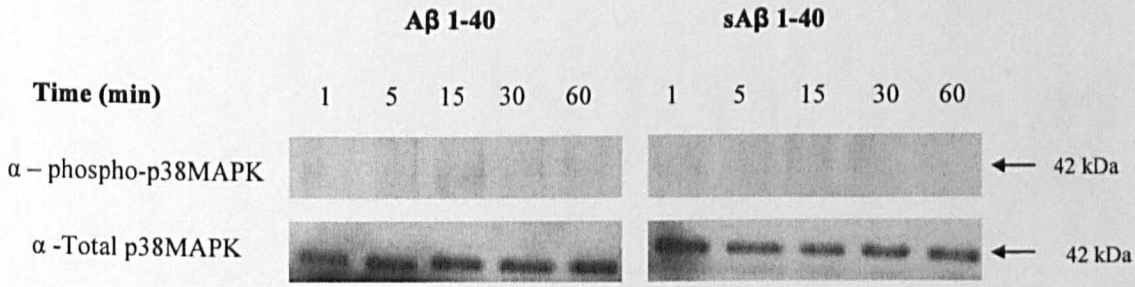

Figure 5.3. The effect of Aβ 1-40 treatment on the activation of JNK and p38MAPK by hCMEC/D3 cells over 60 min. (a) Fully confluent hCMEC/D3 cells were incubated with Aβ 1-40 or sAβ 1-40 for 1, 5, 15, 30 and 60 min. The cells were then lysed and the protein levels of active/phosphorylated JNK (rabbit polyclonal IgG) and total JNK (rabbit polyclonal IgG) was assessed via western blotting techniques. **(b)** Active and total p38MAPK (both rabbit polyclonal IgG) after Aβ 1-40 incubation. Results are from one experiment representative of 3 with single samples.

(a) JNK

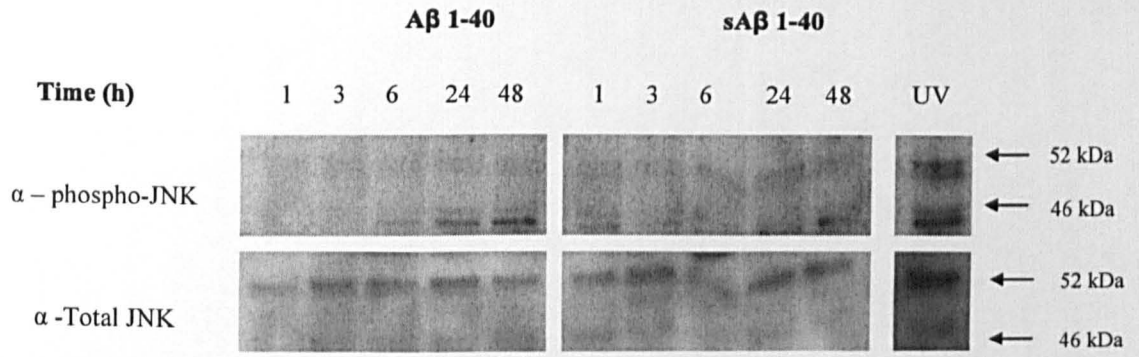

(b) ERK

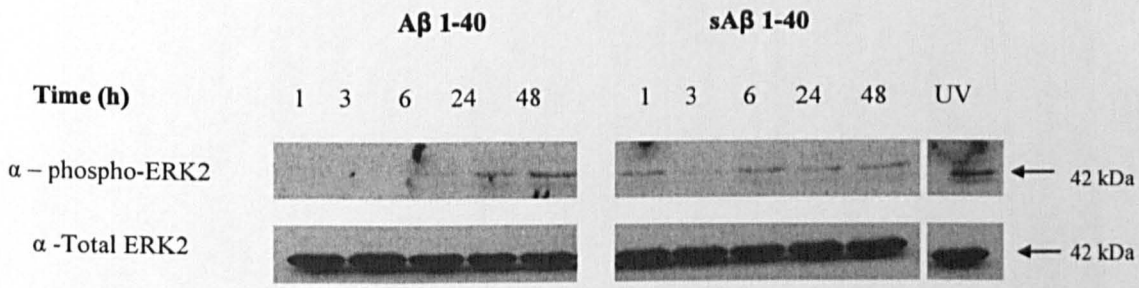

(c) p38MAPK

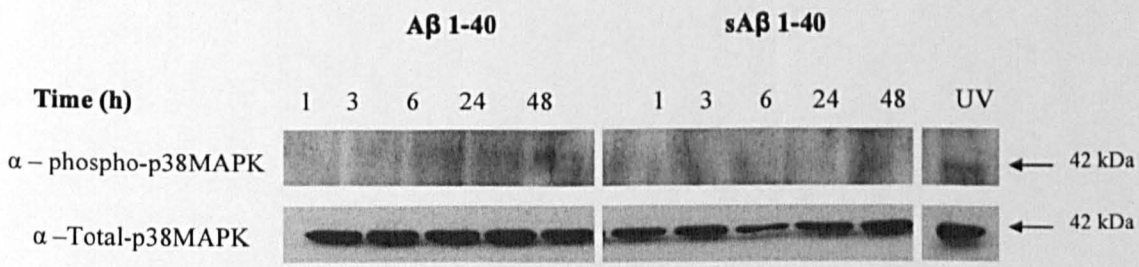

Figure 5.4. The effect of Aβ 1-40 treatment on the activation of JNK, ERK, p38MAPK by hCMEC/D3 cells over 48 h. (a) Fully confluent hCMEC/D3 cells were incubated with Aβ 1-40 for 1, 3, 6, 24 and 48 h. The cells were then lysed and the protein levels of active and total JNK (rabbit polyclonal IgG) was assessed via western blotting. **(b)** Active (mouse monoclonal IgG_1) and total ERK2 (mouse monoclonal IgG_{2a}) after Aβ incubation. (c) Active (rabbit polyclonal IgG) and total p38MAPK (rabbit polyclonal IgG) after Aβ incubation. Results are from one experiment representative of two.

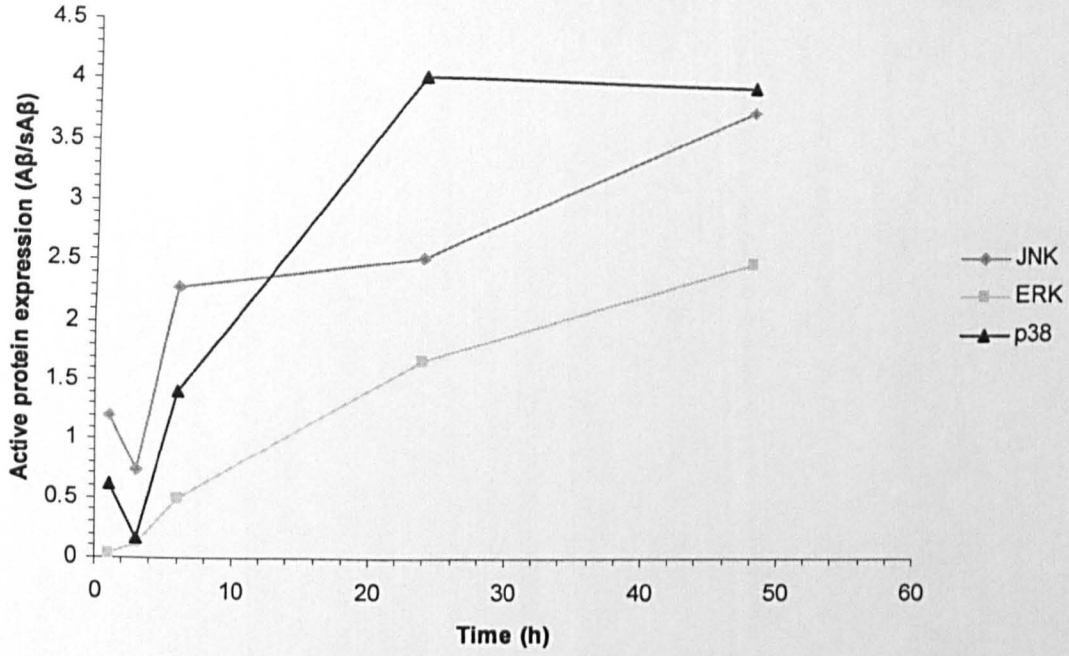

Figure 5.5. The activation of JNK, ERK and p38MAPK over 48 h after treatment with Aβ 1-40 as assessed by optical density analysis of western blots. The OD of the active JNK (46 kDa) ERK2 and p38MAPK bands from Figure 5.4 were divided by total JNK, ERK and p38MAPK respectively (arbitrary units) and normalised to sAβ control.

(a) JNK

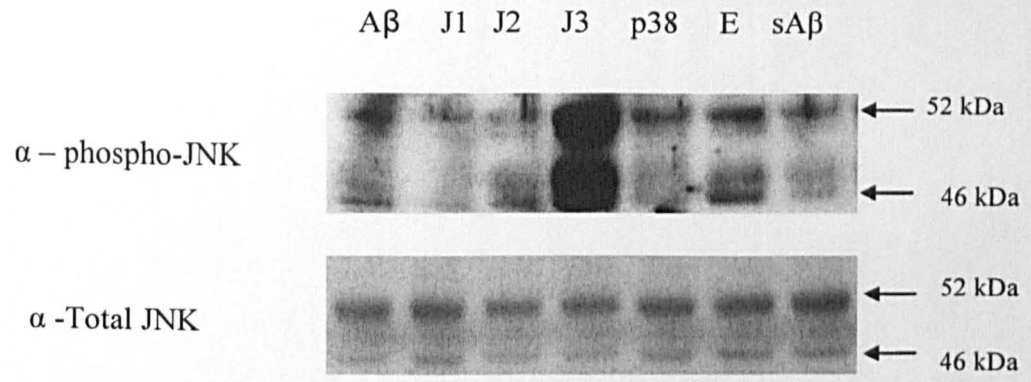

(b) p38MAPK

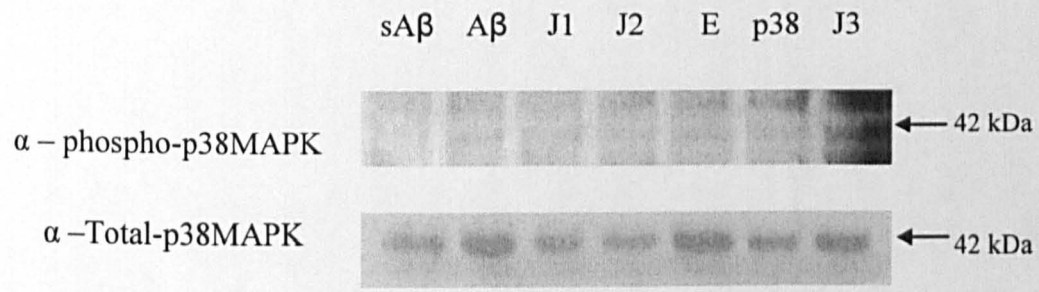

(c) ERK

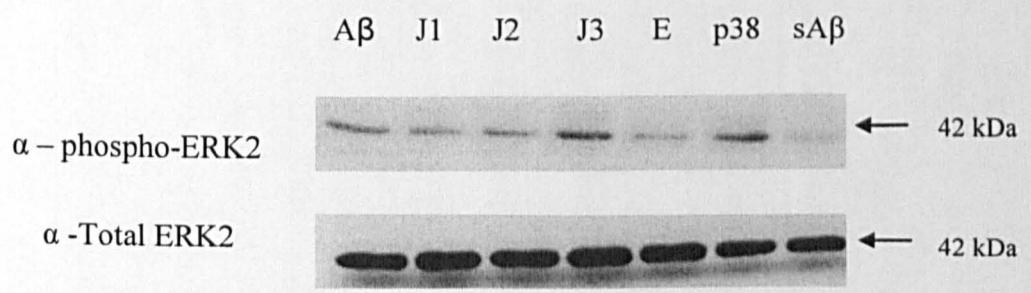

Key:

J1 = SP600125,
J2 = TAT-TI-$JIP_{153-163}$.
J3 = N-(3-Cyano-4,5,6,7-tetrahydro-1-benzothien-2-yl)-1-naphthamide.
E = PD98059.
p38 = SB203580.

Figure 5.6. The role of signalling pathway inhibition on the activation of JNK, ERK and p38MAPK by hCMEC/D3 cells following Aβ 1-40 incubation for 48 h. (a) Fully confluent hCMEC/D3 cells were pre-incubated with SP600125 (50 μM), TAT-TI-$JIP_{153-163}$ (10 μM), PD98059 (50 μM), SB203580 (20 μM) or N-(3-Cyano-4,5,6,7-tetrahydro-1-benzothien-2-yl)-1-naphthamide (0.5 μM) for 30 min and then incubated with Aβ 1-40 or sAβ 1-40 for 48 h. The expression of active and total JNK was then assessed via western blotting techniques. **(b)** The expression of active and total p38MAPK and **(c)** ERK was also measured. Results are from one experiment representative of two.

(a)

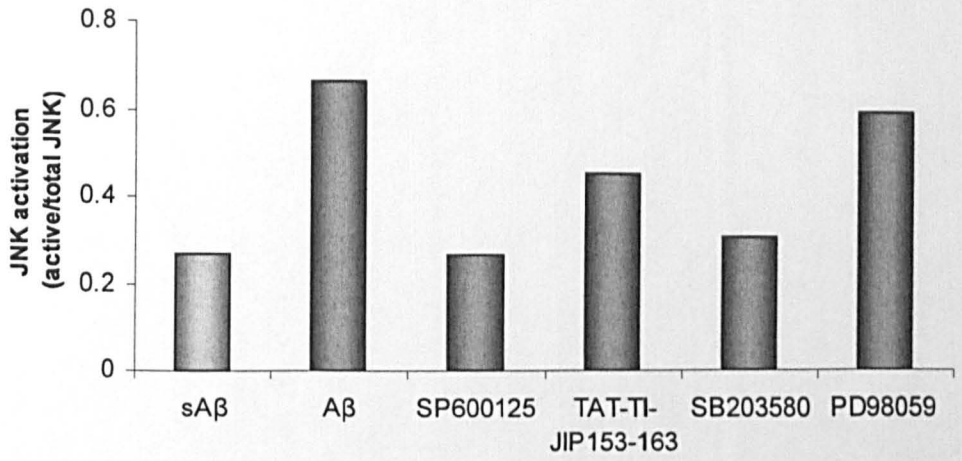

(b)

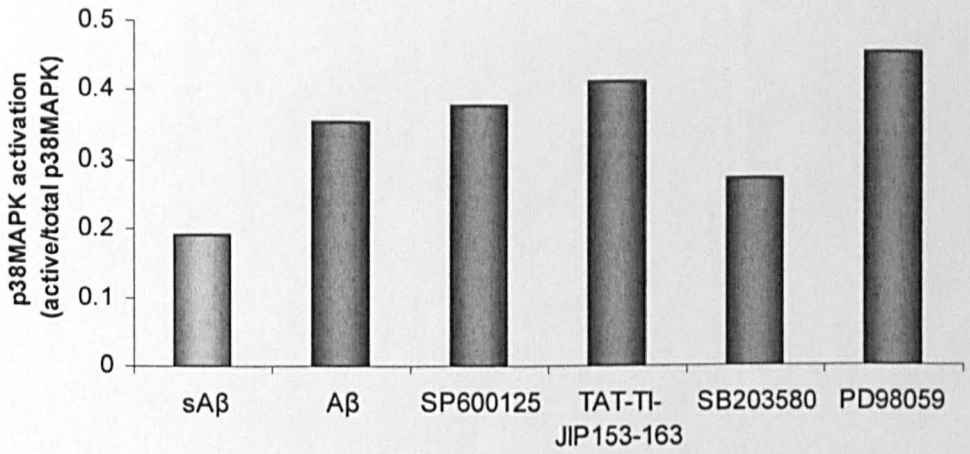

(c)

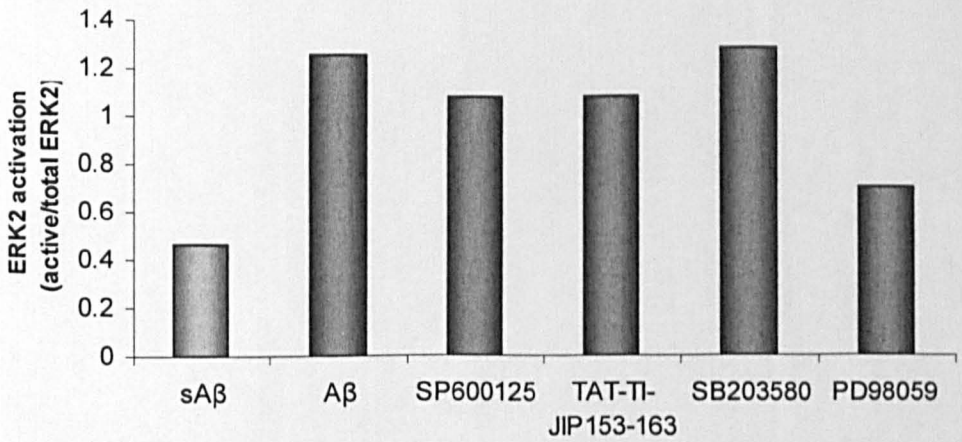

Figure 5.7. The role of signalling pathway inhibition on the relative activation of JNK, ERK and p38MAPK by hCMEC/D3 cells following Aβ incubation for 48 h as assessed by optical density analysis of western blots. Fully confluent hCMEC/D3 were pre-incubated with SP600125, TAT-TI-$JIP_{153-163}$, PD98059, SB203580 or for 30 min and then incubated with Aβ1-40 or sAβ 1-40 for 48 h. The OD of the active JNK (46 kDa) ERK2 and p38MAPK bands from Figure 5.6 were divided by total JNK, ERK and p38MAPK respectively.

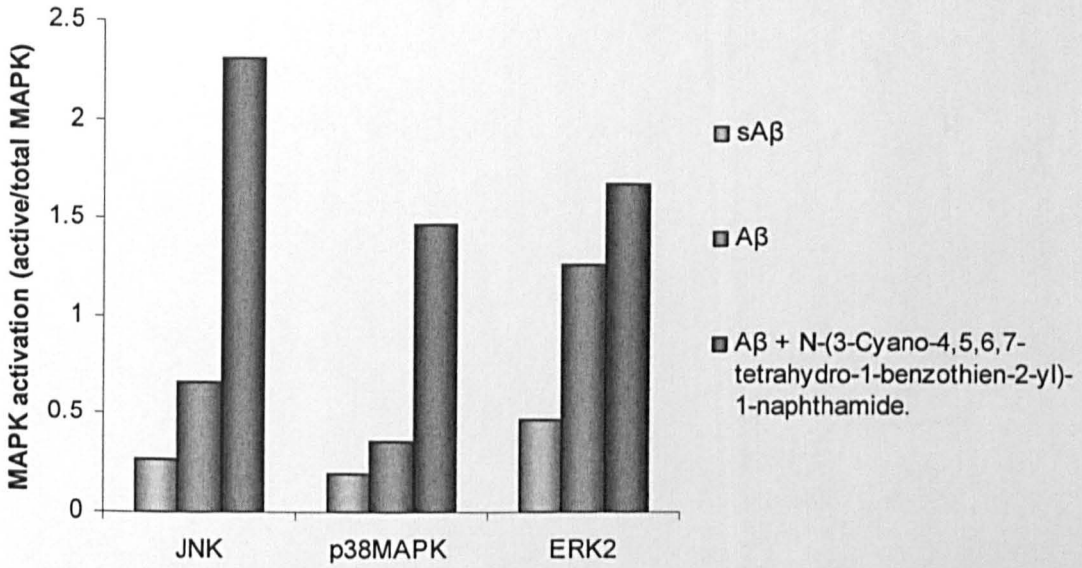

Figure 5.8. The activation of JNK, p38MAPK and ERK2 after Aβ 1-40 incubation with N-(3-Cyano-4,5,6,7-tetrahydro-1-benzothien-2-yl)-1-naphthamide as assessed via optical density analysis by hCMEC/D3 cells. Fully confluent hCMEC/D3 were pre-incubated with N-(3-Cyano-4,5,6,7-tetrahydro-1-benzothien-2-yl)-1-naphthamide or for 30 min and then incubated with Aβ1-40 or sAβ 1-40 for 48 h. The OD of the active JNK (46 kDa) ERK2 and p38MAPK bands from Figure 5.6 were divided by total JNK, ERK and p38MAPK respectively. The data was then normalised to Aβ 1-40.

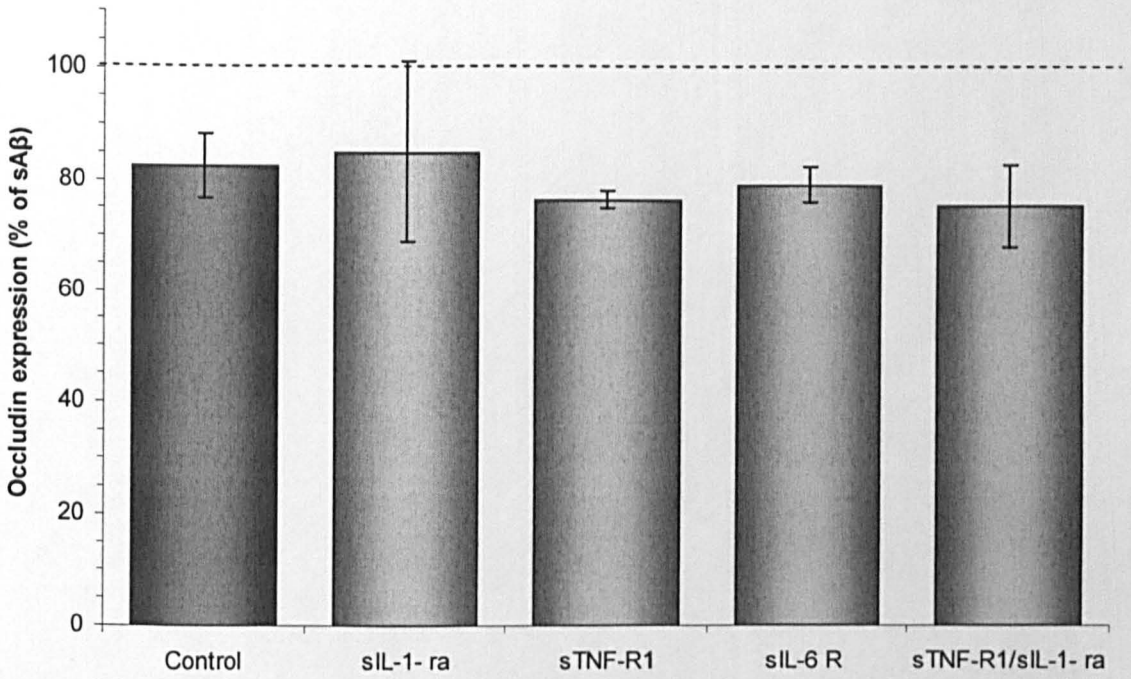

Figure 5.9. The effect of soluble cytokine receptors on Aβ 1-40-mediated occludin down-regulation by hCMEC/D3 cells. Fully confluent hCMEC/D3 cells were incubated with Aβ 1-40 or sAβ 1-40 in the presence or absence of sTNF-R, sIL-l ra, sIL-6 receptor or combined sTNF-R and sIL-l ra. Data represents mean ± SEM. n = 3 experiments with duplicate samples. $P > 0.05$ using a Student's t test comparing each treatment to their sAβ counterparts.

		TEER Ω.cm^2	
		Pre incubation	*Post incubation*
Control	Aβ 1-40	29 ± 1.5	29 ± 2.0
	sAβ 1-40	29 ± 1.3	28 ± 1.6
SP600125	Aβ 1-40	30 ± 2.5	28 ± 1.3
	sAβ 1-40	30 ± 2.4	29 ± 2.8
TAT-JI-JIP$_{153-163}$	Aβ 1-40	30 ± 1.8	28 ± 1.59
	sAβ 1-40	30 ± 1.7	29 ± 2.2
SB203580	Aβ 1-40	29 ± 1.5	28 ± 1.09
	sAβ 1-40	29 ± 1.1	28 ± 0.9

Figure 5.10. The trans-endothelial electrical resistance (TEER) of hCMEC/D3 cells after 48 h Aβ 1-40 incubation with JNK and p38MAPK inhibitors. hCMEC/D3 cells were grown to confluence on collagen- and fibronectin- coated transwell filter inserts, pre-incubated with TAT-TI-JIP$_{153-163}$ (10 μM), SB203580 (20 μM), SP600125 (50 μM) and incubated with 5 μM Aβ 1-40 or sAβ1-40 for 48. The trans-endothelial cell electrical resistance of hCMEC/D3 cells was recorded before and after Aβ incubation. n = 3 with duplicate samples. $P > 0.05$ using a paired t test compared cells incubated with sAβ 1-40 to those treated with Aβ 1-40.

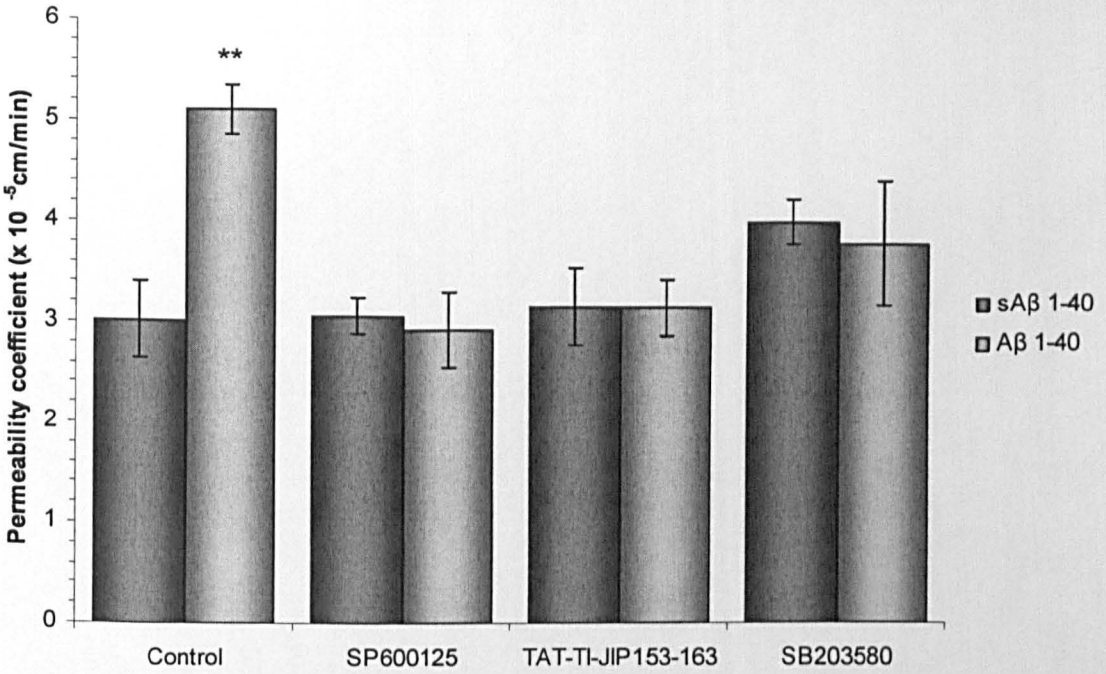

Figure 5.11. The effect of JNK and p38MAPK inhibition on Aβ 1-40- mediated increased hCMEC/D3 cell permeability to 70 kDa FITC-dextran. hCMEC/D3 cells were grown to confluence on collagen and fibronectin coated- tranwell filter inserts, pre-incubated with TAT-TI-$JIP_{153-163}$ (10 μM), SB203580 (20 μM), SP600125 (50 μM) and incubated with 5 μM Aβ 1-40 or sAβ1-40 for 48 h. The permeability of the cells to 70-kDa FITC dextran was then investigated. Data represents mean ± SEM. n = 3 experiments with duplicate samples. ** $P < 0.01$ using a paired t test comparing each treatment to the sAβ 1-40 control.

(a) Supernatant.

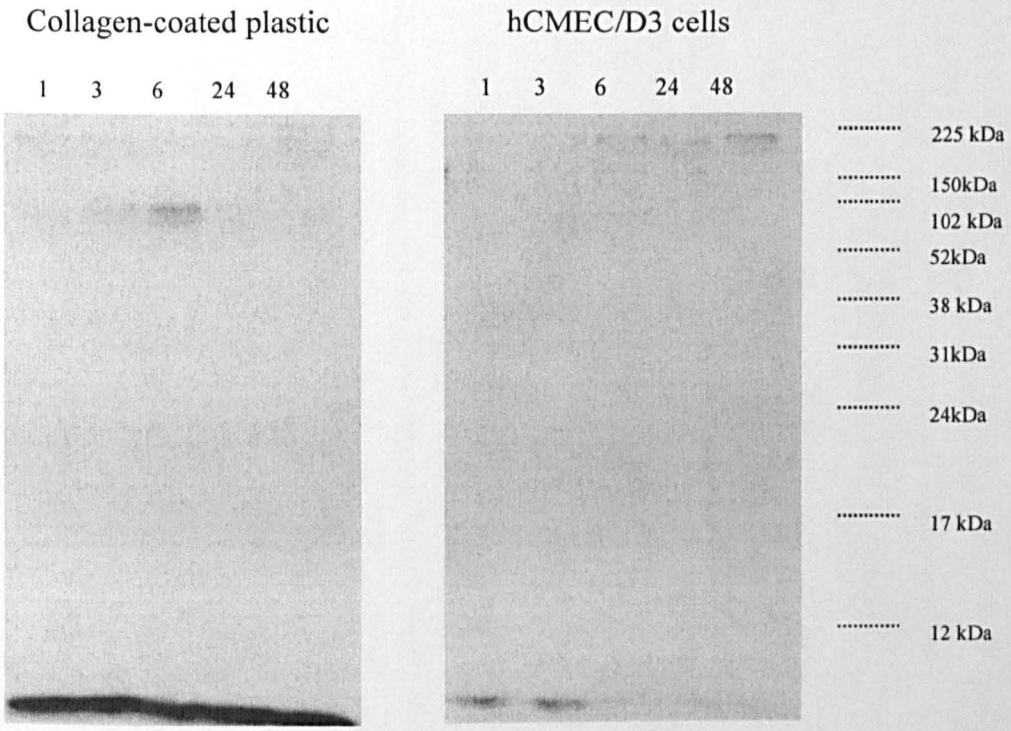

(b) Cell lysate.

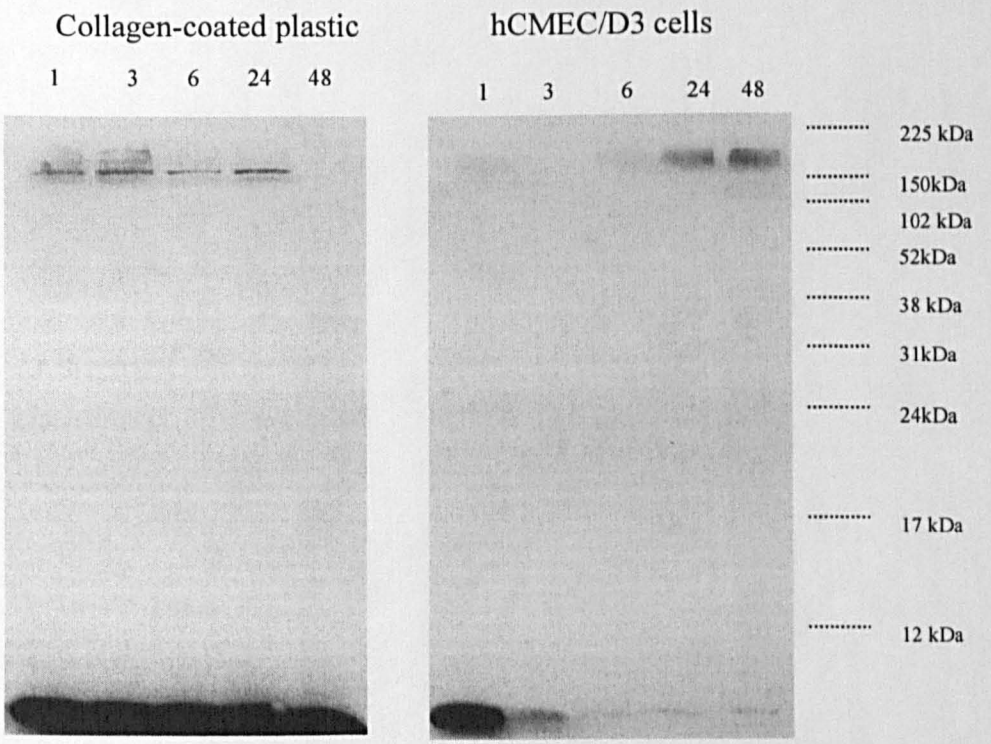

Figure 5.12. Aβ 1-40 in cells and supernatants after 48 h incubation with hCMEC/D3 cells or collagen coated plastic. (a) Aβ 1-40 was added to either a collagen-coated tissue culture plate or hCMEC/D3 cells for 1, 6, 24 or 48 h. The supernatant was collected and the protein levels of Aβ (6E10, mouse monoclonal IgG_1) was investigated using western bloting techniques and a 15 % acrylamide gel. **(b)** The protein levels of Aβ were measured in cell lysate at each time point on 15 % acrylamide gels. The experiment was carried out once.

(a) Aβ 1-40

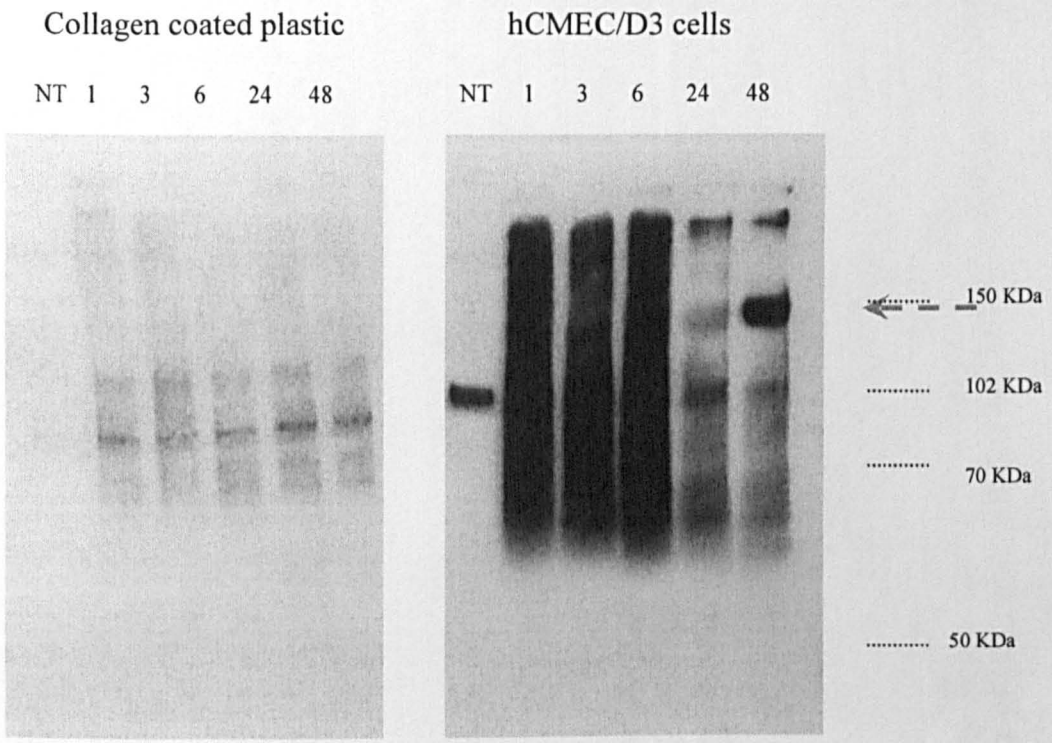

(b) APP

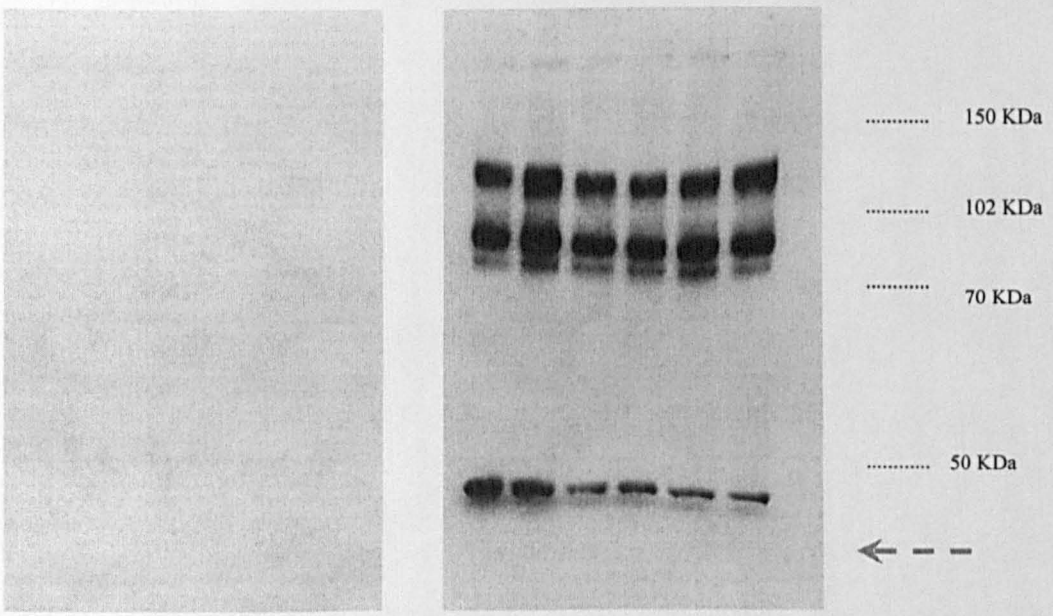

Figure 5.13. Aβ 1-40 in cells after 48 h incubation with hCMEC/D3 or collagen coated plastic. (a) Aβ 1-40 was added to either a collagen- coated tissue culture plate or hCMEC/D3 cells for 1, 6, 24 or 48 h. The cell lysate was collected and the protein levels of Aβ (6E10, mouse monoclonal IgG_1) and **(b)** APP (22C11, mouse monoclonal IgG_1) was investigated using western blotting techniques and a 8 % acrylamide gel. Result from one experiment, representative of three. No treatment (NT) corresponds to wells to which no Aβ was added to the supernatant.

(a) Aβ1-40

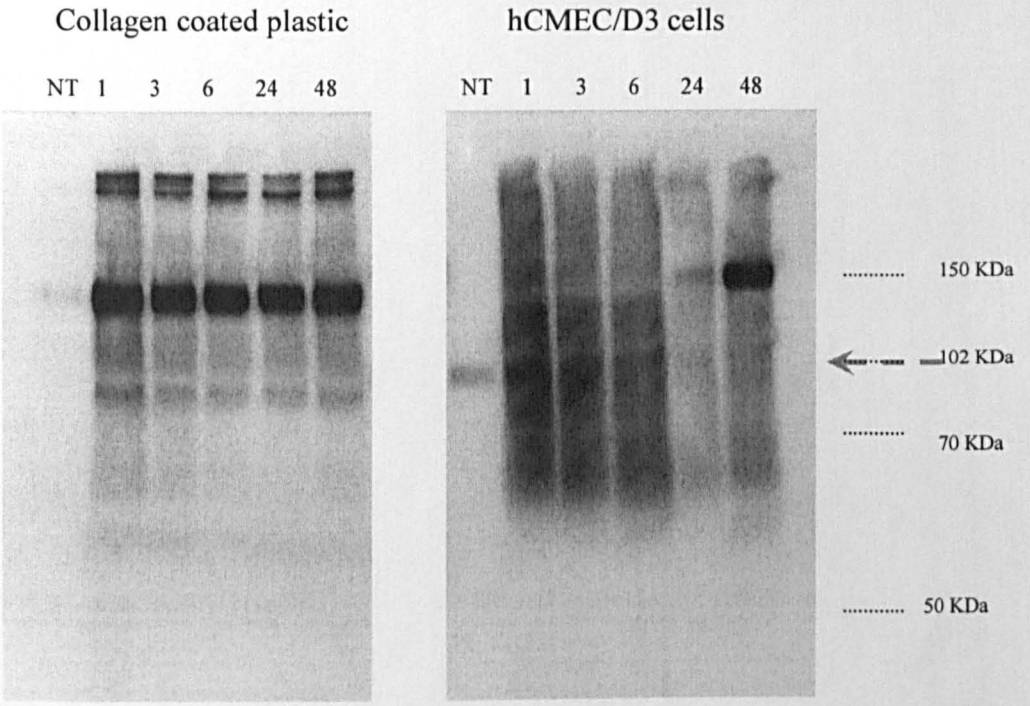

(b) APP

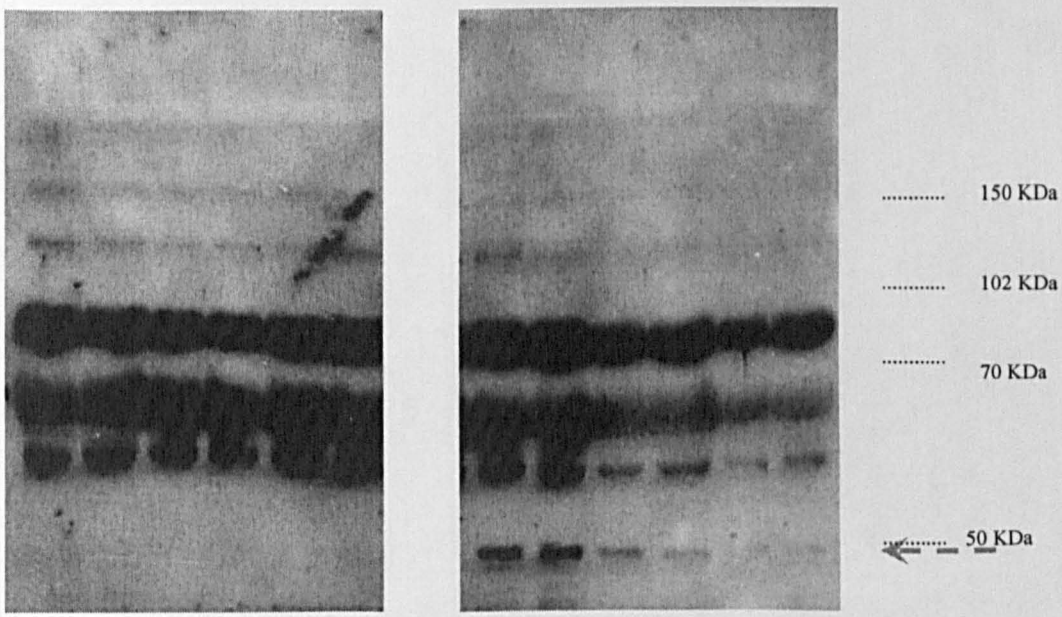

Figure 5.14. Aβ 1-40 in supernatants after 48 h incubation with hCMEC/D3 or collagen coated plastic. (a) Aβ 1-40 was added to either a collagen coated tissue culture plate or hCMEC/D3 cells for 1, 6, 24 or 48 h. The supernatant was collected and the protein levels of Aβ (6E10, mouse monoclonal IgG_1) and **(b)** APP (22C11, mouse monoclonal IgG_1) was investigated using western blotting techniques and a 8 % acrylamide gel. Result from one experiment, representative of three. No treatment (NT) corresponds to wells to which no Aβ was added to the supernatant.

5.4 Discussion

5.4.1 Role of intracellular signalling pathways involved in Aβ 1-40- mediated occludin down-regulation

A main aim of this study was to investigate the signalling pathway(s) involved in Aβ-mediated occludin down-regulation in hCMEC/D3 cells. The intracellular regulation of occludin is potentially very complex (reviewed in [131]) and therefore only pathways activated by Aβ or those most likely to be involved in the regulation of occludin expression were investigated.

Src, a non-receptor tyrosine kinase, is suggested to play a role in TJ assembly [657]. Sabath *et al* [657] identified Src as a key component of the TJ complex in MDCK cells. Furthermore, the group found that activation of the G protein G α12, induced Src phosphorylation of ZO-1 and dissociation of occludin and Cl-1 from the TJ complex. If Aβ was acting via Src in hCMEC/D3 cells, disruption in ZO-1 and possibly Cl-5 expression would be expected, however this was not observed at the protein or mRNA level. There are no reports of Src activation by Aβ in the literature and so it is unsurprising that its inhibition had no effect on Aβ-mediated occludin down-regulation.

Rho-associated kinases (ROCK) are serine/threonine kinases which can alter TJ protein expression (discussed in [131]). Persidsky *et al* [132], have demonstrated that the migration of HIV-1 infected monocytes across primary hBECs *in vitro*, occurs via rho/ROCK activation. In that study the activation of Rho/ROCK in hBECs induced the phosphorylation and disruption of occludin and Cl-5. In this study ROCK inhibition did not alter Aβ-induced occludin down-regulation and there was no alteration in Cl-5 levels.

PKC is a family of Ser/Thr specific kinases of which 12 isoforms exist. The activation of PKC, rather than inhibition, is a suggested therapeutic target for AD, (reviewed in [658]) as a preventative measure for neuronal cell death. The effect of PKC on occludin is complex and isoform-specific. For example, Andreeva *et al* [659] have

found that PKCα activation can cause TJ disassembly whilst PKCδ can mediate TJ assembly in MDCK cells. Bisindolylmaleimide -1 used here, is a non-specific PKC inhibitor and did not alter the Aβ-mediated occludin decrease in hCMEC/D3 cells.

PKC, ROCK and Src appear to act via modifications of TJ protein phosphorlyation, or to alter the association of each TJ protein with each other. In general these processes are post-translational in nature and can occur quite rapidly. For example, ROCK- dependent migration of HIV monocytes occurs within hours [132], whilst TJ disruption as the result of low Ca^+ levels, used in many models to investigate junction assembly, occurs within 20 h [659]. In the current study, a reduction in occludin at the protein level occurred only after 48 h, and occludin was also down-regulated at the mRNA level. This implies that Aβ may be acting at the level of transcriptional activity and/or of mRNA stability. For this reason, transcription factors or signalling pathways leading to modification in transcriptional activity (NF-κB, JNK, GSK-3β) were investigated.

NF-κB is an inducible transcription factor found in many cell types including ECs [660], neurones and glia [642]. NF-kB is activated by multiple signalling molecules including TNF-α, IL-1, LPS and Aβ (summarised in [642]). High levels of NF-kB activation induced by Aβ can lead to neuronal cell death *in vitro* [351, 641], whilst low activation might afford neuroprotection [344, 642]. Indeed, Kalschmidt *et al* [344, 642] have found that TNF-α at low concentrations (2 ng/ml) protects primary rat cerebellar granule cells against Aβ 1-40- mediated toxicity via NF-kB activation. In the present study however NF-kB inhibition did not reverse occludin down-regulation.

The PI3K, AKT, GSK-3β/α pathway is commonly described as an AD therapeutic target [628, 629]. Class 1 PI3K converts phosphatidyinositol 4,5 diphosphate (PI 4,5) to 3, 4, 5 triphosphate on the inner leaflet of the plasma membrane. PI 3,4,5 tri-phosphate causes AKT/PKB translocation to the membrane. Subsequent AKT activation, by phosphorylation at Ser473 and Thr308, suppresses the activity of GSK-3β, via phosphorylation at serine 9. GSK-3β activation has been noted in response to ROS [661, 662] and Aβ [345, 347] in

neuronal cell cultures. Schafer *et al* [661] have found that treatment of murine hippocampal cells with LiCl (GSK-3β inhibitor,10 mM), increases their resistance to glutamate and hydrogen peroxide- induced oxidative stress. Aβ-induced activation of GSK-3β has been observed in both neuronal [345, 347] and EC cultures [630]. In neuronal cultures, Aβ neurotoxicity is associated with GSK-3β activation. Koh *et al* [345] found that LiCl at 5 and 10 mM increased the survival of rat hippocampal neuronal cell cultures treated with 20 μM Aβ 1-42. In a follow up study, Lee *et al* [347] have found that PI3K activation can also reverse the Aβ- mediated toxicity. Specifically, for ECs, Suhara *et al* [630] have demonstrated that virally- encoded Aβ 1-42 was pro-apoptotic, via the inhibition of AKT phosphorylation and GSK activation, in HUVEC cells. The role of PI3K in TJ regulation is not fully known. PI3K activation in response to TGF-β can result in the translocation of ZO-1 from the TJ [663]. It the present study, the finding that LiCl did not reverse Aβ-mediated occludin down-regulation does not rule out that cytoxic effects at higher concentrations of Aβ may occur via the GSK-3β pathway. It is unsurprising however, that the PI3K inhibitor used in this study had no effect on occludin down-regulation, as there are no reports on Aβ directly activating PI3K. A future study into the signalling pathways mediating Aβ cytotoxicity in hCMEC/D3 cells would be interesting. It is noteworthy that other pathways converging on GSK-3β, such as the GSK-3β inhibitory protein Wnt [664], are also proposed targets in AD.

MAPK are Ser/Thr kinases that respond to a variety of stimuli (e.g. stress), and act to regulate a plethora of activities including gene expression, mitosis and apoptosis. There are three main groups called ERK, p38MAPK and JNK. MAPK signalling has a demonstrable role of TJ expression (reviewed in [131]). The activation of p38MAPK and ERK 1/2 can cause an increase or a decrease in TJ protein expression, depending on the stimulus and cell type [131]. The MAPK family are implicated in AD pathogenesis [665], since ERK [666, 667], JNK [633] and p38MAPK[668] are all found to be up-regulated in neurones from AD patients. Furthermore, Aβ-mediated neuronal cell death *in vitro* has

been reported as being JNK-dependent [353, 634]. In this study, inhibitors of JNK (SP600125 TAT-TI-$JIP_{153-163}$) and p38MAPK (SB203580) prevented Aβ -mediated occludin down-regulation and Aβ-mediated increased hCMEC/D3 cell permeability.

Alternative explanations for these results are that both p38MAPK and JNK pathways are important for the occludin down-regulation, or that the inhibitors used in this study are not specific for one pathway. Both SP600125 and TAT-TI-$JIP_{153-163}$ inhibited JNK but not p38MAPK or ERK2, however SB203580 inhibited both JNK and p38MAPK. The key pathway in Aβ 1-40-mediated occludin down-regulation appears therefore to be JNK, whereas the role of p38MAPK remains to be determined.

The specificity of SP600125 [669] and SB203580 [670] has recently been investigated *in vitro*. Using an *in vitro* kinase assay, SP600125 at 10 μM, was found to inhibit in addition to JNK 1/2, thirteen other protein kinases (including SGK, S6K1, AMPK, CDK2, CK1δ and DYRKIA) [669]. Numerous studies have used SP600125 for the inhibition of JNK (discussed in [654, 671, 672]). However to confirm the finding of Aβ 1-40 mediated occludin down-regulation via JNK activation; TAT-TI-$JIP_{153-163}$ was used. Scaffold proteins known as JNK-interacting proteins (JIP) are thought to form an important part of the JNK pathway, by permitting JNK activation. A short conserved sequence of JIP1 has been demonstrated to bind to and inhibit JNK, by preventing JIP1-JNK inteactions [645, 654, 671-674]. TAT-TI-$JIP_{153-163}$ is a small cell permeable peptide [675], containing an inhibitor sequence for JNK. TI-$JIP_{153-163}$ *in vitro* was shown to not inhibit ERK or p38MAPK [673]. TAT-TI-$JIP_{153-163}$, like SP600125, completely reversed occludin down-regulation.

In contrast to the JNK inhibitors used, SB203580 may not be specific for p38MAPK. Using an *in vitro* kinase assay, Bain *et al* [670] have demonstrated that SB203580 at 1 μM inhibits not only p38MAPK, but also GSK-3β, CK1, RIP2 and GAK. Furthermore SB203580 also decreased the activation of two of the three JNK isoforms; JNK2 (40 % inhibition) and JNK3 (72 % inhibition). In this study, SB203580 inhibited

JNK activation, occludin down-regulation and the increase in paracellular permeability as a result of Aβ treatment. SB203580 may therefore prevent the actions of Aβ to hCMEC/D3 cells by the inhibition of JNK rather than p38MAPK. Bain *et al* [670] also found that pp2, a src inhibitor, could decrease the activity of p38MAPK α/β isoforms by 57 % and 62 % respectively. In the present study pp2 did not reverse the Aβ-mediated occludin down-regulation, and therefore the p38MAPK pathway is not likely to be involved.

5.4.2 Role of extracellular soluble factors in Aβ 1-40- mediated occludin down-regulation by hCMEC/D3 cells

Although the data described above points to JNK rather than p38MAPK activation as being involved in the Aβ1-40-mediated occludin down-regulation in hCMEC/D3 cells, it has been shown that p38MAPK activation is associated with the production of inflammatory cytokines. Microglia activation by Aβ is associated with the production of inflammatory cytokines [374]. *In vitro*, various cytokines including IL-1, TNF and IL-6 are produced after Aβ incubation in a p38MAPK- dependent manner by microglia [676, 677], and in isolated glia from AD patients [678]. Crucially, a novel p38MAPK inhibitor was found to suppress hippocampus levels of TNF-α and IL-1β following intracerebroventricular infusion of Aβ 1-42 in mice [378]. In that study, synaptic dysfunction and behavioural deficits were attenuated after treatment. Aβ peptides have also been demonstrated to induce IFN-γ and IL-1β production in HUVEC cells [679]. Increased cytokine levels are found in AD patients, particularly IL-1β, TNF-α and IL-6 [377, 680]. IL-1β [265-268] and TNF-α [655, 656] can induce increased permeability in cell lines that form TJs. Importantly, IL-1 β has been shown to decrease occludin at the mRNA level in a human retinal pigment epithelial [265] and HUVEC [660] cell lines, whilst TNF-α has been shown to decrease occludin at the protein level in HUVEC cells [681]. It is therefore possible that Aβ activates p38MAPK in hCMEC/D3 cells, to produce a cytokine, which

could act to down-regulate occludin. In this study however, sIL-1-ra and sTNF-R1, when used singly or in combination, had no effect on Aβ- mediated occludin down-regulation. IL-6 is relatively unique, in that the soluble form of the receptor (sIL-6) can bind to IL-6 and function as a signalling receptor via gp130 activation [682-684]. ECs express gp130 [682], and therefore, if IL-6 was produced by hCMEC/D3 cells, one would predict that sIL-6 would enhance occludin down-regulation. The possibility remains that when hCMEC/D3 cells are treated with Aβ, a soluble factor is released such as IFN-γ [685-688], though this has yet to be accounted for. It is of note however, that the activation of p38MAPK was not found at time points earlier than 6 h and the activation of p38MAPK, JNK and ERK all occurred around the same time. It therefore seems unlikely that a p38MAPK-dependent secreted factor is acting on hCMEC/D3 cells, or p38MAPK activation would occur prior to JNK and ERK activation. These results imply that JNK is likely to be the key pathway in Aβ-mediated occludin down-regulation in hCMEC/D3 cells.

5.4.3 JNK as a therapeutic target in AD

JNK is a promising therapeutic target for AD, potentially decreasing Aβ production [689], offering protection for neurones and, as found in this study, preventing occludin down-regulation in BEC. There are three genes that encode JNK in mammalian systems- *jnk1*, *jnk2*, *jnk3*; and each gene is alternatively spliced to create 46 and 55 kDa forms of the proteins [654, 672, 690]. The significance of each variant is not fully known, however JNK 1 and 2 are widely expressed whilst JNK3 is largely restricted to the brain (reviewed in [654]). Morishima *et al* [635] have demonstrated that Aβ 25-35 toxicity is significantly reduced in cortical neurones derived from JNK3 knock-out mice compared to control neurones, however they also state that JNK1-deficient neurones are also resistant to apoptosis. Fogarty *et al* [691] concur with the involvement of JNK1 in neuronal cell death,

as they found that rat cortical neurones were resistant to Aβ-induced apoptosis if JNK1, but not JNK2, was depleted using antisense technology. SP600125 [692] and TAT-TI-$JIP_{153-163}$ [645, 675] are non-specific JNK inhibitors, whilst N-(3-Cyano-4,5,6,7-tetrahydro-1-benzothien-2-yl)-1-naphthamide has been demonstrated to inhibit JNK2 and 3, but not JNK1 [646]. In this study, N-(3-Cyano-4,5,6,7-tetrahydro-1-benzothien-2-yl)-1-naphthamide was found to be toxic to hCMEC/D3 cells at doses in excess of 0.5 μM. At a non-toxic concentration, N-(3-Cyano-4,5,6,7-tetrahydro-1-benzothien-2-yl)-1-naphthamide did not reverse the Aβ-mediated occludin down-regulation. Indeed, western blotting analysis revealed that this compound activated rather than inhibited JNK. It therefore appears that N-(3-Cyano-4,5,6,7-tetrahydro-1-benzothien-2-yl)-1-naphthamide, at the concentrations used here, initiates a cascade(s) that activates JNK, potentially leading to hCMEC/D3 cell death. There are no current reports of N-(3-Cyano-4,5,6,7-tetrahydro-1-benzothien-2-yl)-1-naphthamide used in cell culture settings, and it is possible that this compound may act on an as yet unidentified pathway to stimulate JNK. This part of the investigation has shown that JNK inhibition can reverse Aβ-mediated occludin down-regulation; however the JNK isoform involved was not identified. These results further support the view that JNK inhibition might be an attractive therapeutic target in AD, acting to prevent both neuronal cell death and BBB dysfunction.

5.4.3 Role of peptide aggregation in Aβ 1-40-mediated occludin down-regulation by hCMEC/D3 cells

The exact form of Aβ that is toxic to neurones is under debate, although soluble oligomers are emerging as a highly toxic species [357, 359]. Aβ exists as 4 kDa monomer, but has a high tendency to self aggregate to form larger soluble species as wells as larger insoluble fibrils and plaques. In the current study, it was found that the levels of monomeric Aβ 1-40 (4 kDa) were reduced over time in both the supernatant and cell

lysate. This could reflect either the degradation of Aβ by hCMEC/D3 cells, or the aggregation of Aβ. A second finding was the appearance of a large 150 kDa component at 24 and 48 h, which did not correspond to APP. The appearance of this species coincided with the activation of JNK, ERK and p38MAPK. A literature search revealed that the largest soluble aggregate previously resolved via western blot is 100 kDa in size and corresponds to soluble oligomers [693]. Kuo *et al* [694] were able to resolve a range of non-fibrillar forms of Aβ from AD patients into four molecular weight catagories based on filter exclusion: > 100 kDa, 30-100 kDa, 10 -30 kDa and < 10 kDa. Wu *et al* [617] have identified a 120 kDa Aβ aggregate, which forms after co-incubation with haemoglobin. The 150 kDa Aβ species identified here might therefore correspond to either a large soluble oligomer, or an insoluble aggregate. A future study should be carried out to centrifuge the supernatant (100,000 g, 30 min) to determine if the protein fulfils the criteria of an oligomer. The appearance of the large Aβ form could be explained by self aggregation, binding to a hCMEC/D3 cell- derived molecule, or by the detection of a protein not corresponding to Aβ by the antibody (6E10). A PubMed blast search (National Center for Biotechnology Information http://blast.ncbi.nlm.nih.gov/Blast.cgi) for the sequence detected by 6E10 (amino acids 1-16 of Aβ) did not detect any high molecular weight proteins with the exception of APP. This finding potentially rules out the theory of unspecific recognition by 6E10, unless the protein is as yet unidentified. As yet there are no reports of Aβ binding to proteins to produce a 150 kDa species. The potential aggregation found in this study is interesting in that there are no intermediate species of Aβ, only 4 or 150 kDa. The samples used in this study were under reducing and boiled conditions, which would have disrupted any weak non-covalent interactions. It is therefore possible that aggregation intermediates were disaggregated, whilst the larger aggregate was resistant. Argueing against this explanation is the fact that under reducing conditions Aβ dimers and trimers are successfully resolved on western blotting gels [617]. Whilst there

are no reports of covalent binding of Aβ to an EC secreted factor of 150 kDa in size, this hypothesis cannot be disregarded.

Interestingly, in APP blots, a 50 kDa protein was observed to be decreased over time with Aβ treatment, and this protein was not detected by 6E10. APP typically resolves as three bands between 100 and 130 kDa in size and so it is unlikely that the protein corresponds to full - length APP. To date there are no reports of a 50 kDa product of APP. APP belongs to a gene family that includes APP, APLP1 and APLP2. The possibility that the APP antibody was detecting APLP1/2 was considered. However, the molecular weight of APLP1 or 2 does not correspond to 50 kDa [695-697]. Furthermore a Blast search using the sequence of APP which the antibody recognises did not detect any proteins of 50 kDa which would be recognised by the antibody. The most likely explanation is that this unidentified protein is a fragment of APP.

5.5 Conclusions

The Aβ-mediated increase in permeability was reversed by JNK inhibition, most likely due to the prevention of occludin down-regulation. The JNK pathway might represent a potential therapeutic target of BBB dysfunction in AD.

Chapter 6

General discussion

6.1 The role of P-gp in Aβ transport across the BBB

In the current study, the interactions of P-gp and BCRP with Aβ were investigated using hCMEC/D3 cells. The results described in chapters 2 and 3 demonstrate that P-gp, and to a lesser extent BCRP, can act as Aβ efflux transporters at picomolar but not micromolar concentrations of Aβ. Figure 6.1 summarises the routes of Aβ transport at the BBB, based upon this and other studies (reviewed in [137]). In this study, it has been demonstrated using hCMEC/D3 cells, that both P-gp and BCRP restrict the passage of Aβ in the apical-to-basolateral direction, but do not act to facilitate the basolateral-to-apical passage of Aβ. These novel results are consistent with P-gp and BCRP acting to protect the brain from blood-borne Aβ, but not to clear Aβ peptides localised in the CNS parenchyma into the blood. Unfortunately, comparisons between plasma Aβ concentrations in AD patients and non-demented controls are difficult due to the binding of Aβ to plasma proteins [320, 613], oligomerisation of Aβ [698] and high intra- and inter- person variability [699]. None-the-less, there are numerous reports of increased Aβ 1-40 and Aβ 1-42 in the plasma of AD patients compared to controls [321, 699-703]. Quoted concentrations of free Aβ are in the nM to pM range, for example Mehta *et al* [703] found that plasma levels of Aβ 1-40 were higher in AD patients (0.063 nM) than in controls (0.052). Kuo *et al* [320] have recently demonstrated that, once released from plasma proteins, Aβ 1-40 levels in serum are higher in AD patients (2.53 nM) compared to elderly non-demented subjects (1.83 nM). P-gp and BCRP may serve as a protective mechanism for the brain if any of the Aβ bound to plasma proteins is released free [319, 701]. Sagare *et al* [319] recently demonstrated that sLRP, a major plasma Aβ-binding protein, is ~32.5

% lower in AD patients than controls, and this effect is associated with an elevated level of free unbound Aβ 1-40 (22 pM compared to 5 pM in controls). The concentrations of free Aβ in the plasma of AD patients are within the range used in this study, suggesting that P-gp and BCRP could indeed act to protect the brain from circulating unbound Aβ. The increased plasma Aβ levels found in AD could represent either increased production by the brain, or a peripherally produced pool of Aβ. In support of the latter hypothesis, Galloway *et al* [704, 705] have found that small intestine epithelial cells can secrete Aβ. Interestingly a high saturated fat and cholesterol diet, a high risk factor for AD, can induce Aβ production by epithelial cells [94]. Increased plasma Aβ levels, might saturate P-gp and BCRP, allowing blood-to-brain transport via diffusion or RAGE. There is not much evidence for the increased production of Aβ by brain resident cells in AD. However, transgenic mice produced from single or double mutations found in FAD have increased levels of Aβ in the brain parenchyma [331, 332], and neuronal cultures can be induced to increase their production of Aβ by oxidative stress [689]. Aβ produced within the brain could diffuse or be transported across the BBB, and P-gp could act to limit its re-entry into the CNS.

Decreased Aβ clearance from the brain parenchyma is emerging as a potential mechanism in AD pathogenesis [137]. LRP-1 binding at the abluminal membrane of BECs causes brain-to-blood Aβ transport, and decreased LRP-1 expression has been noted in AD patients [384]. To date, P-gp was also hypothesised to mediate brain-to-blood Aβ transport since decreased BEC P-gp expression is associated with plaque deposition [409] and *in vitro* evidence demonstrates P-gp-Aβ binding [406]. In addition, Cirrito *et al* [408] demonstrated *in vivo*, that tariquidar treatment increases Aβ ISF levels in APP mice. By contrast, the results presented here are constant with no significant P-gp or BCRP transport of Aβ in the brain-blood direction, possibly since most P-gp is located on the luminal membrane. The finding of Cirrito *et al* [408], might reflect inhibition of blood-to-brain Aβ transport, as indicated by this study, or an inhibition of P-gp expressed by other cells which

act to uptake Aβ e.g. astrocytes, epithelial cells. In AD, P-gp may therefore be important for the prevention of blood-to-brain Aβ transport, unlike LRP-1 which acts as a brain-to-blood Aβ transporter. It is also possible that P-gp down-regulation is a feature of BBB dysfunction observed in AD (Dr Barrand, Cambridge University, personal communication). If this is the case, brain Aβ load would probably increase by diffusion of the blood-borne peptide across BECs. However, a direct effect of Aβ on hCMEC/D3 cell expression of P-gp was not observed in this study, suggesting that an alternate indirect mechanism e.g. cytokines may induce the down-regulation of P-gp by brain capillaries.

The results of this study have opened up further questions, including whether Aβ transported across BECs is a degradation product or intact Aβ. BECs express enzymes capable of Aβ degradation (e.g. NEP, ICE, ECE) and it has been noted by Nazer *et al* [561], using MDCK cells grown on filters, that LRP can transport degraded peptides. It would be interesting therefore to distinguish between intact and degraded peptides in transport experiments. This could be achieved by re-suspending the supernatants in trichloroacaetic acid and centrifuging to precipitate the intact peptide before counting the radiation in both separated fractions [561]. In addition to Aβ degradation, aggregation of Aβ might also be a factor affecting the ability of P-gp or BCRP to bind Aβ. It would be interesting to pre-aggregate Aβ and determine the efflux and permeability characteristics of Aβ across this *in vitro* BBB model. This could be carried out with non-tagged Aβ and ELISA techniques or tagged Aβ.

A further question raised by the results is the concentration range within which the efflux and transport of Aβ by BCRP or P-gp may operate. In order to test this, increasing concentrations of ^{125}I Aβ 1-40 or native Aβ peptides could be used for efflux and permeability experiments with BCRP and P-gp inhibitors. Alternatively, hCMEC/D3 cells could be made to express increasing levels of P-gp following cell transfection with vectors containing the MDR1 gene, in order to investigate whether higher concentrations of Aβ could be effluxed or transported. In terms of the permeability of hCMEC/D3 cells, the

effect on transport of increasing Aβ concentrations on the basolateral and apical sides should be investigated further. This would be achieved by altering the concentration of Aβ to achieve either equal concentrations on each side, or higher concentrations in the basolateral chamber. This is potentially significant in AD, as if increased brain production of Aβ is the cause of AD, any potential protective effect of P-gp or BCRP pumping Aβ out of BECs into the plasma could be insignificant when compared to bulk flow out from the brain. There are no reports of BCRP-Aβ interactions in the literature and to further demonstrate BCRP –Aβ interactions, dual immunolabelling should be carried out. This could be performed *in vitro*, by incubating Aβ with hCMEC/D3 cells and co-immunolabelling to investigate sub-cellular localisation, and also *in vivo* using brain tissue from AD mouse models.

Finally, a general limitation of a two dimensional cell culture model of BECs is that is does not take into account the role of the cerebral blood flow. A novel technique has been developed [474] which uses hCMEC/D3 cells grown in the lumen of hollow microporous fibers that are exposed to a physiological pulsatile flow. This model would be useful to investigate Aβ mediated P-gp and BCRP transport as the conditions mimic more appropriately the *in vivo* situation. Furthermore, to extrapolate the findings to the *in vivo*, rodents could be pretreated with a P-gp inhibitor or vehicle control, and then *in situ* perfusion carried out with Aβ alone or with a P-gp inhibitor, and the cerebral ISF levels measured.

6.2 Aβ mediated down-regulation of Glut-1 at the BBB

An interesting finding of this study is that Aβ can induce robust Glut-1 down-regulation in hCMEC/D3 cells. This result is in agreement with data from AD CNS tissue samples, in which decreased Glut-1 expression is a common feature [146, 586, 587]. Decreased Glut-1 expression could have the effect of decreasing the amount of glucose

available to neurones, causing an energy crisis. Indeed, decreased glucose metabolism is a common feature of AD patients [430, 431]. The finding that Aβ is sufficient to decrease Glut-1 expression *in vitro* should be taken further experimentally. Firstly, it should be determined whether Glut-1 down-regulation by hCMEC/D3 cells results in a functional decrease in glucose transport. This could be carried out by measuring the intracellular accumulation of $^{14}C/^{3}H$-2-deoxyglucose in Aβ-treated cells. Secondly, inhibitors for pathways activated by Aβ could be employed in an attempt to reverse Glut-1 down-regulation. Thirdly, the mechanisms of Aβ-mediated Glut-1 down-regulation could be investigated further using hCMEC/D3 cells transfected with vectors containing the Glut-1 promoter, to determine if Aβ suppresses transcriptional activity of the Glut-1 promoter.

6.3 Role of JNK in Aβ-mediated increased BBB permeability

In this study, the effect of Aβ on the expression of BEC proteins and permeability was investigated. The results from this study have demonstrated that Aβ *in vitro* can increase the permeability of BECs to paracellular markers. This data is in agreement with the findings that in AD patients increased BBB permeability [579] is observed as indicated by the abnormal presence of plasma proteins on the brain parenchyma. Increased BBB permeability could induce local neuronal degeneration through disruption of homeostasis. The present study provides evidence that increased Aβ levels might be the causative factor for increased BBB permeability. As described previously, elevated plasma levels of Aβ are reported in AD patients [319] and elevated brain levels of Aβ are hypothesised to be critical in the pathogenesis of AD [302]. Furthermore, in a vast majority of AD patients, cerebral amyloid angiopathy occurs in which Aβ is deposited on the vasculature walls [643]. Therefore, high local concentrations of Aβ could in principle lead to a leaky BBB. In fact, the results from chapters 4 and 5 show that Aβ added to the luminal side of the hCMEC/D3 cell cultures was sufficient to induce increased hCMEC/D3 cell permeability.

Results from this study also imply that specific occludin down-regulation at the TJs is responsible for the increased permeability of hCMEC/D3 cells. This is in agreement with Marco and Skaper [486], who found a partial decrease in occludin levels in rat BECs after Aβ incubation and Tachehci *et al* [94], who demonstrated, using an *in vivo* model (APP/PS1 mice), down-regulation of occludin and increased BBB permeability. Overall, the results described here expand on the mechanisms leading to a leaky BBB in AD and identify Aβ as having a central role in this effect, acting to decrease occludin expression by BECs.

A novel finding of the present study is that JNK inhibition can prevent the Aβ-induced increased permeability and occludin down-regulation in BECs. This finding demonstrates that JNK inhibitors might be a potential therapeutic target for the treatment of AD, preventing a leaky BBB. Further experimentation should be carried out both *in vitro* and *in vivo* in order to fully characterise the interplay between Aβ, JNK and occludin down-regulation.

Although the results imply that JNK rather than p38MAPK is the main pathway involved in Aβ-mediated occludin down-regulation, the results from this study have not exclusively ruled out p38MAPK involvement. To confirm involvement of different components of the MAPK family, BECs could be stimulated by Aβ in the presence or absence of MAPK inhibitors and quantitatively assessed for MAPK activity using various available ELISA kits. In addition, AD patient tissue from different BRAAK stages and areas of the brain could be stained for plasma proteins as a guide of BBB leakiness and examined for correlation with decreased occludin levels and phosphorylated MAPK family members, as well as other TJ proteins. This would determine whether JNK and/or p38MAPK activation is associated with decreased occludin expression at the BBB in AD patients. Furthermore, transgenic mouse models could be used. Tg2576 [584] and TASTPM [706] mice show increased BBB permeability. TJ protein expression and JNK activation should also be investigated at the levels of the BBB in these mice.

Another area for further investigation is the mechanism of Aβ-induced JNK activation. The activity of upstream JNK activators (e.g MAPKK, MAPKKK) could be assessed via western blotting using phosphorylated-state specific antibodies in hCMEC/D3 cells after Aβ incubation. MKK4 and MKK7 are the two MAPKKs that activate JNK, which themselves are activated by a range of MAPKKKs. For example, TNF-1 and IL-1, known stimulators of the JNK pathway, stimulate the MAPKKK TAK1 [707]. Once and if identified, the gene of each identified signalling component could be silenced in hCMEC/D3 cells using siRNA, and the effects on Aβ mediated occludin down-regulation assessed. Furthermore, AD patient tissue and transgenic models could be stained for each identified signalling component. Aβ may also activate reactive oxygen species (ROS), which in turn could lead to JNK activation. This mechanism of JNK activation could be investigated *in vitro*, by measuring whether Aβ increases ROS levels in hCMEC/D3 cells.

In addition, the downstream consequences of JNK activation by Aβ could be investigated. Potentially, JNK could act to suppress occludin at the transcriptional level, on mRNA stability, directly at the protein level or even a combination of all three (Figure 6.2). To investigate Aβ-induced changes at the transcriptional level, the promoter of occludin could be cloned into reporter vectors and then transfected into hCMEC/D3 cells. The effect of Aβ on occludin promoter activity could then be investigated in the presence or absence of JNK inhibitors to determine if this is a significant mechanism of occludin down-regulation. Subsequent experiments (e.g. EMSA) could then be carried out to determine which transcription factor(s) are involved in this effect. To investigate JNK effects on occludin mRNA stability, qRT-PCR could be carried out. This could be achieved by investigating whether Aβ enhances the degradation of occludin mRNA in the presence of transcriptional inhibitors, i.e. actinomycin D, and also the effects of JNK inhibitors on this process. To investigate any possible direct effects of JNK at the protein

level, occludin could be isolated via immunoprecipitation and the phosphorylated state of different splice forms investigated in the presence and absence of JNK inhibitors assessed via western blotting. Once indentified *in vitro*, the results could be investigated *in vivo* from both AD patient tissue and AD transgenic mouse models. Using both AD patient tissue and AD transgenic mouse models, binding of any transcription factors to the occludin promoter in hCMEC/D3 cells could be investigated by chromatin immunoprecipitation, and compared to age matched controls.

It would also be interesting to identify the JNK isoform activated by Aβ. siRNA knockdown of each JNK isoform in hCMEC/D3 cells could be carried out, and the effect of Aβ on occludin down-regulation determined. Alternatively, kinase assays on Aβ hCMEC/D3 cell lysates could be analysed for the levels of each active JNK isoform.

The combined results of these experiments would elucidate the molecular pathway(s) leading to the down-regulation of occludin by Aβ, and perhaps suggest novel therapeutic ways of manipulating these pathway(s). A major future direction for this work, would be the assessment of JNK inhibitors as an AD therapeutic agent. Tg2756 and TASTPM mice could be treated with JNK inhibitors and the effect on BBB leakiness and occludin expression observed. A water maze assessment could also be carried out to investigate whether a reversal in BBB effects improves cognition in the mouse models. Since JNK inhibition can also protect neurones, a detailed neuronal investigation should also be carried out in regions susceptible to AD e.g. the hippocampus. The diagnosis of AD is based on symptoms and significant neurodegeneration and BBB dysfunction might have already occured. Therefore, as therapeutic agents, JNK inhibitors would most likely be administered after the onset of any damage. Further *in vitro* and *in vivo* evaluation of the ability of JNK inhibition to stall disease progression, or better yet, reverse vascular and neuronal dysfunction after symptoms have already occurred could be carried out in the mouse models of AD.

In principle, JNK might represent an attractive dual target, preventing both neurotoxicity and increased BBB leakiness. Indeed, JNK inhibition can prevent Aβ-induced neuronal death *in vitro* [353, 634, 636], and activated JNK is found in neurones from AD patient's tissue [632, 633]. It is thus possible, that with earlier diagnosis of AD in patients, administration of JNK inhibitors may become a novel therapy to protect against any further damaging effects of Aβ at the level of both neurons and the cerebral vasculature.

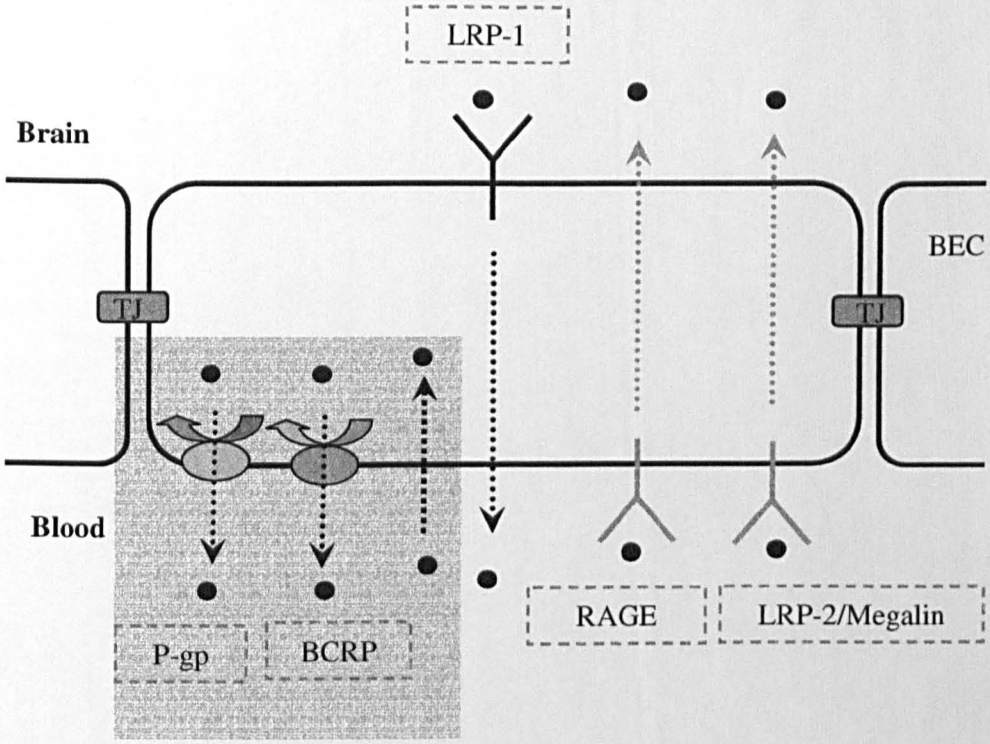

Figure 6.1. The transport of Aβ at the BBB mediated via LRP, P-gp and RAGE. The blood-to-brain transport of Aβ (black dot) is mediated by RAGE and LRP-2/megalin, whilst the brain-to-blood transport is mediated by LRP-1. The results of this study, indicated by a grey box, have demonstrated that P-gp and BCRP form a blood-brain Aβ transport barrier.

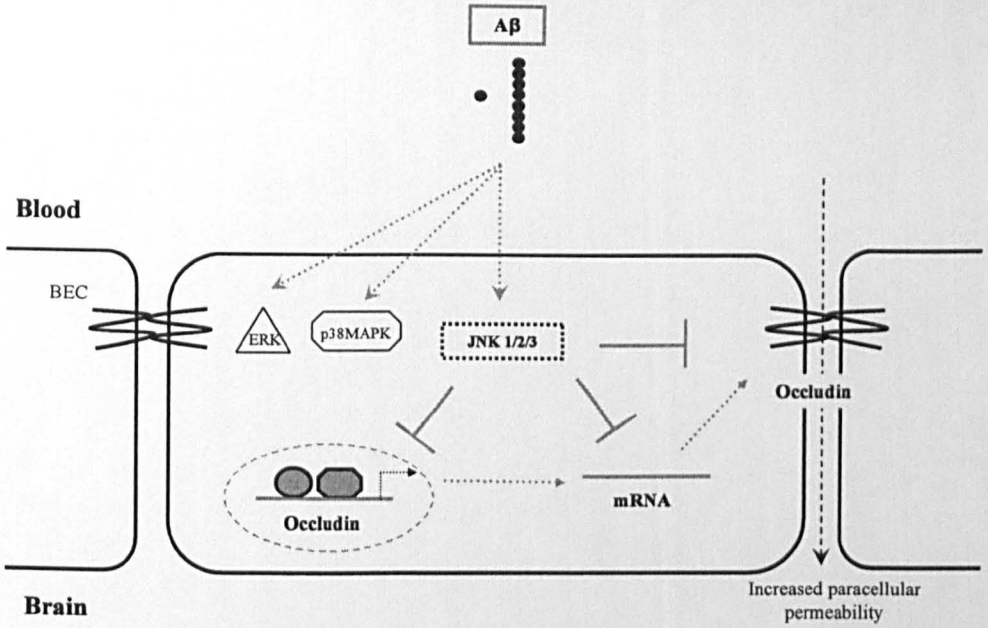

Figure 6.2. Potential mechanisms of Aβ-mediated increased permeability in hCMEC/D3 cells. Aβ induces down-regulation of occludin via JNK activation in hCMEC/D3 cells. JNK activation could theoretically act to alter occludin levels via transcription activity suppression, mRNA degradation or a direct effect on occludin at the protein level. ● = Aβ monomer ● = oligomer species

References

1. Erlich, P., *Das Sauerstoff-Bedurfnisdes Organismus. Eine farbenanalytische Studie.* Verlag von August Hirschwald, 1885.
2. Lewandowski, M., *Zur Lehre von der Cerebrospinalflussigkeit.* Z.Klein Forsch, 1900. **40**: p. 480-494.
3. Bechmann, I., I. Galea, and V.H. Perry, *What is the blood-brain barrier (not)?* Trends Immunol, 2007. **28**(1): p. 5-11.
4. Goldmann, E., *Vitalfärbungen am Zentralnervensystem. Beitrag zur Physio-Pathologie des Plexus Choroideus und der Hirnhäute. Abhandlungen der königlich preußischen Akademie der Wissenschaften.* Physikalisch-Mathematische Classe 1 (1913), pp. 1–64., 1913.
5. Reese, T.S. and M.J. Karnovsky, *Fine structural localization of a blood-brain barrier to exogenous peroxidase.* J Cell Biol, 1967. **34**(1): p. 207-17.
6. Hawkins, B.T. and T.P. Davis, *The blood-brain barrier/neurovascular unit in health and disease.* Pharmacol Rev, 2005. **57**(2): p. 173-85.
7. Leis, J.A., L.K. Bekar, and W. Walz, *Potassium homeostasis in the ischemic brain.* Glia, 2005. **50**(4): p. 407-16.
8. Walz, W., *Role of glial cells in the regulation of the brain ion microenvironment.* Prog Neurobiol, 1989. **33**(4): p. 309-33.
9. Walz, W., *Role of astrocytes in the clearance of excess extracellular potassium.* Neurochem Int, 2000. **36**(4-5): p. 291-300.
10. Rao, K.V., et al., *Astrocytes protect neurons from ammonia toxicity.* Neurochem Res, 2005. **30**(10): p. 1311-8.
11. Suarez, I., G. Bodega, and B. Fernandez, *Glutamine synthetase in brain: effect of ammonia.* Neurochem Int, 2002. **41**(2-3): p. 123-42.
12. Tsacopoulos, M., *Metabolic signaling between neurons and glial cells: a short review.* J Physiol Paris, 2002. **96**(3-4): p. 283-8.
13. Benarroch, E.E., *Neuron-astrocyte interactions: partnership for normal function and disease in the central nervous system.* Mayo Clin Proc, 2005. **80**(10): p. 1326-38.
14. Pellerin, L., et al., *Activity-dependent regulation of energy metabolism by astrocytes: an update.* Glia, 2007. **55**(12): p. 1251-62.
15. Tsacopoulos, M. and P.J. Magistretti, *Metabolic coupling between glia and neurons.* J Neurosci, 1996. **16**(3): p. 877-85.
16. Abbott, N.J., *Astrocyte-endothelial interactions and blood-brain barrier permeability.* J Anat, 2002. **200**(6): p. 629-38.
17. Bauer, H.C. and H. Bauer, *Neural induction of the blood-brain barrier: still an enigma.* Cell Mol Neurobiol, 2000. **20**(1): p. 13-28.
18. Haseloff, R.F., et al., *In search of the astrocytic factor(s) modulating blood-brain barrier functions in brain capillary endothelial cells in vitro.* Cell Mol Neurobiol, 2005. **25**(1): p. 25-39.
19. Dehouck, M.P., et al., *An easier, reproducible, and mass-production method to study the blood-brain barrier in vitro.* J Neurochem, 1990. **54**(5): p. 1798-801.
20. Sobue, K., et al., *Induction of blood-brain barrier properties in immortalized bovine brain endothelial cells by astrocytic factors.* Neurosci Res, 1999. **35**(2): p. 155-64.
21. Janzer, R.C. and M.C. Raff, *Astrocytes induce blood-brain barrier properties in endothelial cells.* Nature, 1987. **325**(6101): p. 253-7.
22. Maxwell, K., J.A. Berliner, and P.A. Cancilla, *Induction of gamma-glutamyl transpeptidase in cultured cerebral endothelial cells by a product released by astrocytes.* Brain Res, 1987. **410**(2): p. 309-14.

23. Rubin, L.L., et al., *A cell culture model of the blood-brain barrier.* J Cell Biol, 1991. **115**(6): p. 1725-35.
24. Tran, N.D., et al., *Transforming growth factor-beta mediates astrocyte-specific regulation of brain endothelial anticoagulant factors.* Stroke, 1999. **30**(8): p. 1671-8.
25. el Hafny, B., J.M. Bourre, and F. Roux, *Synergistic stimulation of gamma-glutamyl transpeptidase and alkaline phosphatase activities by retinoic acid and astroglial factors in immortalized rat brain microvessel endothelial cells.* J Cell Physiol, 1996. **167**(3): p. 451-60.
26. Lee, S.W., et al., *SSeCKS regulates angiogenesis and tight junction formation in blood-brain barrier.* Nat Med, 2003. **9**(7): p. 900-6.
27. Schroeter, M.L., et al., *Astrocytes enhance radical defence in capillary endothelial cells constituting the blood-brain barrier.* FEBS Lett, 1999. **449**(2-3): p. 241-4.
28. Estrada, C., et al., *Astrocyte growth stimulation by a soluble factor produced by cerebral endothelial cells in vitro.* J Neuropathol Exp Neurol, 1990. **49**(6): p. 539-49.
29. Balabanov, R. and P. Dore-Duffy, *Role of the CNS microvascular pericyte in the blood-brain barrier.* J Neurosci Res, 1998. **53**(6): p. 637-44.
30. Lai, C.H. and K.H. Kuo, *The critical component to establish in vitro BBB model: Pericyte.* Brain Res Brain Res Rev, 2005. **50**(2): p. 258-65.
31. Peppiatt, C.M., et al., *Bidirectional control of CNS capillary diameter by pericytes.* Nature, 2006. **443**(7112): p. 700-4.
32. Simionescu, M., et al., *The cerebral microvasculature of the rat: structure and luminal surface properties during early development.* J Submicrosc Cytol Pathol, 1988. **20**(2): p. 243-61.
33. Hellstrom, M., et al., *Role of PDGF-B and PDGFR-beta in recruitment of vascular smooth muscle cells and pericytes during embryonic blood vessel formation in the mouse.* Development, 1999. **126**(14): p. 3047-55.
34. Lindahl, P., et al., *Pericyte loss and microaneurysm formation in PDGF-B-deficient mice.* Science, 1997. **277**(5323): p. 242-5.
35. Puri, M.C., et al., *The receptor tyrosine kinase TIE is required for integrity and survival of vascular endothelial cells.* Embo J, 1995. **14**(23): p. 5884-91.
36. Ramsauer, M., D. Krause, and R. Dermietzel, *Angiogenesis of the blood-brain barrier in vitro and the function of cerebral pericytes.* Faseb J, 2002. **16**(10): p. 1274-6.
37. Hori, S., et al., *A pericyte-derived angiopoietin-1 multimeric complex induces occludin gene expression in brain capillary endothelial cells through Tie-2 activation in vitro.* J Neurochem, 2004. **89**(2): p. 503-13.
38. Dohgu, S., et al., *Brain pericytes contribute to the induction and up-regulation of blood-brain barrier functions through transforming growth factor-beta production.* Brain Res, 2005. **1038**(2): p. 208-15.
39. Herman, I.M. and P.A. D'Amore, *Microvascular pericytes contain muscle and nonmuscle actins.* J Cell Biol, 1985. **101**(1): p. 43-52.
40. Oishi, K., T. Kamiyashiki, and Y. Ito, *Isometric contraction of microvascular pericytes from mouse brain parenchyma.* Microvasc Res, 2007. **73**(1): p. 20-8.
41. Bennett, H.S., J.H. Luft, and J.C. Hampton, *Morphological classifications of vertebrate blood capillaries.* Am J Physiol, 1959. **196**(2): p. 381-90.
42. Pasqualini, R., W. Arap, and D.M. McDonald, *Probing the structural and molecular diversity of tumor vasculature.* Trends Mol Med, 2002. **8**(12): p. 563-71.
43. Simionescu, M., N. Simionescu, and G.E. Palade, *Segmental differentiations of cell junctions in the vascular endothelium. Arteries and veins.* J Cell Biol, 1976. **68**(3): p. 705-23.

44. Cornford, E.M., et al., *Comparison of lipid-mediated blood-brain-barrier penetrability in neonates and adults.* Am J Physiol, 1982. **243**(3): p. C161-8.
45. Crone, C. and S.P. Olesen, *Electrical resistance of brain microvascular endothelium.* Brain Res, 1982. **241**(1): p. 49-55.
46. Deli, M.A., et al., *Permeability studies on in vitro blood-brain barrier models: physiology, pathology, and pharmacology.* Cell Mol Neurobiol, 2005. **25**(1): p. 59-127.
47. Olesen, S.P. and C. Crone, *Electrical resistance of muscle capillary endothelium.* Biophys J, 1983. **42**(1): p. 31-41.
48. Muhleisen, H., H. Wolburg, and E. Betz, *Freeze-fracture analysis of endothelial cell membranes in rabbit carotid arteries subjected to short-term atherogenic stimuli.* Virchows Arch B Cell Pathol Incl Mol Pathol, 1989. **56**(6): p. 413-7.
49. Wolburg, H., et al., *Modulation of tight junction structure in blood-brain barrier endothelial cells. Effects of tissue culture, second messengers and cocultured astrocytes.* J Cell Sci, 1994. **107 (Pt 5)**: p. 1347-57.
50. Engelhardt, B., *Development of the blood-brain barrier.* Cell Tissue Res, 2003. **314**(1): p. 119-29.
51. Nagy, Z., H. Peters, and I. Huttner, *Fracture faces of cell junctions in cerebral endothelium during normal and hyperosmotic conditions.* Lab Invest, 1984. **50**(3): p. 313-22.
52. Tsukita, S., M. Furuse, and M. Itoh, *Multifunctional strands in tight junctions.* Nat Rev Mol Cell Biol, 2001. **2**(4): p. 285-93.
53. Engelhardt, B., K. Wolburg-Buchholz, and H. Wolburg, *Involvement of the choroid plexus in central nervous system inflammation.* Microsc Res Tech, 2001. **52**(1): p. 112-29.
54. Duvernoy, H.M. and P.Y. Risold, *The circumventricular organs: an atlas of comparative anatomy and vascularization.* Brain Res Rev, 2007. **56**(1): p. 119-47.
55. Fry, M. and A.V. Ferguson, *The sensory circumventricular organs: brain targets for circulating signals controlling ingestive behavior.* Physiol Behav, 2007. **91**(4): p. 413-23.
56. Oldendorf, W.H., M.E. Cornford, and W.J. Brown, *The large apparent work capability of the blood-brain barrier: a study of the mitochondrial content of capillary endothelial cells in brain and other tissues of the rat.* Ann Neurol, 1977. **1**(5): p. 409-17.
57. Betz, A.L., J.A. Firth, and G.W. Goldstein, *Polarity of the blood-brain barrier: distribution of enzymes between the luminal and antiluminal membranes of brain capillary endothelial cells.* Brain Res, 1980. **192**(1): p. 17-28.
58. Ghersi-Egea, J.F., et al., *Localization of drug-metabolizing enzyme activities to blood-brain interfaces and circumventricular organs.* J Neurochem, 1994. **62**(3): p. 1089-96.
59. Ghersi-Egea, J.F., A. Minn, and G. Siest, *A new aspect of the protective functions of the blood-brain barrier: activities of four drug-metabolizing enzymes in isolated rat brain microvessels.* Life Sci, 1988. **42**(24): p. 2515-23.
60. Minn, A., et al., *Drug metabolizing enzymes in the brain and cerebral microvessels.* Brain Res Brain Res Rev, 1991. **16**(1): p. 65-82.
61. Schroeter, M.L., et al., *Astrocytes induce manganese superoxide dismutase in brain capillary endothelial cells.* Neuroreport, 2001. **12**(11): p. 2513-7.
62. Schulze, C. and J.A. Firth, *Immunohistochemical localization of adherens junction components in blood-brain barrier microvessels of the rat.* J Cell Sci, 1993. **104 (Pt 3)**: p. 773-82.
63. Wallez, Y. and P. Huber, *Endothelial adherens and tight junctions in vascular homeostasis, inflammation and angiogenesis.* Biochim Biophys Acta, 2008. **1778**(3): p. 794-809.

64. Lampugnani, M.G., et al., *A novel endothelial-specific membrane protein is a marker of cell-cell contacts.* J Cell Biol, 1992. **118**(6): p. 1511-22.
65. Brown, R.C. and T.P. Davis, *Calcium modulation of adherens and tight junction function: a potential mechanism for blood-brain barrier disruption after stroke.* Stroke, 2002. **33**(6): p. 1706-11.
66. Abbruscato, T.J. and T.P. Davis, *Combination of hypoxia/aglycemia compromises in vitro blood-brain barrier integrity.* J Pharmacol Exp Ther, 1999. **289**(2): p. 668-75.
67. Ebnet, K., *Organization of multiprotein complexes at cell-cell junctions.* Histochem Cell Biol, 2008. **130**(1): p. 1-20.
68. Hawkins, R.A., D.R. Peterson, and J.R. Vina, *The complementary membranes forming the blood-brain barrier.* IUBMB Life, 2002. **54**(3): p. 101-7.
69. Wolburg, H. and A. Lippoldt, *Tight junctions of the blood-brain barrier: development, composition and regulation.* Vascul Pharmacol, 2002. **38**(6): p. 323-37.
70. Schneeberger, E.E. and R.D. Lynch, *The tight junction: a multifunctional complex.* Am J Physiol Cell Physiol, 2004. **286**(6): p. C1213-28.
71. Furuse, M., et al., *Occludin: a novel integral membrane protein localizing at tight junctions.* J Cell Biol, 1993. **123**(6 Pt 2): p. 1777-88.
72. Lippoldt, A., et al., *Structural alterations of tight junctions are associated with loss of polarity in stroke-prone spontaneously hypertensive rat blood-brain barrier endothelial cells.* Brain Res, 2000. **885**(2): p. 251-61.
73. Hirase, T., et al., *Occludin as a possible determinant of tight junction permeability in endothelial cells.* J Cell Sci, 1997. **110 (Pt 14)**: p. 1603-13.
74. Ando-Akatsuka, Y., et al., *Interspecies diversity of the occludin sequence: cDNA cloning of human, mouse, dog, and rat-kangaroo homologues.* J Cell Biol, 1996. **133**(1): p. 43-7.
75. Papadopoulos, M.C., et al., *Occludin expression in microvessels of neoplastic and non-neoplastic human brain.* Neuropathol Appl Neurobiol, 2001. **27**(5): p. 384-95.
76. Fanning, A.S., et al., *The tight junction protein ZO-1 establishes a link between the transmembrane protein occludin and the actin cytoskeleton.* J Biol Chem, 1998. **273**(45): p. 29745-53.
77. Furuse, M., et al., *Direct association of occludin with ZO-1 and its possible involvement in the localization of occludin at tight junctions.* J Cell Biol, 1994. **127**(6 Pt 1): p. 1617-26.
78. Saitou, M., et al., *Complex phenotype of mice lacking occludin, a component of tight junction strands.* Mol Biol Cell, 2000. **11**(12): p. 4131-42.
79. Schulzke, J.D., et al., *Epithelial transport and barrier function in occludin-deficient mice.* Biochim Biophys Acta, 2005. **1669**(1): p. 34-42.
80. Saitou, M., et al., *Occludin-deficient embryonic stem cells can differentiate into polarized epithelial cells bearing tight junctions.* J Cell Biol, 1998. **141**(2): p. 397-408.
81. Tsukita, S. and M. Furuse, *Occludin and claudins in tight-junction strands: leading or supporting players?* Trends Cell Biol, 1999. **9**(7): p. 268-73.
82. McCarthy, K.M., et al., *Occludin is a functional component of the tight junction.* J Cell Sci, 1996. **109 (Pt 9)**: p. 2287-98.
83. Balda, M.S., et al., *Functional dissociation of paracellular permeability and transepithelial electrical resistance and disruption of the apical-basolateral intramembrane diffusion barrier by expression of a mutant tight junction membrane protein.* J Cell Biol, 1996. **134**(4): p. 1031-49.
84. Chen, Y., et al., *COOH terminus of occludin is required for tight junction barrier function in early Xenopus embryos.* J Cell Biol, 1997. **138**(4): p. 891-9.

85. Yu, A.S., et al., *Knockdown of occludin expression leads to diverse phenotypic alterations in epithelial cells.* Am J Physiol Cell Physiol, 2005. **288**(6): p. C1231-41.
86. Antonetti, D.A., et al., *Vascular endothelial growth factor induces rapid phosphorylation of tight junction proteins occludin and zonula occluden 1. A potential mechanism for vascular permeability in diabetic retinopathy and tumors.* J Biol Chem, 1999. **274**(33): p. 23463-7.
87. Antonetti, D.A., et al., *Vascular permeability in experimental diabetes is associated with reduced endothelial occludin content: vascular endothelial growth factor decreases occludin in retinal endothelial cells. Penn State Retina Research Group.* Diabetes, 1998. **47**(12): p. 1953-9.
88. Hirase, T., et al., *Regulation of tight junction permeability and occludin phosphorylation by Rhoa-p160ROCK-dependent and -independent mechanisms.* J Biol Chem, 2001. **276**(13): p. 10423-31.
89. Stamatovic, S.M., et al., *Protein kinase Calpha-RhoA cross-talk in CCL2-induced alterations in brain endothelial permeability.* J Biol Chem, 2006. **281**(13): p. 8379-88.
90. DeMaio, L., et al., *Oxidized phospholipids mediate occludin expression and phosphorylation in vascular endothelial cells.* Am J Physiol Heart Circ Physiol, 2006. **290**(2): p. H674-83.
91. Bolton, S.J., D.C. Anthony, and V.H. Perry, *Loss of the tight junction proteins occludin and zonula occludens-1 from cerebral vascular endothelium during neutrophil-induced blood-brain barrier breakdown in vivo.* Neuroscience, 1998. **86**(4): p. 1245-57.
92. Brooks, T.A., et al., *Chronic inflammatory pain leads to increased blood-brain barrier permeability and tight junction protein alterations.* Am J Physiol Heart Circ Physiol, 2005. **289**(2): p. H738-43.
93. Mark, K.S. and T.P. Davis, *Cerebral microvascular changes in permeability and tight junctions induced by hypoxia-reoxygenation.* Am J Physiol Heart Circ Physiol, 2002. **282**(4): p. H1485-94.
94. Takechi, R., et al., *Chylomicron amyloid-beta in the aetiology of Alzheimer's disease.* Atheroscler Suppl, 2008.
95. Furuse, M., et al., *Claudin-1 and -2: novel integral membrane proteins localizing at tight junctions with no sequence similarity to occludin.* J Cell Biol, 1998. **141**(7): p. 1539-50.
96. Erickson, K.K., J.M. Sundstrom, and D.A. Antonetti, *Vascular permeability in ocular disease and the role of tight junctions.* Angiogenesis, 2007. **10**(2): p. 103-17.
97. Morita, K., et al., *Claudin multigene family encoding four-transmembrane domain protein components of tight junction strands.* Proc Natl Acad Sci U S A, 1999. **96**(2): p. 511-6.
98. Itoh, M., et al., *Direct binding of three tight junction-associated MAGUKs, ZO-1, ZO-2, and ZO-3, with the COOH termini of claudins.* J Cell Biol, 1999. **147**(6): p. 1351-63.
99. Furuse, M., H. Sasaki, and S. Tsukita, *Manner of interaction of heterogeneous claudin species within and between tight junction strands.* J Cell Biol, 1999. **147**(4): p. 891-903.
100. Furuse, M., et al., *A single gene product, claudin-1 or -2, reconstitutes tight junction strands and recruits occludin in fibroblasts.* J Cell Biol, 1998. **143**(2): p. 391-401.
101. Liebner, S., et al., *Claudin-1 and claudin-5 expression and tight junction morphology are altered in blood vessels of human glioblastoma multiforme.* Acta Neuropathol, 2000. **100**(3): p. 323-31.

102. Wolburg, H., et al., *Localization of claudin-3 in tight junctions of the blood-brain barrier is selectively lost during experimental autoimmune encephalomyelitis and human glioblastoma multiforme.* Acta Neuropathol, 2003. **105**(6): p. 586-92.
103. Nitta, T., et al., *Size-selective loosening of the blood-brain barrier in claudin-5-deficient mice.* J Cell Biol, 2003. **161**(3): p. 653-60.
104. Bazzoni, G., *The JAM family of junctional adhesion molecules.* Curr Opin Cell Biol, 2003. **15**(5): p. 525-30.
105. Del Maschio, A., et al., *Leukocyte recruitment in the cerebrospinal fluid of mice with experimental meningitis is inhibited by an antibody to junctional adhesion molecule (JAM).* J Exp Med, 1999. **190**(9): p. 1351-6.
106. Aurrand-Lions, M., et al., *Heterogeneity of endothelial junctions is reflected by differential expression and specific subcellular localization of the three JAM family members.* Blood, 2001. **98**(13): p. 3699-707.
107. Liu, Y., et al., *Human junction adhesion molecule regulates tight junction resealing in epithelia.* J Cell Sci, 2000. **113 (Pt 13)**: p. 2363-74.
108. Bazzoni, G., et al., *Interaction of junctional adhesion molecule with the tight junction components ZO-1, cingulin, and occludin.* J Biol Chem, 2000. **275**(27): p. 20520-6.
109. Ebnet, K., et al., *Junctional adhesion molecule interacts with the PDZ domain-containing proteins AF-6 and ZO-1.* J Biol Chem, 2000. **275**(36): p. 27979-88.
110. Citi, S., et al., *Cingulin: characterization and localization.* J Cell Sci, 1989. **93 (Pt 1)**: p. 107-22.
111. Stevenson, B.R., et al., *ZO-1 and cingulin: tight junction proteins with distinct identities and localizations.* Am J Physiol, 1989. **257**(4 Pt 1): p. C621-8.
112. Yamamoto, T., et al., *The Ras target AF-6 interacts with ZO-1 and serves as a peripheral component of tight junctions in epithelial cells.* J Cell Biol, 1997. **139**(3): p. 785-95.
113. Yamamoto, T., et al., *In vivo interaction of AF-6 with activated Ras and ZO-1.* Biochem Biophys Res Commun, 1999. **259**(1): p. 103-7.
114. Zhong, Y., et al., *Localization of the 7H6 antigen at tight junctions correlates with the paracellular barrier function of MDCK cells.* Exp Cell Res, 1994. **214**(2): p. 614-20.
115. Zhong, Y., et al., *Sequential decrease in tight junctions as revealed by 7H6 tight junction-associated protein during rat hepatocarcinogenesis.* Jpn J Cancer Res, 1994. **85**(4): p. 351-6.
116. Stevenson, B.R., et al., *Identification of ZO-1: a high molecular weight polypeptide associated with the tight junction (zonula occludens) in a variety of epithelia.* J Cell Biol, 1986. **103**(3): p. 755-66.
117. Gumbiner, B., T. Lowenkopf, and D. Apatira, *Identification of a 160-kDa polypeptide that binds to the tight junction protein ZO-1.* Proc Natl Acad Sci U S A, 1991. **88**(8): p. 3460-4.
118. Haskins, J., et al., *ZO-3, a novel member of the MAGUK protein family found at the tight junction, interacts with ZO-1 and occludin.* J Cell Biol, 1998. **141**(1): p. 199-208.
119. Gonzalez-Mariscal, L., A. Betanzos, and A. Avila-Flores, *MAGUK proteins: structure and role in the tight junction.* Semin Cell Dev Biol, 2000. **11**(4): p. 315-24.
120. te Velthuis, A.J., J.F. Admiraal, and C.P. Bagowski, *Molecular evolution of the MAGUK family in metazoan genomes.* BMC Evol Biol, 2007. **7**: p. 129.
121. Wittchen, E.S., J. Haskins, and B.R. Stevenson, *Protein interactions at the tight junction. Actin has multiple binding partners, and ZO-1 forms independent complexes with ZO-2 and ZO-3.* J Biol Chem, 1999. **274**(49): p. 35179-85.

122. Itoh, M., K. Morita, and S. Tsukita, *Characterization of ZO-2 as a MAGUK family member associated with tight as well as adherens junctions with a binding affinity to occludin and alpha catenin.* J Biol Chem, 1999. **274**(9): p. 5981-6.
123. Schmidt, A., et al., *Occludin binds to the SH3-hinge-GuK unit of zonula occludens protein 1: potential mechanism of tight junction regulation.* Cell Mol Life Sci, 2004. **61**(11): p. 1354-65.
124. Umeda, K., et al., *ZO-1 and ZO-2 independently determine where claudins are polymerized in tight-junction strand formation.* Cell, 2006. **126**(4): p. 741-54.
125. Itoh, M., et al., *Involvement of ZO-1 in cadherin-based cell adhesion through its direct binding to alpha catenin and actin filaments.* J Cell Biol, 1997. **138**(1): p. 181-92.
126. Muller, S.L., et al., *The tight junction protein occludin and the adherens junction protein alpha-catenin share a common interaction mechanism with ZO-1.* J Biol Chem, 2005. **280**(5): p. 3747-56.
127. McNeil, E., C.T. Capaldo, and I.G. Macara, *Zonula occludens-1 function in the assembly of tight junctions in Madin-Darby canine kidney epithelial cells.* Mol Biol Cell, 2006. **17**(4): p. 1922-32.
128. Umeda, K., et al., *Establishment and characterization of cultured epithelial cells lacking expression of ZO-1.* J Biol Chem, 2004. **279**(43): p. 44785-94.
129. Katsuno, T., et al., *Deficiency of Zonula Occludens-1 Causes Embryonic Lethal Phenotype Associated with Defected Yolk Sac Angiogenesis and Apoptosis of Embryonic Cells.* Mol Biol Cell, 2008. **19**(6): p. 2465-2475.
130. Abbott, N.J., *Inflammatory mediators and modulation of blood-brain barrier permeability.* Cell Mol Neurobiol, 2000. **20**(2): p. 131-47.
131. Gonzalez-Mariscal, L., R. Tapia, and D. Chamorro, *Crosstalk of tight junction components with signaling pathways.* Biochim Biophys Acta, 2008. **1778**(3): p. 729-56.
132. Persidsky, Y., et al., *Rho-mediated regulation of tight junctions during monocyte migration across the blood-brain barrier in HIV-1 encephalitis (HIVE).* Blood, 2006. **107**(12): p. 4770-80.
133. Ma, T.Y., et al., *Mechanism of extracellular calcium regulation of intestinal epithelial tight junction permeability: role of cytoskeletal involvement.* Microsc Res Tech, 2000. **51**(2): p. 156-68.
134. Balda, M.S., et al., *Assembly and sealing of tight junctions: possible participation of G-proteins, phospholipase C, protein kinase C and calmodulin.* J Membr Biol, 1991. **122**(3): p. 193-202.
135. Balda, M.S., et al., *Assembly of the tight junction: the role of diacylglycerol.* J Cell Biol, 1993. **123**(2): p. 293-302.
136. Klingler, C., et al., *Disruption of epithelial tight junctions is prevented by cyclic nucleotide-dependent protein kinase inhibitors.* Histochem Cell Biol, 2000. **113**(5): p. 349-61.
137. Zlokovic, B.V., *The blood-brain barrier in health and chronic neurodegenerative disorders.* Neuron, 2008. **57**(2): p. 178-201.
138. Simpson, I.A., A. Carruthers, and S.J. Vannucci, *Supply and demand in cerebral energy metabolism: the role of nutrient transporters.* J Cereb Blood Flow Metab, 2007. **27**(11): p. 1766-91.
139. Pardridge, W.M., R.J. Boado, and C.R. Farrell, *Brain-type glucose transporter (GLUT-1) is selectively localized to the blood-brain barrier. Studies with quantitative western blotting and in situ hybridization.* J Biol Chem, 1990. **265**(29): p. 18035-40.
140. Birnbaum, M.J., H.C. Haspel, and O.M. Rosen, *Cloning and characterization of a cDNA encoding the rat brain glucose-transporter protein.* Proc Natl Acad Sci U S A, 1986. **83**(16): p. 5784-8.

141. Cornford, E.M., S. Hyman, and W.M. Pardridge, *An electron microscopic immunogold analysis of developmental up-regulation of the blood-brain barrier GLUT1 glucose transporter.* J Cereb Blood Flow Metab, 1993. **13**(5): p. 841-54.
142. Cornford, E.M., S. Hyman, and B.E. Swartz, *The human brain GLUT1 glucose transporter: ultrastructural localization to the blood-brain barrier endothelia.* J Cereb Blood Flow Metab, 1994. **14**(1): p. 106-12.
143. Dick, A.P., et al., *Identification and characterization of the glucose transporter of the blood-brain barrier by cytochalasin B binding and immunological reactivity.* Proc Natl Acad Sci U S A, 1984. **81**(22): p. 7233-7.
144. Farrell, C.L. and W.M. Pardridge, *Blood-brain barrier glucose transporter is asymmetrically distributed on brain capillary endothelial lumenal and ablumenal membranes: an electron microscopic immunogold study.* Proc Natl Acad Sci U S A, 1991. **88**(13): p. 5779-83.
145. Farrell, C.L., J. Yang, and W.M. Pardridge, *GLUT-1 glucose transporter is present within apical and basolateral membranes of brain epithelial interfaces and in microvascular endothelia with and without tight junctions.* J Histochem Cytochem, 1992. **40**(2): p. 193-9.
146. Harik, S.I., *Changes in the glucose transporter of brain capillaries.* Can J Physiol Pharmacol, 1992. **70 Suppl**: p. S113-7.
147. Simpson, I.A., et al., *Glucose transporter asymmetries in the bovine blood-brain barrier.* J Biol Chem, 2001. **276**(16): p. 12725-9.
148. Lee, W.J., et al., *Glucose transport by isolated plasma membranes of the bovine blood-brain barrier.* Am J Physiol, 1997. **272**(5 Pt 1): p. C1552-7.
149. Simpson, I.A., et al., *Blood-brain barrier glucose transporter: effects of hypo- and hyperglycemia revisited.* J Neurochem, 1999. **72**(1): p. 238-47.
150. Moos, T. and E.H. Morgan, *Transferrin and transferrin receptor function in brain barrier systems.* Cell Mol Neurobiol, 2000. **20**(1): p. 77-95.
151. Moos, T., et al., *Iron trafficking inside the brain.* J Neurochem, 2007. **103**(5): p. 1730-40.
152. Angelova-Gateva, P., *Iron transferrin receptors in rat and human cerebrum.* Agressologie, 1980. **21**(1): p. 27-30.
153. Jefferies, W.A., et al., *Transferrin receptor on endothelium of brain capillaries.* Nature, 1984. **312**(5990): p. 162-3.
154. Moos, T. and E.H. Morgan, *The significance of the mutated divalent metal transporter (DMT1) on iron transport into the Belgrade rat brain.* J Neurochem, 2004. **88**(1): p. 233-45.
155. Hawkins, R.A., et al., *Structure of the blood-brain barrier and its role in the transport of amino acids.* J Nutr, 2006. **136**(1 Suppl): p. 218S-26S.
156. Oldendorf, W.H. and J. Szabo, *Amino acid assignment to one of three blood-brain barrier amino acid carriers.* Am J Physiol, 1976. **230**(1): p. 94-8.
157. Sanchez del Pino, M.M., D.R. Peterson, and R.A. Hawkins, *Neutral amino acid transport characterization of isolated luminal and abluminal membranes of the blood-brain barrier.* J Biol Chem, 1995. **270**(25): p. 14913-8.
158. Mann, G.E., D.L. Yudilevich, and L. Sobrevia, *Regulation of amino acid and glucose transporters in endothelial and smooth muscle cells.* Physiol Rev, 2003. **83**(1): p. 183-252.
159. Smith, Q.R., *The blood-brain barrier and the regulation of amino acid uptake and availability to brain.* Adv Exp Med Biol, 1991. **291**: p. 55-71.
160. White, M.F., *The transport of cationic amino acids across the plasma membrane of mammalian cells.* Biochim Biophys Acta, 1985. **822**(3-4): p. 355-74.
161. Lee, W.J., et al., *Glutamine transport by the blood-brain barrier: a possible mechanism for nitrogen removal.* Am J Physiol, 1998. **274**(4 Pt 1): p. C1101-7.

162. Benrabh, H. and J.M. Lefauconnier, *Glutamate is transported across the rat blood-brain barrier by a sodium-independent system.* Neurosci Lett, 1996. **210**(1): p. 9-12.
163. Betz, A.L., *Sodium transport from blood to brain: inhibition by furosemide and amiloride.* J Neurochem, 1983. **41**(4): p. 1158-64.
164. Eisenberg, H.M. and R.L. Suddith, *Cerebral vessels have the capacity to transport sodium and potassium.* Science, 1979. **206**(4422): p. 1083-5.
165. Somjen, G.G., *Ion regulation in the brain: implications for pathophysiology.* Neuroscientist, 2002. **8**(3): p. 254-67.
166. Hsu, P., et al., *pHi in piglet cerebral microvascular endothelial cells: recovery from an acid load.* Proc Soc Exp Biol Med, 1996. **212**(3): p. 256-62.
167. O'Donnell, M.E., et al., *Bumetanide inhibition of the blood-brain barrier Na-K-Cl cotransporter reduces edema formation in the rat middle cerebral artery occlusion model of stroke.* J Cereb Blood Flow Metab, 2004. **24**(9): p. 1046-56.
168. Taylor, C.J., et al., *Transporters involved in regulation of intracellular pH in primary cultured rat brain endothelial cells.* J Physiol, 2006. **576**(Pt 3): p. 769-85.
169. Dean, M., Y. Hamon, and G. Chimini, *The human ATP-binding cassette (ABC) transporter superfamily.* J Lipid Res, 2001. **42**(7): p. 1007-17.
170. Higgins, C.F., *ABC transporters: from microorganisms to man.* Annu Rev Cell Biol, 1992. **8**: p. 67-113.
171. Loscher, W. and H. Potschka, *Drug resistance in brain diseases and the role of drug efflux transporters.* Nat Rev Neurosci, 2005. **6**(8): p. 591-602.
172. Loscher, W. and H. Potschka, *Role of drug efflux transporters in the brain for drug disposition and treatment of brain diseases.* Prog Neurobiol, 2005. **76**(1): p. 22-76.
173. Juliano, R.L. and V. Ling, *A surface glycoprotein modulating drug permeability in Chinese hamster ovary cell mutants.* Biochim Biophys Acta, 1976. **455**(1): p. 152-62.
174. Juranka, P.F., R.L. Zastawny, and V. Ling, *P-glycoprotein: multidrug-resistance and a superfamily of membrane-associated transport proteins.* Faseb J, 1989. **3**(14): p. 2583-92.
175. Ueda, K., et al., *The mdr1 gene, responsible for multidrug-resistance, codes for P-glycoprotein.* Biochem Biophys Res Commun, 1986. **141**(3): p. 956-62.
176. Zhou, S.F., *Structure, function and regulation of P-glycoprotein and its clinical relevance in drug disposition.* Xenobiotica, 2008. **38**(7): p. 802-32.
177. Callen, D.F., et al., *Localization of the human multiple drug resistance gene, MDR1, to 7q21.1.* Hum Genet, 1987. **77**(2): p. 142-4.
178. Chin, J.E., et al., *Structure and expression of the human MDR (P-glycoprotein) gene family.* Mol Cell Biol, 1989. **9**(9): p. 3808-20.
179. Gottesman, M.M. and I. Pastan, *Biochemistry of multidrug resistance mediated by the multidrug transporter.* Annu Rev Biochem, 1993. **62**: p. 385-427.
180. Childs, S., et al., *Identification of a sister gene to P-glycoprotein.* Cancer Res, 1995. **55**(10): p. 2029-34.
181. Gerloff, T., et al., *The sister of P-glycoprotein represents the canalicular bile salt export pump of mammalian liver.* J Biol Chem, 1998. **273**(16): p. 10046-50.
182. Ruetz, S. and P. Gros, *Phosphatidylcholine translocase: a physiological role for the mdr2 gene.* Cell, 1994. **77**(7): p. 1071-81.
183. van Helvoort, A., et al., *MDR1 P-glycoprotein is a lipid translocase of broad specificity, while MDR3 P-glycoprotein specifically translocates phosphatidylcholine.* Cell, 1996. **87**(3): p. 507-17.
184. Rao, U.S. and S.L. Nuti, *Identification of two different states of P-glycoprotein in its catalytic cycle: role of the linker region in the transition between these two states.* J Biol Chem, 2003. **278**(47): p. 46576-82.

185. Linton, K.J., *Structure and function of ABC transporters.* Physiology (Bethesda), 2007. **22**: p. 122-30.
186. Schinkel, A.H., *P-Glycoprotein, a gatekeeper in the blood-brain barrier.* Adv Drug Deliv Rev, 1999. **36**(2-3): p. 179-194.
187. Schinkel, A.H. and J.W. Jonker, *Mammalian drug efflux transporters of the ATP binding cassette (ABC) family: an overview.* Adv Drug Deliv Rev, 2003. **55**(1): p. 3-29.
188. Cabrera, M.A., et al., *A topological substructural approach for the prediction of P-glycoprotein substrates.* J Pharm Sci, 2006. **95**(3): p. 589-606.
189. Cianchetta, G., et al., *A pharmacophore hypothesis for P-glycoprotein substrate recognition using GRIND-based 3D-QSAR.* J Med Chem, 2005. **48**(8): p. 2927-35.
190. Crivori, P., et al., *Computational models for identifying potential P-glycoprotein substrates and inhibitors.* Mol Pharm, 2006. **3**(1): p. 33-44.
191. Huang, J., et al., *Identifying P-glycoprotein substrates using a support vector machine optimized by a particle swarm.* J Chem Inf Model, 2007. **47**(4): p. 1638-47.
192. Penzotti, J.E., et al., *A computational ensemble pharmacophore model for identifying substrates of P-glycoprotein.* J Med Chem, 2002. **45**(9): p. 1737-40.
193. Wang, R.B., et al., *Structure-activity relationship: analyses of p-glycoprotein substrates and inhibitors.* J Clin Pharm Ther, 2003. **28**(3): p. 203-28.
194. Pleban, K., et al., *P-glycoprotein substrate binding domains are located at the transmembrane domain/transmembrane domain interfaces: a combined photoaffinity labeling-protein homology modeling approach.* Mol Pharmacol, 2005. **67**(2): p. 365-74.
195. Romsicki, Y. and F.J. Sharom, *Phospholipid flippase activity of the reconstituted P-glycoprotein multidrug transporter.* Biochemistry, 2001. **40**(23): p. 6937-47.
196. Canaparo, R., et al., *Expression of CYP3A isoforms and P-glycoprotein in human stomach, jejunum and ileum.* Clin Exp Pharmacol Physiol, 2007. **34**(11): p. 1138-44.
197. Chiou, W.L., et al., *A comprehensive account on the role of efflux transporters in the gastrointestinal absorption of 13 commonly used substrate drugs in humans.* Int J Clin Pharmacol Ther, 2001. **39**(3): p. 93-101.
198. Lee, Y.J., S.J. Chung, and C.K. Shim, *Limited role of P-glycoprotein in the intestinal absorption of cyclosporin A.* Biol Pharm Bull, 2005. **28**(4): p. 760-3.
199. Lin, J.H., *How significant is the role of P-glycoprotein in drug absorption and brain uptake?* Drugs Today (Barc), 2004. **40**(1): p. 5-22.
200. Sakaeda, T., et al., *Molecular and pharmacokinetic properties of 222 commercially available oral drugs in humans.* Biol Pharm Bull, 2001. **24**(8): p. 935-40.
201. Ogihara, T., et al., *What kinds of substrates show P-glycoprotein-dependent intestinal absorption? Comparison of verapamil with vinblastine.* Drug Metab Pharmacokinet, 2006. **21**(3): p. 238-44.
202. Westphal, K., et al., *Oral bioavailability of digoxin is enhanced by talinolol: evidence for involvement of intestinal P-glycoprotein.* Clin Pharmacol Ther, 2000. **68**(1): p. 6-12.
203. Meerum Terwogt, J.M., et al., *Co-administration of cyclosporin enables oral therapy with paclitaxel.* Lancet, 1998. **352**(9124): p. 285.
204. Choudhuri, S. and C.D. Klaassen, *Structure, function, expression, genomic organization, and single nucleotide polymorphisms of human ABCB1 (MDR1), ABCC (MRP), and ABCG2 (BCRP) efflux transporters.* Int J Toxicol, 2006. **25**(4): p. 231-59.
205. Lecureur, V., et al., *Expression and regulation of hepatic drug and bile acid transporters.* Toxicology, 2000. **153**(1-3): p. 203-19.

206. Ceckova-Novotna, M., P. Pavek, and F. Staud, *P-glycoprotein in the placenta: expression, localization, regulation and function.* Reprod Toxicol, 2006. **22**(3): p. 400-10.
207. Stewart, P.A., R. Beliveau, and K.A. Rogers, *Cellular localization of P-glycoprotein in brain versus gonadal capillaries.* J Histochem Cytochem, 1996. **44**(7): p. 679-85.
208. Golden, P.L. and W.M. Pardridge, *P-Glycoprotein on astrocyte foot processes of unfixed isolated human brain capillaries.* Brain Res, 1999. **819**(1-2): p. 143-6.
209. Pardridge, W.M., et al., *Brain microvascular and astrocyte localization of P-glycoprotein.* J Neurochem, 1997. **68**(3): p. 1278-85.
210. Beaulieu, E., et al., *P-glycoprotein is strongly expressed in the luminal membranes of the endothelium of blood vessels in the brain.* Biochem J, 1997. **326 (Pt 2)**: p. 539-44.
211. Tatsuta, T., et al., *Functional involvement of P-glycoprotein in blood-brain barrier.* J Biol Chem, 1992. **267**(28): p. 20383-91.
212. Seetharaman, S., et al., *Multidrug resistance-related transport proteins in isolated human brain microvessels and in cells cultured from these isolates.* J Neurochem, 1998. **70**(3): p. 1151-9.
213. Bendayan, R., et al., *In situ localization of P-glycoprotein (ABCB1) in human and rat brain.* J Histochem Cytochem, 2006. **54**(10): p. 1159-67.
214. Schinkel, A.H., et al., *Disruption of the mouse mdr1a P-glycoprotein gene leads to a deficiency in the blood-brain barrier and to increased sensitivity to drugs.* Cell, 1994. **77**(4): p. 491-502.
215. Schinkel, A.H., et al., *Absence of the mdr1a P-Glycoprotein in mice affects tissue distribution and pharmacokinetics of dexamethasone, digoxin, and cyclosporin A.* J Clin Invest, 1995. **96**(4): p. 1698-705.
216. Miller, D.S., B. Bauer, and A.M. Hartz, *Modulation of p-glycoprotein at the blood-brain barrier: opportunities to improve central nervous system pharmacotherapy.* Pharmacol Rev, 2008. **60**(2): p. 196-209.
217. Drion, N., et al., *Role of P-glycoprotein in the blood-brain transport of colchicine and vinblastine.* J Neurochem, 1996. **67**(4): p. 1688-93.
218. Kemper, E.M., et al., *Increased penetration of paclitaxel into the brain by inhibition of P-Glycoprotein.* Clin Cancer Res, 2003. **9**(7): p. 2849-55.
219. Chen, Y.N., et al., *Characterization of adriamycin-resistant human breast cancer cells which display overexpression of a novel resistance-related membrane protein.* J Biol Chem, 1990. **265**(17): p. 10073-80.
220. Doyle, L.A., et al., *A multidrug resistance transporter from human MCF-7 breast cancer cells.* Proc Natl Acad Sci U S A, 1998. **95**(26): p. 15665-70.
221. Doyle, L.A. and D.D. Ross, *Multidrug resistance mediated by the breast cancer resistance protein BCRP (ABCG2).* Oncogene, 2003. **22**(47): p. 7340-58.
222. Miyake, K., et al., *Molecular cloning of cDNAs which are highly overexpressed in mitoxantrone-resistant cells: demonstration of homology to ABC transport genes.* Cancer Res, 1999. **59**(1): p. 8-13.
223. Allikmets, R. and M. Dean, *Cloning of novel ABC transporter genes.* Methods Enzymol, 1998. **292**: p. 116-30.
224. Koshiba, S., et al., *Human ABC transporters ABCG2 (BCRP) and ABCG4.* Xenobiotica, 2008. **38**(7): p. 863-88.
225. Krishnamurthy, P. and J.D. Schuetz, *Role of ABCG2/BCRP in biology and medicine.* Annu Rev Pharmacol Toxicol, 2006. **46**: p. 381-410.
226. Mitomo, H., et al., *A functional study on polymorphism of the ATP-binding cassette transporter ABCG2: critical role of arginine-482 in methotrexate transport.* Biochem J, 2003. **373**(Pt 3): p. 767-74.

227. Eisenblatter, T., S. Huwel, and H.J. Galla, *Characterisation of the brain multidrug resistance protein (BMDP/ABCG2/BCRP) expressed at the blood-brain barrier.* Brain Res, 2003. **971**(2): p. 221-31.
228. Cisternino, S., et al., *Expression, up-regulation, and transport activity of the multidrug-resistance protein Abcg2 at the mouse blood-brain barrier.* Cancer Res, 2004. **64**(9): p. 3296-301.
229. Cooray, H.C., et al., *Localisation of breast cancer resistance protein in microvessel endothelium of human brain.* Neuroreport, 2002. **13**(16): p. 2059-63.
230. Sarkadi, B., et al., *ABCG2 -- a transporter for all seasons.* FEBS Lett, 2004. **567**(1): p. 116-20.
231. Youdim, K.A., et al., *Flavonoid permeability across an in situ model of the blood-brain barrier.* Free Radic Biol Med, 2004. **36**(5): p. 592-604.
232. Muller, H., et al., *New functional assay of P-glycoprotein activity using Hoechst 33342.* Bioorg Med Chem, 2007. **15**(23): p. 7470-9.
233. Scharenberg, C.W., M.A. Harkey, and B. Torok-Storb, *The ABCG2 transporter is an efficient Hoechst 33342 efflux pump and is preferentially expressed by immature human hematopoietic progenitors.* Blood, 2002. **99**(2): p. 507-12.
234. Ejendal, K.F. and C.A. Hrycyna, *Differential sensitivities of the human ATP-binding cassette transporters ABCG2 and P-glycoprotein to cyclosporin A.* Mol Pharmacol, 2005. **67**(3): p. 902-11.
235. El-Masry, E.M. and M.B. Abou-Donia, *Interaction of pyridostigmine bromide and N,N-diethyl-m-toluamide alone and in combination with P-glycoprotein expressed in Escherichia coli leaky mutant.* J Toxicol Environ Health A, 2006. **69**(10): p. 919-33.
236. Krishnamurthy, P., et al., *The stem cell marker Bcrp/ABCG2 enhances hypoxic cell survival through interactions with heme.* J Biol Chem, 2004. **279**(23): p. 24218-25.
237. Hubensack, M., et al., *Effect of the ABCB1 modulators elacridar and tariquidar on the distribution of paclitaxel in nude mice.* J Cancer Res Clin Oncol, 2008. **134**(5): p. 597-607.
238. Pan, G., N. Giri, and W.F. Elmquist, *Abcg2/Bcrp1 mediates the polarized transport of antiretroviral nucleosides abacavir and zidovudine.* Drug Metab Dispos, 2007. **35**(7): p. 1165-73.
239. Bauer, B., et al., *Pregnane X receptor up-regulation of P-glycoprotein expression and transport function at the blood-brain barrier.* Mol Pharmacol, 2004. **66**(3): p. 413-9.
240. Bauer, B., et al., *In vivo activation of human pregnane X receptor tightens the blood-brain barrier to methadone through P-glycoprotein up-regulation.* Mol Pharmacol, 2006. **70**(4): p. 1212-9.
241. Goralski, K.B., et al., *Downregulation of mdr1a expression in the brain and liver during CNS inflammation alters the in vivo disposition of digoxin.* Br J Pharmacol, 2003. **139**(1): p. 35-48.
242. Seelbach, M.J., et al., *Peripheral inflammatory hyperalgesia modulates morphine delivery to the brain: a role for P-glycoprotein.* J Neurochem, 2007. **102**(5): p. 1677-90.
243. Bauer, B., A.M. Hartz, and D.S. Miller, *Tumor necrosis factor alpha and endothelin-1 increase P-glycoprotein expression and transport activity at the blood-brain barrier.* Mol Pharmacol, 2007. **71**(3): p. 667-75.
244. Regina, A., et al., *Dexamethasone regulation of P-glycoprotein activity in an immortalized rat brain endothelial cell line, GPNT.* J Neurochem, 1999. **73**(5): p. 1954-63.
245. Mandi, Y., et al., *Nitric oxide production and MDR expression by human brain endothelial cells.* Anticancer Res, 1998. **18**(4C): p. 3049-52.

246. Theron, D., et al., *Influence of tumor necrosis factor-alpha on the expression and function of P-glycoprotein in an immortalised rat brain capillary endothelial cell line, GPNT.* Biochem Pharmacol, 2003. **66**(4): p. 579-87.
247. Yang, H.W., et al., *Increased P-glycoprotein function and level after long-term exposure of four antiepileptic drugs to rat brain microvascular endothelial cells in vitro.* Neurosci Lett, 2008. **434**(3): p. 299-303.
248. Volk, H., H. Potschka, and W. Loscher, *Immunohistochemical localization of P-glycoprotein in rat brain and detection of its increased expression by seizures are sensitive to fixation and staining variables.* J Histochem Cytochem, 2005. **53**(4): p. 517-31.
249. Zhu, H.J. and G.Q. Liu, *Glutamate up-regulates P-glycoprotein expression in rat brain microvessel endothelial cells by an NMDA receptor-mediated mechanism.* Life Sci, 2004. **75**(11): p. 1313-22.
250. Felix, R.A. and M.A. Barrand, *P-glycoprotein expression in rat brain endothelial cells: evidence for regulation by transient oxidative stress.* J Neurochem, 2002. **80**(1): p. 64-72.
251. Xiao-Dong, L., Y. Zhi-Hong, and Y. Hui-Wen, *Repetitive/temporal hypoxia increased P-glycoprotein expression in cultured rat brain microvascular endothelial cells in vitro.* Neurosci Lett, 2008. **432**(3): p. 184-7.
252. Hayashi, K., et al., *HIV-Tat protein induces P-glycoprotein expression in brain microvascular endothelial cells.* J Neurochem, 2005. **93**(5): p. 1231-41.
253. Dohgu, S., et al., *Transforming growth factor-beta1 upregulates the tight junction and P-glycoprotein of brain microvascular endothelial cells.* Cell Mol Neurobiol, 2004. **24**(3): p. 491-7.
254. Hong, H., et al., *Up-regulation of P-glycoprotein expression by glutathione depletion-induced oxidative stress in rat brain microvessel endothelial cells.* J Neurochem, 2006. **98**(5): p. 1465-73.
255. http://www.mssociety.org.uk/about_ms/index.html.
256. Lassmann, H., *Mechanisms of inflammation induced tissue injury in multiple sclerosis.* J Neurol Sci, 2008.
257. Lassmann, H., W. Bruck, and C. Lucchinetti, *Heterogeneity of multiple sclerosis pathogenesis: implications for diagnosis and therapy.* Trends Mol Med, 2001. **7**(3): p. 115-21.
258. Werring, D.J., et al., *The pathogenesis of lesions and normal-appearing white matter changes in multiple sclerosis: a serial diffusion MRI study.* Brain, 2000. **123 (Pt 8)**: p. 1667-76.
259. Wuerfel, J., et al., *Changes in cerebral perfusion precede plaque formation in multiple sclerosis: a longitudinal perfusion MRI study.* Brain, 2004. **127**(Pt 1): p. 111-9.
260. Kirk, J., et al., *Tight junctional abnormality in multiple sclerosis white matter affects all calibres of vessel and is associated with blood-brain barrier leakage and active demyelination.* J Pathol, 2003. **201**(2): p. 319-27.
261. Leech, S., et al., *Persistent endothelial abnormalities and blood-brain barrier leak in primary and secondary progressive multiple sclerosis.* Neuropathol Appl Neurobiol, 2007. **33**(1): p. 86-98.
262. Plumb, J., et al., *Abnormal endothelial tight junctions in active lesions and normal-appearing white matter in multiple sclerosis.* Brain Pathol, 2002. **12**(2): p. 154-69.
263. Forster, C., *Tight junctions and the modulation of barrier function in disease.* Histochem Cell Biol, 2008. **130**(1): p. 55-70.
264. Minagar, A. and J.S. Alexander, *Blood-brain barrier disruption in multiple sclerosis.* Mult Scler, 2003. **9**(6): p. 540-9.

265. Abe, T., et al., *Interleukin-1beta and barrier function of retinal pigment epithelial cells (ARPE-19): aberrant expression of junctional complex molecules.* Invest Ophthalmol Vis Sci, 2003. **44**(9): p. 4097-104.
266. Afonso, P.V., et al., *Human blood-brain barrier disruption by retroviral-infected lymphocytes: role of myosin light chain kinase in endothelial tight-junction disorganization.* J Immunol, 2007. **179**(4): p. 2576-83.
267. Al-Sadi, R., et al., *Mechanism of IL-1beta-induced increase in intestinal epithelial tight junction permeability.* J Immunol, 2008. **180**(8): p. 5653-61.
268. Al-Sadi, R.M. and T.Y. Ma, *IL-1beta causes an increase in intestinal epithelial tight junction permeability.* J Immunol, 2007. **178**(7): p. 4641-9.
269. Luna, J.D., et al., *Blood-retinal barrier (BRB) breakdown in experimental autoimmune uveoretinitis: comparison with vascular endothelial growth factor, tumor necrosis factor alpha, and interleukin-1beta-mediated breakdown.* J Neurosci Res, 1997. **49**(3): p. 268-80.
270. Marcus, B.C., et al., *Cytokine-induced increases in endothelial permeability occur after adhesion molecule expression.* Surgery, 1996. **120**(2): p. 411-6; discussion 416-7.
271. del Zoppo, G.J. and T. Mabuchi, *Cerebral microvessel responses to focal ischemia.* J Cereb Blood Flow Metab, 2003. **23**(8): p. 879-94.
272. Witt, K.A., et al., *Effects of hypoxia-reoxygenation on rat blood-brain barrier permeability and tight junctional protein expression.* Am J Physiol Heart Circ Physiol, 2003. **285**(6): p. H2820-31.
273. Fischer, S., et al., *Hypoxia-induced hyperpermeability in brain microvessel endothelial cells involves VEGF-mediated changes in the expression of zonula occludens-1.* Microvasc Res, 2002. **63**(1): p. 70-80.
274. Wang, W., W.L. Dentler, and R.T. Borchardt, *VEGF increases BMEC monolayer permeability by affecting occludin expression and tight junction assembly.* Am J Physiol Heart Circ Physiol, 2001. **280**(1): p. H434-40.
275. van Bruggen, N., et al., *VEGF antagonism reduces edema formation and tissue damage after ischemia/reperfusion injury in the mouse brain.* J Clin Invest, 1999. **104**(11): p. 1613-20.
276. Mark, K.S., et al., *Nitric oxide mediates hypoxia-induced changes in paracellular permeability of cerebral microvasculature.* Am J Physiol Heart Circ Physiol, 2004. **286**(1): p. H174-80.
277. *American Psychiatric Association. Diagnostic and Statistical Manual of Mental Disorders* 2000: p. Fourth Edition.
278. Wimo, A., L. Jonsson, and B. Winblad, *An estimate of the worldwide prevalence and direct costs of dementia in 2003.* Dement Geriatr Cogn Disord, 2006. **21**(3): p. 175-81.
279. Ferri, C.P., et al., *Global prevalence of dementia: a Delphi consensus study.* Lancet, 2005. **366**(9503): p. 2112-7.
280. Lobo, A., et al., *Prevalence of dementia and major subtypes in Europe: A collaborative study of population-based cohorts. Neurologic Diseases in the Elderly Research Group.* Neurology, 2000. **54**(11 Suppl 5): p. S4-9.
281. van der Flier, W.M. and P. Scheltens, *Epidemiology and risk factors of dementia.* J Neurol Neurosurg Psychiatry, 2005. **76 Suppl 5**: p. v2-7.
282. Brunnstrom, H., et al., *Prevalence of dementia subtypes: A 30-year retrospective survey of neuropathological reports.* Arch Gerontol Geriatr, 2008.
283. http://www.alzheimers.org.uk/site/scripts/documents_info.php?categoryID=200120&documentID=341.
284. Selkoe, D.J., *Alzheimer's disease: genes, proteins, and therapy.* Physiol Rev, 2001. **81**(2): p. 741-66.

285. Selkoe, D.J. and M.B. Podlisny, *Deciphering the genetic basis of Alzheimer's disease.* Annu Rev Genomics Hum Genet, 2002. **3**: p. 67-99.
286. Alzheimer, A., et al., *An English translation of Alzheimer's 1907 paper, "Uber eine eigenartige Erkankung der Hirnrinde".* Clin Anat, 1995. **8**(6): p. 429-31.
287. Graeber, M.B. and P. Mehraein, *Reanalysis of the first case of Alzheimer's disease.* Eur Arch Psychiatry Clin Neurosci, 1999. **249 Suppl 3**: p. 10-3.
288. Jellinger, K.A., *Alzheimer 100--highlights in the history of Alzheimer research.* J Neural Transm, 2006. **113**(11): p. 1603-23.
289. Moller, H.J. and M.B. Graeber, *The case described by Alois Alzheimer in 1911. Historical and conceptual perspectives based on the clinical record and neurohistological sections.* Eur Arch Psychiatry Clin Neurosci, 1998. **248**(3): p. 111-22.
290. http://www.alz.org/national/documents/topicsheet_stages.pdf.
291. Glenner, G.G. and C.W. Wong, *Alzheimer's disease: initial report of the purification and characterization of a novel cerebrovascular amyloid protein.* Biochem Biophys Res Commun, 1984. **120**(3): p. 885-90.
292. Kang, J., et al., *The precursor of Alzheimer's disease amyloid A4 protein resembles a cell-surface receptor.* Nature, 1987. **325**(6106): p. 733-6.
293. Masters, C.L., et al., *Neuronal origin of a cerebral amyloid: neurofibrillary tangles of Alzheimer's disease contain the same protein as the amyloid of plaque cores and blood vessels.* Embo J, 1985. **4**(11): p. 2757-63.
294. Masters, C.L., et al., *Amyloid plaque core protein in Alzheimer disease and Down syndrome.* Proc Natl Acad Sci U S A, 1985. **82**(12): p. 4245-9.
295. Iqbal, K. and M. Novak, *From tangles to tau protein.* Bratisl Lek Listy, 2006. **107**(9-10): p. 341-2.
296. Iqbal, K., et al., *Defective brain microtubule assembly in Alzheimer's disease.* Lancet, 1986. **2**(8504): p. 421-6.
297. Braak, H. and E. Braak, *Neuropathological stageing of Alzheimer-related changes.* Acta Neuropathol, 1991. **82**(4): p. 239-59.
298. Thal, D.R., et al., *The development of amyloid beta protein deposits in the aged brain.* Sci Aging Knowledge Environ, 2006. **2006**(6): p. re1.
299. Thal, D.R., et al., *Phases of A beta-deposition in the human brain and its relevance for the development of AD.* Neurology, 2002. **58**(12): p. 1791-800.
300. Thal, D.R., et al., *Sequence of Abeta-protein deposition in the human medial temporal lobe.* J Neuropathol Exp Neurol, 2000. **59**(8): p. 733-48.
301. Oddo, S. and F.M. LaFerla, *The role of nicotinic acetylcholine receptors in Alzheimer's disease.* J Physiol Paris, 2006. **99**(2-3): p. 172-9.
302. Hardy, J., *Alzheimer's disease: the amyloid cascade hypothesis: an update and reappraisal.* J Alzheimers Dis, 2006. **9**(3 Suppl): p. 151-3.
303. Hardy, J.A. and G.A. Higgins, *Alzheimer's disease: the amyloid cascade hypothesis.* Science, 1992. **256**(5054): p. 184-5.
304. Blennow, K., M.J. de Leon, and H. Zetterberg, *Alzheimer's disease.* Lancet, 2006. **368**(9533): p. 387-403.
305. Small, S.A. and S. Gandy, *Sorting through the cell biology of Alzheimer's disease: intracellular pathways to pathogenesis.* Neuron, 2006. **52**(1): p. 15-31.
306. Thinakaran, G. and E.H. Koo, *APP trafficking, processing and function.* J Biol Chem, 2008.
307. Zheng, H. and E.H. Koo, *The amyloid precursor protein: beyond amyloid.* Mol Neurodegener, 2006. **1**: p. 5.
308. Cirrito, J.R., et al., *Synaptic activity regulates interstitial fluid amyloid-beta levels in vivo.* Neuron, 2005. **48**(6): p. 913-22.
309. http://www.ncbi.nlm.nih.gov/entrez/viewer.fcgi?db=protein&val=41406057.

310. Radde, R., et al., *The value of incomplete mouse models of Alzheimer's disease.* Eur J Nucl Med Mol Imaging, 2008. **35 Suppl 1**: p. S70-4.
311. Bates, K.A., et al., *Clearance mechanisms of Alzheimer's amyloid-beta peptide: implications for therapeutic design and diagnostic tests.* Mol Psychiatry, 2008.
312. Jellinger, K.A., et al., *Biomarkers for early diagnosis of Alzheimer disease: 'ALZheimer ASsociated gene'- a new blood biomarker?* J Cell Mol Med, 2008. **12**(4): p. 1094-117.
313. Lichtlen, P. and M.H. Mohajeri, *Antibody-based approaches in Alzheimer's research: safety, pharmacokinetics, metabolism, and analytical tools.* J Neurochem, 2008. **104**(4): p. 859-74.
314. Bishop, G.M. and S.R. Robinson, *The amyloid hypothesis: let sleeping dogmas lie?* Neurobiol Aging, 2002. **23**(6): p. 1101-5.
315. Davis, D.G., et al., *Alzheimer neuropathologic alterations in aged cognitively normal subjects.* J Neuropathol Exp Neurol, 1999. **58**(4): p. 376-88.
316. Gong, Y., et al., *Alzheimer's disease-affected brain: presence of oligomeric A beta ligands (ADDLs) suggests a molecular basis for reversible memory loss.* Proc Natl Acad Sci U S A, 2003. **100**(18): p. 10417-22.
317. Nordberg, A., *Amyloid plaque imaging in vivo: current achievement and future prospects.* Eur J Nucl Med Mol Imaging, 2008. **35 Suppl 1**: p. S46-50.
318. Klunk, W.E., et al., *Imaging brain amyloid in Alzheimer's disease with Pittsburgh Compound-B.* Ann Neurol, 2004. **55**(3): p. 306-19.
319. Sagare, A., et al., *Clearance of amyloid-beta by circulating lipoprotein receptors.* Nat Med, 2007. **13**(9): p. 1029-31.
320. Kuo, Y.M., et al., *Amyloid-beta peptides interact with plasma proteins and erythrocytes: implications for their quantitation in plasma.* Biochem Biophys Res Commun, 2000. **268**(3): p. 750-6.
321. van Oijen, M., et al., *Plasma Abeta(1-40) and Abeta(1-42) and the risk of dementia: a prospective case-cohort study.* Lancet Neurol, 2006. **5**(8): p. 655-60.
322. Formichi, P., et al., *Cerebrospinal fluid tau, A beta, and phosphorylated tau protein for the diagnosis of Alzheimer's disease.* J Cell Physiol, 2006. **208**(1): p. 39-46.
323. Strozyk, D., et al., *CSF Abeta 42 levels correlate with amyloid-neuropathology in a population-based autopsy study.* Neurology, 2003. **60**(4): p. 652-6.
324. Fagan, A.M., et al., *Inverse relation between in vivo amyloid imaging load and cerebrospinal fluid Abeta42 in humans.* Ann Neurol, 2006. **59**(3): p. 512-9.
325. Teller, J.K., et al., *Presence of soluble amyloid beta-peptide precedes amyloid plaque formation in Down's syndrome.* Nat Med, 1996. **2**(1): p. 93-5.
326. Tokuda, T., et al., *Plasma levels of amyloid beta proteins Abeta1-40 and Abeta1-42(43) are elevated in Down's syndrome.* Ann Neurol, 1997. **41**(2): p. 271-3.
327. Mann, D.M., P.O. Yates, and B. Marcyniuk, *Alzheimer's presenile dementia, senile dementia of Alzheimer type and Down's syndrome in middle age form an age related continuum of pathological changes.* Neuropathol Appl Neurobiol, 1984. **10**(3): p. 185-207.
328. Motte, J. and R.S. Williams, *Age-related changes in the density and morphology of plaques and neurofibrillary tangles in Down syndrome brain.* Acta Neuropathol, 1989. **77**(5): p. 535-46.
329. Olson, M.I. and C.M. Shaw, *Presenile dementia and Alzheimer's disease in mongolism.* Brain, 1969. **92**(1): p. 147-56.
330. Prasher, V.P., et al., *Molecular mapping of Alzheimer-type dementia in Down's syndrome.* Ann Neurol, 1998. **43**(3): p. 380-3.
331. Duyckaerts, C., M.C. Potier, and B. Delatour, *Alzheimer disease models and human neuropathology: similarities and differences.* Acta Neuropathol, 2008. **115**(1): p. 5-38.

332. Gotz, J. and L.M. Ittner, *Animal models of Alzheimer's disease and frontotemporal dementia.* Nat Rev Neurosci, 2008. **9**(7): p. 532-44.
333. Scheuner, D., et al., *Secreted amyloid beta-protein similar to that in the senile plaques of Alzheimer's disease is increased in vivo by the presenilin 1 and 2 and APP mutations linked to familial Alzheimer's disease.* Nat Med, 1996. **2**(8): p. 864-70.
334. Farrer, L.A., et al., *Effects of age, sex, and ethnicity on the association between apolipoprotein E genotype and Alzheimer disease. A meta-analysis. APOE and Alzheimer Disease Meta Analysis Consortium.* Jama, 1997. **278**(16): p. 1349-56.
335. Lavretsky, H., et al., *Apolipoprotein epsilon4 allele status, depressive symptoms, and cognitive decline in middle-aged and elderly persons without dementia.* Am J Geriatr Psychiatry, 2003. **11**(6): p. 667-73.
336. Gearing, M., H. Mori, and S.S. Mirra, *Abeta-peptide length and apolipoprotein E genotype in Alzheimer's disease.* Ann Neurol, 1996. **39**(3): p. 395-9.
337. Rebeck, G.W., et al., *Apolipoprotein E in sporadic Alzheimer's disease: allelic variation and receptor interactions.* Neuron, 1993. **11**(4): p. 575-80.
338. Baum, L., et al., *Apolipoprotein E isoforms in Alzheimer's disease pathology and etiology.* Microsc Res Tech, 2000. **50**(4): p. 278-81.
339. Bales, K.R., et al., *Lack of apolipoprotein E dramatically reduces amyloid beta-peptide deposition.* Nat Genet, 1997. **17**(3): p. 263-4.
340. Martel, C.L., et al., *Isoform-specific effects of apolipoproteins E2, E3, and E4 on cerebral capillary sequestration and blood-brain barrier transport of circulating Alzheimer's amyloid beta.* J Neurochem, 1997. **69**(5): p. 1995-2004.
341. Alvarez, A.R., et al., *Wnt-3a overcomes beta-amyloid toxicity in rat hippocampal neurons.* Exp Cell Res, 2004. **297**(1): p. 186-96.
342. Busciglio, J., A. Lorenzo, and B.A. Yankner, *Methodological variables in the assessment of beta amyloid neurotoxicity.* Neurobiol Aging, 1992. **13**(5): p. 609-12.
343. Garrido, J.L., et al., *Protein kinase C inhibits amyloid beta peptide neurotoxicity by acting on members of the Wnt pathway.* Faseb J, 2002. **16**(14): p. 1982-4.
344. Kaltschmidt, B., et al., *Inhibition of NF-kappaB potentiates amyloid beta-mediated neuronal apoptosis.* Proc Natl Acad Sci U S A, 1999. **96**(16): p. 9409-14.
345. Koh, S.H., M.Y. Noh, and S.H. Kim, *Amyloid-beta-induced neurotoxicity is reduced by inhibition of glycogen synthase kinase-3.* Brain Res, 2008. **1188**: p. 254-62.
346. Lambert, M.P., et al., *Diffusible, nonfibrillar ligands derived from Abeta1-42 are potent central nervous system neurotoxins.* Proc Natl Acad Sci U S A, 1998. **95**(11): p. 6448-53.
347. Lee, K.Y., et al., *Phosphatidylinositol-3-kinase activation blocks amyloid beta-induced neurotoxicity.* Toxicology, 2008. **243**(1-2): p. 43-50.
348. Nassif, M., et al., *Beta-amyloid peptide toxicity in organotypic hippocampal slice culture involves Akt/PKB, GSK-3beta, and PTEN.* Neurochem Int, 2007. **50**(1): p. 229-35.
349. Pike, C.J., et al., *Neurodegeneration induced by beta-amyloid peptides in vitro: the role of peptide assembly state.* J Neurosci, 1993. **13**(4): p. 1676-87.
350. Pike, C.J., et al., *In vitro aging of beta-amyloid protein causes peptide aggregation and neurotoxicity.* Brain Res, 1991. **563**(1-2): p. 311-4.
351. Valerio, A., et al., *NF-kappaB pathway: a target for preventing beta-amyloid (Abeta)-induced neuronal damage and Abeta42 production.* Eur J Neurosci, 2006. **23**(7): p. 1711-20.
352. Vitolo, O.V., et al., *Amyloid beta -peptide inhibition of the PKA/CREB pathway and long-term potentiation: reversibility by drugs that enhance cAMP signaling.* Proc Natl Acad Sci U S A, 2002. **99**(20): p. 13217-21.

353. Wei, W., X. Wang, and J.W. Kusiak, *Signaling events in amyloid beta-peptide-induced neuronal death and insulin-like growth factor I protection.* J Biol Chem, 2002. **277**(20): p. 17649-56.
354. Hu, N.W., et al., *Soluble amyloid-{beta} peptides potently disrupt hippocampal synaptic plasticity in the absence of cerebrovascular dysfunction in vivo.* Brain, 2008.
355. Irvine, G.B., et al., *Protein aggregation in the brain: the molecular basis for Alzheimer's and Parkinson's diseases.* Mol Med, 2008. **14**(7-8): p. 451-64.
356. Klein, W.L., *Abeta toxicity in Alzheimer's disease: globular oligomers (ADDLs) as new vaccine and drug targets.* Neurochem Int, 2002. **41**(5): p. 345-52.
357. Klein, W.L., W.B. Stine, Jr., and D.B. Teplow, *Small assemblies of unmodified amyloid beta-protein are the proximate neurotoxin in Alzheimer's disease.* Neurobiol Aging, 2004. **25**(5): p. 569-80.
358. Viola, K.L., P.T. Velasco, and W.L. Klein, *Why Alzheimer's is a disease of memory: the attack on synapses by A beta oligomers (ADDLs).* J Nutr Health Aging, 2008. **12**(1): p. 51S-7S.
359. Walsh, D.M. and D.J. Selkoe, *A beta oligomers - a decade of discovery.* J Neurochem, 2007. **101**(5): p. 1172-84.
360. Oda, T., et al., *Clusterin (apoJ) alters the aggregation of amyloid beta-peptide (A beta 1-42) and forms slowly sedimenting A beta complexes that cause oxidative stress.* Exp Neurol, 1995. **136**(1): p. 22-31.
361. Stine, W.B., Jr., et al., *The nanometer-scale structure of amyloid-beta visualized by atomic force microscopy.* J Protein Chem, 1996. **15**(2): p. 193-203.
362. Klein, W.L., G.A. Krafft, and C.E. Finch, *Targeting small Abeta oligomers: the solution to an Alzheimer's disease conundrum?* Trends Neurosci, 2001. **24**(4): p. 219-24.
363. De Felice, F.G., et al., *Alzheimer's disease-type neuronal tau hyperphosphorylation induced by A beta oligomers.* Neurobiol Aging, 2008. **29**(9): p. 1334-47.
364. LaFerla, F.M. and S. Oddo, *Alzheimer's disease: Abeta, tau and synaptic dysfunction.* Trends Mol Med, 2005. **11**(4): p. 170-6.
365. Marcello, E., R. Epis, and M. Di Luca, *Amyloid flirting with synaptic failure: towards a comprehensive view of Alzheimer's disease pathogenesis.* Eur J Pharmacol, 2008. **585**(1): p. 109-18.
366. Selkoe, D.J., *Alzheimer's disease is a synaptic failure.* Science, 2002. **298**(5594): p. 789-91.
367. Small, D.H., *Network dysfunction in Alzheimer's disease: does synaptic scaling drive disease progression?* Trends Mol Med, 2008. **14**(3): p. 103-8.
368. Venkitaramani, D.V., et al., *Beta-amyloid modulation of synaptic transmission and plasticity.* J Neurosci, 2007. **27**(44): p. 11832-7.
369. Klyubin, I., et al., *Amyloid beta protein dimer-containing human CSF disrupts synaptic plasticity: prevention by systemic passive immunization.* J Neurosci, 2008. **28**(16): p. 4231-7.
370. Gotz, J., et al., *Formation of neurofibrillary tangles in P301l tau transgenic mice induced by Abeta 42 fibrils.* Science, 2001. **293**(5534): p. 1491-5.
371. Lewis, J., et al., *Enhanced neurofibrillary degeneration in transgenic mice expressing mutant tau and APP.* Science, 2001. **293**(5534): p. 1487-91.
372. Avila, J., *Tau phosphorylation and aggregation in Alzheimer's disease pathology.* FEBS Lett, 2006. **580**(12): p. 2922-7.
373. Higuchi, Y., et al., *Ultrastructural changes of blood vessels in the cerebral cortex in Alzheimer's disease.* Jpn J Psychiatry Neurol, 1987. **41**(2): p. 283-90.
374. Bamberger, M.E. and G.E. Landreth, *Microglial interaction with beta-amyloid: implications for the pathogenesis of Alzheimer's disease.* Microsc Res Tech, 2001. **54**(2): p. 59-70.

375. Miyakawa, T., et al., *Morphological changes of microvessels in the brain with Alzheimer's disease.* Jpn J Psychiatry Neurol, 1988. **42**(4): p. 819-24.
376. Stewart, P.A., et al., *A morphometric study of the blood-brain barrier in Alzheimer's disease.* Lab Invest, 1992. **67**(6): p. 734-42.
377. Rojo, L.E., et al., *Neuroinflammation: implications for the pathogenesis and molecular diagnosis of Alzheimer's disease.* Arch Med Res, 2008. **39**(1): p. 1-16.
378. Munoz, L., et al., *A novel p38 alpha MAPK inhibitor suppresses brain proinflammatory cytokine up-regulation and attenuates synaptic dysfunction and behavioral deficits in an Alzheimer's disease mouse model.* J Neuroinflammation, 2007. **4**: p. 21.
379. LeBlanc, A.C., et al., *Processing of amyloid precursor protein in human primary neuron and astrocyte cultures.* J Neurochem, 1997. **68**(3): p. 1183-90.
380. Citron, M., et al., *Mutation of the beta-amyloid precursor protein in familial Alzheimer's disease increases beta-protein production.* Nature, 1992. **360**(6405): p. 672-4.
381. Citron, M., et al., *Mutant presenilins of Alzheimer's disease increase production of 42-residue amyloid beta-protein in both transfected cells and transgenic mice.* Nat Med, 1997. **3**(1): p. 67-72.
382. Weller, R.O., et al., *Perivascular drainage of amyloid-beta peptides from the brain and its failure in cerebral amyloid angiopathy and Alzheimer's disease.* Brain Pathol, 2008. **18**(2): p. 253-66.
383. Deane, R., Z. Wu, and B.V. Zlokovic, *RAGE (yin) versus LRP (yang) balance regulates alzheimer amyloid beta-peptide clearance through transport across the blood-brain barrier.* Stroke, 2004. **35**(11 Suppl 1): p. 2628-31.
384. Donahue, J.E., et al., *RAGE, LRP-1, and amyloid-beta protein in Alzheimer's disease.* Acta Neuropathol, 2006. **112**(4): p. 405-15.
385. Miller, M.C., et al., *Hippocampal RAGE immunoreactivity in early and advanced Alzheimer's disease.* Brain Res, 2008.
386. Yan, S.D., et al., *RAGE and amyloid-beta peptide neurotoxicity in Alzheimer's disease.* Nature, 1996. **382**(6593): p. 685-91.
387. Arancio, O., et al., *RAGE potentiates Abeta-induced perturbation of neuronal function in transgenic mice.* Embo J, 2004. **23**(20): p. 4096-105.
388. Chen, X., et al., *RAGE: a potential target for Abeta-mediated cellular perturbation in Alzheimer's disease.* Curr Mol Med, 2007. **7**(8): p. 735-42.
389. Mackic, J.B., et al., *Human blood-brain barrier receptors for Alzheimer's amyloid-beta 1- 40. Asymmetrical binding, endocytosis, and transcytosis at the apical side of brain microvascular endothelial cell monolayer.* J Clin Invest, 1998. **102**(4): p. 734-43.
390. Deane, R., et al., *RAGE mediates amyloid-beta peptide transport across the blood-brain barrier and accumulation in brain.* Nat Med, 2003. **9**(7): p. 907-13.
391. Emanuele, E., et al., *Circulating levels of soluble receptor for advanced glycation end products in Alzheimer disease and vascular dementia.* Arch Neurol, 2005. **62**(11): p. 1734-6.
392. Zlokovic, B.V., et al., *Glycoprotein 330/megalin: probable role in receptor-mediated transport of apolipoprotein J alone and in a complex with Alzheimer disease amyloid beta at the blood-brain and blood-cerebrospinal fluid barriers.* Proc Natl Acad Sci U S A, 1996. **93**(9): p. 4229-34.
393. Narita, M., et al., *Alpha2-macroglobulin complexes with and mediates the endocytosis of beta-amyloid peptide via cell surface low-density lipoprotein receptor-related protein.* J Neurochem, 1997. **69**(5): p. 1904-11.
394. Shibata, M., et al., *Clearance of Alzheimer's amyloid-ss(1-40) peptide from brain by LDL receptor-related protein-1 at the blood-brain barrier.* J Clin Invest, 2000. **106**(12): p. 1489-99.

395. Deane, R., et al., *LRP/amyloid beta-peptide interaction mediates differential brain efflux of Abeta isoforms.* Neuron, 2004. **43**(3): p. 333-44.
396. Kang, D.E., et al., *Modulation of amyloid beta-protein clearance and Alzheimer's disease susceptibility by the LDL receptor-related protein pathway.* J Clin Invest, 2000. **106**(9): p. 1159-66.
397. Baum, L., et al., *Low density lipoprotein receptor related protein gene exon 3 polymorphism association with Alzheimer's disease in Chinese.* Neurosci Lett, 1998. **247**(1): p. 33-6.
398. Christoforidis, M., R. Schober, and K. Krohn, *Genetic-morphologic association study: association between the low density lipoprotein-receptor related protein (LRP) and cerebral amyloid angiopathy.* Neuropathol Appl Neurobiol, 2005. **31**(1): p. 11-9.
399. Hollenbach, E., et al., *Confirmation of an association between a polymorphism in exon 3 of the low-density lipoprotein receptor-related protein gene and Alzheimer's disease.* Neurology, 1998. **50**(6): p. 1905-7.
400. Kamboh, M.I., R.E. Ferrell, and S.T. DeKosky, *Genetic association studies between Alzheimer's disease and two polymorphisms in the low density lipoprotein receptor-related protein gene.* Neurosci Lett, 1998. **244**(2): p. 65-8.
401. Kang, D.E., et al., *Genetic association of the low-density lipoprotein receptor-related protein gene (LRP), an apolipoprotein E receptor, with late-onset Alzheimer's disease.* Neurology, 1997. **49**(1): p. 56-61.
402. Causevic, M., et al., *Lack of association between the levels of the low-density lipoprotein receptor-related protein (LRP) and either Alzheimer dementia or LRP exon 3 genotype.* J Neuropathol Exp Neurol, 2003. **62**(10): p. 999-1005.
403. Fallin, D., et al., *No association between the low density lipoprotein receptor-related protein (LRP) gene and late-onset Alzheimer's disease in a community-based sample.* Neurosci Lett, 1997. **233**(2-3): p. 145-7.
404. McIlroy, S.P., et al., *Common polymorphisms in LRP and A2M do not affect genetic risk for Alzheimer disease in Northern Ireland.* Am J Med Genet, 2001. **105**(6): p. 502-6.
405. Sanchez-Guerra, M., et al., *Case-control study and meta-analysis of low density lipoprotein receptor-related protein gene exon 3 polymorphism in Alzheimer's disease.* Neurosci Lett, 2001. **316**(1): p. 17-20.
406. Lam, F.C., et al., *beta-Amyloid efflux mediated by p-glycoprotein.* J Neurochem, 2001. **76**(4): p. 1121-8.
407. Kuhnke, D., et al., *MDR1-P-Glycoprotein (ABCB1) Mediates Transport of Alzheimer's amyloid-beta peptides--implications for the mechanisms of Abeta clearance at the blood-brain barrier.* Brain Pathol, 2007. **17**(4): p. 347-53.
408. Cirrito, J.R., et al., *P-glycoprotein deficiency at the blood-brain barrier increases amyloid-beta deposition in an Alzheimer disease mouse model.* J Clin Invest, 2005. **115**(11): p. 3285-90.
409. Vogelgesang, S., et al., *Deposition of Alzheimer's beta-amyloid is inversely correlated with P-glycoprotein expression in the brains of elderly non-demented humans.* Pharmacogenetics, 2002. **12**(7): p. 535-41.
410. de la Torre, J.C., *Pathophysiology of neuronal energy crisis in Alzheimer's disease.* Neurodegener Dis, 2008. **5**(3-4): p. 126-32.
411. de la Torre, J.C., *Alzheimer's Disease Prevalence can be Lowered with Non-Invasive Testing.* J Alzheimers Dis, 2008. **14**(3): p. 353-9.
412. de la Torre, J.C. and G.B. Stefano, *Evidence that Alzheimer's disease is a microvascular disorder: the role of constitutive nitric oxide.* Brain Res Brain Res Rev, 2000. **34**(3): p. 119-36.
413. Farkas, E. and P.G. Luiten, *Cerebral microvascular pathology in aging and Alzheimer's disease.* Prog Neurobiol, 2001. **64**(6): p. 575-611.

414. Girouard, H. and C. Iadecola, *Neurovascular coupling in the normal brain and in hypertension, stroke, and Alzheimer disease.* J Appl Physiol, 2006. **100**(1): p. 328-35.
415. Henry-Feugeas, M.C., *MRI of the 'Alzheimer syndrome'.* J Neuroradiol, 2007. **34**(4): p. 220-7.
416. Henry-Feugeas, M.C., *Alzheimer's disease in late-life dementia: a minor toxic consequence of devastating cerebrovascular dysfunction.* Med Hypotheses, 2008. **70**(4): p. 866-75.
417. Iadecola, C., *Neurovascular regulation in the normal brain and in Alzheimer's disease.* Nat Rev Neurosci, 2004. **5**(5): p. 347-60.
418. Kalaria, R.N., *Vascular factors in Alzheimer's disease.* Int Psychogeriatr, 2003. **15 Suppl 1**: p. 47-52.
419. Roy, S. and A. Rauk, *Alzheimer's disease and the 'ABSENT' hypothesis: mechanism for amyloid beta endothelial and neuronal toxicity.* Med Hypotheses, 2005. **65**(1): p. 123-37.
420. Zlokovic, B.V., *New therapeutic targets in the neurovascular pathway in Alzheimer's disease.* Neurotherapeutics, 2008. **5**(3): p. 409-14.
421. de la Torre, J.C., *Is Alzheimer's disease a neurodegenerative or a vascular disorder? Data, dogma, and dialectics.* Lancet Neurol, 2004. **3**(3): p. 184-90.
422. Ruitenberg, A., et al., *Cerebral hypoperfusion and clinical onset of dementia: the Rotterdam Study.* Ann Neurol, 2005. **57**(6): p. 789-94.
423. Kogure, D., et al., *Longitudinal evaluation of early Alzheimer's disease using brain perfusion SPECT.* J Nucl Med, 2000. **41**(7): p. 1155-62.
424. Okamura, N., et al., *[Prediction of progression in patients with mild cognitive impairment using IMP-SPECT].* Nippon Ronen Igakkai Zasshi, 2000. **37**(12): p. 974-8.
425. Snowdon, D.A., et al., *Brain infarction and the clinical expression of Alzheimer disease. The Nun Study.* Jama, 1997. **277**(10): p. 813-7.
426. Vermeer, S.E., et al., *Silent brain infarcts and the risk of dementia and cognitive decline.* N Engl J Med, 2003. **348**(13): p. 1215-22.
427. Bennett, S.A., et al., *Cleavage of amyloid precursor protein elicited by chronic cerebral hypoperfusion.* Neurobiol Aging, 2000. **21**(2): p. 207-14.
428. Pappas, B.A., et al., *Chronic ischemia: memory impairment and neural pathology in the rat.* Ann N Y Acad Sci, 1997. **826**: p. 498-501.
429. Wu, Z., et al., *Role of the MEOX2 homeobox gene in neurovascular dysfunction in Alzheimer disease.* Nat Med, 2005. **11**(9): p. 959-65.
430. Hoyer, S., R. Nitsch, and K. Oesterreich, *Predominant abnormality in cerebral glucose utilization in late-onset dementia of the Alzheimer type: a cross-sectional comparison against advanced late-onset and incipient early-onset cases.* J Neural Transm Park Dis Dement Sect, 1991. **3**(1): p. 1-14.
431. Fukuyama, H., et al., *Altered cerebral energy metabolism in Alzheimer's disease: a PET study.* J Nucl Med, 1994. **35**(1): p. 1-6.
432. de Leon, M.J., et al., *The radiologic prediction of Alzheimer disease: the atrophic hippocampal formation.* AJNR Am J Neuroradiol, 1993. **14**(4): p. 897-906.
433. Ogawa, M., et al., *Altered energy metabolism in Alzheimer's disease.* J Neurol Sci, 1996. **139**(1): p. 78-82.
434. Killiany, R.J., et al., *Use of structural magnetic resonance imaging to predict who will get Alzheimer's disease.* Ann Neurol, 2000. **47**(4): p. 430-9.
435. Johnson, K.A., et al., *Preclinical prediction of Alzheimer's disease using SPECT.* Neurology, 1998. **50**(6): p. 1563-71.
436. de Leon, M.J., et al., *Prediction of cognitive decline in normal elderly subjects with 2-[(18)F]fluoro-2-deoxy-D-glucose/poitron-emission tomography (FDG/PET).* Proc Natl Acad Sci U S A, 2001. **98**(19): p. 10966-71.

437. Hooijmans, C.R., et al., *Amyloid beta deposition is related to decreased glucose transporter-1 levels and hippocampal atrophy in brains of aged APP/PS1 mice.* Brain Res, 2007. **1181**: p. 93-103.
438. Mooradian, A.D., H.C. Chung, and G.N. Shah, *GLUT-1 expression in the cerebra of patients with Alzheimer's disease.* Neurobiol Aging, 1997. **18**(5): p. 469-74.
439. Zipser, B.D., et al., *Microvascular injury and blood-brain barrier leakage in Alzheimer's disease.* Neurobiol Aging, 2007. **28**(7): p. 977-86.
440. Dickstein, D.L., et al., *Abeta peptide immunization restores blood-brain barrier integrity in Alzheimer disease.* Faseb J, 2006. **20**(3): p. 426-33.
441. Su, G.C., et al., *Intravascular infusions of soluble beta-amyloid compromise the blood-brain barrier, activate CNS glial cells and induce peripheral hemorrhage.* Brain Res, 1999. **818**(1): p. 105-17.
442. Blanc, E.M., et al., *Amyloid beta-peptide induces cell monolayer albumin permeability, impairs glucose transport, and induces apoptosis in vascular endothelial cells.* J Neurochem, 1997. **68**(5): p. 1870-81.
443. Gonzalez-Velasquez, F.J., J.A. Kotarek, and M.A. Moss, *Soluble aggregates of the amyloid-beta protein selectively stimulate permeability in human brain microvascular endothelial monolayers.* J Neurochem, 2008.
444. Strazielle, N., et al., *In vitro evidence that beta-amyloid peptide 1-40 diffuses across the blood-brain barrier and affects its permeability.* J Neuropathol Exp Neurol, 2000. **59**(1): p. 29-38.
445. Birks, J., *Cholinesterase inhibitors for Alzheimer's disease.* Cochrane Database Syst Rev, 2006(1): p. CD005593.
446. Kaduszkiewicz, H., et al., *Cholinesterase inhibitors for patients with Alzheimer's disease: systematic review of randomised clinical trials.* Bmj, 2005. **331**(7512): p. 321-7.
447. Raina, P., et al., *Effectiveness of cholinesterase inhibitors and memantine for treating dementia: evidence review for a clinical practice guideline.* Ann Intern Med, 2008. **148**(5): p. 379-97.
448. Takeda, A., et al., *A systematic review of the clinical effectiveness of donepezil, rivastigmine and galantamine on cognition, quality of life and adverse events in Alzheimer's disease.* Int J Geriatr Psychiatry, 2006. **21**(1): p. 17-28.
449. Raschetti, R., et al., *Cholinesterase inhibitors in mild cognitive impairment: a systematic review of randomised trials.* PLoS Med, 2007. **4**(11): p. e338.
450. Cacabelos, R., M. Takeda, and B. Winblad, *The glutamatergic system and neurodegeneration in dementia: preventive strategies in Alzheimer's disease.* Int J Geriatr Psychiatry, 1999. **14**(1): p. 3-47.
451. McShane, R., A. Areosa Sastre, and N. Minakaran, *Memantine for dementia.* Cochrane Database Syst Rev, 2006(2): p. CD003154.
452. Bard, F., et al., *Peripherally administered antibodies against amyloid beta-peptide enter the central nervous system and reduce pathology in a mouse model of Alzheimer disease.* Nat Med, 2000. **6**(8): p. 916-9.
453. Janus, C., et al., *A beta peptide immunization reduces behavioural impairment and plaques in a model of Alzheimer's disease.* Nature, 2000. **408**(6815): p. 979-82.
454. Lemere, C.A., et al., *Nasal A beta treatment induces anti-A beta antibody production and decreases cerebral amyloid burden in PD-APP mice.* Ann N Y Acad Sci, 2000. **920**: p. 328-31.
455. Morgan, D., et al., *A beta peptide vaccination prevents memory loss in an animal model of Alzheimer's disease.* Nature, 2000. **408**(6815): p. 982-5.
456. Schenk, D., et al., *Immunization with amyloid-beta attenuates Alzheimer-disease-like pathology in the PDAPP mouse.* Nature, 1999. **400**(6740): p. 173-7.

457. Sigurdsson, E.M., et al., *An attenuated immune response is sufficient to enhance cognition in an Alzheimer's disease mouse model immunized with amyloid-beta derivatives.* J Neurosci, 2004. **24**(28): p. 6277-82.
458. Sigurdsson, E.M., et al., *Immunization with a nontoxic/nonfibrillar amyloid-beta homologous peptide reduces Alzheimer's disease-associated pathology in transgenic mice.* Am J Pathol, 2001. **159**(2): p. 439-47.
459. Weiner, H.L., et al., *Nasal administration of amyloid-beta peptide decreases cerebral amyloid burden in a mouse model of Alzheimer's disease.* Ann Neurol, 2000. **48**(4): p. 567-79.
460. Wilcock, D.M., et al., *Passive amyloid immunotherapy clears amyloid and transiently activates microglia in a transgenic mouse model of amyloid deposition.* J Neurosci, 2004. **24**(27): p. 6144-51.
461. Wisniewski, T. and U. Konietzko, *Amyloid-beta immunisation for Alzheimer's disease.* Lancet Neurol, 2008. **7**(9): p. 805-11.
462. Ito, S., et al., *Induction of matrix metalloproteinases (MMP3, MMP12 and MMP13) expression in the microglia by amyloid-beta stimulation via the PI3K/Akt pathway.* Exp Gerontol, 2007. **42**(6): p. 532-7.
463. Yin, K.J., et al., *Abeta25-35 alters Akt activity, resulting in Bad translocation and mitochondrial dysfunction in cerebrovascular endothelial cells.* J Cereb Blood Flow Metab, 2005. **25**(11): p. 1445-55.
464. Eisenhauer, P.B., et al., *Toxicity of various amyloid beta peptide species in cultured human blood-brain barrier endothelial cells: increased toxicity of dutch-type mutant.* J Neurosci Res, 2000. **60**(6): p. 804-10.
465. Hughes, E., R.M. Burke, and A.J. Doig, *Inhibition of toxicity in the beta-amyloid peptide fragment beta -(25-35) using N-methylated derivatives: a general strategy to prevent amyloid formation.* J Biol Chem, 2000. **275**(33): p. 25109-15.
466. Iversen, L.L., et al., *The toxicity in vitro of beta-amyloid protein.* Biochem J, 1995. **311 (Pt 1)**: p. 1-16.
467. Scorziello, A., et al., *beta 25-35 alters calcium homeostasis and induces neurotoxicity in cerebellar granule cells.* J Neurochem, 1996. **66**(5): p. 1995-2003.
468. Gu, X., et al., *Brain and retinal vascular endothelial cells with extended life span established by ectopic expression of telomerase.* Invest Ophthalmol Vis Sci, 2003. **44**(7): p. 3219-25.
469. Kannan, R., et al., *GSH transport in human cerebrovascular endothelial cells and human astrocytes: evidence for luminal localization of Na+-dependent GSH transport in HCEC.* Brain Res, 2000. **852**(2): p. 374-82.
470. Kusch-Poddar, M., et al., *Evaluation of the immortalized human brain capillary endothelial cell line BB19 as a human cell culture model for the blood-brain barrier.* Brain Res, 2005. **1064**(1-2): p. 21-31.
471. Muruganandam, A., et al., *Development of immortalized human cerebromicrovascular endothelial cell line as an in vitro model of the human blood-brain barrier.* Faseb J, 1997. **11**(13): p. 1187-97.
472. Stins, M.F., J. Badger, and K. Sik Kim, *Bacterial invasion and transcytosis in transfected human brain microvascular endothelial cells.* Microb Pathog, 2001. **30**(1): p. 19-28.
473. Weksler, B.B., et al., *Blood-brain barrier-specific properties of a human adult brain endothelial cell line.* Faseb J, 2005. **19**(13): p. 1872-4.
474. Cucullo, L., et al., *Immortalized human brain endothelial cells and flow-based vascular modeling: a marriage of convenience for rational neurovascular studies.* J Cereb Blood Flow Metab, 2008. **28**(2): p. 312-28.
475. Holloway, K., et al., *Action of transcription factors in the control of transferrin receptor expression in human brain endothelium.* J Mol Biol, 2007. **365**(5): p. 1271-84.

476. Lim, J.C., et al., *Activation of beta-catenin signalling by GSK-3 inhibition increases p-glycoprotein expression in brain endothelial cells.* J Neurochem, 2008. **106**(4): p. 1855-65.
477. Maru, S.V., et al., *Chemokine production and chemokine receptor expression by human glioma cells: Role of CXCL10 in tumour cell proliferation.* J Neuroimmunol, 2008. **199**(1-2): p. 35-45.
478. Mordelet, E., et al., *Chemokine transport across human vascular endothelial cells.* Endothelium, 2007. **14**(1): p. 7-15.
479. Schreibelt, G., et al., *Reactive oxygen species alter brain endothelial tight junction dynamics via RhoA, PI3 kinase, and PKB signaling.* Faseb J, 2007. **21**(13): p. 3666-76.
480. Wilhelm, I., et al., *Regulation of cerebral endothelial cell morphology by extracellular calcium.* Phys Med Biol, 2007. **52**(20): p. 6261-74.
481. Wilhelm, I., et al., *Hyperosmotic stress induces Axl activation and cleavage in cerebral endothelial cells.* J Neurochem, 2008.
482. Miller, D.S., et al., *Xenobiotic transport across isolated brain microvessels studied by confocal microscopy.* Mol Pharmacol, 2000. **58**(6): p. 1357-67.
483. Virgintino, D., et al., *Expression of P-glycoprotein in human cerebral cortex microvessels.* J Histochem Cytochem, 2002. **50**(12): p. 1671-6.
484. Schlachetzki, F. and W.M. Pardridge, *P-glycoprotein and caveolin-1alpha in endothelium and astrocytes of primate brain.* Neuroreport, 2003. **14**(16): p. 2041-6.
485. Forster, C., et al., *Differential effects of hydrocortisone and TNFalpha on tight junction proteins in an in vitro model of the human blood-brain barrier.* J Physiol, 2008. **586**(7): p. 1937-49.
486. Marco, S. and S.D. Skaper, *Amyloid beta-peptide1-42 alters tight junction protein distribution and expression in brain microvessel endothelial cells.* Neurosci Lett, 2006. **401**(3): p. 219-24.
487. Fox, E. and S.E. Bates, *Tariquidar (XR9576): a P-glycoprotein drug efflux pump inhibitor.* Expert Rev Anticancer Ther, 2007. **7**(4): p. 447-59.
488. Dale, I.L., et al., *Reversal of P-glycoprotein-mediated multidrug resistance by XR9051, a novel diketopiperazine derivative.* Br J Cancer, 1998. **78**(7): p. 885-92.
489. Acharya, P., et al., *P-Glycoprotein (P-gp) expressed in a confluent monolayer of hMDR1-MDCKII cells has more than one efflux pathway with cooperative binding sites.* Biochemistry, 2006. **45**(51): p. 15505-19.
490. Evers, R., et al., *Inhibitory effect of the reversal agents V-104, GF120918 and Pluronic L61 on MDR1 Pgp-, MRP1- and MRP2-mediated transport.* Br J Cancer, 2000. **83**(3): p. 366-74.
491. Smith, A.J., et al., *Availability of PSC833, a substrate and inhibitor of P-glycoproteins, in various concentrations of serum.* J Natl Cancer Inst, 1998. **90**(15): p. 1161-6.
492. Lohner, K., et al., *Flavonoids alter P-gp expression in intestinal epithelial cells in vitro and in vivo.* Mol Nutr Food Res, 2007. **51**(3): p. 293-300.
493. Shaw, N.J., et al., *Autosomal recessive hypoparathyroidism with renal insufficiency and developmental delay.* Arch Dis Child, 1991. **66**(10): p. 1191-4.
494. Endter, S., et al., *P-glycoprotein (MDR1) functional activity in human alveolar epithelial cell monolayers.* Cell Tissue Res, 2007. **328**(1): p. 77-84.
495. Campbell, L., et al., *Constitutive expression of p-glycoprotein in normal lung alveolar epithelium and functionality in primary alveolar epithelial cultures.* J Pharmacol Exp Ther, 2003. **304**(1): p. 441-52.
496. Smith, M., Y. Omidi, and M. Gumbleton, *Primary porcine brain microvascular endothelial cells: biochemical and functional characterisation as a model for drug transport and targeting.* J Drug Target, 2007. **15**(4): p. 253-68.

497. Hira, A., et al., *Role of P-glycoprotein in accumulation and cytotoxicity of amrubicin and amrubicinol in MDR1 gene-transfected LLC-PK1 cells and human A549 lung adenocarcinoma cells.* Biochem Pharmacol, 2008. **75**(4): p. 973-80.
498. Xia, S., S. Yu, and X. Yuan, *Effects of hypoxia on expression of P-gp and mutltidrug resistance protein in human lung adenocarcinoma A549 cell line.* J Huazhong Univ Sci Technolog Med Sci, 2005. **25**(3): p. 279-81.
499. Pesic, M., et al., *Induced resistance in the human non small cell lung carcinoma (NCI-H460) cell line in vitro by anticancer drugs.* J Chemother, 2006. **18**(1): p. 66-73.
500. Hoffmaster, K.A., et al., *P-glycoprotein expression, localization, and function in sandwich-cultured primary rat and human hepatocytes: relevance to the hepatobiliary disposition of a model opioid peptide.* Pharm Res, 2004. **21**(7): p. 1294-302.
501. Lecureur, V., A. Guillouzo, and O. Fardel, *Differential regulation of mdr genes in response to 2-acetylaminofluorene treatment in cultured rat and human hepatocytes.* Carcinogenesis, 1996. **17**(5): p. 1157-60.
502. Manov, I., et al., *High-dose acetaminophen inhibits the lethal effect of doxorubicin in HepG2 cells: the role of P-glycoprotein and mitogen-activated protein kinase p44/42 pathway.* J Pharmacol Exp Ther, 2007. **322**(3): p. 1013-22.
503. Kitano, T., et al., *Conditionally immortalized syncytiotrophoblast cell lines as new tools for study of the blood-placenta barrier.* Biol Pharm Bull, 2004. **27**(6): p. 753-9.
504. Perriere, N., et al., *A functional in vitro model of rat blood-brain barrier for molecular analysis of efflux transporters.* Brain Res, 2007. **1150**: p. 1-13.
505. Roux, F. and P.O. Couraud, *Rat brain endothelial cell lines for the study of blood-brain barrier permeability and transport functions.* Cell Mol Neurobiol, 2005. **25**(1): p. 41-58.
506. Hosoya, K., et al., *Conditionally immortalized brain capillary endothelial cell lines established from a transgenic mouse harboring temperature-sensitive simian virus 40 large T-antigen gene.* AAPS PharmSci, 2000. **2**(3): p. E27.
507. Omidi, Y., et al., *Evaluation of the immortalised mouse brain capillary endothelial cell line, b.End3, as an in vitro blood-brain barrier model for drug uptake and transport studies.* Brain Res, 2003. **990**(1-2): p. 95-112.
508. Yang, T., K.E. Roder, and T.J. Abbruscato, *Evaluation of bEnd5 cell line as an in vitro model for the blood-brain barrier under normal and hypoxic/aglycemic conditions.* J Pharm Sci, 2007. **96**(12): p. 3196-213.
509. Teifel, M. and P. Friedl, *Establishment of the permanent microvascular endothelial cell line PBMEC/C1-2 from porcine brains.* Exp Cell Res, 1996. **228**(1): p. 50-7.
510. Zhang, Y., et al., *Porcine brain microvessel endothelial cells as an in vitro model to predict in vivo blood-brain barrier permeability.* Drug Metab Dispos, 2006. **34**(11): p. 1935-43.
511. Durieu-Trautmann, O., et al., *Immortalization of brain capillary endothelial cells with maintenance of structural characteristics of the blood-brain barrier endothelium.* In Vitro Cell Dev Biol, 1991. **27A**(10): p. 771-8.
512. Hughes, C.C. and P.L. Lantos, *Brain capillary endothelial cells in vitro lack surface IgG Fc receptors.* Neurosci Lett, 1986. **68**(1): p. 100-6.
513. Ramsby, M.L., G.S. Makowski, and E.A. Khairallah, *Differential detergent fractionation of isolated hepatocytes: biochemical, immunochemical and two-dimensional gel electrophoresis characterization of cytoskeletal and noncytoskeletal compartments.* Electrophoresis, 1994. **15**(2): p. 265-77.
514. Begley, D.J., et al., *Functional expression of P-glycoprotein in an immortalised cell line of rat brain endothelial cells, RBE4.* J Neurochem, 1996. **67**(3): p. 988-95.

515. Demeule, M., et al., *Drug transport to the brain: key roles for the efflux pump P-glycoprotein in the blood-brain barrier.* Vascul Pharmacol, 2002. **38**(6): p. 339-48.
516. Regina, A., et al., *Mrp1 multidrug resistance-associated protein and P-glycoprotein expression in rat brain microvessel endothelial cells.* J Neurochem, 1998. **71**(2): p. 705-15.
517. Barrand, M.A., K.J. Robertson, and S.F. von Weikersthal, *Comparisons of P-glycoprotein expression in isolated rat brain microvessels and in primary cultures of endothelial cells derived from microvasculature of rat brain, epididymal fat pad and from aorta.* FEBS Lett, 1995. **374**(2): p. 179-83.
518. Deli, M.A., et al., *Tissue plasminogen activator inhibits P-glycoprotein activity in brain endothelial cells.* Eur J Pharmacol, 2001. **411**(1-2): p. R3-R5.
519. Demeuse, P., et al., *Puromycin selectively increases mdr1a expression in immortalized rat brain endothelial cell lines.* J Neurochem, 2004. **88**(1): p. 23-31.
520. Marchi, N., et al., *Determinants of drug brain uptake in a rat model of seizure-associated malformations of cortical development.* Neurobiol Dis, 2006. **24**(3): p. 429-42.
521. Tishler, D.M., et al., *MDR1 gene expression in brain of patients with medically intractable epilepsy.* Epilepsia, 1995. **36**(1): p. 1-6.
522. Cornford, E.M., *Epilepsy and the blood brain barrier: endothelial cell responses to seizures.* Adv Neurol, 1999. **79**: p. 845-62.
523. Shirai, A., et al., *Transport of cyclosporin A across the brain capillary endothelial cell monolayer by P-glycoprotein.* Biochim Biophys Acta, 1994. **1222**(3): p. 400-4.
524. Rabindran, S.K., et al., *Reversal of a novel multidrug resistance mechanism in human colon carcinoma cells by fumitremorgin C.* Cancer Res, 1998. **58**(24): p. 5850-8.
525. Rabindran, S.K., et al., *Fumitremorgin C reverses multidrug resistance in cells transfected with the breast cancer resistance protein.* Cancer Res, 2000. **60**(1): p. 47-50.
526. Robey, R.W., et al., *Overexpression of the ATP-binding cassette half-transporter, ABCG2 (Mxr/BCrp/ABCP1), in flavopiridol-resistant human breast cancer cells.* Clin Cancer Res, 2001. **7**(1): p. 145-52.
527. Breuzard, G., et al., *Energy transfer to analyse membrane-integrated mitoxantrone in BCRP-overexpressed cells.* J Photochem Photobiol B, 2007. **87**(2): p. 113-23.
528. Wang, Q., et al., *Application and limitation of inhibitors in drug-transporter interactions studies.* Int J Pharm, 2008. **356**(1-2): p. 12-8.
529. Garimella, T.S., et al., *Plasma pharmacokinetics and tissue distribution of the breast cancer resistance protein (BCRP/ABCG2) inhibitor fumitremorgin C in SCID mice bearing T8 tumors.* Cancer Chemother Pharmacol, 2005. **55**(2): p. 101-9.
530. McDevitt, C.A. and R. Callaghan, *How can we best use structural information on P-glycoprotein to design inhibitors?* Pharmacol Ther, 2007. **113**(2): p. 429-41.
531. Mistry, P., et al., *In vitro and in vivo reversal of P-glycoprotein-mediated multidrug resistance by a novel potent modulator, XR9576.* Cancer Res, 2001. **61**(2): p. 749-58.
532. Roe, M., et al., *Reversal of P-glycoprotein mediated multidrug resistance by novel anthranilamide derivatives.* Bioorg Med Chem Lett, 1999. **9**(4): p. 595-600.
533. Bains, O.S. and C.J. Kennedy, *Alterations in respiration rate of isolated rainbow trout hepatocytes exposed to the P-glycoprotein substrate rhodamine 123.* Toxicology, 2005. **214**(1-2): p. 87-98.
534. Choo, E.F., et al., *Differential in vivo sensitivity to inhibition of P-glycoprotein located in lymphocytes, testes, and the blood-brain barrier.* J Pharmacol Exp Ther, 2006. **317**(3): p. 1012-8.

535. van Vliet, E.A., et al., *Inhibition of the multidrug transporter P-glycoprotein improves seizure control in phenytoin-treated chronic epileptic rats.* Epilepsia, 2006. **47**(4): p. 672-80.
536. van Vliet, E.A., et al., *Region-specific overexpression of P-glycoprotein at the blood-brain barrier affects brain uptake of phenytoin in epileptic rats.* J Pharmacol Exp Ther, 2007. **322**(1): p. 141-7.
537. Walker, J., C. Martin, and R. Callaghan, *Inhibition of P-glycoprotein function by XR9576 in a solid tumour model can restore anticancer drug efficacy.* Eur J Cancer, 2004. **40**(4): p. 594-605.
538. Jordan, M.A., D. Thrower, and L. Wilson, *Mechanism of inhibition of cell proliferation by Vinca alkaloids.* Cancer Res, 1991. **51**(8): p. 2212-22.
539. Lobert, S., J.W. Ingram, and J.J. Correia, *Additivity of dilantin and vinblastine inhibitory effects on microtubule assembly.* Cancer Res, 1999. **59**(19): p. 4816-22.
540. Toso, R.J., et al., *Kinetic stabilization of microtubule dynamic instability in vitro by vinblastine.* Biochemistry, 1993. **32**(5): p. 1285-93.
541. Klement, G., et al., *Continuous low-dose therapy with vinblastine and VEGF receptor-2 antibody induces sustained tumor regression without overt toxicity.* J Clin Invest, 2000. **105**(8): p. R15-24.
542. Vacca, A., et al., *Antiangiogenesis is produced by nontoxic doses of vinblastine.* Blood, 1999. **94**(12): p. 4143-55.
543. van der Sandt, I.C., et al., *P-glycoprotein inhibition leads to enhanced disruptive effects by anti-microtubule cytostatics at the in vitro blood-brain barrier.* Pharm Res, 2001. **18**(5): p. 587-92.
544. Bijman, M.N., et al., *Microtubule-targeting agents inhibit angiogenesis at subtoxic concentrations, a process associated with inhibition of Rac1 and Cdc42 activity and changes in the endothelial cytoskeleton.* Mol Cancer Ther, 2006. **5**(9): p. 2348-57.
545. McLucas, E., et al., *Global gene expression analysis of the effects of vinblastine on endothelial cells, when eluted from a thermo-responsive polymer.* J Biomed Mater Res A, 2006. **79**(2): p. 246-53.
546. Perriere, N., et al., *Puromycin-based purification of rat brain capillary endothelial cell cultures. Effect on the expression of blood-brain barrier-specific properties.* J Neurochem, 2005. **93**(2): p. 279-89.
547. Ji, B.S., L. He, and G.Q. Liu, *Modulation of P-glycoprotein function by amlodipine derivatives in brain microvessel endothelial cells of rats.* Acta Pharmacol Sin, 2005. **26**(2): p. 166-70.
548. Zhang, W., et al., *The expression and functional characterization of ABCG2 in brain endothelial cells and vessels.* Faseb J, 2003. **17**(14): p. 2085-7.
549. Alqawi, O., S. Bates, and E. Georges, *Arginine482 to threonine mutation in the breast cancer resistance protein ABCG2 inhibits rhodamine 123 transport while increasing binding.* Biochem J, 2004. **382**(Pt 2): p. 711-6.
550. Allen, J.D., S.C. Jackson, and A.H. Schinkel, *A mutation hot spot in the Bcrp1 (Abcg2) multidrug transporter in mouse cell lines selected for Doxorubicin resistance.* Cancer Res, 2002. **62**(8): p. 2294-9.
551. Gaillard, P.J., et al., *Astrocytes increase the functional expression of P-glycoprotein in an in vitro model of the blood-brain barrier.* Pharm Res, 2000. **17**(10): p. 1198-205.
552. Cho, C.W., et al., *Ultrasound-induced mild hyperthermia as a novel approach to increase drug uptake in brain microvessel endothelial cells.* Pharm Res, 2002. **19**(8): p. 1123-9.
553. Fontaine, M., W.F. Elmquist, and D.W. Miller, *Use of rhodamine 123 to examine the functional activity of P-glycoprotein in primary cultured brain microvessel endothelial cell monolayers.* Life Sci, 1996. **59**(18): p. 1521-31.

554. Kubota, H., et al., *Distribution and functional activity of P-glycoprotein and multidrug resistance-associated proteins in human brain microvascular endothelial cells in hippocampal sclerosis.* Epilepsy Res, 2006. **68**(3): p. 213-28.
555. Ng, K.Y., et al., *Effect of heat preconditioning on the uptake and permeability of R123 in brain microvessel endothelial cells during mild heat treatment.* J Pharm Sci, 2004. **93**(4): p. 896-907.
556. Tanzi, R.E., R.D. Moir, and S.L. Wagner, *Clearance of Alzheimer's Abeta peptide: the many roads to perdition.* Neuron, 2004. **43**(5): p. 605-8.
557. Beffert, U., C. Arguin, and J. Poirier, *The polymorphism in exon 3 of the low density lipoprotein receptor-related protein gene is weakly associated with Alzheimer's disease.* Neurosci Lett, 1999. **259**(1): p. 29-32.
558. Hatanaka, Y., et al., *Low density lipoprotein receptor-related protein gene polymorphisms and risk for late-onset Alzheimer's disease in a Japanese population.* Clin Genet, 2000. **58**(4): p. 319-23.
559. Ito, S., et al., *Cerebral clearance of human amyloid-beta peptide (1-40) across the blood-brain barrier is reduced by self-aggregation and formation of low-density lipoprotein receptor-related protein-1 ligand complexes.* J Neurochem, 2007. **103**(6): p. 2482-90.
560. Ito, S., S. Ohtsuki, and T. Terasaki, *Functional characterization of the brain-to-blood efflux clearance of human amyloid-beta peptide (1-40) across the rat blood-brain barrier.* Neurosci Res, 2006. **56**(3): p. 246-52.
561. Nazer, B., S. Hong, and D.J. Selkoe, *LRP promotes endocytosis and degradation, but not transcytosis, of the amyloid-beta peptide in a blood-brain barrier in vitro model.* Neurobiol Dis, 2008. **30**(1): p. 94-102.
562. Poduslo, J.F., et al., *Receptor-mediated transport of human amyloid beta-protein 1-40 and 1-42 at the blood-brain barrier.* Neurobiol Dis, 1999. **6**(3): p. 190-9.
563. Qiu, Z., et al., *Alpha2-macroglobulin enhances the clearance of endogenous soluble beta-amyloid peptide via low-density lipoprotein receptor-related protein in cortical neurons.* J Neurochem, 1999. **73**(4): p. 1393-8.
564. Yang, D.S., et al., *Apolipoprotein E promotes the binding and uptake of beta-amyloid into Chinese hamster ovary cells in an isoform-specific manner.* Neuroscience, 1999. **90**(4): p. 1217-26.
565. Tamaki, C., et al., *Major involvement of low-density lipoprotein receptor-related protein 1 in the clearance of plasma free amyloid beta-peptide by the liver.* Pharm Res, 2006. **23**(7): p. 1407-16.
566. Vogelgesang, S., et al., *Cerebrovascular P-glycoprotein expression is decreased in Creutzfeldt-Jakob disease.* Acta Neuropathol, 2006. **111**(5): p. 436-43.
567. Miners, J.S., et al., *Abeta-degrading enzymes in Alzheimer's disease.* Brain Pathol, 2008. **18**(2): p. 240-52.
568. Howell, S., J. Nalbantoglu, and P. Crine, *Neutral endopeptidase can hydrolyze beta-amyloid(1-40) but shows no effect on beta-amyloid precursor protein metabolism.* Peptides, 1995. **16**(4): p. 647-52.
569. Iwata, N., et al., *Identification of the major Abeta1-42-degrading catabolic pathway in brain parenchyma: suppression leads to biochemical and pathological deposition.* Nat Med, 2000. **6**(2): p. 143-50.
570. Kurochkin, I.V. and S. Goto, *Alzheimer's beta-amyloid peptide specifically interacts with and is degraded by insulin degrading enzyme.* FEBS Lett, 1994. **345**(1): p. 33-7.
571. Eckman, E.A., D.K. Reed, and C.B. Eckman, *Degradation of the Alzheimer's amyloid beta peptide by endothelin-converting enzyme.* J Biol Chem, 2001. **276**(27): p. 24540-8.

572. Hu, J., et al., *Angiotensin-converting enzyme degrades Alzheimer amyloid beta-peptide (A beta); retards A beta aggregation, deposition, fibril formation; and inhibits cytotoxicity.* J Biol Chem, 2001. **276**(51): p. 47863-8.
573. Eckman, E.A. and C.B. Eckman, *Abeta-degrading enzymes: modulators of Alzheimer's disease pathogenesis and targets for therapeutic intervention.* Biochem Soc Trans, 2005. **33**(Pt 5): p. 1101-5.
574. Wang, D.S., D.W. Dickson, and J.S. Malter, *beta-Amyloid Degradation and Alzheimer's Disease.* J Biomed Biotechnol, 2006. **2006**(3): p. 58406.
575. Leissring, M.A., et al., *Kinetics of amyloid beta-protein degradation determined by novel fluorescence- and fluorescence polarization-based assays.* J Biol Chem, 2003. **278**(39): p. 37314-20.
576. Kuo, Y.M., et al., *High levels of circulating Abeta42 are sequestered by plasma proteins in Alzheimer's disease.* Biochem Biophys Res Commun, 1999. **257**(3): p. 787-91.
577. Berzin, T.M., et al., *Agrin and microvascular damage in Alzheimer's disease.* Neurobiol Aging, 2000. **21**(2): p. 349-55.
578. Elovaara, I., et al., *Serum and cerebrospinal fluid proteins and the blood-brain barrier in Alzheimer's disease and multi-infarct dementia.* Eur Neurol, 1987. **26**(4): p. 229-34.
579. Matsumoto, Y., et al., *Blood-brain barrier permeability correlates with medial temporal lobe atrophy but not with amyloid-beta protein transport across the blood-brain barrier in Alzheimer's disease.* Dement Geriatr Cogn Disord, 2007. **23**(4): p. 241-5.
580. Skoog, I., et al., *A population study on blood-brain barrier function in 85-year-olds: relation to Alzheimer's disease and vascular dementia.* Neurology, 1998. **50**(4): p. 966-71.
581. Wada, H., *Blood-brain barrier permeability of the demented elderly as studied by cerebrospinal fluid-serum albumin ratio.* Intern Med, 1998. **37**(6): p. 509-13.
582. Cantara, S., et al., *TAT-BH4 counteracts Abeta toxicity on capillary endothelium.* FEBS Lett, 2007. **581**(4): p. 702-6.
583. Sutton, E.T., G.R. Hellermann, and T. Thomas, *beta-amyloid-induced endothelial necrosis and inhibition of nitric oxide production.* Exp Cell Res, 1997. **230**(2): p. 368-76.
584. Ujiie, M., et al., *Blood-brain barrier permeability precedes senile plaque formation in an Alzheimer disease model.* Microcirculation, 2003. **10**(6): p. 463-70.
585. Liu, Y., et al., *Decreased glucose transporters correlate to abnormal hyperphosphorylation of tau in Alzheimer disease.* FEBS Lett, 2008. **582**(2): p. 359-64.
586. Horwood, N. and D.C. Davies, *Immunolabelling of hippocampal microvessel glucose transporter protein is reduced in Alzheimer's disease.* Virchows Arch, 1994. **425**(1): p. 69-72.
587. Kalaria, R.N. and S.I. Harik, *Reduced glucose transporter at the blood-brain barrier and in cerebral cortex in Alzheimer disease.* J Neurochem, 1989. **53**(4): p. 1083-8.
588. Pfaffl, M.W., *A new mathematical model for relative quantification in real-time RT-PCR.* Nucleic Acids Res, 2001. **29**(9): p. e45.
589. Smith, M.A., et al., *Iron accumulation in Alzheimer disease is a source of redox-generated free radicals.* Proc Natl Acad Sci U S A, 1997. **94**(18): p. 9866-8.
590. Balcells, M., J.S. Wallins, and E.R. Edelman, *Amyloid beta toxicity dependent upon endothelial cell state.* Neurosci Lett, 2008.
591. Shankar, G.M., et al., *Amyloid-beta protein dimers isolated directly from Alzheimer's brains impair synaptic plasticity and memory.* Nat Med, 2008.

592. Sukhai, M., et al., *Decreased expression of P-glycoprotein in interleukin-1beta and interleukin-6 treated rat hepatocytes.* Inflamm Res, 2001. **50**(7): p. 362-70.
593. Hartmann, G., H. Kim, and M. Piquette-Miller, *Regulation of the hepatic multidrug resistance gene expression by endotoxin and inflammatory cytokines in mice.* Int Immunopharmacol, 2001. **1**(2): p. 189-99.
594. Fernandez, C., et al., *Influence of the pro-inflammatory cytokines on P-glycoprotein expression and functionality.* J Pharm Pharm Sci, 2004. **7**(3): p. 359-71.
595. Castellani, R.J., et al., *Iron: the Redox-active center of oxidative stress in Alzheimer disease.* Neurochem Res, 2007. **32**(10): p. 1640-5.
596. Rottkamp, C.A., et al., *Redox-active iron mediates amyloid-beta toxicity.* Free Radic Biol Med, 2001. **30**(4): p. 447-50.
597. Kalaria, R.N., et al., *Transferrin receptors of rat and human brain and cerebral microvessels and their status in Alzheimer's disease.* Brain Res, 1992. **585**(1-2): p. 87-93.
598. Morris, C.M., et al., *Transferrin receptors in the normal human hippocampus and in Alzheimer's disease.* Neuropathol Appl Neurobiol, 1994. **20**(5): p. 473-7.
599. Yoshida, T., et al., *Activated microglia cause iron-dependent lipid peroxidation in the presence of ferritin.* Neuroreport, 1998. **9**(9): p. 1929-33.
600. Moroo, I., et al., *Identification of a novel route of iron transcytosis across the mammalian blood-brain barrier.* Microcirculation, 2003. **10**(6): p. 457-62.
601. Bradbury, M.W., *Transport of iron in the blood-brain-cerebrospinal fluid system.* J Neurochem, 1997. **69**(2): p. 443-54.
602. Frolich, L., et al., *Integrity of the blood-CSF barrier in dementia of Alzheimer type: CSF/serum ratios of albumin and IgG.* Eur Arch Psychiatry Clin Neurosci, 1991. **240**(6): p. 363-6.
603. Kay, A.D., et al., *CSF and serum concentrations of albumin and IgG in Alzheimer's disease.* Neurobiol Aging, 1987. **8**(1): p. 21-5.
604. Leonardi, A., et al., *The integrity of the blood-brain barrier in Alzheimer's type and multi-infarct dementia evaluated by the study of albumin and IgG in serum and cerebrospinal fluid.* J Neurol Sci, 1985. **67**(2): p. 253-61.
605. Wardlaw, J.M., et al., *Is breakdown of the blood-brain barrier responsible for lacunar stroke, leukoaraiosis, and dementia?* Stroke, 2003. **34**(3): p. 806-12.
606. Correale, J. and A. Villa, *The blood-brain-barrier in multiple sclerosis: functional roles and therapeutic targeting.* Autoimmunity, 2007. **40**(2): p. 148-60.
607. van Vliet, E.A., et al., *Blood-brain barrier leakage may lead to progression of temporal lobe epilepsy.* Brain, 2007. **130**(Pt 2): p. 521-34.
608. Karssen, A.M., et al., *Multidrug resistance P-glycoprotein hampers the access of cortisol but not of corticosterone to mouse and human brain.* Endocrinology, 2001. **142**(6): p. 2686-94.
609. Smith, Q.R. and S.I. Rapoport, *Cerebrovascular permeability coefficients to sodium, potassium, and chloride.* J Neurochem, 1986. **46**(6): p. 1732-42.
610. Landfield, P.W., et al., *A new glucocorticoid hypothesis of brain aging: implications for Alzheimer's disease.* Curr Alzheimer Res, 2007. **4**(2): p. 205-12.
611. Hooper, C., D.L. Taylor, and J.M. Pocock, *Pure albumin is a potent trigger of calcium signalling and proliferation in microglia but not macrophages or astrocytes.* J Neurochem, 2005. **92**(6): p. 1363-76.
612. Moser, K.V. and C. Humpel, *Blood-derived serum albumin contributes to neurodegeneration via astroglial stress fiber formation.* Pharmacology, 2007. **80**(4): p. 286-92.
613. Biere, A.L., et al., *Amyloid beta-peptide is transported on lipoproteins and albumin in human plasma.* J Biol Chem, 1996. **271**(51): p. 32916-22.
614. Akiyama, H., et al., *Thrombin accumulation in brains of patients with Alzheimer's disease.* Neurosci Lett, 1992. **146**(2): p. 152-4.

615. Kalaria, R.N. and G. Perry, *Amyloid P component and other acute-phase proteins associated with cerebellar A beta-deposits in Alzheimer's disease.* Brain Res, 1993. **631**(1): p. 151-5.
616. Stone, J., *What initiates the formation of senile plaques? The origin of Alzheimer-like dementias in capillary haemorrhages.* Med Hypotheses, 2008. **71**(3): p. 347-59.
617. Wu, C.W., et al., *Hemoglobin promotes Abeta oligomer formation and localizes in neurons and amyloid deposits.* Neurobiol Dis, 2004. **17**(3): p. 367-77.
618. Lin, W.R., et al., *Herpesviruses in brain and Alzheimer's disease.* J Pathol, 2002. **197**(3): p. 395-402.
619. Ball, M.J., *The essential lesion of Alzheimer disease: a surprise in retrospect.* J Alzheimers Dis, 2006. **9**(3 Suppl): p. 29-33.
620. Kinoshita, J., *Pathogens as a cause of Alzheimer's disease.* Neurobiol Aging, 2004. **25**(5): p. 639-40.
621. Folin, M., et al., *Effects of beta-amyloid on rat neuromicrovascular endothelial cells cultured in vitro.* Int J Mol Med, 2005. **15**(6): p. 929-35.
622. Chi, X., et al., *Potassium channel openers prevent beta-amyloid toxicity in bovine vascular endothelial cells.* Neurosci Lett, 2000. **290**(1): p. 9-12.
623. Price, J.M., et al., *Physiological levels of beta-amyloid induce cerebral vessel dysfunction and reduce endothelial nitric oxide production.* Neurol Res, 2001. **23**(5): p. 506-12.
624. Cantara, S., M. Ziche, and S. Donnini, *Opposite effects of beta amyloid on endothelial cell survival: role of fibroblast growth factor-2 (FGF-2).* Pharmacol Rep, 2005. **57 Suppl**: p. 138-43.
625. Magrane, J., et al., *Dissociation of ERK and Akt signaling in endothelial cell angiogenic responses to beta-amyloid.* Exp Cell Res, 2006. **312**(7): p. 996-1010.
626. Xu, J., et al., *Amyloid beta peptide-induced cerebral endothelial cell death involves mitochondrial dysfunction and caspase activation.* J Cereb Blood Flow Metab, 2001. **21**(6): p. 702-10.
627. Small, D.H., S.S. Mok, and J.C. Bornstein, *Alzheimer's disease and Abeta toxicity: from top to bottom.* Nat Rev Neurosci, 2001. **2**(8): p. 595-8.
628. Balaraman, Y., et al., *Glycogen synthase kinase 3beta and Alzheimer's disease: pathophysiological and therapeutic significance.* Cell Mol Life Sci, 2006. **63**(11): p. 1226-35.
629. Takashima, A., *GSK-3 is essential in the pathogenesis of Alzheimer's disease.* J Alzheimers Dis, 2006. **9**(3 Suppl): p. 309-17.
630. Suhara, T., et al., *Abeta42 generation is toxic to endothelial cells and inhibits eNOS function through an Akt/GSK-3beta signaling-dependent mechanism.* Neurobiol Aging, 2003. **24**(3): p. 437-51.
631. Okazawa, H. and S. Estus, *The JNK/c-Jun cascade and Alzheimer's disease.* Am J Alzheimers Dis Other Demen, 2002. **17**(2): p. 79-88.
632. Shoji, M., et al., *JNK activation is associated with intracellular beta-amyloid accumulation.* Brain Res Mol Brain Res, 2000. **85**(1-2): p. 221-33.
633. Zhu, X., et al., *Activation and redistribution of c-jun N-terminal kinase/stress activated protein kinase in degenerating neurons in Alzheimer's disease.* J Neurochem, 2001. **76**(2): p. 435-41.
634. Bozyczko-Coyne, D., et al., *CEP-1347/KT-7515, an inhibitor of SAPK/JNK pathway activation, promotes survival and blocks multiple events associated with Abeta-induced cortical neuron apoptosis.* J Neurochem, 2001. **77**(3): p. 849-63.
635. Morishima, Y., et al., *Beta-amyloid induces neuronal apoptosis via a mechanism that involves the c-Jun N-terminal kinase pathway and the induction of Fas ligand.* J Neurosci, 2001. **21**(19): p. 7551-60.

636. Troy, C.M., et al., *beta-Amyloid-induced neuronal apoptosis requires c-Jun N-terminal kinase activation.* J Neurochem, 2001. **77**(1): p. 157-64.
637. Kaltschmidt, B., et al., *Transcription factor NF-kappaB is activated in primary neurons by amyloid beta peptides and in neurons surrounding early plaques from patients with Alzheimer disease.* Proc Natl Acad Sci U S A, 1997. **94**(6): p. 2642-7.
638. Terai, K., A. Matsuo, and P.L. McGeer, *Enhancement of immunoreactivity for NF-kappa B in the hippocampal formation and cerebral cortex of Alzheimer's disease.* Brain Res, 1996. **735**(1): p. 159-68.
639. Ferrer, I., et al., *NF-kB immunoreactivity is observed in association with beta A4 diffuse plaques in patients with Alzheimer's disease.* Neuropathol Appl Neurobiol, 1998. **24**(4): p. 271-7.
640. Boissiere, F., et al., *Nuclear translocation of NF-kappaB in cholinergic neurons of patients with Alzheimer's disease.* Neuroreport, 1997. **8**(13): p. 2849-52.
641. Kuner, P., R. Schubenel, and C. Hertel, *Beta-amyloid binds to p57NTR and activates NFkappaB in human neuroblastoma cells.* J Neurosci Res, 1998. **54**(6): p. 798-804.
642. Kaltschmidt, B., D. Widera, and C. Kaltschmidt, *Signaling via NF-kappaB in the nervous system.* Biochim Biophys Acta, 2005. **1745**(3): p. 287-99.
643. Gravina, S.A., et al., *Amyloid beta protein (A beta) in Alzheimer's disease brain. Biochemical and immunocytochemical analysis with antibodies specific for forms ending at A beta 40 or A beta 42(43).* J Biol Chem, 1995. **270**(13): p. 7013-6.
644. Krumenacker, J.S., A. Kots, and F. Murad, *Effects of the JNK inhibitor anthra[1,9-cd]pyrazol-6(2H)-one (SP-600125) on soluble guanylyl cyclase alpha1 gene regulation and cGMP synthesis.* Am J Physiol Cell Physiol, 2005. **289**(4): p. C778-84.
645. Barr, R.K., et al., *Reverse two-hybrid screening identifies residues of JNK required for interaction with the kinase interaction motif of JNK-interacting protein-1.* J Biol Chem, 2004. **279**(41): p. 43178-89.
646. Angell, R.M., et al., *N-(3-Cyano-4,5,6,7-tetrahydro-1-benzothien-2-yl)amides as potent, selective, inhibitors of JNK2 and JNK3.* Bioorg Med Chem Lett, 2007. **17**(5): p. 1296-301.
647. Sarker, K.P., et al., *Inhibition of caspase-3 activation by SB 203580, p38 mitogen-activated protein kinase inhibitor in nitric oxide-induced apoptosis of PC-12 cells.* J Mol Neurosci, 2000. **15**(3): p. 243-50.
648. Hur, E., et al., *Mitogen-activated protein kinase kinase inhibitor PD98059 blocks the trans-activation but not the stabilization or DNA binding ability of hypoxia-inducible factor-1alpha.* Mol Pharmacol, 2001. **59**(5): p. 1216-24.
649. Daoud, G., et al., *Src family kinases play multiple roles in differentiation of trophoblasts from human term placenta.* J Physiol, 2006. **571**(Pt 3): p. 537-53.
650. Narumiya, S., T. Ishizaki, and M. Uehata, *Use and properties of ROCK-specific inhibitor Y-27632.* Methods Enzymol, 2000. **325**: p. 273-84.
651. Root, C.N., et al., *Entry of influenza viruses into cells is inhibited by a highly specific protein kinase C inhibitor.* J Gen Virol, 2000. **81**(Pt 11): p. 2697-705.
652. Yano, H., et al., *Biochemical and pharmacological studies with KT7692 and LY294002 on the role of phosphatidylinositol 3-kinase in Fc epsilon RI-mediated signal transduction.* Biochem J, 1995. **312 (Pt 1)**: p. 145-50.
653. Lin, Y.Z., et al., *Inhibition of nuclear translocation of transcription factor NF-kappa B by a synthetic peptide containing a cell membrane-permeable motif and nuclear localization sequence.* J Biol Chem, 1995. **270**(24): p. 14255-8.
654. Bogoyevitch, M.A., *The isoform-specific functions of the c-Jun N-terminal Kinases (JNKs): differences revealed by gene targeting.* Bioessays, 2006. **28**(9): p. 923-34.
655. Mazzon, E. and S. Cuzzocrea, *Role of TNF-alpha in lung tight junction alteration in mouse model of acute lung inflammation.* Respir Res, 2007. **8**: p. 75.

656. Mazzon, E. and S. Cuzzocrea, *Role of TNF-alpha in ileum tight junction alteration in mouse model of restraint stress.* Am J Physiol Gastrointest Liver Physiol, 2008. **294**(5): p. G1268-80.
657. Sabath, E., et al., *Galpha12 regulates protein interactions within the MDCK cell tight junction and inhibits tight-junction assembly.* J Cell Sci, 2008. **121**(Pt 6): p. 814-24.
658. Olariu, A., K. Yamada, and T. Nabeshima, *Amyloid pathology and protein kinase C (PKC): possible therapeutics effects of PKC activators.* J Pharmacol Sci, 2005. **97**(1): p. 1-5.
659. Andreeva, A.Y., et al., *Assembly of tight junction is regulated by the antagonism of conventional and novel protein kinase C isoforms.* Int J Biochem Cell Biol, 2006. **38**(2): p. 222-33.
660. Williams, M.R., et al., *Gene expression of endothelial cells due to interleukin-1 beta stimulation and neutrophil transmigration.* Endothelium, 2008. **15**(1): p. 73-165.
661. Schafer, M., et al., *Inhibition of glycogen synthase kinase 3 beta is involved in the resistance to oxidative stress in neuronal HT22 cells.* Brain Res, 2004. **1005**(1-2): p. 84-9.
662. Maiese, K. and Z.Z. Chong, *Insights into oxidative stress and potential novel therapeutic targets for Alzheimer disease.* Restor Neurol Neurosci, 2004. **22**(2): p. 87-104.
663. Bakin, A.V., et al., *Phosphatidylinositol 3-kinase function is required for transforming growth factor beta-mediated epithelial to mesenchymal transition and cell migration.* J Biol Chem, 2000. **275**(47): p. 36803-10.
664. Inestrosa, N.C., et al., *Synaptotoxicity in Alzheimer's disease: the Wnt signaling pathway as a molecular target.* IUBMB Life, 2007. **59**(4-5): p. 316-21.
665. Zhu, X., et al., *Differential activation of neuronal ERK, JNK/SAPK and p38 in Alzheimer disease: the 'two hit' hypothesis.* Mech Ageing Dev, 2001. **123**(1): p. 39-46.
666. Hyman, B.T., T.E. Elvhage, and J. Reiter, *Extracellular signal regulated kinases. Localization of protein and mRNA in the human hippocampal formation in Alzheimer's disease.* Am J Pathol, 1994. **144**(3): p. 565-72.
667. Perry, G., et al., *Activation of neuronal extracellular receptor kinase (ERK) in Alzheimer disease links oxidative stress to abnormal phosphorylation.* Neuroreport, 1999. **10**(11): p. 2411-5.
668. Zhu, X., et al., *Activation of p38 kinase links tau phosphorylation, oxidative stress, and cell cycle-related events in Alzheimer disease.* J Neuropathol Exp Neurol, 2000. **59**(10): p. 880-8.
669. Bain, J., et al., *The specificities of protein kinase inhibitors: an update.* Biochem J, 2003. **371**(Pt 1): p. 199-204.
670. Bain, J., et al., *The selectivity of protein kinase inhibitors: a further update.* Biochem J, 2007. **408**(3): p. 297-315.
671. Bogoyevitch, M.A., *Therapeutic promise of JNK ATP-noncompetitive inhibitors.* Trends Mol Med, 2005. **11**(5): p. 232-9.
672. Bogoyevitch, M.A. and B. Kobe, *Uses for JNK: the many and varied substrates of the c-Jun N-terminal kinases.* Microbiol Mol Biol Rev, 2006. **70**(4): p. 1061-95.
673. Barr, R.K., T.S. Kendrick, and M.A. Bogoyevitch, *Identification of the critical features of a small peptide inhibitor of JNK activity.* J Biol Chem, 2002. **277**(13): p. 10987-97.
674. Bogoyevitch, M.A. and P.G. Arthur, *Inhibitors of c-Jun N-terminal kinases: JuNK no more?* Biochim Biophys Acta, 2008. **1784**(1): p. 76-93.

675. Guan, Q.H., et al., *Neuroprotection against ischemic brain injury by a small peptide inhibitor of c-Jun N-terminal kinase (JNK) via nuclear and non-nuclear pathways.* Neuroscience, 2006. **139**(2): p. 609-27.
676. Pyo, H., et al., *Mitogen-activated protein kinases activated by lipopolysaccharide and beta-amyloid in cultured rat microglia.* Neuroreport, 1998. **9**(5): p. 871-4.
677. Franciosi, S., et al., *Broad-spectrum effects of 4-aminopyridine to modulate amyloid beta1-42-induced cell signaling and functional responses in human microglia.* J Neurosci, 2006. **26**(45): p. 11652-64.
678. Walker, D.G., S.U. Kim, and P.L. McGeer, *Complement and cytokine gene expression in cultured microglial derived from postmortem human brains.* J Neurosci Res, 1995. **40**(4): p. 478-93.
679. Suo, Z., et al., *Alzheimer's beta-amyloid peptides induce inflammatory cascade in human vascular cells: the roles of cytokines and CD40.* Brain Res, 1998. **807**(1-2): p. 110-7.
680. Weisman, D., E. Hakimian, and G.J. Ho, *Interleukins, inflammation, and mechanisms of Alzheimer's disease.* Vitam Horm, 2006. **74**: p. 505-30.
681. McKenzie, J.A. and A.J. Ridley, *Roles of Rho/ROCK and MLCK in TNF-alpha-induced changes in endothelial morphology and permeability.* J Cell Physiol, 2007. **213**(1): p. 221-8.
682. Hooper, W.C., D.J. Phillips, and B.L. Evatt, *Endothelial cell protein S synthesis is upregulated by the complex of IL-6 and soluble IL-6 receptor.* Thromb Haemost, 1997. **77**(5): p. 1014-9.
683. Poree, B., et al., *Interleukin-6 (IL-6) and/or soluble IL-6 receptor down-regulation of human type II collagen gene expression in articular chondrocytes requires a decrease of Sp1.Sp3 ratio and of the binding activity of both factors to the COL2A1 promoter.* J Biol Chem, 2008. **283**(8): p. 4850-65.
684. Yamaguchi, T., et al., *IL-6/sIL-6R enhances cathepsin B and L production via caveolin-1-mediated JNK-AP-1 pathway in human gingival fibroblasts.* J Cell Physiol, 2008.
685. Bailey, T.L., et al., *The nature and effects of cortical microvascular pathology in aging and Alzheimer's disease.* Neurol Res, 2004. **26**(5): p. 573-8.
686. Bruewer, M., et al., *Interferon-gamma induces internalization of epithelial tight junction proteins via a macropinocytosis-like process.* Faseb J, 2005. **19**(8): p. 923-33.
687. Chiba, H., et al., *The significance of interferon-gamma-triggered internalization of tight-junction proteins in inflammatory bowel disease.* Sci STKE, 2006. **2006**(316): p. pe1.
688. Li, Q., et al., *Interferon-gamma and tumor necrosis factor-alpha disrupt epithelial barrier function by altering lipid composition in membrane microdomains of tight junction.* Clin Immunol, 2008. **126**(1): p. 67-80.
689. Shen, C., et al., *Hydrogen peroxide promotes Abeta production through JNK-dependent activation of gamma-secretase.* J Biol Chem, 2008. **283**(25): p. 17721-30.
690. Davis, R.J., *Signal transduction by the JNK group of MAP kinases.* Cell, 2000. **103**(2): p. 239-52.
691. Fogarty, M.P., E.J. Downer, and V. Campbell, *A role for c-Jun N-terminal kinase 1 (JNK1), but not JNK2, in the beta-amyloid-mediated stabilization of protein p53 and induction of the apoptotic cascade in cultured cortical neurons.* Biochem J, 2003. **371**(Pt 3): p. 789-98.
692. Bennett, B.L., et al., *SP600125, an anthrapyrazolone inhibitor of Jun N-terminal kinase.* Proc Natl Acad Sci U S A, 2001. **98**(24): p. 13681-6.
693. Dahlgren, K.N., et al., *Oligomeric and fibrillar species of amyloid-beta peptides differentially affect neuronal viability.* J Biol Chem, 2002. **277**(35): p. 32046-53.

694. Kuo, Y.M., et al., *Water-soluble Abeta (N-40, N-42) oligomers in normal and Alzheimer disease brains.* J Biol Chem, 1996. **271**(8): p. 4077-81.
695. Holback, S., L. Adlerz, and K. Iverfeldt, *Increased processing of APLP2 and APP with concomitant formation of APP intracellular domains in BDNF and retinoic acid-differentiated human neuroblastoma cells.* J Neurochem, 2005. **95**(4): p. 1059-68.
696. Li, Q. and T.C. Sudhof, *Cleavage of amyloid-beta precursor protein and amyloid-beta precursor-like protein by BACE 1.* J Biol Chem, 2004. **279**(11): p. 10542-50.
697. Maloney, B., et al., *Presence of a "CAGA box" in the APP gene unique to amyloid plaque-forming species and absent in all APLP-1/2 genes: implications in Alzheimer's disease.* Faseb J, 2004. **18**(11): p. 1288-90.
698. Stenh, C., et al., *Amyloid-beta oligomers are inefficiently measured by enzyme-linked immunosorbent assay.* Ann Neurol, 2005. **58**(1): p. 147-50.
699. Abdullah, L., et al., *The influence of diagnosis, intra- and inter-person variability on serum and plasma Abeta levels.* Neurosci Lett, 2007. **428**(2-3): p. 53-8.
700. Ertekin-Taner, N., et al., *Plasma amyloid beta protein is elevated in late-onset Alzheimer disease families.* Neurology, 2008. **70**(8): p. 596-606.
701. Matsubara, E., et al., *Soluble Abeta homeostasis in AD and DS: impairment of anti-amyloidogenic protection by lipoproteins.* Neurobiol Aging, 2004. **25**(7): p. 833-41.
702. Mayeux, R., et al., *Plasma A[beta]40 and A[beta]42 and Alzheimer's disease: relation to age, mortality, and risk.* Neurology, 2003. **61**(9): p. 1185-90.
703. Mehta, P.D., et al., *Plasma and cerebrospinal fluid levels of amyloid beta proteins 1-40 and 1-42 in Alzheimer disease.* Arch Neurol, 2000. **57**(1): p. 100-5.
704. Galloway, S., et al., *Synergistic effects of high fat feeding and apolipoprotein E deletion on enterocytic amyloid-beta abundance.* Lipids Health Dis, 2008. **7**: p. 15.
705. Pallebage-Gamarallage, M.M., et al., *The effect of exogenous cholesterol and lipid-modulating agents on enterocytic amyloid-beta abundance.* Br J Nutr, 2008: p. 1-8.
706. Howlett, D.R., et al., *Abeta deposition and related pathology in an APP x PS1 transgenic mouse model of Alzheimer's disease.* Histol Histopathol, 2008. **23**(1): p. 67-76.
707. Krishna, M. and H. Narang, *The complexity of mitogen-activated protein kinases (MAPKs) made simple.* Cell Mol Life Sci, 2008.